University of Alberta

Factors Affecting Sediment Oxygen Demand of The Athabasca River Sediment Under Ice Cover

by

Kusumakar Sharma

A thesis submitted to the Faculty of Graduate Studies and Research
in partial fulfillment of the requirements for the degree of

Doctor of Philosophy
in
Environmental Engineering

Civil and Environmental Engineering

©Kusumakar Sharma
Fall 2012
Edmonton, Alberta

Permission is hereby granted to the University of Alberta Libraries to reproduce single copies of this thesis and to lend or sell such copies for private, scholarly or scientific research purposes only. Where the thesis is converted to, or otherwise made available in digital form, the University of Alberta will advise potential users of the thesis of these terms.

The author reserves all other publication and other rights in association with the copyright in the thesis and, except as herein before provided, neither the thesis nor any substantial portion thereof may be printed or otherwise reproduced in any material form whatsoever without the author's prior written permission.

ABSTRACT

This research was conducted in a response to the dissolved oxygen (DO) decline in winter in the Athabasca River. Sediment oxygen demand (SOD) is considered as one of the major factors contributing to the DO decline in the Athabasca River. The SOD is influenced by physical phenomena, chemical reaction and microbial activities in river water as well as in the sediment. The overall objective of this thesis research was to determine factors affecting the SOD in river sediment in winter. The factors that influence the SOD in this research were: water chemistry, sediment characteristics, nutrient flux across the sediment water interface (SWI) and microbially mediated nitrogen dynamics inside sediment.

In the first phase of the research, sediment samples collected at different sites along the Athabasca River were incubated in sediment cores to determine the SOD. In order to obtain reliable SOD, a newly designed SOD measurement technique was used. The new SOD measurement technique has addressed the issue of hydrodynamics inside the benthic chamber, continuous DO monitoring, and its flexibility in operation at low temperature. Furthermore, advanced features added to the technique enabled us to conduct a study on nutrient fluxes across the SWI. The fall and winter SOD measurement revealed that the SOD was correlated with water chemistry in the fall season, but not in the winter season. In general, total organic carbon (TOC) was the main driving force for the SOD variations in fall and winter seasons. The SOD was also correlated with porosity in both fall and winter seasons. The nutrient flux analysis of three sites along the Athabasca

River in winter revealed that an efflux (from sediment to water column) of ammonium was observed. The ammonium efflux was correlated with the SOD. This indicates that nutrient rich sediment exerts higher SOD.

Having determined the relationship between ammonium flux and the SOD, the research in the second phase aimed to study microbially mediated nitrogen transformation in the sediment and the impact of the nitrogen transformation on the SOD. The impact of increased nutrient load on the SOD was also studied by spiking the overlying water of the sediment core with nutrients. To undertake this study, a suite of microsensors were used to measure concentrations profiles of oxygen, ammonium, nitrate and pH in the sediment at near zero temperature. The concentration profiles revealed that oxygen penetration depth in the sediment reduced when the water was spiked with nutrient load. Higher amount of oxygen consumption was observed due to an increase in the microbially mediated ammonium oxidation when nutrient was added. Therefore addition of nutrient increased SOD in the experimental condition. Although addition of particulate TOC did not increase microbial activity immediately in winter, the solubilisation process in the long run would affect ammonium oxidation. In order to maintain the DO level in the river in winter, the result suggested that either nutrient load should be reduced or supply of oxygen should be increased.

ACKNOWLEDGEMENT

I would like to express my profound gratitude to my co-supervisors, Dr. Tong Yu and Dr. Preston McEachern for their valuable guidance, suggestions and encouragement throughout the period of research. Dr. Tong Yu gave me freedom on my vision and path, and always provided resources for the research. Dr. Preston McEachern showed me the course of my research. Without their guidance and support this work would not have been possible. I also would like to express gratitude to the members who served in the Doctoral Examination Committee.

Sincere appreciation is due to Dr. Jian Peng of University of Saskatchewan for kindly considering of being the external examiner for this dissertation. His constructive and professional comments are highly appreciated.

I want to acknowledge the consortium of Natural Science and Engineering Research Council of Canada (NSERC), Alberta Environment, Alberta Newsprint Co., Alberta Pacific Forest Industries Inc. (ALPAC), Hinton Pulp, Millar Western Forest Products Ltd. and Slave Lake Pulp for funding the research.

I want to thank many others who provided helpful assistance on this project. Maria Demeter helped me on my laboratory setup and analysis. Assistance from Shujie Ren, Sabinus Okafor, Hong Liu and Shuying Tan during microsensor fabrication and measurement is greatly appreciated. Nathan Findlay, Slav

Stanislawski, Brian Jackson, Chris Ware, Roderick Hazenkewel, Dr. Gen Wu, Dr. Xiao-Hong Zhou helped in the field sampling. Dr. Prem Bhandari helped in the statistical analysis.

I would like to thank Ved P. Sharma and Ai B. Gurung for giving me good orientation in the initial stages of my life at the University as well as in Canada. The coffee group I formed during my research, the composition changed a lot over the time and included Ved, Ashim, Umesh, Santosh, Janak, Remant, Prem, Krishna, Hukum, Saurav, Mohan, Rishi, shared their views and sympathized on my frustrations during the research period.

Above all, I express my deep gratitude to my beloved wife Lalita, daughter Pritha and son Archit for their great support, patience and understanding throughout the research. My wife's endless love and encouragement to complete Ph. D., and my children's 'are you done yet?', were guiding path during my life's high and low times. I would not miss this opportunity to express appreciation and thanks to my brother Guru Prasad Sharma who always guided me to move forward.

This work is dedicated to my parents late Mr. Bhubaneswar Upadhyaya and late Mrs. Mana Devi Sharma who made me to stand in this world.

TABLE OF CONTENTS

LIST OF TABLES

LIST OF FIGURES

NOMENCLATURE

φ	Porosity
μM	micromol/litre
μS	microSiemens
θ	Tortuosity
ψ	Temperature correction factor
ρ_{sed}	Density of sediment
ρ_w	Density of water
Ag	Silver
AgCl	Silver Chloride
Ag/|AgCl	Chloride coated silver wire
A_{sed}	Area of the sediment surface
AOB	Ammonium oxidizing bacteria
BOD	Biological oxygen demand
BOD_5	5-day biological oxygen demand
BSA	Bovine Serum Albumen
C	Concentration
$CaCO_3$	Calcium Carbonate
CO_2	Carbon dioxide
COD	Chemical Oxygen Demand
d	day
D_i	Irrigation diffusion coefficient of oxygen

D_o	Molecular diffusion coefficient of oxygen
DO	Dissolved Oxygen
DOC	Dissolved organic carbon
DON	Dissolved organic nitrogen
DOM	Dissolved organic matter
D_s	Effective diffusion coefficient of oxygen in sediment
D/S	Downstream
D_t	Turbulent diffusion coefficient of oxygen
EMF	Electromotive force
hr	hour
H_2S	Hydrogen sulphide
HS^-	Hydrogen sulphide ion
ID	Inner diameter
ISmE	Ion selective liquid membrane microsensor
J_o	Flux of oxygen
k_0	Zero order rate constant
k_1	First order rate constant
k_b	Rate constant
k_c	Half saturation concentration
$KMnO_4$	Potassium permanganate
L	Litre
mV	millivolt
nA	nanoampere

NH_3	Ammonia
NH_4^+	Ammonium ion
NH_4Cl	Ammonium Chloride
NOB	Nitrite oxidizing bacteria
NO_2^-	Nitrite ion
NO_3^-	Nitrate ion
NO_x^-	$NO_2^- + NO_3^-$
O_2	Oxygen
OD	Outer diameter
pA	picoampere
PO_4^{3-}	Phosphate
POM	Particulate organic matter
RC	Reduced Chemicals
r_n	Reaction kinetics of oxygen in the sediment porewater
r_{n1}	First-order reaction kinetics of oxygen in the sediment porewater
r_{nM}	Monod reaction kinetics of oxygen in the sediment porewater
SO_4^{2-}	Sulphate
SOD	Sediment oxygen demand
SWI	Sediment water interface
T	Temperature
t	Time
TC	Total carbon

TDP	Total dissolved phosphorus
TIN	Total organic nitrogen ($NH_4^+ + NO_2^- + NO_3^-$)
TN	Total nitrogen
TOC	Total organic carbon
TP	Total phosphorus
TSS	Total suspended solids
U/S	Upstream
V_{olw}	Volume of overlying water
x_f	Dry mass of sediment in unit volume of wet sediment
z	depth of the sediment measured from the sediment water interface

Chapter 1

GENERAL INTRODUCTION

1.1 Background

The decline of the dissolved oxygen (DO) concentration in river water during low flow, especially during winter in cold regions, is of prime concern, as it affects the aquatic ecosystem. The Athabasca River is fully covered with snow and ice in winter limiting reaeration and reducing photosynthetic activity. Pollutant loads from effluents of pulp mills and municipal wastes discharged to the Athabasca River exacerbates the balance of the river's DO budget. In the winter of 2003, the DO level reached below 6.5 mg/L, a chronic level according to guidelines established by the Canadian Council of Ministers of the Environment (CCME). This observation prompted an investigation on factors affecting the Athabasca River's DO budget. The oxygen demand exerted by the decaying activity in the sediment known as sediment oxygen demand (SOD), one of the sinks for DO budget in the river, could be a significant factor for the DO deficit (Ellis and Stefan, 1989).

Extensive literatures evaluate the impact of the SOD on the DO budget (Belanger, 1981; Murphy and Hicks, 1986; Traux et al., 1995). The SOD has been shown to be responsible for half the portion of the DO depletion in the stream (Matlock et

al., 2003). Previous studies in the Athabasca River investigated the SOD's spatial and seasonal changes (Casey, 1990; Monenco, 1992; HBT, 1993; Noton, 1995; Tian et. al., 2004). Yu (2006) studied the impact of the impulse carbon load on the SOD in Athabasca River sediment and found that labile carbon load increased SOD. These studies indicate the transfer phenomena of oxygen from bulk water into sediment controls the SOD and hence the DO budget (Boudreau, 1997). The oxygen transfer is influenced by temperature, flow velocity, DO concentration, availability of organic matter, and sediment porosity (Di Toro, 2001).

Various types of microorganisms mediate organic matter degradation and other biochemical processes through processes known as diagenesis (Fenchel and Blackburn, 1979). In diagenesis, the oxygen demand in the sediment is elevated by microorganisms that degrade organic carbon and oxidize reduced chemical species, such as ammonia, sulphides, and methane, for microbial growth and metabolism. The Athabasca River receives organic matter and nutrients from municipal waste discharges and pulp mill effluents that increase nutrient load in the river sediment. Once nutrients in particulate form settle onto the river bed or the dissolved nutrients are transferred to the sediment, they provide food for microorganisms for their metabolic activities. These processes contribute to the increase of the SOD.

1.2 Problem Statement and Objectives

Substantial impact of the SOD on river system's oxygen budget makes the SOD imperative to be included in DO modeling (Hatcher, 1986). Continuous SOD monitoring in any river is a challenge using available SOD measurement techniques. SOD values differ from site to site and season to season (Wood, 2001; Ghrenz, 2003). The changes have also been observed in diurnal SOD values (Nakamura et al., 2004). The development of reliable SOD measurement techniques (either field-based or laboratory-based) and understanding factors influencing the SOD (Noton, 1996) is required. The correct estimation of the SOD would reduce uncertainty in DO modeling (Di Toro, 2001).

Numerous SOD studies have been conducted in temperate climates, estuaries, lakes, and on the sea floor (Boudreau, 2001; Di Toro, 2001). There is not much literature available about the SOD in river sediment (Matlock et al., 1998; Wood, 2001; House, 2003; Haag et al., 2006). The majority of literature focuses on the effect of physical parameters such as flow velocity (Nakamura and Stefan, 1994; Mackenthum and Stefan, 1998), hydrodynamic state (Higashino et al., 2003), porosity (Boudreau, 1997) and sediment composition (House, 2003; Haag et al., 2006), on the SOD. In addition to the effect of physical parameters on the SOD, the chemical reactions occurring inside sediment for organic carbon degradation and nutrient transformation are considered responsible for giving rise to the SOD (Boulding, 1968; Berner, 1980; Boudreau and Jorgensen, 2001). Moreover, inclusion of early diagenesis, which describes carbon and nutrient recycling inside sediment, into a DO model is challenging as early diagenesis couples diffusion

and reaction components. One way is to estimate the nutrient budget across the SWI. The nutrient flux measurement can be used to estimate the nutrient budget across the SWI. The nutrient flux exchanges across the SWI regulate the DO demand, thus rendering changes in the SOD (Denis et al., 2003).

Given the Athabasca River's conditions in the winter, when it is covered with ice, the SOD results obtained from previous studies in other type of climate and aquatic systems are not directly applicable. Precious studies estimating SOD in the Athabasca River sediment (Noton, 1996; Tian, 2005; Yu, 2006) have not elucidated the factors affecting SOD variations spatially nor temporally. As the Athabasca River receives loads of organic matter and nutrients from effluent discharges from pulp mills and waste treatment plants, it is hypothesized that this load increases the concentrations of water quality parameters pertaining to organic carbon and nutrients, and this process elevates the SOD. Similarly, during the period of ice cover, the SOD could be the only major sink to imbalance the DO budget in the river water column.

Nutrient recycling has been shown to regulate the DO demand within sediment, thus making the nutrient flux an important component of the global nutrient budget (Stief et al., 2003). So far no study has determined nutrient flux and the impact of biogeochemistry on the nutrient flux in the river systems under ice cover. The nutrient flux estimate at the SWI helps to determine the nutrient budget, but it does not give a quantitative description of processes governing

nutrient transformation. In nitrogen transformation process ammonium is converted to nitrate by a set of autotrophic microbes. In this process a significant amount of DO is consumed (Altman, 2003). Nitrogen transformation could also exert a DO demand in river sediment at near zero temperature, when the river is covered with ice. Until now no study has been reported about ammonium oxidation and nitrification in river sediment in such condition. The autotrophic microorganisms found in sediment biofilm are responsible for ammonium oxidation and nitrification (Revsbech et al., 2006). Thus, investigating the activity of these nitrifiers could provide reaction rates which in turn could be used to estimate the DO demand and ultimately the SOD.

In view of the gap in research about the SOD of the river sediment under ice cover, this thesis had the following objectives:

(1) To develop a suitable method and apparatus for SOD determination and evaluate its applicability at near zero temperature condition
(2) To determine the SOD in Athabasca River sediment in the fall season (without ice cover) and winter season (with ice cover)
(3) To evaluate the spatial variation of the SOD in Athabasca River sediment
(4) To determine factors affecting the SOD, the factors being water quality parameters, the season (fall and winter), and physical characteristics of the sediment (porosity and composition)
(5) To investigate nutrient flux across SWI at near zero temperature conditions in relation to the sediment biogeochemistry

(6) To fabricate and evaluate the performance of a suite of microsensors, including combined oxygen, ammonium, nitrate, and pH at near zero temperature

(7) To profile concentrations of O_2, NH_4^+, NO_3^-, and pH in micro-scale vertically along the depth of sediment at near zero temperature

(8) To determine the activity of ammonium oxidizing and nitrifying bacteria from concentration profiles and determine conversion rates at near zero temperature

(9) To determine the impact of a spiked load of NH_4^+ and TOC on ammonium oxidation and oxygen consumption based on concentration profiles at near zero temperature

1.3 Thesis Outline

The overall objectives of this thesis were to investigate the variation of the SOD in river sediment and factors affecting it, determine the flux of nutrients across the SWI in the winter, and evaluate the potential application of a suite of microsensors to obtain insight into the activity of nitrogen transformation and its impact on the SOD. The following section provides a short summary of investigations and experiments in this thesis.

A literature study (included in Chapter 2) was conducted to understand the meaning of the SOD and its relationship with the DO budget in the river. With the

acknowledgement of spatial and temporal variations of the SOD, the study looked at what factors mostly affect the SOD. From the literature study it was found that the availability of organic matter and nutrients in both the water column and sediment, influence the SOD. In addition to this, the sediment characteristics that provide the niche for microbial activity are also important in affecting SOD. In the context that the Athabasca River is different from the rivers in warm climates, the main question was to analyze at what magnitude are those factors found in the literature are relevant to Athabasca River.

Chapter 3 gives details about the materials and methods used in this research. The research was conducted on river sediment collected at different locations in and along the Athabasca River (upstream of Hinton to downstream of the Calling River confluence with the Athabasca River). Accessibility and availability of the sediment dictated the number of sampling locations. Fifteen locations were sampled in the fall of 2006, but only 10 sampling locations were accessible in the winter of 2007. The number of sampling locations decreased in later survey periods. In order to measure SOD a new laboratory based technique was developed. The new technique consists of a sediment core tube which has addressed the issues of appropriate mixing of overlying water in the core; shape, size and content in the core; DO monitoring; and flexibility of its operation for other purposes. The additional features of the technique allow intermittent sampling for nutrient flux analysis. Details are included in the materials and methods section.

In the first investigative research (Chapter 4), the SOD was determined for the fall and winter seasons from fall 2006 to fall 2008. The SOD was found to vary in space and time at all sampling periods along the Athabasca River. The mean SOD in the fall ranged from 0.00 $g/m^2 \cdot d$ to 0.71 $g/m^2 \cdot d$ and the mean SOD in the winter ranged from 0.02 $g/m^2 \cdot d$ to 0.48 $g/m^2 \cdot d$. All reported SOD values are at 4^oC, unless otherwise stated. In general, the SOD was higher at downstream sampling locations of the river compared to upstream locations. The SOD did not consistently exhibit any trend of changes in the SOD above and below nutrient discharge points. This led to an acknowledgement of the existence of other factors apart from the nutrient load in the river. Within this context, the physical property of sediment (porosity, granulometry) at the top 2 cm of the active layer was regressed against the SOD. The SOD was correlated with porosity in the fall sampling period as well as in the winter sampling period. The porosity was influenced by the silt and clay portion as well as the organic matter content of the sediment. In general, the finer the sediment grains, more organic matter was retained and the higher SOD observed. The result indicated that sediment porosity is one of the factors affecting the SOD variations in the Athabasca River.

Nutrient flux analysis of NH_4^+, NO_x^-, PO_4^{3-}, SO_4^{2-} (Chapter 4) was done for sediment samples collected at three locations along the Athabasca River. To determine the flux, changes in concentrations of nutrients in overlying water of the sediment core during the incubation period were used. An efflux of NH_4^+ and

NO_x^- from the sediment to the water column was observed at two sites. An influx of PO_4^{3-} from the water column to the sediment was observed in one of three sites. No change was observed for SO_4^{2-} at all sites. The NH_4^+ flux was correlated with the organic matter and total nitrogen content of the sediment. NH_4^+ flux was positively correlated with the SOD. The result indicated that ammonium flux from sediment to water column in nutrient rich sediment is responsible for a higher DO demand, thus increasing SOD.

In an attempt to provide general guidance for calibrating oxygen modeling, Chapter 5 presents an analysis of the relationship between the Athabasca River's SOD and water quality parameters. The SOD of all fall and winter seasons were regressed with seasonal water quality parameters, respectively. The water quality parameters were total organic carbon (TOC), 5-day biochemical oxygen demand (BOD_5), total suspended solids (TSS), total organic nitrogen (TIN), total dissolved phosphorus (TDP), Chlorophyll-a, Fe, conductivity, and alkalinity. In fall, pair-wise correlation indicated that SOD was positively correlated with water quality parameters, the TOC, TDP, Chlorophyll-a, Fe, and a negative correlation with alkalinity and conductivity. SOD was not correlated with BOD_5. The reason could be that SOD is the outcome of biological degradation of organic matter (labile and refractory) in the sediment, whereas BOD_5 is a measure of biodegradability of organic matter and BOD_5 sensitive to labile organic matter in water column. The principal component analysis of all fall data confirmed the pair-wise correlation. But in the winter seasons the SOD did not show a correlation with any of the fall

water chemistry except alkalinity and TSS. TOC was positively correlated with TDP, which was positively correlated with TSS. Although TOC was not statistically correlated with SOD in winter, but TOC was the driving force for the SOD variation. Based on the fall season results, a classification of the SOD as developed which will be a useful tool for water quality modellers in the Athabasca River.

In light of the flux investigation, it was imperative to understand the dynamics of nutrients at the sediment water interface (SWI). With the findings of increased ammonium and nitrate concentration and an efflux of ammonium from the sediment to the water column in the winter, it was necessary to gain insight into nitrogen dynamics and the transformation inside sediment. In order to have insight into this phenomenon, a suite of microsensors (O_2, NH_4^+, NO_3^-, pH), were fabricated and evaluated (Chapter 6) in our lab. The evaluation and deployment of liquid type ion selective microsensors (ISmE) at near zero temperature is the first of its kind in river sediment. During the microsensor evaluation process, the impact of temperature change in the microsensor's performance was examined. Temperature did not appear to affect the O_2 microsensor's performance. The performance of pH microsensor was stable at all temperatures; however, the NH_4^+ and NO_3^- microsensors' performances exhibited the effects of temperature. To minimize the temperature's effect on microsensor performance, the calibration of all microsensors was done at the same temperature as the experimental solution.

Chapter 7 presents the microsensor measurement of nutrient concentrations inside sediment at near zero temperature. The microsensors were used to profile concentrations of O_2, NH_4^+, NO_3^-, and pH along the depth of sediment samples. Moreover, the impact of nutrient addition was evaluated by spiking the water of the sediment core with NH_4^+ alone and combination of NH_4^+ and TOC and incubating sediment core for more than two months. The O_2 microsensors were used to determine oxygen penetration depth inside sediment in the dark, illuminated, and under flow conditions. The NH_4^+, NO_3^-, and pH microsensors could not be used in flow conditions because of noisy signals due to flow.

The profiles revealed that once ammonium was added to water overlying the sediment, there was a higher consumption of oxygen, thus diminishing thickness of aerobic zone. Ammonium oxidation due to the metabolic activities of AOB and nitrate production due to NOB in the aerobic zone was the main reason for the oxygen consumption. Diurnal changes (light and dark) did not show a significant effect on ammonium oxidation. Addition of particulate TOC did not increase ammonium oxidation in the short term likely due to a lack of solubilisation of particulate organic carbon, but the TOC would be responsible for diagenesis in the sediment once the particulate TOC is converted to soluble form. The results indicated that addition of nutrient increases oxygen consumption rate in the sediment, exerting higher oxygen demand. This microbially mediated phenomenon increases SOD thus reducing the DO level in the Athabasca River.

In order to maintain DO level in the Athabasca River, the nutrient load needs to be controlled.

Chapter 2

FACTORS AFFECTING SEDIMENT OXYGEN DEMAND

A LITERATURE REVIEW

2.1 General

The DO concentration in water bodies indicates the state of its quality. The availability of DO in water bodies affects and sustains the aquatic ecosystem in balance. Any alteration in DO concentration, especially during the stage when its quantity has been reduced, results in environmental stress, rendering changes in the activity level of individual elements in the aquatic ecosystem. The impact of low DO concentration in rivers is manifested by fish mortality, odours, and other aesthetic nuisances (Cox, 2003).

Many factors lead to the variability in DO in rivers, and the major influences can be categorised as being either sources or sinks of DO in the rivers (Cox, 2003). The major sources of DO are: (1) reaeration from the atmosphere caused by turbulence, (2) photosynthetic oxygen production, and (3) the introduction of DO from other sources such as tributaries. The main causes of oxygen depletion, the sinks, are: (1) the oxidation of organic material and other reduced matter in the water column, (2) degassing of oxygen in supersaturated water, (3) respiration by aquatic plants, and (4) the oxygen demand exerted by the riverbed.

The dominant processes that relate to the oxygen balance of a river are (Bennett and Rathburn, 1972): (1) the oxygen demand of the carbonaceous and nitrogenous wastes in the water, (2) the oxygen demand of the bottom deposits, (3) any immediate chemical oxygen demand (COD), (4) the oxygen required for plant respiration, (5) the oxygen produced by plant photosynthesis, and (6) the oxygen gained from atmospheric reaeration. With this understanding, Figure 2.1 presents an idealized representation of sources and sinks in balancing the DO in the river water column. The straight lines represent the sources and the wavy lines represent the sinks. The thickness of the line indicates the significance of either the source or sink.

The SOD is the rate of oxygen removal from overlying water, either by biological means or chemical oxidation of substances in the bottom material of a water body (Veenstra and Nolen, 1991; Traux et al., 1995; Hatcher, 1986). The SOD is a major sink in the dissolved oxygen (DO) budget balance in aquatic environments including rivers, lakes, and channels (Thommann and Mueller, 1987), as depicted in Figure 2.1. As observed by Hanes and Irvine (1966), the SOD at a certain location of a given section of a river is responsible for about 50% of oxygen depletion. Many researchers have concluded that the SOD is one of the major sinks for oxygen in the aquatic system (Belanger, 1981; Murphy and Hicks, 1986; Traux et al., 1995). Matlock et al. (2003) also found that the SOD was responsible for 50% of the total oxygen depletion within the stream, adding weight to the idea

that the SOD is one of the most important parameters within the DO budget balance.

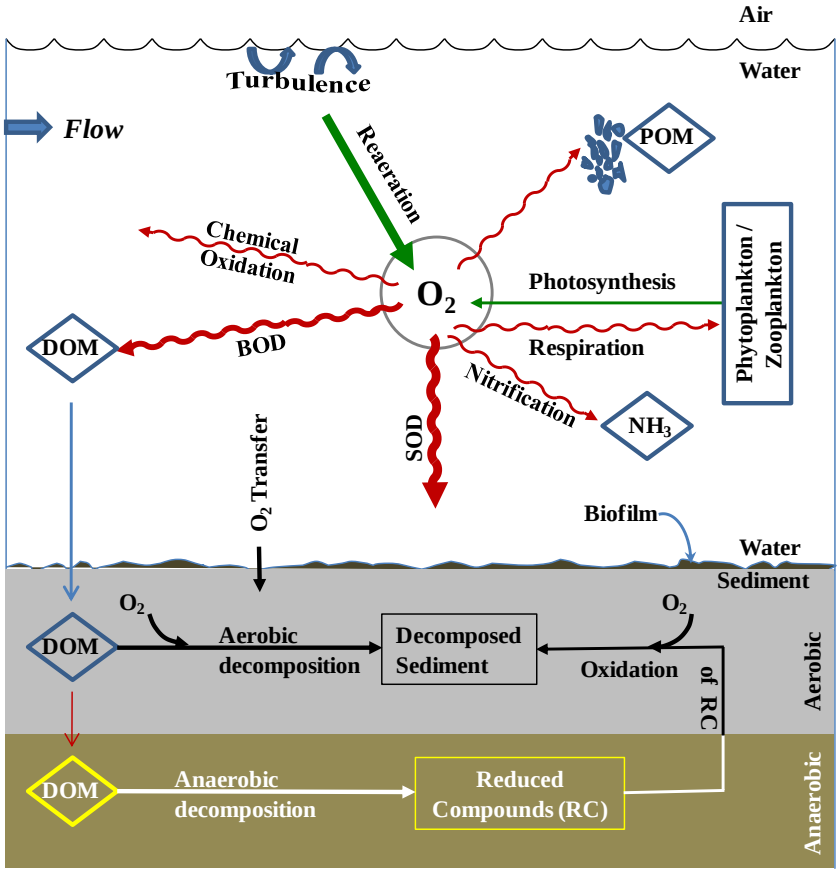

Figure 2.1 Idealized representation of overlying water column on the bottom sediment layer of the Athabasca River in the fall season. The DO budget balance is shown by sources (straight lines) and sinks (wavy lines). Inside sediment the O_2 is consumed in bacterial mediated oxidation/reduction reactions.

2.2 Sediment Oxygen Demand and its Determination

The SOD is a natural phenomenon that consists of two parts: (1) exertion of oxygen demand due to biological respiration, and (2) microbially mediated

chemical oxidation of reduced substances derived from sediment. The primary contributing factor to SOD is the deposition and subsequent decomposition of organic matter transported to the benthic layer. As shown in Figure 2.1, the dissolved organic matter (DOM) is decomposed by bacteria by taking up oxygen in aerobic respiration. At the same time, ammonia is nitrified by autotrophic bacteria in aerobic conditions (Tchobanoglous et al., 2003). In a deeper layer of sediment, the DOM is decomposed anaerobically to produce reduced compounds, such as methane, hydrogen sulphide, and ammonia. These reduced compounds, when transported to aerobic sediment layer, get oxidised, exerting an oxygen demand. Again, the chemical oxidation of reduced compounds in this process is facilitated by microbial organisms.

The SOD measurements are useful when they accurately predict the SOD of a system (Parkhill and Gulliver, 1997). In view of this notion, there are three broad methods used for the SOD measurements, which are (Hatcher, 1986): (1) whole core incubation, (2) use of microsensors, and (3) use of SOD models. A comprehensive review of the SOD measurement techniques is presented by Bowman and Delfino (1980), Hall and Berkas (1989) and Traux et al. (1995). Tian (2005) and Yu (2006) have written a literature review of the SOD measurement techniques applicable to ice-covered rivers and lakes.

The whole core incubation and microsensor methods could be used as laboratory or in-situ methods to determine the SOD. Microsensors are robust with very high

spatial resolution, making them a reliable tool to elucidate the concentration profiles of chemical species with no or minimized physical disturbance (Revsbech et al., 1980). The principle of whole core incubation is to measure total oxygen demand, while that for microsensor usage is to measure diffusive oxygen demand (Rabouillea et al., 2003). In the core incubation method, either *in situ* or laboratory, the SOD is obtained from the change of oxygen concentration over the period of incubation time, in a fixed volume of water overlying the sediment (Haag, 2006). In the microsensor method, the SOD is calculated from the oxygen profiles by using an appropriate molecular diffusion coefficient (in vertical direction only) (Kuhl and Revsbech, 2001). The microsensor method gives an accurate diffusive flux, since this does not disturb the natural condition at the sediment-water interface. The biggest challenge is that microsensors measure diffusion only, and physical processes are ignored (Vigil, 1992).

There are pros and cons to using any of the methods for the SOD measurements. The researchers have focused on the factors that relate to similarities or differences in the results of in-situ or laboratory measurement of the SOD. The laboratory technique often yields data of high precision (Bowman and Delfino, 1980) and can be performed under more uniform conditions (especially temperature). The in-situ technique tends to yield SOD values that are substantially different than those generated by the laboratory technique (Murphy and Hicks, 1986; Hall and Berkas, 1988). This difference has been attributed to

disruption of the sediment's microbial flora and physicochemical characteristics during core collection, handling, and analysis.

The in-situ methods are more specific to the site conditions and the SOD values differ in space and time. The most observed drawback of this method is non-reproducibility to satisfy statistical significance. This method gives erroneous SOD values when employed in a season in which DO concentration is below 3 mg/L near the sediment surface (Murphy and Hicks, 1986; Doyle and Lynch, 2005). Another drawback of this method is that the field crews require considerable lead time, special equipment, and training (Hatcher, 1986).

The third method for determining SOD is using models. Researchers have developed various types of the SOD models. Earlier models have determined the SOD assuming a zero order areal reaction with an oxygen uptake rate that is constant over time (Di Toro et al., 1990). Empirical formulations have been developed that relate the SOD to the composition of the sediments, including parameters such as COD and volatile solids concentration (Baity, 1938; Fair et al., 1940), or physical parameters such as temperature and sediment mixing depth (Hargrave, 1969, 1973). Other formulations have related the SOD to the DO in the water overlying the sediments and temperature (Walker and Snodgrass, 1986). Most of these empirical formulations yield only weak correlations between the SOD and input parameters (Park and Jaffe, 1999).

The first deterministic SOD model was derived from a one-dimensional mass balance equation for DO at the sediment-water interface, neglecting advection (Boulding, 1968). This model assumed that the oxygen consumption is zero order and constant over the sediment depth. The SOD was computed from the simulated slope of the DO profile in the sediments. In a further refinement of this formulation, the oxygen consumption was divided between the carbonaceous and nitrogenous oxygen consumption (Klpwijk and Snodgrass, 1986), describing both of them via a zero-order constant consumption rate.

Di Toro (1986) developed a diagenetic model that estimates the SOD based on the load of particulate organic matter (POM) to the sediments and the flux of oxygen into the sediments required for the degradation of this organic matter. This model does not account for the diffusive flux of the individual reduced species followed by their oxidation. Some of these processes have been accounted for in a diagenetic model developed by Di Toro et al. (1990), which included the oxidation of methane and ammonia produced in the sediments.

The Di Toro (1990) model was further expanded to include the diagenesis of reduced species that exert oxygen demand, such as Fe^{2+}, Mn^{2+}, Ca^{2+}, Cd^{2+}, and HS^{-} (Di Toro, 2001). The one-dimensional (z-axis) mass balance equations for the rate of DO change in the diffusive boundary layer and inside the sediment (considering electron transfer species) can be written as (DiToro, 2001):

$$\frac{\partial(O_z)}{\partial t} = (D_o + D_t + D_i)\frac{\partial^2 O_z}{\partial z^2} \qquad \text{(overlying water)} \qquad (2.1)$$

$$\frac{\partial(O_z)}{\partial t} = D_s \frac{\partial^2(O_z)}{\partial z^2} - r_n \qquad \text{(inside sediment)} \qquad (2.2)$$

where, D_o, D_t, and D_i are molecular, turbulent and irrigation diffusion coefficients for DO in water, D_s is the effective diffusion coefficient of oxygen in the sediment, O_z is the DO concentration in the porewater, t is the time, z is the distance from the SWI, and r_n is a function describing the net reaction of DO in pore water. The net reaction may include biochemical reactions involving the oxidation of organic matter by microbes and chemical redox reactions.

Equation (2.1) is subject to boundary conditions $O_z = O_0$ at $z = 0$ for $t \geq 0$. When the diffusion is the dominant factor for oxygen transfer, the flux of oxygen into the sediment is the sediment-oxygen demand and is proportional to the oxygen concentration gradient at the SWI (Matisoff and Neeson, 2005), using Fick's First Law:

$$SOD = Flux = J_{Oz} = -\varphi D_s \frac{\partial(O_z)}{\partial z}\Big|_{z=0} \qquad (2.3)$$

The effective diffusion coefficient, D_s, in pore water (i.e., porous medium) is related to the value of the molecular diffusion coefficient in free solution, D_o, but is not equal due to the tortuous movement of molecules in a porous medium. Thus, the flux is written as (Boudreau, 1997):

$$SOD = J_{Oz} = -D_0 \frac{\varphi}{\theta^2}\frac{\partial(O_z)}{\partial z} \qquad (2.4)$$

where φ is porosity and θ is tortuosity, $\theta^2 = 1 - \ln(\varphi^2)$ (Boudreau, 1997), which eliminates the tedious job of determining tortuosity, and D_o can be calculated from the temperature relationship (Han and Bartels, 1996) as: $Log_{10}(D_o) = - 4.410 + 773.8/T - (506.4/T)^2$, T is temperature in Kelvin.

Several equations have been used to describe the reaction of oxygen (r_n) in the sediment pore water by researchers (House, 2003):

(a) Zero-order reaction kinetics

$$r_{n_0} = k_0 x_f \tag{2.5}$$

where $x_f = \rho_{sed}(1-\varphi)$ is the dry mass of sediment in the unit volume of wet sediment, k_0 is the zero-order rate constant, ρ_{sed} is the density of sediment particles, and φ is the sediment porosity.

(b) First-order reaction kinetics

$$r_{n_1} = k_1 O_z \tag{2.6}$$

where k_1 is the first-order reaction rate constant

(c) Monod equation

$$r_{n_M} = z_f \frac{k_b O_z}{(O_z + k_c)} \tag{2.7}$$

where k_b and k_c are constants. If $k_c << O_z$, then $k_b = k_c$ in equation (2.6).

The use of a diagenetic model depends on the DO concentration in the sediment. Since the DO penetration depth is limited to a few millimeters of the sediment (Cai and Sayless, 1996), microsensors can be effectively used to get the oxygen penetration depth and profile oxygen concentrations in micron levels along the depth of sediment (Revsbech, 1986).

Recently a chamberless SOD measurement method has been developed (Osborn et al., 2008). In this method, water quality parameters, stream velocity, and sediment oxygen uptake rates are incorporated in model equations on a spreadsheet to calculate the SOD. This method tries to replace the *in situ* chamber measurement of the SOD; however, if the sediment oxygen uptake rate is not readily available, a laboratory measurement is necessary.

2.3 SOD Studies on the Athabasca River

The SOD study on the Athabasca River makes it different from other places, especially rivers in the southern part of the United States, because the Athabasca River experiences an ice-covered stage for more than four months during the winter season. The idealized representation of the DO budget balance presented in Figure 2.1 has to be modified for the Athabasca River in the winter season (Figure 2.2). In this period, there is no reaeration from the atmosphere, as the river is covered with ice and snow. In addition, photosynthesis is minimized because the ice and snow cover obstructs solar radiation. All the sources of DO are

nullified in the river, but the sinks are left intact. The SOD bears the brunt of the sinks as microbial activities in the sediment continue.

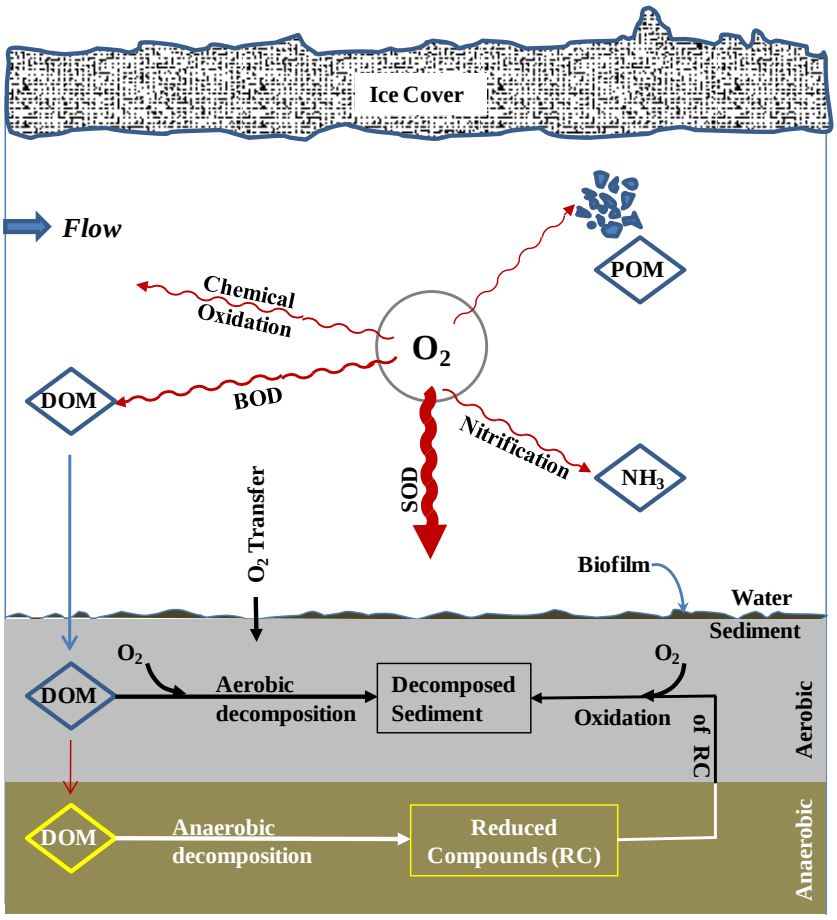

Figure 2.2 Idealized representation of overlying water column on the bottom sediment layer of the Athabsca River in the winter season. The ice and snow cover eliminates sources of DO, thus leaving the sinks intact. The SOD becomes major sink of DO in the Athabasca River.

The SOD study in the Athabasca River started in 1988 (Casey and Noton, 1989). Several other studies have focused on the spatial variability of the SOD along the Athabasca River (Casey and Noton, 1989; HBT, 1993; Monenco, 1993; Noton, 1996). Tian (2005) investigated three methods for estimating the SOD and

demonstrated that the closed chamber method used in previous studies was unreliable. Yu (2006) further developed core and microsensor methods that allowed increased replicates to be incubated under controlled conditions. She found that improper mixing in a closed chamber was a major factor that led to previous underestimates of the SOD. Yu (2006) investigated the impact of organic carbon and nutrients on the SOD and found that the SOD was stimulated by nutrients in the presence of labial carbon. Table 2.1 presents the SOD measured in the Athabasca River at different times. The SOD varied with time and space in the range of 0.09 g/m^2•d to 1.25 g/m^2•d at 20^oC. The highest SOD was observed at downstream of Millar Western Mill effluent discharge point.

2.4 Factors Affecting SOD

Several biotic and abiotic factors described in the literature that influence the SOD are: the DO concentration in the overlying water column, the temperature of the overlying water column, the flow velocity of the water above sediment, the organic load and toxic materials in the water column, sediment characteristics (organic content as well as granulometry), and microbial activity in the sediment. Primary focus is often given to the biological components such as the organic content of the benthic sediment and microbial concentrations. In addition, the measurement technique influences the SOD, thus acquiring site-specific consideration (Bowman and Delfino, 1980).

Table 2.1 Measured SOD along the Athabasca River

Site	SOD (g/m^2•d) @ 20^oC	
	2004 Fall[#]	1990 – 1995*
Upstream of Hinton Pulp	0.30	0.11
Emerson Bridge	0.22	0.37 (0.31 – 0.46)
Upstream of McLeod River		0.26
2 km downstream of Millar Western Mill		0.74 (0.50 – 1.25)
Blue Ridge		0.31 (0.22 – 0.46)
Fort Assiniboine	0.60	0.33 (0.09 – 0.53)
Chisholm	0.11	0.11
Smith		0.28 (0.22 – 0.44)
Upstream of ALPAC Mill Water Intake		0.39 (0.33 – 0.46)
Downstream of Calling River	0.34	0.20
Pelican River	0.61	

[#] Yu (2006): Averaged SOD for 24 hour and 48 hour incubation
* Averaged SOD for 1989 to 1995 period, ranges are in parentheses (Tian, 2005)

2.4.1 DO Concentration in Overlying Water

The DO concentration in overlying water is shown to influence the SOD as it increases the depth of oxygen penetration inside sediment. Increasing the depth of oxygen penetration increases the volume of aerobic sediment involved in aerobic respiration, and thereby increases the SOD (Steeby et al., 2004). Low dissolved oxygen levels in the water column (below 2-3 mg/L) may negatively influence the SOD by limiting the supply of DO (Bowman and Delfino, 1980), since the DO would become a limiting parameter for microbial as well as chemical reactions. Doyle and Lynch (2005) reported that the SOD was not affected at higher oxygen concentrations in the water column. The DO concentration in the Athabasca River is well above 3 mg/L, thus minimizing the effect of DO concentration on the SOD.

2.4.2 Temperature

The water temperature at the SWI greatly impacts the SOD. A temperature increase results in increased rates of bacterial respiration, yielding higher SOD. McDonnell & Hall (1969), for example, reported that biological activities increase two-fold for each 10 ℃ rise in temperature. However, in the Athabasca River, the low DO event occurs in the winter, when there is low flow due to cut off in flow from frozen tributaries (NREI, 2004). When the SOD values in the Athabasca River in the winter in Table 2.1 are compared to the SOD values in the rivers of warm climate in Table 2.2, the temperature's impact on the SOD is significant. The SOD values in the rivers of warm climate are many folds higher than those in the Athabasca River. But Casey and Noton (1990) compared fall and winter SOD of three sites, Windfall Bridge, Whitecourt, and Fort Assiniboine in the Athabasca River, and found similar results for both seasons. This indicates that although the river is open to the atmosphere in the fall and covered with ice and snow in winter, the benthic redox-oxidation reactions facilitated by microbial activity are similar in both seasons, thus producing similar SOD.

In order to compare SOD it is important to correct the rate to a constant temperature, typically 20 ℃, using the modified van't Hoff form of the Arrehnius equation:

$$SOD_T = SOD_{20}\psi^{T-20} \tag{2.8}$$

where, SOD_{20} is the SOD value normalized to 20°C, SOD_T is the SOD at incubation temperature, T is the incubation temperature in degree Celsius (°C), and ψ is the temperature correction coefficient. The value of ψ ranges from 1.04 to 1.13 at a ranging temperature of 2°C to 30°C (Whittemore, 1986). Stefan (1992) suggested a lower value of temperature coefficient at low temperatures.

Table 2.2 SOD (20°C) reported in river water systems

SN	River	SOD (g/m^2 d)	Reference
1	Saddle River and Salem River Watersheds, New Jersey, USA	0.6 - 7.1	Heckathorn and Gibs, 2010
2	Blackwater Streams of Georgia, USA	0.1 - 2.3	Utley et al., 2008
3	Klamath River, Oregon, USA	0.3 - 2.9	Doyle and Lynch, 2005
4	Semariang Batu River, Malaysia	0.76 - 21.4	Ling et al., 2009
5	Keelung River, Taiwan	0.24 - 1.58	Liu, 2009

2.4.3 Flow Velocity or Mixing

The flow velocity of water above sediment significantly impacts the SOD. The increasing flow velocity of the overlying water exposed to the sediment increases the SOD. Specifically, the SOD increases linearly with velocity at low velocities (<10 cm/s) (Mackenthun and Stefan, 1998) but becomes independent at high velocities (Nakamura and Stefan, 1994). A variety of processes are influenced by the flow velocity, e.g., DO gradients enhance mass transfer as tangential velocities

increase, as do transfer rates for soluble organics in the water column (Truax, et al., 1995). Turbulence may influence biological and chemical reaction rates and/or cause suspension of sediments, resulting in an increased active surface area.

Researchers have suggested that the oxygen loss rate measured with sediment chambers at low velocities reflects the physical transport rate of oxygen from the overlying water to the SWI rather than the actual maximum rate of oxygen consumption by reactions occurring in that sediment (Parkhill and Gulliver, 1997). If this were the case, then an increase in the chamber circulation velocity would cause a corresponding increase in the oxygen loss rate at the SWI. At a high enough mixing rate, the physical transport rate would become faster than the rate of oxygen consumption in the sediments, and the measured oxygen loss rate would reflect the rate of oxygen utilization by chemical and biological reactions at the SWI. Figure 2.3 presents an idealized representation of the effect of flow velocity on the SOD inside a sediment chamber (Doyle and Rounds, 2003).

At low flow velocities, the benthic boundary layer's thickness at the SWI regulates the DO transport, because diffusional transport takes over the advective transport of oxygen (Revsbech, 1986). At high flow velocities, sediment particles get resuspended, which increases the SOD. Therefore, flow rates for the laboratory and in-situ measurements of the SOD must be selected based on expected velocities of which sediment will be exposed (Belanger, 1980).

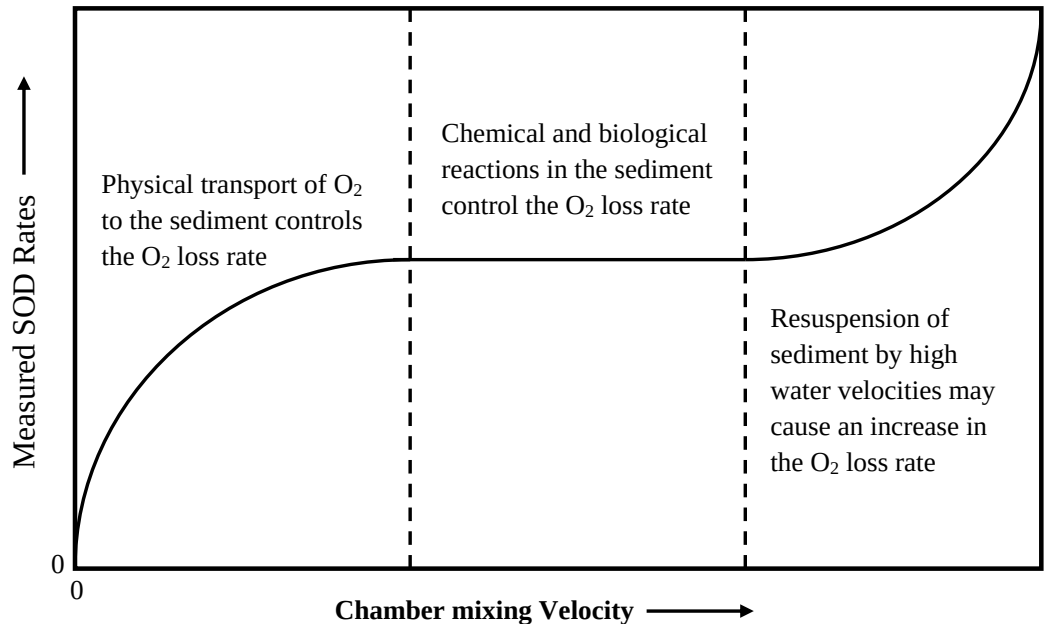

Figure 2.3 Idealized representation of the effect of flow velocity on the SOD

2.4.4 Organic Waste Load in Water Column

The waste load in the water column is increased by the continuous discharge of organic matter and nutrients from point sources, such as wastewater treatment plants, industries, and non-point sources. Over time, these substances settle onto the riverbed, making the sediment surface organic-rich where bacterial activities flourish. The SOD values measured in stream systems vary greatly and the variability can be enhanced by point-source pollution. For example, Truax et al. (1995) reported that values from 0.1 to 33 g/m^2•day have been measured downstream from paper mills in the southeastern U.S. An availability of organic matter in the sediment has been shown to increase SOD (Heckathorn and Gibs, 2010). Ling (2009) reported the highest SOD (21.4 g/m^2•d) below the discharge

point of a shrimp farm. The contribution of nutrients from the shrimp farm was responsible for higher SOD.

Effluents from three wastewater treatment plants and five pulp mills are discharged into the Athabasca River. Historically, the Athabasca River received 3727 kg/day BOD_5, 1033 kg/day total nitrogen (TN), and 331 kg/day total phosphorus (TP) load from the effluent discharges of five pulp mills (Chambers et al., 2006). In addition to this, municipal sewage treatment discharge added 160 kg/day TN and 41 kg/day TP during the period of 1989-1994 (Chambers, 2000). Although a new biological treatment system adopted by pulp mills reduced the BOD_5 load significantly, the nutrient load remained unchanged or increased in recent years (NREI, 2004). The continuous addition of the waste load to the Athabasca River is of concern. Chambers et al. (1997) reported DO sag below the effluent discharge points from the pulp mills. Yu (2006) studied the impact of organic carbon and nutrient addition in the water column on the SOD and found that the SOD was stimulated by adding a labile carbon source. However, the impact of the discharge from pulp mills on the SOD in the Athabasca River is yet to be determined.

2.4.5 Sediment Characteristics and Contents

The SOD in rivers and shallow fresh water systems vary greatly depending on the sediment deposition and supply and recycling of organic compounds in the

sediment (Utley, 2008). The organic matter reaches the stream sediment from either a source outside the system, such as leaf litter, and municipal or industrial discharge or it may be generated inside the system through plant growth (Bowie et. al., 1985). The organic matter also reaches the sediment matrix by being adsorbed to the sediment particle. The biomass that reaches the sediment matrix is fed upon by microorganisms living within the aerobic and anaerobic zones of the sediment. As the organisms within the aerobic zone feed, they require oxygen to respire and turn the organic matter into energy, therefore placing a demand on oxygen within the SWI (Bowie et. al., 1985). Sediments with higher organic matter content are shown to have higher SOD due to the creation of a feast for microorganisms to act upon (Raboulie et al., 2003, Doyle and Lynch, 1997).

Studies have found that sediment type (portion of finer or coarser particles) influences the SOD (Ghrenz et al., 2003), with sediments rich in organics consuming the most oxygen. Minute amounts of biodegradable organics that exist in sandy environments can also efficiently consume oxygen (Seiki et al., 1994). Rounds and Doyle (1997) observed the lowest SOD for sediment with high sand components and little organic matter in the Tulatin River, USA. However, there was no statistically significant correlation between measured SOD and sediment characteristics in the Williamette River in Oregon, USA (Caldwell and Doyle, 1995). Casey (1990) reported that sediment properties, with finer and higher organic matter content in three sites of the Athabasca River, were correlated with the SOD, but in other sites the sediment properties, having coarser sediment, were

not correlated with the SOD. It is assumed that the sediment with a higher portion of finer particle, such as clay and silt, can retain organic matter since the porosity of the sediment is higher than that of sandy sediment (Denis et al., 2003). Moreover, the porosity of the sediment is directly related to the SOD (Di Toro, 2001; Boudreau, 2001)

2.4.6 Oxidation-Redox Reactions in the Sediment

Organic matter is decomposed by heterotrophic bacteria in aerobic condition. Therefore the aerobic degradation is limited to the sediment's aerobic zone. In the deeper layer of the sediment, anaerobic condition exists. In the anaerobic condition, the end products of microbial activity on organic matter are reduced compounds such as methane, ammonia, and sulphide. In organic rich sediments, continuous degradation occurs in aerobic as well as anaerobic zones. Reduced compounds are transported from the sediment's anaerobic zone to its aerobic zone due to concentration gradient of chemicals. These reduced compounds get oxidized in the aerobic zone, thus exerting added oxygen demand (Gelda et al., 1995). A stoicheometric representation is given in Table 2.3 to explain the additional oxygen demand required to oxidize compounds such as ammonia, methane, and hydrogen sulphide. In the anaerobic reaction, metals such as iron and manganese play important roles, and are also included in Table 2.3. The microbial oxidation of methane and sulphide require higher amounts of oxygen

than ammonia. This gives the autotrophic bacteria an opportunity to oxidize ammonia even in smaller concentration of oxygen (Tchobanoglous et al., 2003).

Table 2.3 Stoichiometry for reduced species oxidation

Species	Reaction	Oxygen Equivalent
Ammonia	$NH_3 + 2O_2 \rightarrow NO_3^- + H_2O + H^+$	
	$\frac{5}{8}CH_4 + HNO_3 \rightarrow \frac{5}{8}CO_2 + 0.5N_2 + \frac{7}{4}H_2O$	
Overall	$NH_3 + 0.75O_2 \rightarrow 0.5N_2 + 1.5H_2O$	1.71 g of O_2/g of N
Iron	$4Fe^{2+} + O_2 + 6H_2O \rightarrow 4FeOOH + 8H^+$	0.14 g of O_2/g of Fe
Manganese	$2Mn^{2+} + O_2 + 2H_2O \rightarrow 2MnO_2 + 4H^+$	0.29 g of O_2/g of Mn
Methane	$CH_4 + 2O_2 \rightarrow CO_2 + 2H_2O$	4.0 g of O_2/g of CH_4
Sulphide	$HS^- + 2O_2 \rightarrow SO4^{2-} + H^+$	2.0 g of O_2/g of S

Studies have shown that the rate of organic matter supply to the sediments is the factor that ultimately controls the potential magnitude of sediment nutrient fluxes (Cowan et al., 1996). In the riverbed system ammonia flux is important (Revsbech et al., 2006) because ammonia is converted to nitrate by microorganisms consuming oxygen. The nitrate is denitrified to nitrogen gas in anoxic/anaerobic condition, which completes the nitrogen cycle. The increased flux of ammonia from the anaerobic to the aerobic zone increases the SOD in the sediment (Revsbech et al., 2006). Given the quantity of nitrogen load in the Athabasca River and possible supply to the sediment, the study on nitrogen transformation is

important. The amount of oxygen consumed during the nitrogen transformation could give an estimate of metabolic rates in the Athabasca River sediment.

The ammonium oxidation and nitrification process comprises two sequential steps, which are mediated by two groups of bacteria known as ammonium oxidizing bacteria (AOB) and nitrite oxidizing bacteria (NOB). Under aerobic condition NH_4^+ is oxidized to NO_2^- by AOB, and NO_2^- is oxidized to NO_3^- by NOB (Wetzel, 2007):

$$NH_4^+ + 1½\ O_2 + 2\ OH^- \rightarrow NO_2^- + 3\ H_2O \qquad \Delta G0 + -287\ kJ\ mol^{-1} \qquad (2.9)$$

$$NO_2^- + ½\ O_2 \rightarrow NO_3^- \qquad \Delta G0 + -74.1\ kJ\ mol^{-1} \qquad (2.10)$$

For the oxidation of 1 mol of NH_4^+, 2 mol of O_2 are consumed, implying a relatively high O_2 demand for the performance of nitrification in aquatic sediments. The nitrifiers are autotrophic organisms, the growth is slow, and the small amount of the energy obtained during the nitrification process is used to produce biomass (Tchobanoglous et al., 2003). As a result, autotrophs have to compete for substrate with heterotrophs that consume O_2 to degrade organic matter.

In sediment, oxygen is often depleted in an active layer within a few millimetres of the surface, limiting nitrification to a very narrow zone. Nitrifiers are therefore

challenged with a limited supply of O_2. Also, these microorganisms have to compete with metabolically superior microorganisms for their substrates, the O_2 and NH_4^+. Altman (2003) reported that nitrification can consume up to 90% of the total sedimentary O_2 consumption and that the nitrification rate is often comparable to the rate of denitrification (Lorenzen et al., 1998; Meyer et al., 2001). In view of this fact, a nitrogen transformation study was undertaken for this research.

For the microscale investigation of nitrification, measuring tools are needed that allow a sufficiently high spatial resolution to determine nitrification rates. Because of their small size, microsensors are useful tools to investigate processes occurring at a very fine scale as is the case with sediment (de Beer, 1999), where diffusion and reaction processes create steep physiochemical gradients within micrometer distances. Use of microsensors minimizes the disturbance of these gradients and other microenviromental conditions such as boundary layers, diffusion and flow patterns on the microscale (Amann and Kuhl, 1998). Moreover, the microsensors' fine spatial resolution allows the functional separation of different layers and, hence, the spatially differentiated interpretation of the processes that occur in close vicinity (e.g. nitrification and denitrification). Therefore using microsensors, one can determine activity of microorganism that mediate the nitrogen transformation.

2.4.7 Flux of Nutrient Across Sediment Water Interface

As mentioned earlier, the SOD could be divided into oxygen diffusion into the sediment for all aerobic reactions plus the oxygen consumption by the reduced organic substances released from anaerobic reactions in the sediment. When oxygen diffuses into the sediment, organic carbon and nutrients concurrently diffuse into the sediment. In such situation microbial activities inside the sediment mediate the degradation of organic carbon and nutrients and exchange of nutrient flux is created (Berner, 1980). There are two possibilities of nutrient exchanges across the SWI. First, the increased nutrient load in the river water column, which in the case of the Athabasca River comes from discharge from municipal waste treatment and pulp mills, creates an influx of nutrient into sediment. Second, the reduced chemicals accrued inside sediment create concentration gradient across SWI, thus inducing an efflux of nutrients from sediment to the water column. In either case, estimating the nutrient flux across the SWI is important to determine the nutrient budget that regulates organic carbon and the oxygen demand (Denis et al., 2001).

Researchers in the field of biogechemistry are interested mainly in nitrogen fluxes that describe mineralization and/or oxidation of ammonium and nitrification/denitrification. The flux exchange studies have been done, mostly using the whole core method, for the continental shelf (Denis et al., 2001; Jahnke, 2001) and estuaries (Thornton et al., 2007; Cowan and Boynton, 1996). There is a

lack of literature about nutrient flux across the SWI in Canadian rivers, especially in winter when the rivers are covered with ice. The study of nitrogen transformation in the Athabasca River is important, because the ammonia flux is likely an important factor affecting the SOD in the river.

Chapter 3

MATERIALS AND METHODS

3.1 Research Area

The Athabasca River originates from the Rocky Mountains of Alberta and flows in a northeast direction through the province, past the urban centers of Jasper, Hinton, Whitecourt, Athabasca, and Fort McMurray prior to emptying into Lake Athabasca. The drainage area of the Athabasca River basin is about 155,000 square kilometers and contains five pulp mills: Hinton Pulp at Hinton, Alberta News Print Co. (ANC) and Millar Western Forest Products at Whitecourt, Slave Lake Pulp at Lesser Slave Lake, and Alberta Pacific Forest Industries (ALPAC) at the town of Athabasca. The Athabasca River receives discharges from these pulp mills as well as from municipal wastewater from the major towns. Major tributaries, the Berland River, McLeod River, Freeman River, Pembina River, Lesser Slave River, La Biche River, and Calling River, drain into the Athabasca River above Grand Rapids and each is impacted by land use changes, forest, and agriculture.

For this study, 15 sites along the Athabasca River were selected for sediment and water sampling upstream of Grand Rapids. Fig. 3.1 depicts the Athabasca River basin that includes tributaries, approximate pulp mill effluent discharge points,

and sediment sampling sites. Sediment sampling sites were located upstream and downstream of nutrient sources, which were either tributaries or pulp mill effluent discharge.

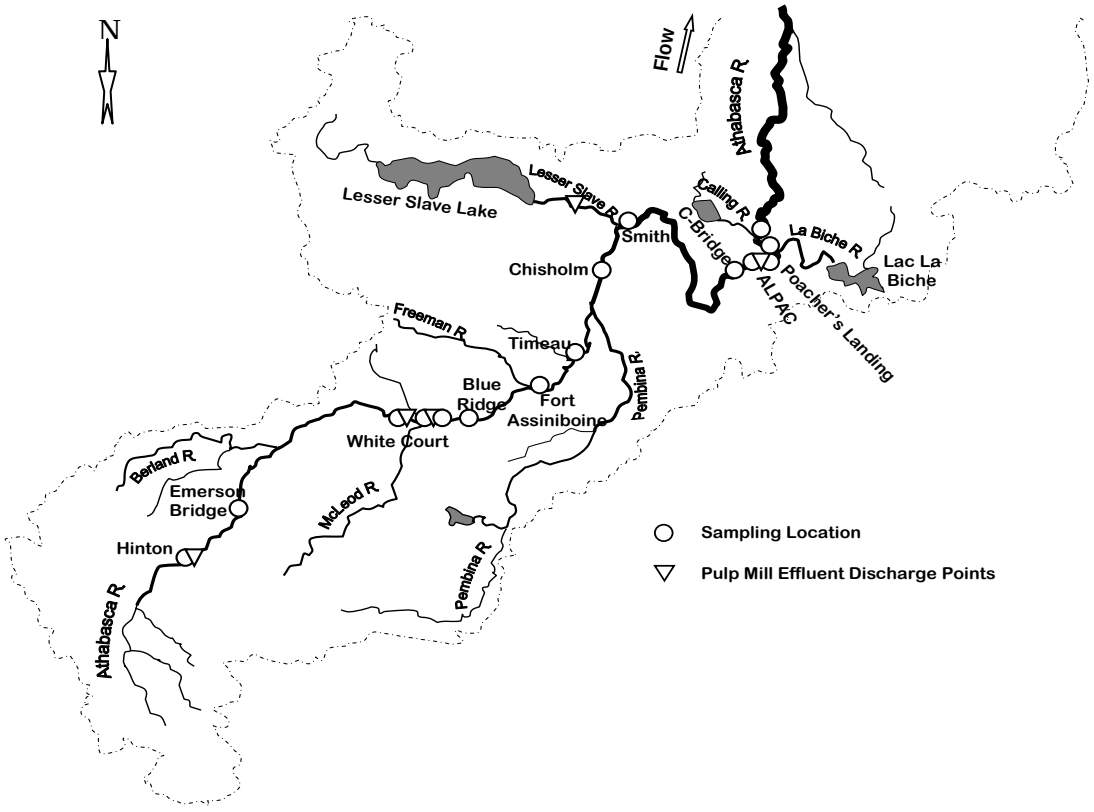

Figure 3.1 Athabasca River basin, 15 sampling sites and five pulp mill locations

3.2 Field Sampling and Research Design

At least two sediment cores and 20 litres of bulk river water were collected at the 15 sites between September 19 and October 16, 2006 (fall); and at 10 sites between February 10 and March 13, 2007 (winter), utilizing 60 cm long (5.72 cm

inner diameter) clear polycarbonate core tubes. In fall 2007, winter 2007 and fall 2008, fewer sites were sampled utilizing a newly developed 34 cm long (6.98 cm diameter) core tube. Because of the inaccessibility to the sediment, sampling was done at fewer sites in other seasons compared to fall 2006.

For the fall sampling, clean cores were pushed at least 10 cm into sediment at river water depths of 50 to 100 cm, depending on the sites. However, at some sites only about a 5 cm depth of sediment could be retrieved. The cores were filled to the top with river water and sealed with a rubber stopper with a compression screw. The core was slowly pulled up, ensuring that sediment stayed inside the core under hydrostatic pressure. Another rubber stopper was inserted at the bottom end of the core. The sediment inside the core was visually observed to estimate its characteristics. Compression screws were tightened carefully to ensure no airspace inside the core. The cores were then kept in ice and wrapped with dark plastic, and placed in wooden racks for transportation to the Environmental Engineering Laboratory at the University of Alberta.

For the winter sampling, the ice cover on the river at each site was drilled with an ice auger to make holes suitable for the core tube moving through and hauling the sediment sample. A number of holes were drilled to obtain a representative sediment sample. The core tube was pushed into the sediment vertically to a depth of at least 10 cm with caution so as not to disturb the sediment surface and structure. In this position, the cylinder was filled with river water and the top of

the core tube was sealed with a rubber stopper. The core tube with a specified depth of sediment sample was moved up slowly without letting the sediment fall by maintaining hydrostatic pressure. While the cylinder was inside the river, its bottom end was sealed with another rubber stopper. Then the sealed core tubes were stacked in a wooden rack covered by dark plastic and transported to the University of Alberta.

The details of site location and sediment characteristics are presented in Table 3.1 for the fall 2006 sampling, and Table 3.2 for the winter 2007 sampling. The sampling for fall 2007, winter 2008 and fall 2008 was done at or proximate to the sites presented in Table 3.1 or Table 3.2.

In the laboratory the cores with sediment and containers with bulk river water were stored in a cold room in the dark. The river water was continuously stirred to maintain O_2 concentration in the container. The SOD determinations commenced the following morning within 24 hours of sample collection. Water in the sediment core was replaced with the bulk river water, which had similarly been kept in the dark at near zero temperatures. A core containing only bulk water served as a control, resulting in two or three sediment cores and one control for each site.

For the fall 2006 and winter 2007 the SOD determinations, the sediment cores and control were equipped with a stirring mechanism consisting of a floating magnetic

Table 3.1 Sampling site locations and characteristics of sediment for the fall 2006

SN	Sampling site	Location	Sampling Date	Sediment Depth in the Core (cm)	Overlying Water Vol. in the Core (L)	Observed Sediment Type
1	U/S of Hinton Pulp (USHP)	N 53^{0}24.135' W 117^{0}36.467'	Oct-12	13.20 - 13.70	1.05 - 1.07	silty detritus on top of sandy layer
2	Emerson Bridge (EBRG)	N 53^{0}41.959' W 117^{0}09.817'	Oct-12	11.40 - 19.70	0.91 - 1.11	fine sediment on top of silty layer
3	U/S of ANC Pulp Mill (UANC)	N 54^{0}10.494' W 115^{0}48.428'	Sep-19	14.73 - 25.75	0.76 - 1.03	fine sediment
4	U/S of McLeod River (USML)	N 54^{0}09.087' W 115^{0}42.550'	Sep-19	16.00 - 17.50	0.96 - 0.99	fine detritus on top of silty layer
5	2 km D/S of Millar Western (DSMW)	N 54^{0}09.574' W 115^{0}40.422'	Sep-22	15.75 - 20.05	0.90 - 1.00	silty sediment on top of sandy layer
6	Blue Ridge (BLRG)	N 54^{0}09.002' W 115^{0}24.789'	Sep-22	15.60 - 18.6	0.93 - 1.01	sandy sediment
7	Fort Assiniboine (FTAS)	N 54^{0}1.699' W 114^{0}22.148'	Oct-03	8.35 - 12.70	1.08 - 1.19	fine sediment on top of silty layer
8	D/S of Timeau River (DSTR)	N 54^{0}30.082' W 114^{0}21.623'	Oct-03	10.10 - 17.75	0.95 - 1.14	silty sediment
9	Chisholm (CHLM)	N 54^{0}54.695' W 114^{0}11.443'	Sep-26	11.03 - 14.15	1.04 - 1.12	silty sediment
10	Smith (SMTH)	N 55^{0}10.233' W 114^{0}02.732'	Sep-26	11.20 - 13.55	1.06 - 1.12	detritus on top of sandy sediment
11	C-Bridge (CBRG)	N 54^{0}56.997' W 112^{0}47.792'	Sep-29	10.40 - 13.25	1.06 - 1.14	fine sediment
12	U/S of ALPAC Intake (USAM)	N 54^{0}58.057' W 112^{0}54.378'	Oct-16	13.55 - 21.6	0.86 - 1.06	very fine detritus on silty layer
13	Poacher's Landing (POLG)	N 54^{0}57.662' W 112^{0}49.674'	Sep-29	20.00 - 21.80	0.85 - 0.90	fine sandy sediment
14	D/S of La Biche River (DSLB)	N 55^{0}01.212' W 112^{0}44.737'	Oct-16	14.00 - 16.25	0.99 - 1.05	fine sediment
15	D/S of Calling River (DSCR)	N 55^{0}05.489' W 112^{0}52.922'	Oct-16	15.00 - 17.70	0.96 - 1.02	fluffy detritus on fine sediment

U/S upstream D/S downstream

bar inside the core cylinder and an inverted stirrer plate at the top of the core cylinder. Stirring speed was held constant below the threshold for sediment resuspension. The sediment cores and control were then incubated in the dark for 24 and 48 hours at 4 ± 1^{o}C. Water column DO concentrations at the start and end of the incubation period were measured by Winkler titration (APHA 1998) to determine the decreased DO concentration in the overlying water column. The

replicate SOD was averaged for each location. For sampling seasons after winter 2007, the SOD determination method was modified, as discussed in 3.3.

Table 3.2 Sampling site locations and characteristics of sediment for winter 2007

SN	Sampling site	Location	Sampling Date	Sediment Depth in the Core (cm)	Overlying Water Vol in the Core (L)	Observed Sediment Type
1	U/S of Hinton Pulp (USHP)	N 53^{0}24.135' W 117^{0}36.467'	Mar-13	7.1 - 9.0	1.20 - 1.25	Fine silty sediment with detritus
2	U/S of McLeod River (USML)	N 54^{0}09.112' W 115^{0}42.568'	Mar-01	15.3 - 19.5	0.90 - 1.03	Fine silty sediment with detritus
3	2 km D/S of Millar Western (DSMW)	N 54^{0}09.574' W 115^{0}40.422	Mar-01	22.0 - 27.5	0.70 - 0.87	Sandy sediment
4	Fort Assiniboine (FTAS)	N 54^{0}19.341' W 114^{0}47.09'	Mar-06	5.3 - 8.2	1.20 - 1.33	Silty sand sediment
5	Smith (SMTH)	N 55^{0}10.233' W 114^{0}02.732'	Feb-27	4.2 - 8.5	1.20 - 1.28	Silty sediment
6	C-Bridge (CBRG)	N 54^{0}56.997' W 112^{0}47.792'	Feb-10	10.0 - 13.4	1.03 - 1.19	Silty sand sediment
7	U/S of ALPAC Intake (USAM)	N 54^{0}58.064' W 112^{0}54.402'	Feb-15	4.7 - 12.1	1.1 - 1.33	Sandy silt sediment on top of fine clay layer
8	Poacher's Landing (POLG)	N 54^{0}57.662' W 112^{0}49.674'	Feb-15	13.5 - 17.0	1.0 - 1.1	Silty sediment
9	D/S of Lac La Biche (DSLB)	N 55^{0}01.212' W 112^{0}44.737'	Feb-10	6.3 - 13.4	1.22 - 1.30	Sandy with clay portion
10	D/S of Calling River (DSCR)	N 55^{0}42.067' W 112^{0}09.963'	Feb-22	8.5 - 18.4	0.9 - 1.23	Orange coloured detritus on top of fine silty sediment

U/S upstream D/S downstream

3.3 SOD Determination in the Athabasca River

3.3.1 Rationale for the Development of Suitable SOD Determination Method

The SOD determination method used in the sampling periods of fall 2006 and winter 2007 was a sediment core method with a mixing mechanism consisting of

a magnetic bar and stirrer plate, as mentioned earlier. This method gave comparable SOD results, but raised some concerns about overlying water mixing and intermittent sampling. The mixing mechanism could not produce uniform and quantifiable water circulation above sediment, because the stirrer cannot control the revolutions of magnetic bars. Since the magnetic bar was revolving at the top surface of the sediment core tube, the rate of mixing near the sediment surface was uncertain. In addition, water analysis was performed only at the start and the end of the incubation period, thus nullifying any intermittent sampling for chemical flux analysis. In view of the above observations and concerns, a suitable and appropriate SOD determination method was deemed necessary after the winter 2007 sampling.

Development of the SOD measurement techniques applicable in the Athabasca River in the winter started in 1989 (Casey and Noton, 1989). The laboratory technique was developed with acrylic cylinders as the sediment core. The top end of the sediment core was filled with paraffin oil to make the system airtight. Water circulation was employed by an external pump, which was connected to two ports positioned slightly above the SWI. Many drawbacks in this system resulted in the need for modifications (Tian, 2005). Tian (2005) used acrylic tubes sealed at both ends with rubber stoppers to determine the SOD. Yu (2006) introduced water circulation in Tian's (2005) sediment core by suspending the magnetic bar wrapped in polyeurathene foam and stirring it with a stirrer plate

placed on the top end of the core in an inverted position. Figure 3.2 shows the Yu (2006) sediment core method and newly developed method.

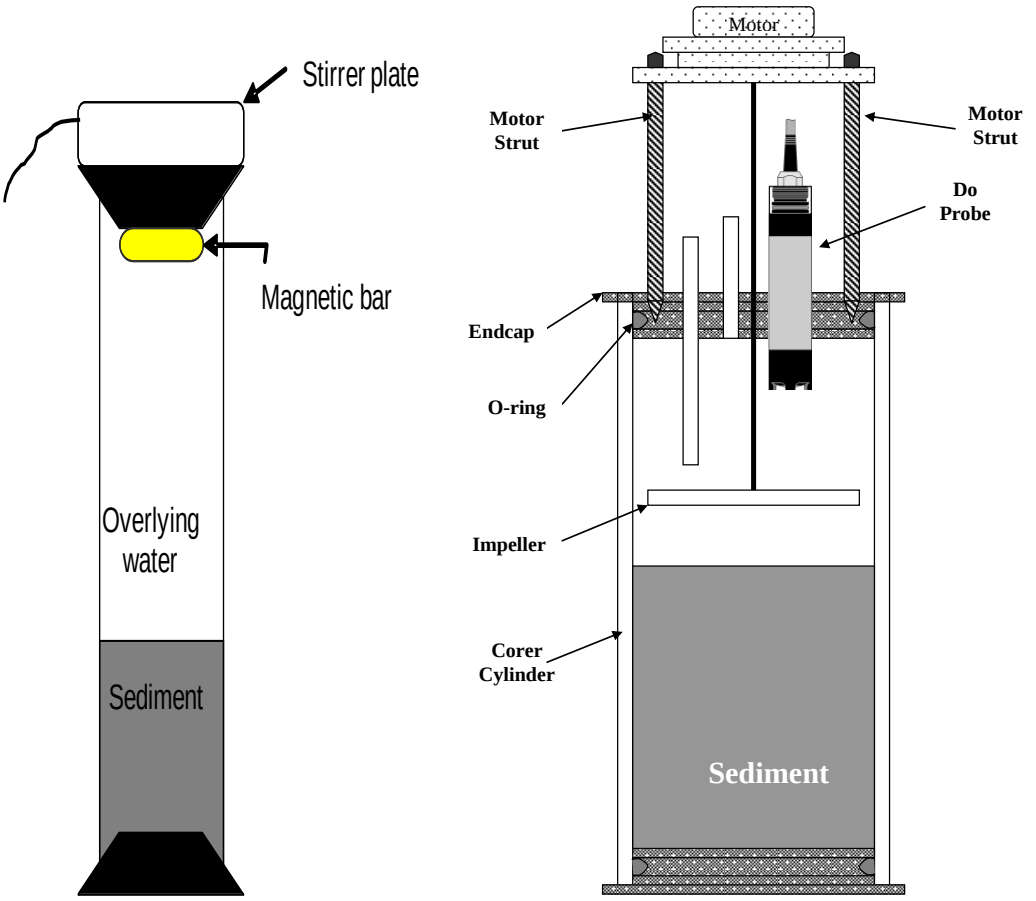

(a) (b)

Figure 3.2 Sediment Core (a) Yu's method, (b) newly developed method

3.3.2 Design Consideration

The depth of the sediment in the sediment core affects the SOD in two ways: (1) the aerobic biological respiration in highly thin layers of sediment (less than 0.5

cm at the surface) affects the SOD (Seiki, 1994), and (2) the reduced chemical substances from the deep layer of sediment when get transferred to the aerobic zone affect the SOD (Truax et al., 1980). Normally researchers have reported that sediment depths greater than 5 cm in sediment cores give reliable SOD results (Lin and Zhu, 2002).

The ratio of the volume of overlying water (V_{olw}) to the surface area of sediment (A_{sed}) at the SWI (V_{olw} / A_{sed}) is important in designing sediment core, since the ratio affects the DO consumption inside the sediment core. The literature shows that for a larger ratio, the measurement time would be too long because of the slow consumption of DO, and that for a smaller ratio the sediment would be resuspended because of the DO supply (Traux et al., 1995). To obtain the suitable DO consumption, overlying water depth in the sediment core is usually maintained at greater than 10 cm.

Increasing the flow velocity of the overlying water exposed to the sediment increases the SOD (Mackenthum and Stefan, 1998). A variety of processes are influenced by the flow velocity, for example: (1) DO gradients enhance mass transfer as tangential velocities increase, as do transfer rates for soluble organics in the water column (Truax, et al., 1995), (2) turbulence may influence biological and chemical reaction rates and/or cause suspension of sediments, resulting in an increased active surface area. Therefore, flow rates for the laboratory and in-situ measurements of SOD must be selected based on the expected velocities to which

sediment will be exposed (Belanger, 1980). In our laboratory, Yu's (2006) introduction of water circulation in the overlying water of the sediment core was unable to quantify the flow velocity rate, since the rate of stirring was uncertain. Therefore we used a timing motor (A.C. Synchronizing Timing Motor, 600 series, manufactured by Hansen Co.) with a speed rate of 20 rpm, which corresponded to the average flow velocity of the Athabasca River bed (Noton, 1996).

Sediment cores, used in a laboratory, are batch type respirometers in which sediment and overlying water are incubated for a certain duration to monitor the DO decline. While designing the sediment cores, physical factors considered are: (1) air tightness, (2) depth of sediment, (3) volume of overlying water, (4) shape and size of the sediment core to determine the ratio of volume to surface area, (5) a water circulation mechanism to mimic the natural benthic condition, (6) the DO recording interval, (7) ease of water sampling, and (8) a provision to replace the water inside the sediment core.

The process for developing and testing of new SOD measurement apparatus included the following steps: (1) selection of sediment core material, (2) determining shape and size of the sediment core by taking into account of field sampling, maintaining suitable ratio of volume to area, and housing facilities for intermittent sampling and DO monitoring, (3) selection of DO probe and its integration with sediment core, (4) determining water circulation in the sediment

core and developing mixing mechanism, assembling DO probe, sampling ports and mixing mechanism on an endcap, and (5) air and water tightness testing.

Researchers have developed numerous sediment cores suitable to a particular research site. Since the experiment in our laboratory is to be conducted at near zero temperatures, applicable to frozen rivers, the methods developed in other places have to be modified. Table 3.3 presents some of the different types of SOD determination techniques used in laboratories around the world. The majority of labs use cylindrical cores as the SOD measurement chambers. There is a great variation in mixing mechanisms in the sediment cores: some use pump recirculation, some use jets, some use magnetic pumps and some have no mixing at all. The techniques are limited to the SOD determination only. Therefore, modification is necessary to include nutrient flux determination along with the SOD determination.

In this research, sediment depth was chosen as 15 cm. The ratio (V_{olw} / A_{sed}) was 145 L/m^2, within a recommended range of 100 - 300 L/m^2 (Murphy and Hicks, 1986). The depth of overlying water in the modified sediment core in this research was 16 cm. The water mixing was performed by an impeller attached to the AC synchronous motor. It has, sometimes, been pointed out that the shaft and impeller's stirring mechanism might introduce some artifacts by allowing oxygen to enter the core. Before the experiment, the sediment core and mixing mechanism in this study were subject to pressure and leakage tests. The hole on the top

Table 3.3 Type of laboratory SOD determination systems

Chamber				Arrangement	Depth (mm)		Vol. to Area Ratio (L/m^2)	Source Water	Mixing Mechanism	Mixing Speed	DO Measured	Flux Determined	Investigators
Type	Shape	Size (mm)	Material		Overlying Water	Sediment							
batch reactor	cylindrical	171 ø, H - 182	plexiglass	external chamber for DO measurement	132	50	132	Synthetic water for BOD test	pump recirculation	110-120 L/min	DO Probe	O_2	Bowman and Delfino (1980)
sediment core	cylindrical	38.1 ø, H - 508	plexiglass	undistrubed sediment cores	408	100	329	filtered lake water	NA	NA	DO Probe	O_2	Belanger (1981)
sediment core	circular chamber	core: 50 ø, H-127 chamber: 254 ø, H - 203.2	lexan	4 sediment cores in series inside a chamber	76.2	127	373	water ways	pump recirculation	0.24 L/min	DO Probe	O_2	Traux et al (1995)
sediment core	rectangular chamber	L - 158, W - 87, H - 340	plexiglass	sampling ports on the top end cap of core	127-144	196-213	127-144	bay water	stirring rod	variable	DO Probe	O_2, nutrients	Cowan and Boynton (1996)
flow through	rectangular chamber	Vol. - 2.9 L, Area - 71.6 cm^2	plexiglass	Sediment at the bottom of the chamber	40.6	50	41	river water	pump recirculation		DO Probe	O_2	Chen et al (2000)
sediment core	cylindrical	150 ø, H - 500	perspex	incubated in thermo regulated cabinet at *in situ* temperature	200	300	200	coastal water	floating magnet	variable	DO Probe, microsensor	O_2	Rabuli et al (2003)
SOD chamber	cylindrical	144 ø, H - 200	perspex	homiginized sample sediment	100	100	100	synthetic water	jet inflows	variable	DO Probe, microsensor	O_2	Areaga and Lee (2005)
sediment core	cylindrical	57.2 ø, H - 600	lexan	undistrubed sediment cores incubated at room temp	450-550	50-150	450-550	river water	NA	NA	Winkler Method	O_2	Tian (2005)
sediment core	cylindrical	57.2 ø, H - 600	lexan	undistrubed sediment cores incubated at room temp	450-550	50-150	450-550	river water	floating magnet	variable	Winkler Method	O_2	Yu (2006)
sediment core	cylindrical	69.8 ø, H - 340	lexan	sampling ports on the top end cap of core	160	150	145	river water	stirring impeller	21 rpm	DO Probe	O_2, nutrients	This Study

ø - diameter, L - length, W - width, H - height
NA - Not applicable

endcap that provided passage for the shaft was sealed with vacuum grease, which only allowed the impeller shaft to rotate. The leakage test confirmed that the vacuum grease was able to provide a complete seal for any gas exchange within the test period. In the pressure test, the core system was subject to the elevated pressure of one bar. No leakage was observed from the shaft hole, sampling ports, or the hole for DO probe. Both tests were conducted to evaluate any changes in the DO concentration inside the sealed core for 96 hours.

In summary, the key features of the newly developed sediment core method are: increased inner diameter of the core tube (6.98 cm) to provide space for the DO probe and sampling ports, reduced length (34 cm) for better handling and mixing, a quantifiable mixing mechanism, and intermittent sampling facility for chemical flux analysis.

3.3.3 Laboratory Nutrient Flux Determination

In the laboratory, sediment samples collected in field cores were transferred to incubation sediment cores (id: 69.86 mm, length: 340 mm). Great precaution was taken not to disturb the SWI while the sediment was being transferred. Three sediment cores with sediment and a core without sediment but with river water, which served as a control core, were incubated in the dark in a thermo-regulated refrigerator ($3 \pm 1^{o}C$). Just prior to beginning the flux measurements, the overlying water in each core was completely replaced with ambient river water to insure that

water quality conditions closely resembled *in situ* conditions. Cores were carefully sealed to exclude any air bubbles and gently stirred with an impeller connected to a motor attached to the top endcap of the sediment core. The motor speed was 20 rpm. Each core was linked by silicon tubing to a 4-litre reserve tank, which was filled with river water. River water in the reserve tank was continuously stirred with the help of stirrer bars to prevent any stratification of oxygen in the tank. Figure 3.3 shows the detail of incubation sediment core setup.

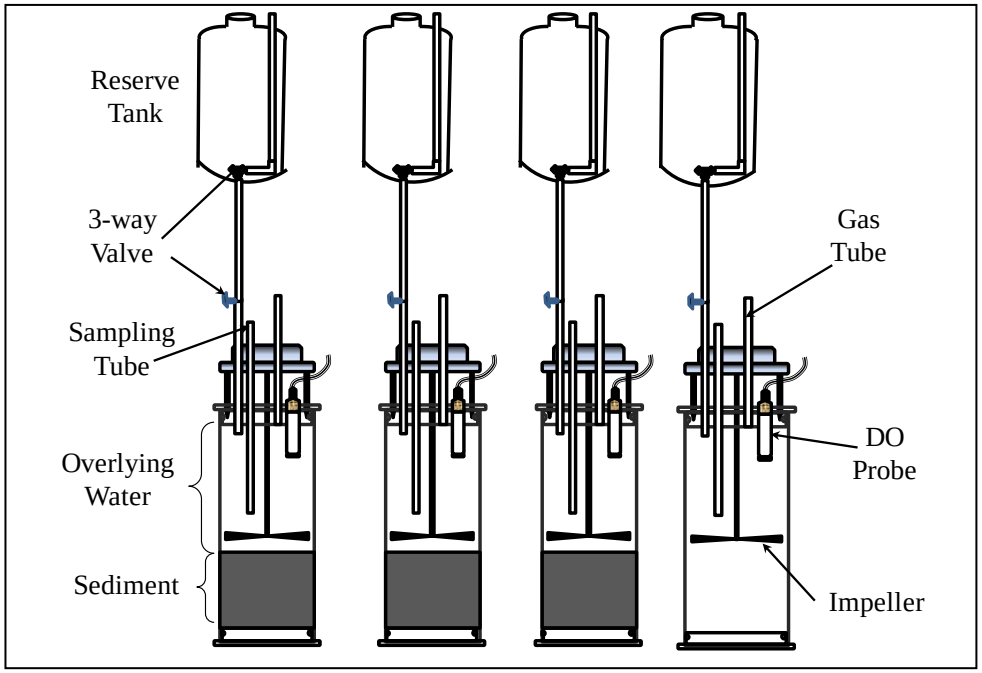

Figure 3.3 Incubation sediment core setup inside thermo-regulated refrigerator

Sampling was done through the sampling tubing in each core and reserve tank, and the volume of overlying water removed from each core was replaced with river water from each reserve tank. In this modified setup, removal and

replacement of water were performed simultaneously by gravity flow. But to avoid contamination, the water in the core was replaced after it was removed from the cores by opening and closing the gas tubing, which also controlled the pressure created by the static head inside the sediment cores. Incubation lasted for 48 hours, during which five water samplings at 12-hour interval were performed. A DO probe (Hach's Intelical LDO) recorded the dissolved oxygen every 15 minutes. The water samples withdrawn from reserve thank and sediment core were analyzed for the concentration of NH_4^+, NO_x^- (NO_2^-+NO_3^-), PO_4^{3-}, and SO_4^{2-}. The change in concentrations of these compounds over the incubation period was used to calculate the flux. The volume correction for the concentration of replacement water was applied in the flux determination. At the end of the incubation period, each core was sliced at 2 cm depth for a porosity profile measurement and granulometric or elemental analysis.

3.4 Porewater Extraction

A centrifuge was used to extract porewater from each 2 cm slice of sediment of fresh duplicate sediment cores. Sectioned 2 cm slices from triplicate sediment cores were combined to extract one sample of porewater for one layer. Aliquots from each sediment section were transferred into polycarbonate centrifuge tubes and tightly closed. The tubes with samples were centrifuged at 10,000 rpm for 20 minutes (Adams, 1994). After centrifugation, supernatant porewater was collected into plastic syringes and passed through 0.02 μm milipore filters.

Sufficient precautions were taken to ensure that the sediment and porewater samples were not exposed to air. The filtered porewater samples were immediately analyzed or acidified and stored at $4^{o}C$ for later analysis (Eaton et al., 2005) of NH_4^+ and NO_x^- concentration.

3.5 Water Analysis

River water collected at each site was analyzed for TOC, BOD_5, TSS, NH_4^+, NO_x^-, TDP, chlorophyll-a, total iron (Fe), and alkalinity. The TIN was the sum of ammonium and nitrite+nitrate. Field DO, temperature, and conductivity were recorded at each site with a polarographic oxygen probe (YSI model 85), while pH was measured in the laboratory with a pH meter (YSI model 65). The river water characteristics presented here are from single grab samples.

TOC was analyzed by a Shimadzu TOC-5000A carbon analyzer. Phosphorus (TDP) and nitrogen (NH_4^+ and NO_x^-) were analyzed by colorimetry with a Lachat 8500 FIA analyzer following Standard Methods (Eaton et al., 2005). TDP samples were filtered through a pre-washed 0.70 μm Millipore filter. Samples for NH_4^+ and NO_x^- analysis were treated with sulfuric acid and stored at $4^{o}C$ temperature for analysis within 14 days after sampling (Eaton et al., 2005). Iron (Fe) was analyzed by an atomic absorption of samples. Chlorophyll-a was analyzed by a spectroflouoro-photometer. All of the above parameters were analyzed at the Biogeochemcal Analytical Laboratory, Department of Science at the University of

Alberta. BOD_5 was determined after 5 days of sample incubation using a polarographic DO meter for DO measurement at Maxxam Analytics Inc., Edmonton.

3.6 Sediment Properties

The water content in the sediment was determined by the loss of weight in the sediment after drying at 105^{o}C, while the loss of weight in the sediment after drying at 375^{o}C for 6h gave the organic matter (OM) content in the sediment. Porosity was determined by dry bulk density and particle density (Percival and Lindsay, 1996). A particle density of 2.65 of quartz was used to determine porosity. The particle size composition or granulometry was determined by utilizing a hydrometer (ASTM, 1994). The total carbon (TC), TOC, and total nitrogen (TN) in sediment aliquots were determined by dry combustion using a Costech 4010 Elemental Analyzer. The granulometry, TC, and TN of the sediment aliquots were analyzed at the Natural Resources Analytical Laboratory, Department of Renewable Resources, while porosity was determined at the Environmental Engineering Laboratory, Department of Civil and Environmental Engineering at the University of Alberta.

A vertical profile of the sediment (physical or chemical) helps in determining the carbon and nutrient dynamics inside the sediment. The 10 cm deep sediment sample was divided in 2 cm deep slices. However, to determine the relationship

between sediment properties and fluxes at the riverbed surface, only the topmost 2 cm slice of sediment was taken into account. This portion of sediment is considered the "active layer," because oxygen diffusion can be observed at few millimetres deep from SWI (Revsbech et al., 2006). In addition, ammonia oxidation and other aerobic microbial processes occur at this layer. Therefore, in order to develop a relationship among measured and calculated parameters, the value of the top 2 cm is taken into account.

3.7 SOD Calculation

Oxygen flux (J_o), is, theoretically, calculated by using (Reimer et al., 2001):

$$J_0 = m\frac{V_{OLW}}{A_{core}} \tag{3.1}$$

where m = $\Delta C/\Delta t$, the change in DO concentration per unit time, V_{OLW} is the volume of overlying water enclosed within the core, and A_{core} is the surface area of the SWI. The clay/sand composition of the sediment cores made it reasonable to apply a smooth surface area, and the SOD (g/m^2 d), in this research, was calculated by (Murphy and Hicks 1986):

$$SOD = \frac{V_{OLW}}{A_{core}}(O_S - O_W) = h(O_S - O_W) \tag{3.2}$$

where, O_s and O_w are the changes in oxygen concentrations (g/m^3) in the sediment core and control core per unit incubation time (d^{-1}) respectively, and *h* is the height of overlying water (m). For reporting purposes the SOD values were transformed to a standard temperature (20^oC) using the following formula:

$$SOD_T = SOD_{20}\psi^{T-20} \tag{3.3}$$

where, SOD_{20} is the SOD value normalized to 20^oC, SOD_T is the SOD at incubation temperature, T is the incubation temperature in ^oC, and ψ is the temperature correction coefficient. A ψ value of 1.04 was used in this study. The value is at the lower end of the range from 1.04 to 1.13 (Whittemore, 1986) due to reduced microbial activity and biochemical reactions at a lower temperature (Stefan, 1992). For compatibility purpose the SOD measured at 3 ± 1^oC were normalized to the SOD at 4 ± 1^oC using above relationship, whenever deemed necessary.

The pollutant loads in the Athabasca River were calculated as the product of constituent concentration and the river flow on the sampling date. Sampling day river flow data were obtained from the Water Survey data warehouse of Environment Canada. The incremental flow of the Athabasca River between hydrometric stations was calculated incorporating flow discharges from tributaries, pulp mills, and municipal effluents.

3.8 Nutrient Flux Calculation

The oxygen and nutrient fluxes were estimated for each core by calculating the mean rate change in concentration during the incubation period using regression analysis (Cowan and Boynton, 1996). Non-significant regressions ($p>0.05$) based on changes over time that were less than the analytical variability were interpreted as zero fluxes. For this study, analytical variability was defined as 2 standard deviations away from the mean of a standard solution within the range of the samples. The control core rate of change was then subtracted from the sediment core rate of change; this volumetric rate of change was then converted to a flux using each core's volume:surface-area-ratio. In spite of the low sampling volume with respect to the overlying water volume, the correction for water replacement (with river water from the reserve tank) was systematically applied (Denis and Grenz, 2003) as the subsequent error sometimes reached up to 28 % for the flux.

3.9 Statistical Analysis

For statistical analysis, the values below the detection limit were assigned to the detection limit. All statistical analyses were performed with SPSS Version 16.0 (2007). All water quality data and the SOD was also normalized by weighted normalization (Bowen, 2006; Mazumdar, 1996):

$$\text{Normalized value of 'i' variable, } N_i = \frac{Variable_i - Variable_{i_{min}}}{Variable_{i_{max}} - Variable_{i_{min}}} \qquad (3.4)$$

where, $Variable_{imin}$ and $Variable_{imax}$ are the minimum and maximum values of variable 'i', respectively.

The normalized data were analyzed by bivariate correlation (Pearson correlation, r) to examine the direction and the degree of association among all variables. A principal component analysis (PCA) (factor analysis) was used to examine the primary drivers for the SOD. Factor scores generated in the PCA were regressed against the normalized the SOD.

3.10 Microsensors Measurement of Ammonium Oxidation

3.10.1 Sediment Incubation on Short Sediment Core

In the laboratory, the sediment was transferred from the field sediment collection cores to the incubation sediment cores (same inner diameter but 100 mm long) using sediment extruder (supplied by Aquatic Research Instruments, ID, USA). Once the sediment, including the fluffy top layer, was transported to the incubation core, the end cap at the bottom of the incubating sediment core was inserted. The sediment core was placed in a 2 L beaker and 1.5 L of river water was poured into the beaker so that about 5 cm of overlying water could be

obtained above the sediment core's top surface. Air was continuously sparged inside the beaker through diffuser stones to facilitate water movement on the sediment surface and to prevent dissolved oxygen stratification in overlying water.

Three sediment cores were incubated for more than two months by spiking the overlying water with nutrients and carbon. The control core was the sediment core that contained only river water with concentrations of NH_4^+ and NO_3^- of 200 μg/L and 300 μg/L, respectively, slightly higher than the historical highest concentrations in the Athabasca River. The reason for increasing the nutrient concentrations in the river water was to effectively obtain the microsensor signals at near zero temperature. Because, at a low temperature the microsensor's performance for its ion selectivity could be affected at a significantly low concentrations of the ions of interest. Other two cores were each spiked with 3 mg/L of NH_4^+, and a combination of 3 mg/L of NH_4^+ and 4 mg/L of TOC, respectively. Table 3.4 presents the nutrient addition strategy. Starch was used as particulate organic carbon source.

3.10.2 Experimental Setup for Microsensor Measurement

The control and nutrient spiked sediment cores, incubated in the temperature-controlled refrigerator, were subjected to the microsensor measurement of concentration profiles along the depth of sediment. Before the microsensor

Table 3.4 Nitrogen and Particulate Organic Carbon Addition in Overlying Water of the Incubation Cores

Spiked Chemicals	Concentration (μg/L)		
	Core 1 Control	Core 2 NH_4^+ Spiked	Core 3 NH_4^+ + TOC Spiked
NH_4^+	200	3000	3000
NO_3^-	300	300	300
NO_2^-	25	25	25
TOC	0	0	4000

measurement started, the top end of the incubating sediment core was inserted into the core receiving hole of a flow cell assembly, as shown in Figure 3.4. Double o-rings were used to prevent any leakage along the sediment core wall. It should be noted here that the top end of the sediment core is level with the bottom of the flow cell. In this way, the top surface of sediment could be levelled with the bottom of the flow cell to avoid scouring of the sediment due to flow.

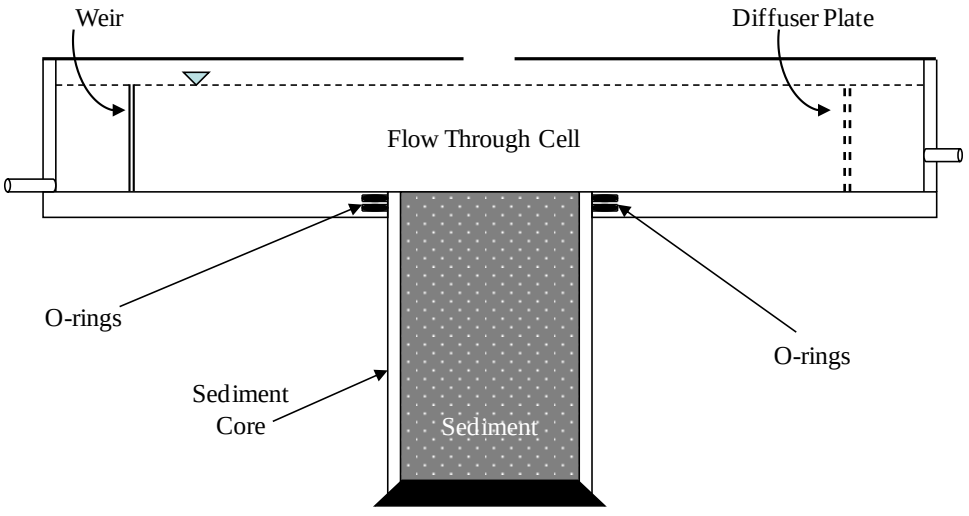

Figure 3.4 Sediment core and flow through cell assembly

The flow cell (300 mm length, 93.5 mm width and 40 mm depth) was made from an acrylic and glass sheet. The viewing side plate and top cover plate were glass sheets. The bottom plate of the flow cell consisted of a hole (63.5 mm diameter) that received the sediment core. The top cover also had a hole (50 mm diameter) for the microsensor movement. The inlet pipe of flow cell was designed to carry flow for a maximum flow velocity of 10 cm/s and, accordingly, a pump was selected. A flow diffuser, 93.5 mm wide and 30 mm deep (with opening area ratio of 11.9%) was equipped to distribute the flow uniformly in the flow cell. The outlet was designed to carry the flow under the gravity. A weir (93.5 mm wide and 30 mm deep acrylic plate) was used to maintain the water level of 30 mm inside the flow cell. Figure 3.5 presents the complete experimental set-up of flow-through cell assembly for this purpose.

Since the experiment was to be done at $3 \pm 1^{o}C$, the sediment core and flow-through cell assembly had to be maintained at this temperature. In order to maintain the desired temperature surrounding the sediment core, an ice bath tank was fitted underneath the flow-through cell, as shown. The sediment core sat on the ice bath tank. Spacers were used to increase height of the sediment, if necessary. The ice bath tank was filled with refrigerated water recirculated with the help of pumps. From time to time, ice cubes were introduced inside the ice bath tank to maintain the temperature. The flow-through cell and ice bath tank were housed inside a sealed styrofoam box for insulation that minimized heat gain

from the surroundings. A thermometer was used to monitor the temperature in the ice bath as well as the water in the flow-through cell.

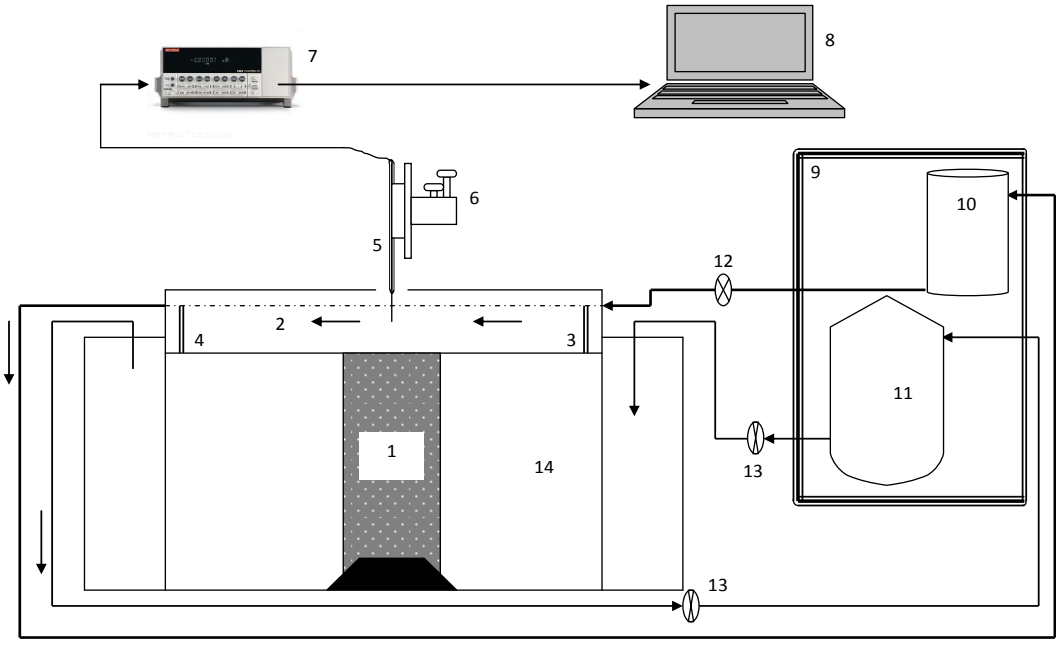

(1) Sediment core (2) Flow cell (3) Flow diffuser (4) Wier (5) Microsensor (6) Micromanipulator (7) Electrochemical Analyzer (8) Computer (9) Thermo-regulated refrigerator (10) River water reservoir (11) Tap water reservoir (12) River water recirculation pump (13) Tap water recirculation pump (14) Ice bath

Figure 3.5 Experimental set up for microseonsor measurement

During the microsensor measurement, river water flowed through insulated tygon tubing from the river water reservoir inside the refrigerator to the flow cell and back to the reservoir with the help of peristaltic pumps. In the same manner, cold water from a tap water reservoir inside the refrigerator flowed through tygon tubing to ice bath tank and back to the water reservoir. The flow rate of 1.4 L/min was maintained in the flow-through cell, which corresponded to a flow velocity of 0.83 cm/s, representing the Athabasca River flow near the bottom. The

microsensor measurements were performed inside a Faraday Cage to block external electrostatic discharges. The oxygen microsensor measurement was performed at stagnant and flowing water conditions. At stagnant water condition, O_2 microsensor measurement was performed by exposing the sediment to dark and illuminated condition. The O_2 Microsensor measurement was performed in the dark during flowing water condition. However, the measurement for other microsensors such as NH_4^+, NO_3^-, and pH ISmEs was performed only at stagnant water conditions because the vibration created by the pumps introduced noise to the electrical signals, making the ISmE microsensor unstable. Therefore the concentration profiles of chemicals obtained by ISmEs were only under stagnant water conditions.

3.10.3 Microsensors Measurement and Data Interpretation

For the concentration profile measurements of O_2, NH_4^+, NO_3^-, and pH, each of the calibrated microsensors (as per Chapter 6) was mounted on a micromanipulator. Cathodic and anodic ends were connected to an electroanalyzer. The electroanalyzer was connected to a computer via a signal-to-electrical current or volt converter. The micromanipulator can achieve movement up to 10 mm of depth, thus limiting its use to this depth. The microsensor's tip was placed inside the overlying water for at least 30 minutes to stabilize the current or potential reading. This step is necessary because the microsensors have a tendency to experience a signal shift due to exposure to different temperatures

and concentrations. Each profile of O_2, NH_4^+, NO_3^-, and pH was taken on the same day to minimize the time-lapse effect.

The microsensor tip was moved downward in a step of 100 μm within sediment. Wherever possible, the electroanalyzer's signal readings were also recorded for overlying water. To identify the SWI, either of the following approaches was adapted: (1) the microscope was used to locate the SWI, or (2) the microsensor was slightly tapped to see the movement of sand particles, which helped to locate the SWI. The profiling of concentrations by all microsensors inside sediment was continued up to the depth where the oxygen concentration became zero. As mentioned earlier, the micromanipulator movement is also restricted to 10 mm. With these limitations, only the ammonium oxidation or nitrification activities were estimated from concentration profiles; and the denitrification activities, which were supposed to be occurring in the sediment section with no oxygen, could not be estimated.

Dark and Illuminated Cycle

Although the sediment core was incubated in the dark, the microsensor measurement was conducted both in the dark and under illuminated conditions. The illumination was achieved with a halogen tube source with a light intensity of 100 lux in a 12-h/12-h light-dark cycle.

Estimation of Consumption and Production Profiles or Activity Profiles

Net metabolic rates of production and consumption of oxygen, ammonium, and nitrate were calculated from the curvature of the concentration profiles (Lorenzen et al., 1998). As the basis for the calculation of net consumption and production rates of O_2, NH_4^+, and NO_3^- from the measured profiles, we used Fick's second law of diffusion including a production and a consumption term (Revsbech et al., 1981):

$$\frac{\partial C_{(z,t)}}{\partial t} = -D_e \frac{\partial^2 C_{(z,t)}}{\partial z^2} - R_{(z)} + P_{(z)} \qquad (3.5)$$

where, $C_{(z,t)}$ is the concentration at time t and depth z, D_e is the effective diffusion coefficient in sediment, R is the respiration rate, and P is the production rate. Assuming the steady state we have, $\partial C_{(z,t)} / \partial t = 0$ and Eq. 3.4 can be reduced to:

$$-D_e \frac{\partial^2 C_{(z,t)}}{\partial z^2} = R_{(z)} - P_{(z)} \qquad (3.6)$$

Equation (3.6) is the fundamental theory behind estimating activity or metabolic rates. For a practical application of Equation (3.6), we have to apply a discrete version of Fick's laws of diffusion. The flux in porous media using Fick's first law (Crank, 1983) is:

$$J = -\varphi \cdot D_s \cdot \frac{\partial C_{(z)}}{\partial z} \qquad (3.7)$$

where, J is the flux, φ is the porosity of the substrate, D_s is the diffusion coefficient in fresh water, and $\partial C/\partial z$ is the inclination of the concentration profile. The fluxes of O_2, NH_4^+, and NO_3^- at a certain depth (z) are thus calculated from the first derivative of the concentration profile. The production or consumption of O_2, NH_4^+, and NO_3^- will result in a change in flux with depth. Activity profiles showing O_2, NH_4^+, and NO_3^- consumption or production rates, in this research, were therefore calculated from the first derivative of the flux profile, which corresponds to the second derivative of the concentration profile. The concentration profiles were analysed mathematically by means of a discrete version of Fick's first law (Meyer et al., 2001):

$$J_{(z+\frac{1}{2}\Delta z)} = -D_{e(z+\frac{1}{2}\Delta z)} \frac{[C_{(z+\Delta z)}] - C_z}{\Delta z} \qquad (3.8)$$

where, $J_{(z+1/2\Delta z)}$ is the flux at the depth between 2 data points, $D_{e(z+1/2\Delta z)}$ is the effective diffusion coefficient in the sediment (= $\varphi \cdot D_s$, as given in equation 3.6) at the same depth, C is the concentration and Δz is the distance between the 2 data points, and D_s is the diffusion coefficient of the ion of interest in fresh water which needed to be corrected for temperature (Li and Gregory, 1974; Broecker

and Peng, 1974). The flux profile was then used to calculate the activity profile by determining the first derivative (Meyer et al., 2003):

$$R_{(z)} - P_{(z)} = \frac{\left[J_{(z-\frac{1}{2}\Delta z)} - J_{(z+\frac{1}{2}\Delta z)} \right]}{2\Delta z} \qquad (3.9)$$

where, $R_{(z)}$ - $P_{(z)}$ is the consumption or production rate at depth z, $J_{(z+1/2\Delta z)}$ and $J_{(z-1/2\Delta z)}$ are the fluxes $1/2\Delta z$ above and below depth z, and Δz is the distance between the data points. This calculation uses a total of 3 data points on the concentration profile for calculating the activity ($C_{(z)}$, $C_{(z+\Delta z)}$, and $C_{(z-\Delta z)}$). Hence, the activity is calculated as the average change in flux over 2 depth intervals ($2\Delta z$).

Differentiation of the raw data in a concentration profile often leads to a very noisy activity profile due to small variations in the data points. To increase the signal-to-noise ratio, an increasing number of data points (i.e. consecutive readings at equally spaced depths) was used to calculate the depth-specific activity. Most of the activity profiles in this study were based on 5 data points (i.e. 2 readings above and 2 readings below the depth for which the activity was calculated). This resulted in smoothening of the activity profile, because the depth-specific activity was calculated as the average change in flux over the

distance from 2*Δz* above and below depth *z*. Therefore, the formula for activity calculation based on 5 data points is as follows:

$$R_{(z)} - P_{(z)} = \frac{\left[J_{(z-1\frac{1}{2}\Delta z)} + J_{(z-\frac{1}{2}\Delta z)} - J_{(z+\frac{1}{2}\Delta z)} - J_{(z+1\frac{1}{2}\Delta z)} \right]}{4\Delta z} \qquad (3.10)$$

The diffusion coefficients of O_2, NH_4^+, and NO_3^- in fresh water were corrected for temperature. The temperature-corrected diffusion coefficient (D_s) for oxygen is 1.28 x 10^{-5} cm^2/s (Broecker and Peng, 1974), while temperature-corrected D_s for NH_4^+ and NO_3^- are 1.097 x 10^{-5} cm^2/s and 1.085 x 10^{-5} cm^2/s, respectively (Li and Gregory, 1974). The average porosity of 0.653 for the top 2 cm of the sediment was used to find the metabolic activities.

Chapter 4

IMPACT OF SEDIMENT PROPERTIES AND NUTRIENT FLUX ON SEDIMENT OXYGEN DEMAND (SOD) OF THE ATHABASCA RIVER

4.1 Introduction

This chapter summarizes research on the relationship between the SOD and sediment characteristics. Specifically, it examines the relationship between sediment porosity and SOD within the context of spatial variability of the SOD along the Athabasca River.

Depletion in the DO concentration in the Athabasca River is observed every winter. In some years concentrations decline to levels that may be harmful to aquatic biota (Chambers et al., 2006; NREI, 2004). This phenomenon is generally attributed to a lack of reaeration due to the ice cover, inputs of oxygen-depleted groundwater, and oxidation of organic material. There has not been a complete understanding of the factors that control DO in the Athabasca River because several water quality models used to make regulatory decisions were unable to predict the DO in the river during extreme years (Tian, 2005). These past models focused on organic matter and nutrients discharged from the pulp mills as the primary components consuming DO in the river. The potential role of the SOD was recognized, but thought to be small and was not included in past models or

was under-represented. The inability of the models to predict low DO suggested the SOD may be more important than previously thought. Improved effluent treatment processes adopted by pulp mills substantially reduced carbonaceous BOD but often increased nutrient load (NREI, 2004) due to the activated sludge treatment processes. We hypothesized that the SOD plays a major role in DO consumption under ice, and that the nutrient load may increase the SOD compared to historic conditions.

SOD along the Athabasca River were investigated in previous studies (Noton, 1996; Moneco, 1993; Casey, 1990) using closed chambers. The SOD showed variability among locations and within a location at different times, ranging from 0.01 g/m^2 d to 0.59 g/m^2 d. The SOD did not show any longitudinal trend along the Athabasca River. Tian (2005) and Yu (2006) investigated three methods for estimating the SOD and found that mixing inside the sediment chamber was important. Yu (2006) investigated the impact of organic carbon and nutrients on the SOD and found that nutrients in the presence of labial carbon stimulated the SOD. Given this background, water quality management in northern Alberta Rivers required further development of processes and concepts captured in existing models to enhance the understanding of factors that control spatial variability and the role of nutrient loads on the SOD.

The effect of sediment properties on benthic oxygen demand have been largely studied in ocean floors, eutrophied lakes, estuaries, and fresh water systems. The sediment properties in lakes and estuaries are different compared to those in a riverbed, as deposition and compaction are continuous phenomena in non-flowing water bodies (Berner, 1980). The sediment properties regulate the SOD, such that in fine grained sediment the advective transport is negligible and molecular diffusion dominates solute transport (Huettel and Webster, 2001), giving rise to higher oxygen demand.

In studying the granulometry of sediment, soil classification with a percentage of clay, silt, and sand is taken into account. However, a combination of clay and silt content, which has the size less than 50 μm, is normally used for fine sediment and the grain size greater than 50 μm is used for coarse (or sandy) sediment (Doyle and Lynch, 2005). In this research we used fine and coarse sediment as per the convention unless otherwise stated.

4.2 Sediment Oxygen Demand in the Athabasca River

The SOD in the Athabasca River was measured in the fall and winter season from fall 2006 until fall 2008. The sampling locations were chosen based on accessibility to the site, availability of sediment, and discharge points (either point or non-point source). Sampling of sediment in 15 sites was possible in fall 2006, and 10 sites the following winter, 2007. Sampling in subsequent seasons, was

possible at a few sites. The sampling of sediment at different seasons and years was done at the same location, so that we could observe the temporal variations. Figure 4.1 presents the longitudinal pattern of mean SOD along the Athabasca River sediment in fall 2006, 2007, and 2008. Figure 4.2 presents the same in winter 2007 and 2008. In fall 2006, the mean SOD ranged from 0.09 g/m^2•d at BLRG to 0.71 g/m^2•d at DSCR (at 4±1^oC). The following fall, the mean SOD ranged from 0.00 g/m^2•d at SMTH to 0.48 g/m^2•d at DSCR. In fall 2008, the mean SOD ranged from 0.04 g/m^2•d at SMTH to 0.32 g/m^2•d at DSCR.

In general, the SOD values at downstream sites of the river were higher than upstream sites of the Athabasca River (Figure 4.1). The highest SOD was observed at the DSCR site during the fall in the sampled years. The SMTH site had lowest mean SOD in fall 2007 and fall 2008. The SOD in fall 2007 and 2008 were lower than the SOD in fall 2006 in most of the sites. The reason for this yearly variation in the SOD could be due to a change in the Athabasca River's flow pattern. Taking the river discharge reported by Environment Canada for the Athabasca Town weather monitoring station, mean monthly river flow averaged over the period of April to October for 2006 was 12567 m^3/s much less than the river flow of 20796 m^3/s and 16159 m^3/s in the same period in 2007 and 2008, respectively. The trend shows that smaller SOD was observed when river velocity was higher. As the river flow increases, the dilution is more pronounced, thus flushing the pollutants away. But at low river flow, the pollutant concentration is higher due to point-source discharges in the river, which enhance the way the

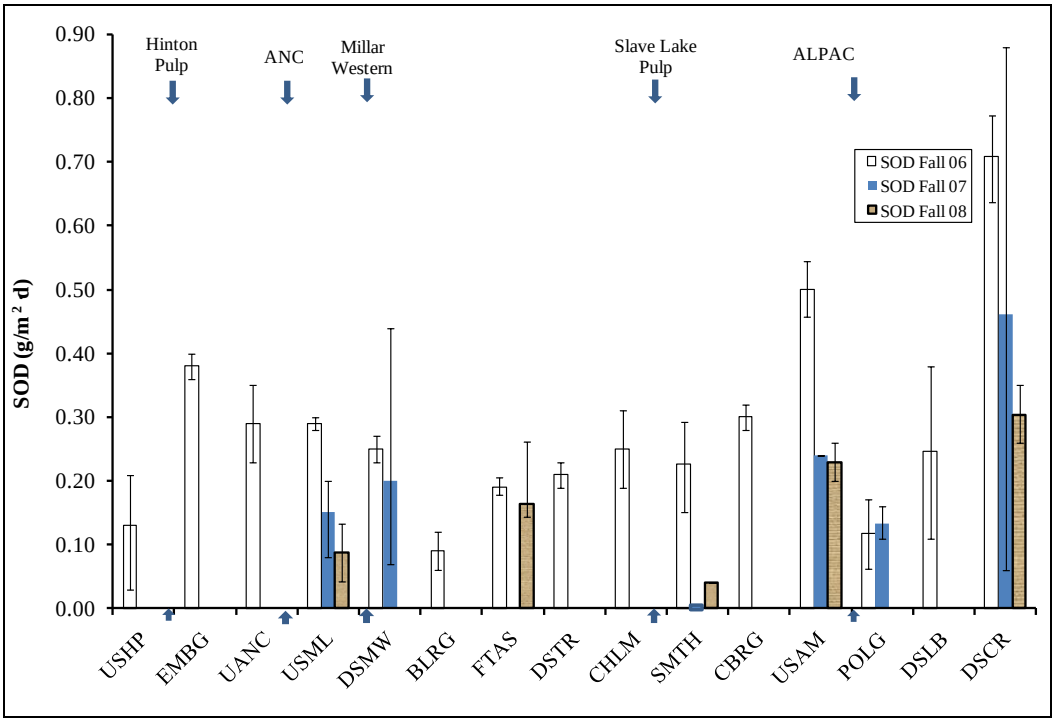

Figure 4.1 Longitudinal pattern of the SOD (at 4±1°C) along the Athabasca River in the fall. The arrows represent approximate pulp mill discharge points to the River

pollutants settle onto the riverbed, thus increasing the SOD. In addition, during high flow in the river the flow velocity increases causing scouring of top layer of the sediment. The net result is smaller SOD due to loss of organic matter and nutrients. The change in the SOD measurement technique in this research could also have some impact on the SOD, as the new technique was used from fall 2007 onwards.

The mean SOD in winter 2007 ranged from 0.02 g/m^2•d at DMSW to 0.48 g/m^2•d at DSCR, while the mean SOD in winter 2008 ranged from 0.21 g/m^2•d at USAM to 0.32 g/m^2•d at USML (4±1°C). A similar longitudinal pattern of the SOD along

the Athabasca River of the fall season was observed in the winter season too. In the winter season, the contribution of pollutant load from non-point sources is minimal, but there is no reaeration in the river water rendering lowered sources to the river's DO budget. It's not just the river flow and water column pollutants that could affect the SOD, but also biological and chemical activities inside the sediment. All these activities take place inside the sediment; thus, the sediment characteristics need to be evaluated. In fall 2006 and winter 2007, sediment sampling was done upstream and downstream of the nutrient discharge points. As seen in Figure 4.1 and Figure 4.2 the impact of point or non-point source

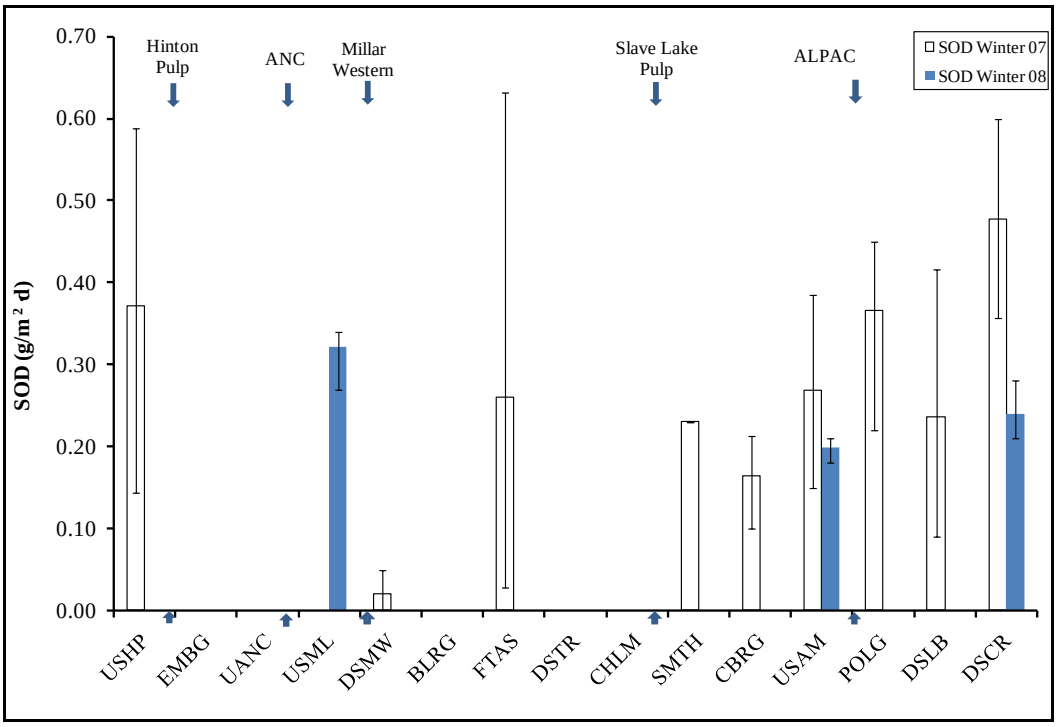

Figure 4.2 Longitudinal pattern of the SOD (at 4 ±1°C) along the Athabasca River in the winter. The arrows represent approximate pulp mill discharge points to the River

discharges on the SOD were observed in some sites only. For example, the SOD at downstream sites of pulp mill discharge points e.g. EMBG in fall 2006 and at POLG in winter 2007 were higher than the upstream sites of the discharge points. Similarly, the SOD at downstream of non-point sources e.g. FTAS and DSLB in fall 2006 were higher than upstream of non-point source (tributaries). The observation indicated that other factors, besides the pollutant load in river water, also contribute to the variation of the SOD. More details of the SOD variation in the Athabasca River and influence of water chemistry on SOD variation is presented in Chapter 5.

4.3 Sediment Characteristics of Athabasca River

Yearly seasonal and climatic variations impact the river water quantity and quality and, thus, sediment deposition and characteristics in the Athabasca River bed. In the spring, there is a slight flow increase after the ice-out on the river, and higher river flows are observed in the summer months because of precipitation. A large quantity of suspended particles is received during the high flow season, which ultimately deposit on the river bed. Scouring of bed material may also take place. In view of this phenomenon, sediment characteristics should be determined at the same time that the SOD is determined.

Figure 4.3 and Figure 4.4 present the sediment porosity along the Athabasca River in fall 2006 and winter 2007. The mean porosity of the Athabasca River sediment

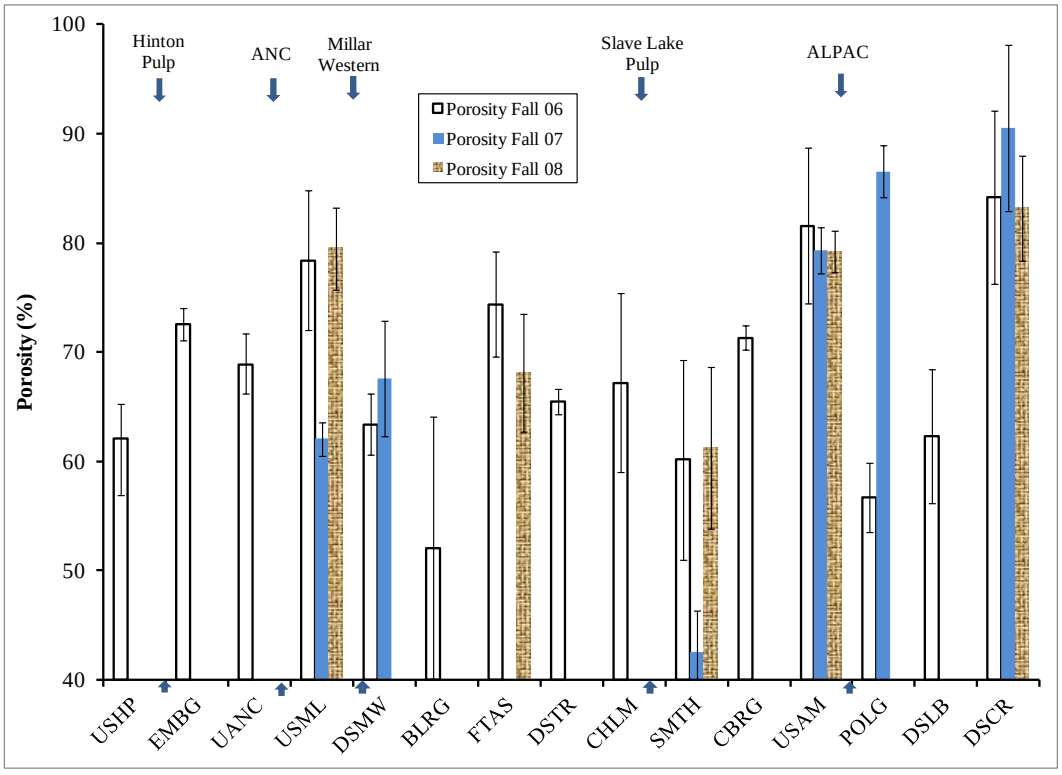

Figure 4.3 Sediment porosity in the fall at different sites along the Athabasca River.

ranges from 60% to 90%. The porosity is influenced by the sediment type, e.g., clay-type sediment has higher porosity compared to sandy soil. The quantity of organic matter present in the sediment also impacts the porosity. In most of the sampling period, the highest porosities (above 70%) were found at USML, USAM, and DSCR sites. The lowest porosity (in the range of 60%) at all times was observed at the SMTH site. The variations in the porosity within a site for different years indicate the impact of river water flow, solids deposition and compaction. For example, the porosities in the fall of sampling years were in the range of 80%, but in the winter the range was 70% to 75%.

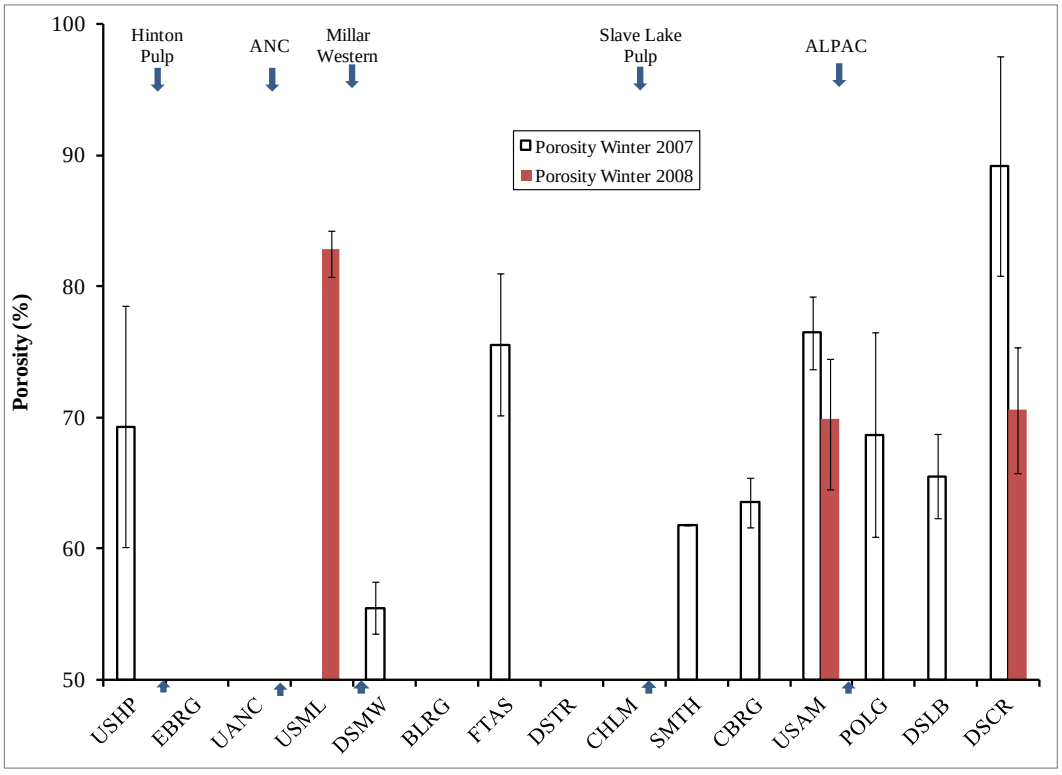

Figure 4.4 Sediment porosity in the winter at different sites along the Athabasca River.

4.4 Impact of Sediment Characteristics on SOD

To evaluate the impact of sediment characteristics, especially the porosity on the SOD, the porosity was regressed against the SOD. As described earlier, the SOD values vary within the site, among sites, and with the season. Figure 4.5, Figure 4.6 and Figure 4.7 present the relationship between mean SOD and mean porosity in fall 2006, fall 2007, and fall 2008, respectively. Figure 4.8 presents the relationship between average SOD and porosity of all sites for fall 2006, fall 2007 and fall 2008. Similarly, Figure 4.9 and Figure 4.10 present the relationship between mean SOD and mean porosity in winter 2007 and winter 2008. Good

correlation between the SOD and porosity was observed in all years and all seasons.

The SOD of 0.25 g/m^2•d at DMSW in the fall of 2006 was smaller than the SOD of 0.29 g/m^2•d at USML, although the Athabasca River received nutrient discharge from the McLeod River, and ANC and Millar Western pulp mills upstream of DMSW. One of the reasons could be that the sediment at DMSW was the coarse grained, sandy type (Table 3.1, Chapter 3) and the porosity was 63% as compared to the fine grained sediment with a porosity of 78% at USML. At BLRG further downstream of DMSW, the SOD was smaller than at DMSW. The porosity at BLRG was 52% compared to 63% at DMSW. A similar case was observed at POLG, downstream of the ALPAC pulp mill discharge in fall 2006. The porosity of 57% at POLG was smaller than the porosity of 82% at USAM.

The changes in the river flow discharge and the direction of flow, especially the meandering, impacts the sediment deposition and scouring. These changes affect the sediment's composition. This composition is reflected in the sediment's porosity. Thus the porosity is not only dependent on the clay, silt, or sand content but also the organic matter present in it. The porosity decreases as the median particle size of the sediment increases (DiToro, 2001).

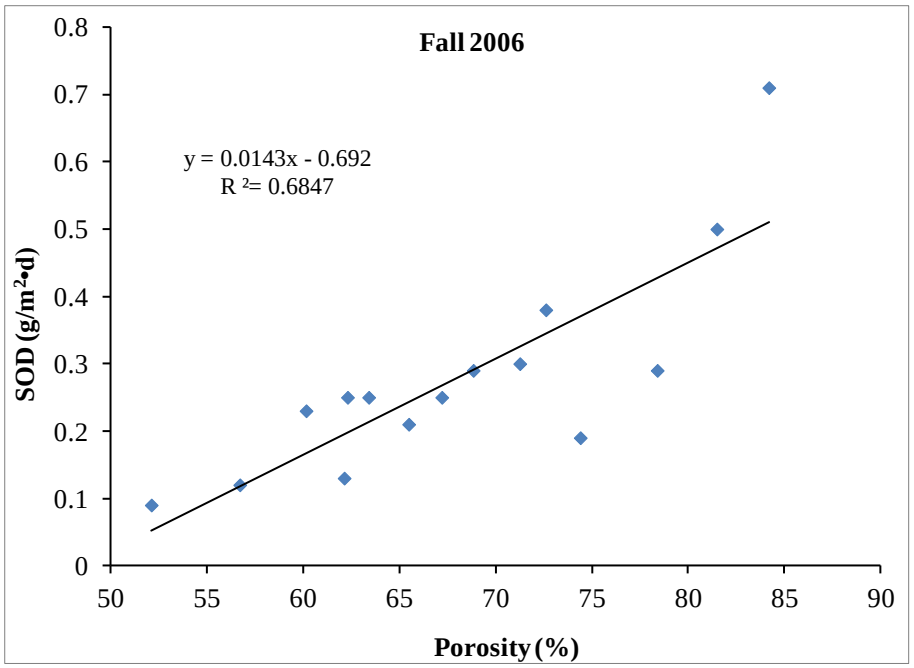

Figure 4.5 Relationship between the SOD and porosity of 15 sites along the Athabasca River in fall 2006

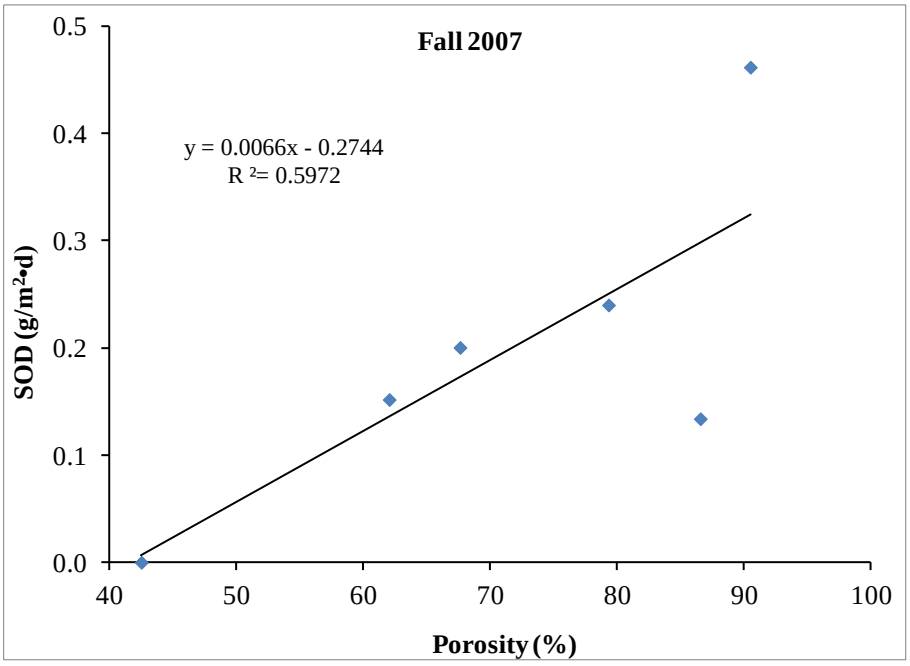

Figure 4.6 Relationship between the SOD and porosity of 6 sites along the Athabasca River in fall 2007

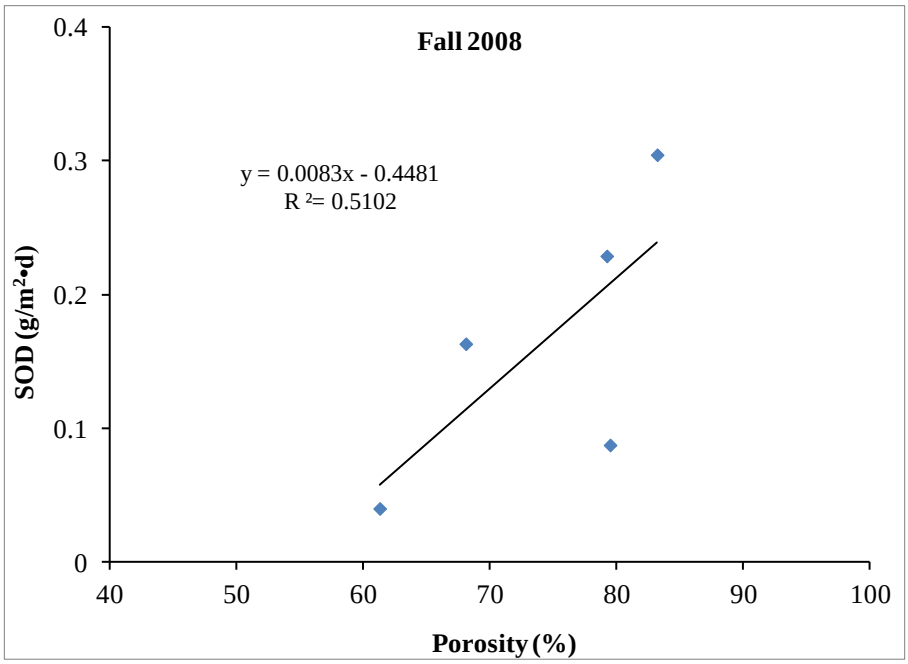

Figure 4.7 Relationship between the SOD and porosity of 5 sites along the Athabasca River in fall 2008

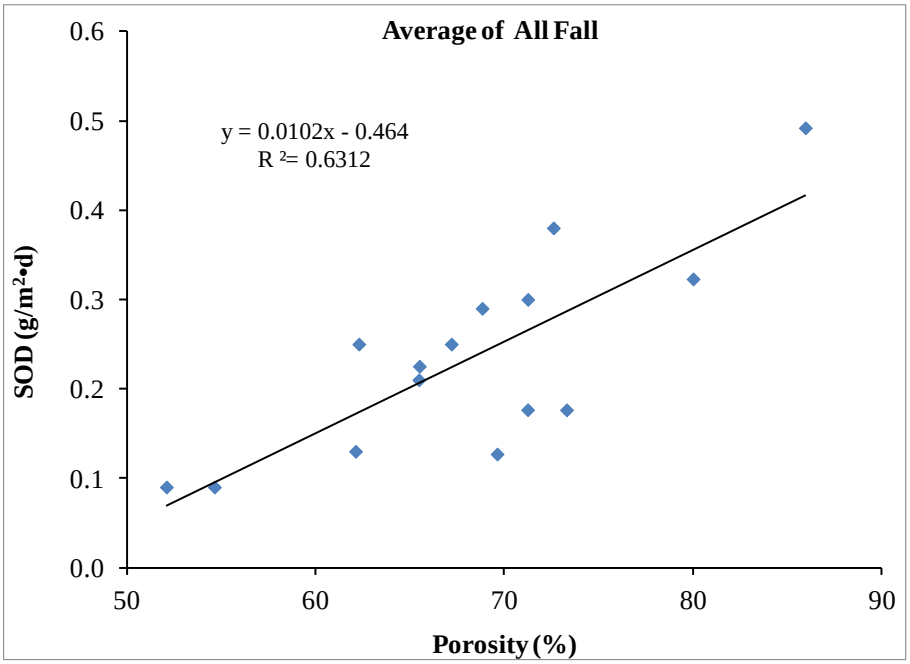

Figure 4.8 Relationship between the SOD and porosity of all sites along the Athabasca River averaged for fall 2006, fall 2007 and fall 2008

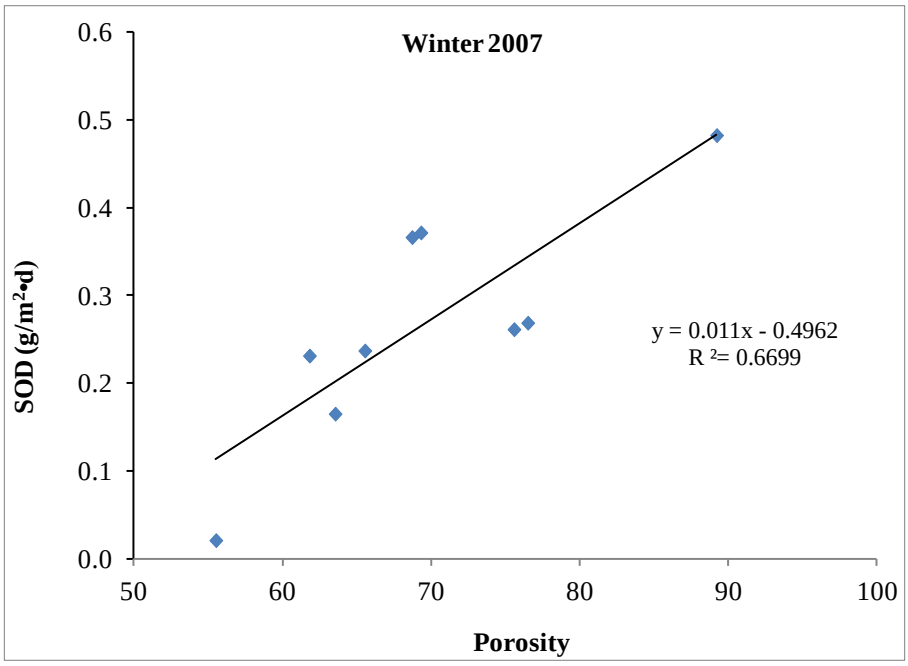

Figure 4.9 Relationship between the SOD and porosity of 9 sites along the Athabasca River in winter 2007

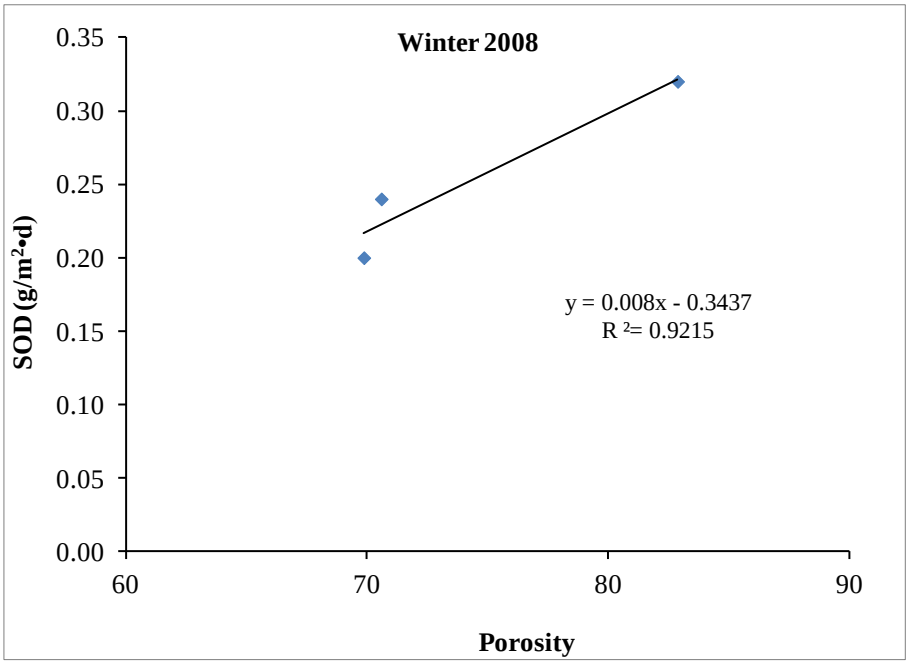

Figure 4.10 Relationship between the SOD and porosity of 3 sites along the Athabasca River in winter 2008

The impact of sediment characteristics on the SOD was seen at the SMTH site. In fall 2006, the SOD was 0.23 g/m^2•d when the porosity was 60%, but the SOD decreased to 0.00 g/m^2•d in fall 2007 as porosity was decreased to 43%. The SOD in fall of 2008 increased slightly to 0.04 g/m^2•d as porosity increased to 61%. Similarly, at the DSCR site, the SOD in fall 2007 was 0.46 g/m^2•d with a porosity of 94% (sand content being 65% and organic matter content being 4.38 g/g) and the SOD decreased to 0.3 g/m^2•d as porosity decreased to 69% (sand content being 70% but organic matter content was 3.01 g/g, as shown in Table 4.1). Therefore larger sand content in the sediment reduced the porosity and the SOD.

In winter 2008, the SOD at DSCR was 0.24 g/m^2•d smaller than the SOD of 0.48 g/m^2•d in winter 2007. The porosity at this site in winter 2008 was 66%, compared to the porosity of 89% in winter 2007. However, the SOD at DSCR was highest most of the time in winter 2008. The SOD of 0.24 g/m^2•d at DSCR was smaller than the SOD of 0.32 g/m^2•d at USML. In that season, the porosity at USML was 83%, higher than the porosity of 66% at DSCR. As shown in table 4.1, the sand content in the sediment at DSCR was 66% and at USML it was 62%. More importantly, the organic matter at DSCR was 2.9 g/g compared to 5.1 g/g at USML. These findings demonstrate that the porosity changes with the composition of the sediment, including the organic matter content. Accordingly, the SOD changed as porosity changed.

4.5 Relationship Between SOD and Nutrient Flux Across the SWI

The sediment pore water analysis of three sites along the Athabasca River, Whitecourt, ALPAC, and downstream of the Calling River confluence revealed that the ammonium concentration increases in deeper sections compared to the SWI, as shown in Table 4.1. The increase of NH_4^+ could be due to the anaerobic degradation of organic matter buried and the nitrogen cycling in the diagenesis process inside sediment. Also, nitrate increased along the depth. Nitrogen transformation from ammonium to nitrate requires a significant amount of oxygen and additional oxygen demand would be exerted if the flux of ammonium is observed from sediment to the river water. If the flux of ammonium is from river water to the sediment, the sediment would be considered as devoid of nutrient. The river water also contains a significant quantity of sulphates. It is imperative to determine the sulphate flux, as the sediment is assumed to be anaerobic in the deeper section of the river sediment. The sulphate recycling is incubation period were used to determine the fluxes of the above nutrients. The PO_4^{3-} was measured as TDP. All the fluxes including oxygen (or SOD) were determined using the slope of the concentration curve and the method used earlier for the SOD. Figure 4.11 and Figure 4.12 give the concentration profiles of oxygen and nutrients, respectively, over the incubation period at the USML site. Figure 4.13 and Figure 4.14 give the concentration profiles of oxygen and nutrients, respectively, over the incubation period at the USAM site. Figure 4.15 and Figure 4.16 give the

concentration profiles of oxygen and nutrients, respectively, over the incubation period at the DSCR site.

Table 4.1 Sediment characteristics and porewater nutrient concentration in three sites

Site	Sediment layer (cm)	Sediment characteristics							Porewater Concentrations (μg N/L)*	
		Chemical			Physical					
		TC (% dry wt)	TN (% dry wt)	OM (% dry wt)	Clay (%)	Silt+Clay (%)	Sand (%)	Porosity (%)	NH_4^+	NO_3^-
USML, White Court Site	0 - 2	7.03	0.17	11.84	9.5	37.9	62.0	82.9	4.85	15.0
	2 - 4	7.42	0.17	10.44	10.4	45.5	54.5	80.5	10.3	13.8
	4 - 6	8.05	0.21	11.17	10.8	47.0	53.0	82.2	15.2	14.0
	6 - 8	6.27	0.14	9.14	11.6	46.1	53.9	78.9	19.0	39.8
	8 - 10	6.71	0.17	9.14	11.3	43.0	56.7	82.3	53.3	13.7
USAM, ALPAC Site	0 - 2	1.55	0.04	2.29	12.3	31.7	68.3	65.3	128.5	16.6
	2 - 4	1.80	0.06	2.03	13.7	32.4	67.6	68.4	257.5	49.2
	4 - 6	1.55	0.04	1.81	13.0	32.2	67.8	67.6	280.8	16.5
	6 - 8	1.68	0.05	2.33	14.0	37.1	62.9	68.0	331.2	14.6
	8 - 10	1.52	0.04	2.37	12.9	36.2	63.8	67.1	485.7	16.4
DSCR, Calling River Site	0 - 2	1.58	0.06	2.88	9.2	34.1	65.9	70.6	989.5	13.0
	2 - 4	1.32	0.03	2.41	7.1	23.1	76.9	69.5	1960.0	22.5
	4 - 6	1.15	0.02	1.66	5.7	18.6	81.4	66.3	1940.0	233.0
	6 - 8	1.09	0.03	1.79	6.9	20.6	79.4	63.3	2870.0	67.0
	8 - 10	1.12	0.03	2.37	8.1	25.3	74.7	65.8	-	-

* The sediment porewater concentrations of NH_4^+ at Upstream of McLeod River site are in mg-N/L

From the concentration profiles it was observed that DO at all sites decreases over the time. The concentration of NH_4^+ increased at the USML and USAM sites, indicating a NH_4^+ flux from sediment to overlying water. The NH_4^+ at DSCR increased slightly after 12 hours of incubation, but decreased later on and levelled off with initial concentration. The concentration of NO_x^--N increased only at the USAM site. The concentration profile of SO_4^{2-} showed a downward flux from the SWI to the sediment at the USML and DSCR sites. The concentration profile of PO_4^{3-} also showed a downward flux at all sites.

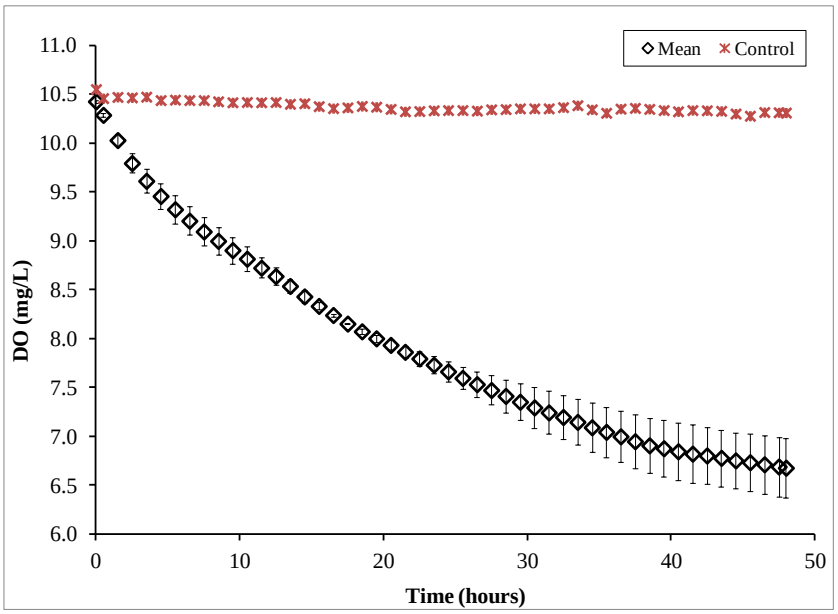

Figure 4.11 Oxygen concentration profile in overlying water of the sediment core over the period of sediment incubation at the USML site

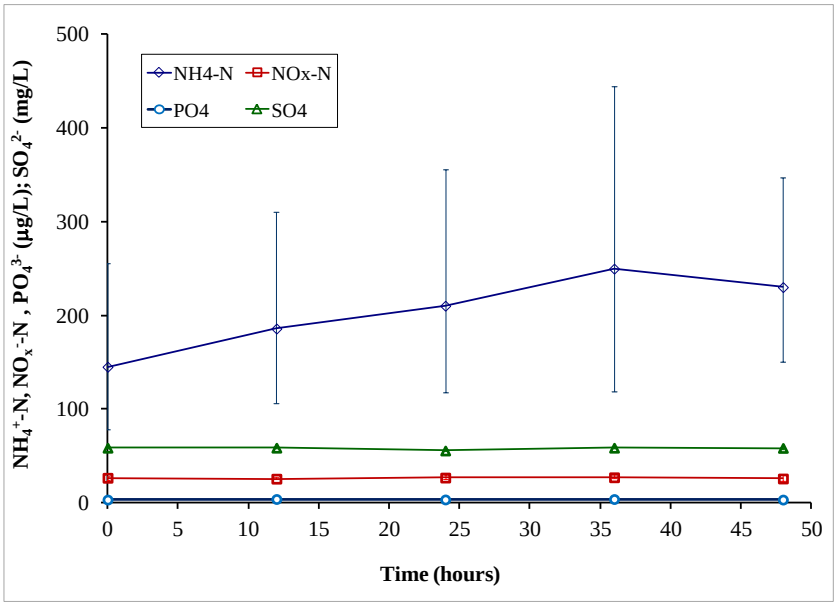

Figure 4.12 NH_4^+-N, NO_x^--N, PO_4^{3-}, and SO_4^{2-} concentration profile in overlying water of the sediment core over the period of sediment incubation at the USML

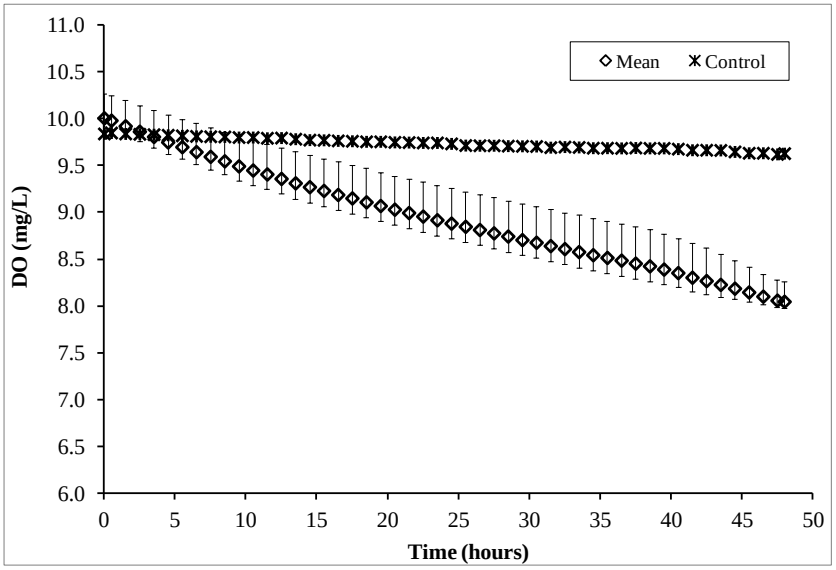

Figure 4.13 Oxygen concentration profile in overlying water of the sediment core over the period of sediment incubation at the USAM site

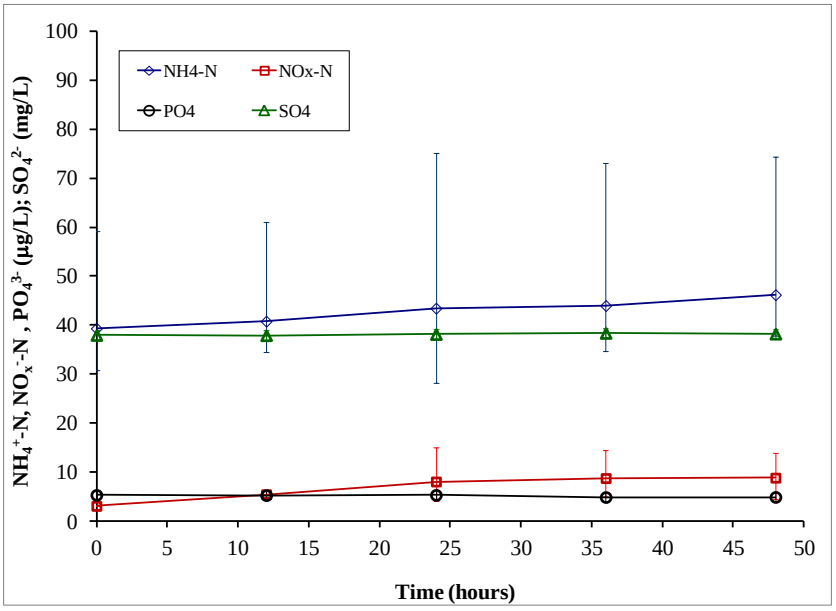

Figure 4.14 NH_4^+-N, NO_x^--N, PO_4^{3-}, and SO_4^{2-} concentration profile in overlying water of the sediment core over the period of sediment incubation at the USAM

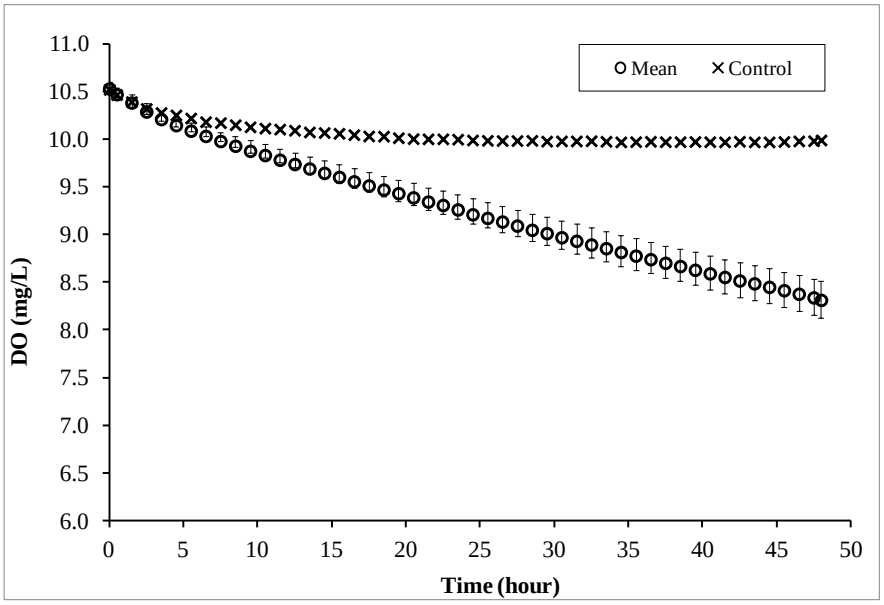

Figure 4.15 Oxygen concentration profile in overlying water of the sediment core over the period of sediment incubation at the DSCR site

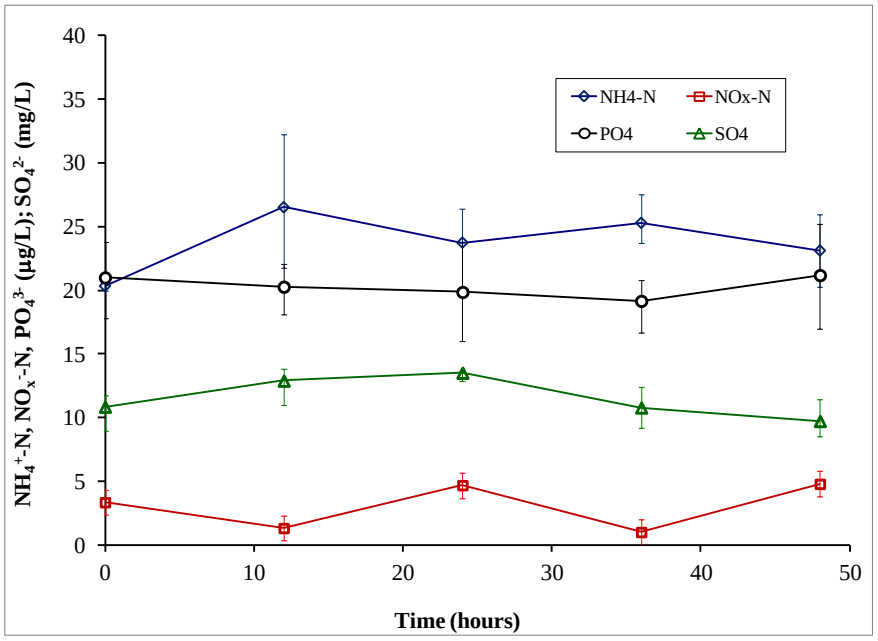

Figure 4.16 NH_4^+-N, NO_x^--N, PO_4^{3-}, and SO_4^{2-} concentration profile in overlying water of the sediment core over the period of sediment incubation at the DSCR site

Table 4.2 shows the SOD and fluxes of NH_4^+-N, NO_x^--N, PO_4^{3-}, and SO_4^{2-}. The NH_4^+-N fluxes of 10.09 mg/m^2•d and 0.91 mg/m^2•d from the sediment to the water column were observed at the Whitecourt and ALPAC sites, respectively. Similarly, NO_x^--N fluxes of 0.46 mg/m^2•d and 0.67 mg/m^2•d from the sediment to the water column were observed at the Whitecourt and ALPAC sites. The PO_4^{3-} and SO_4^{2-} fluxes at the Whitecourt site were considered zero since the time series concentration changes were not significant (R^2 = 0.0202 and 0.0404, respectively). An influx of PO_4^{3-} was observed from the water column to the sediment at the ALPAC site, but there was no SO_4^{2-} flux at any site. At the Calling River site, no nutrient fluxes were observed. The NH_4^+-N flux was corelated with the C/N ratio, as shown in Table 4.3. Therefore higher NH_4^+ flux was observed in nutrient rich sediment. To determine the relationship of these nutrient fluxes with the SOD, the SOD and nutrient fluxes of all three sites were regressed. Figure 4.17 and Figure 4.18 present the relationship of SOD with flux of NH_4^+, NO_x^-, respectively.

Table 4.2 Mean oxygen and nutrient fluxes at the SWI. The fluxes in parenthesis are equivalent to zero. The negative sign indicates influx from the water column to the sediment

	SOD (g/m^2•d)	Flux (mg/m^2•d)			
		NH_4^+-N	NO_x^--N	PO_4^{3-}	SO_4^{2-}
Whitecourt	0.32	10.09	0.46	0 (-0.05)	0 (61.04)
ALPAC	0.20	0.91	0.67	-0.03	0 (38.43)
Calling River	0.24	0 (0.23)	0 (-0.28)	0 (-0.19)	0 (-35.96)

Table 4.3 Sediment content of total organic carbon and total nitrogen (in percentage of dry weight ± SD) at three sites of the Athabasca River

	Total Organic Carbon (% DW)	Total Nitrogen (% DW)	Mean C/N Ratio
White Court	4.03 ± 0.50	0.17 ± 0.03	24.1
ALPAC	0.72 ± 0.01	0.04 ± 0.01	16.3
Calling	0.92 ± 0.06	0.06 ± 0.01	14.6

It was observed that the SOD was correlated with NH_4^+-N flux (R^2 = 0.8375) but not with NO_x^--N flux. The finding is in line with the fact that oxygen is taken up by ammonium oxidizing microbes in aerobic conditions to produce nitrite and nitrate; therefore the SOD was correlated with NH_4^+ flux. The SOD was also correlated with porosity and the sediment classification of silt and clay content at the top 2-cm layer of the sediment, as shown in Table 4.1. The reason for the top 2

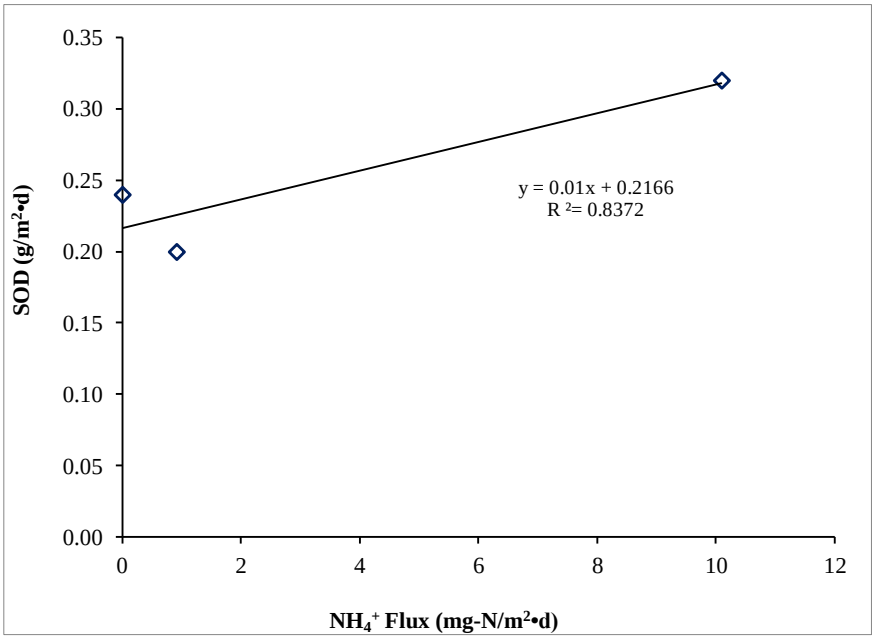

Figure 4.17 Relationship between the SOD and NH_4^+-N flux at three sites of the Athabasca River

cm layer is that most of the microbial activities occur at this layer. The relationship between the SOD and NH_4^+ flux indicated that NH_4^+ flux is also one of the factors that affect the SOD in the winter. The result demonstrates that whenever ammonium accumulates in Athabasca River sediment, it is diffused back to river water. This increased NH_4^+ concentration consumes oxygen, thus giving rise to the higher SOD.

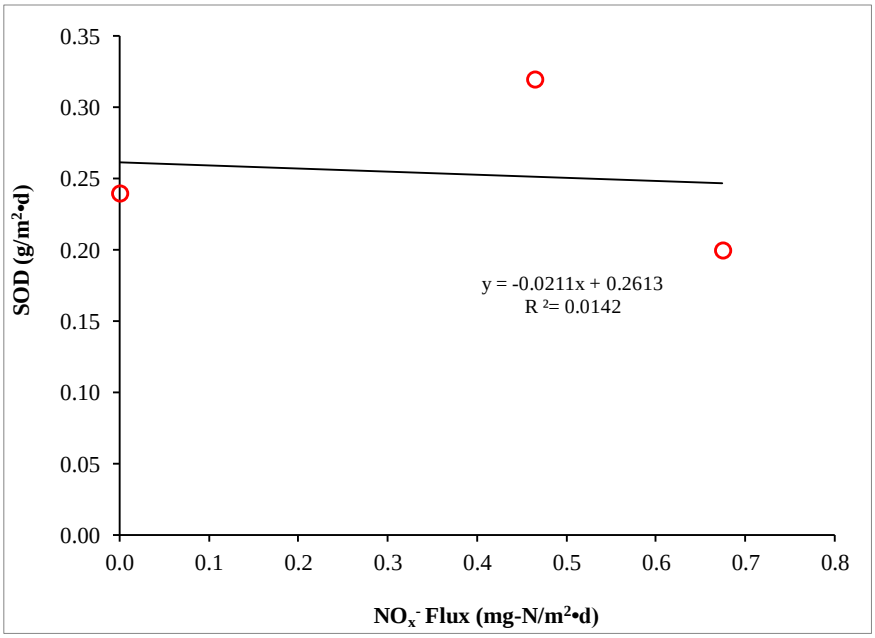

Figure 4.18 Relationship between the SOD and NO_x^--N flux at three sites of the Athabasca River

4.6 Summary and Conclusion

The SOD measurement along the Athabasca River sediment during the fall and winter showed variations among sites, as well as within the site. In addition, the

results showed a variation in the SOD for the fall and winter. The reason for measuring fall and winter SOD was to compare the SOD, such that the fall sampling could be used to estimate winter SOD. There could be several factors causing the variations, but sediment characteristics being a fundamental constituent, we examined the relationship between the SOD and porosity. The results indicated that the SOD is correlated with sediment porosity in all seasons and years. This relationship highlights microbially mediated chemical reactions inside the sediment. The porosity is dependent on the sediment granulometry as well as the organic matter content. The finer the sediment particle, the more organic matter is retained, thus allowing microbes to flourish. This enhances the biochemical reaction inside the sediment. At the sediment layer near the SWI, where aerobic reactions take place, oxygen is consumed, thus exerting oxygen demand. This research found that there are biogeochemical activities inside sediment, even in winter. Therefore, porosity could be one of the key factors that impacts the SOD at a particular site.

Nitrogen transformation mediated by microbial activity near the SWI could also be considered as one of the contributing factors in SOD variations. A newly developed laboratory sediment core incubation method was used to determine the nutrient fluxes of ammonim, nitrate + nitrite, phosphate, and sulphate. The results showed that ammonium and nitrate + nitrite fluxes were significant and the directions of fluxes were from sediment to water column. Upon regression of significant flux with the SOD, it was found that ammonium flux is correlated with

the SOD. The experiment was conducted with samples from three sites, which might not be representative of the Athabasca River. More sites need to be covered to confirm the impact of ammonium flux on the SOD.

From the results of the SOD measurements along the Athabasca River and the relationship between SOD and physico-chemical sediment characteristics the following conclusions are made:

(1) The SOD values varied spatially and temporarily. The SOD values varied in a range of 0 g/m^2•d to 0.71 g/m^2•d in the fall and 0.02 g/m^2•d to 0.48 g/m^2•d in the winter. Higher SOD values were found in the downstream sites of the Athabasca River.

(2) SOD increased with the porosity. The porosity was influenced by the sediment classification, the finer silt and clay portion giving high porosity. In the same way, organic content of the sediment also influenced the porosity.

(3) An efflux of ammonium was found across the SWI directed from sediment to water column in organic rich sediment. The accumulation of ammonium in deeper zones of the sediment and the diffusion of the ammonium to upper zones due to concentration gradient are believed to be the reason behind the efflux of ammonium from the sediment.

(4) The flux of the ammonium from the sediment to the water column is positively correlated to the SOD. This relationship between the SOD and the flux of ammonium indicates that increase in the ammonium flux

increases the SOD in the river. The increase in the SOD will result in lowering the river DO.

(5) An efflux of nitrate was observed, but there was no correlation between flux of nitrate and the SOD. We did not observe any flux of TDP and sulphate at the SWI of the Athabasca River.

Chapter 5

SEDIMENT OXYGEN DEMAND (SOD) IN THE ATHABASCA RIVER AND INFLUENCE OF WATER CHEMISTRY ON SOD

5.1 Introduction

This chapter summarizes study on the relationship between the physical-chemical characteristics of river water and the SOD. Specifically, it examines the relationship between organic carbon, nutrients, and the SOD within the context of spatial variability along the Athabasca River.

5.2 Seasonal and Spatial Variation of SOD along the Athabasca River

Figure 5.1 presents the longitudinal pattern in the SOD and TOC concentration for fall 2006. The mean SOD determined in this study ranged from 0.09 $g/m^2 \cdot d$ at BLRG to 0.71 $g/m^2 \cdot d$ at DSCR. When the values were adjusted to 20^oC, they ranged from 0.17 $g/m^2 \cdot d$ to 1.33 $g/m^2 \cdot d$, respectively. The SOD was generally higher at sites downstream of nutrient sources. Most sites showed good agreement between replications; however, a significant variability was observed between cores at some sites. The SOD values used in all analyses are at 4 ± 1^oC, unless otherwise stated.

The TOC and SOD were positively correlated in the Athabasca River (Figure 5.1). Other studies have shown that the SOD is influenced by the availability of organic matter (Doyle and Linch, 2005; Yu, 2006) and nutrients (Yu, 2006). The SOD value of 0.38 g/m^2•d at EMBG, when compared to the 0.13 g/m^2•d at USHP, highlighted the threefold effect that Hinton Pulp and municipal effluent have on the SOD. Similarly, at FTAS, the SOD value of 0.2 g/m^2•d was two times higher than at the upstream site BLRG (0.09 g/m^2•d) due to loading from the Freeman River between them. A conflicting pattern, in which significant declines in the SOD was observed, occurred between DSMW and BLRG (Whitecourt area), and

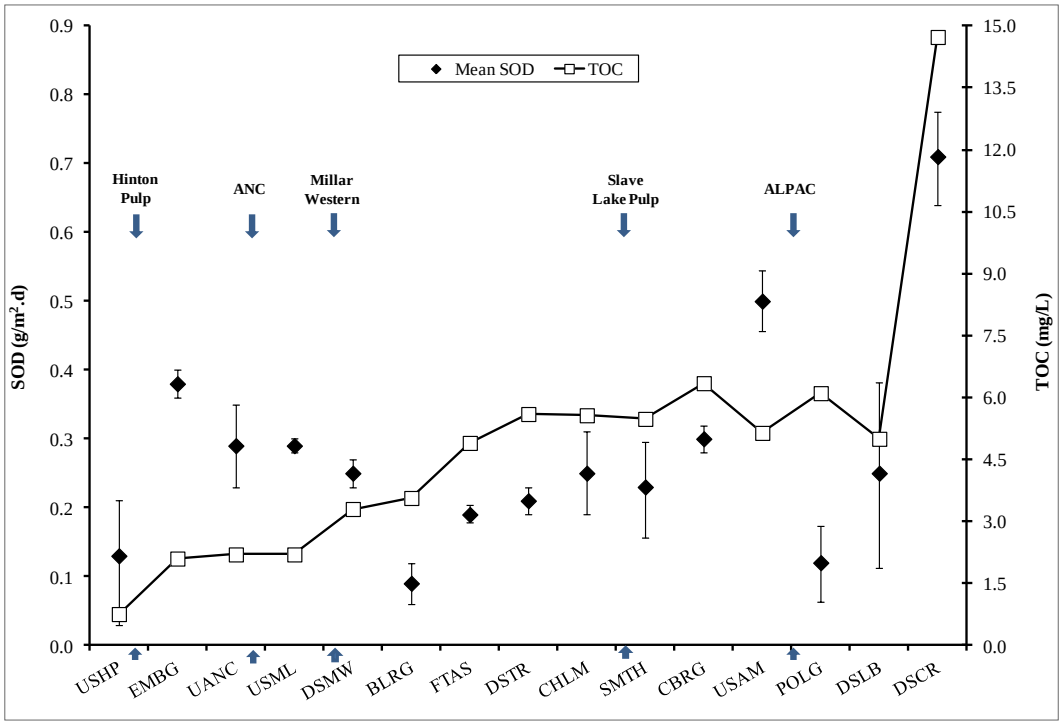

Figure 5.1 Longitudinal pattern of the SOD (at 4±1^{o}C) and TOC concentration along the Athabasca River in fall 2006. The arrows represent approximate discharge points to the River

between USAM and POLG (Athabasca area). These were caused by higher proportions of sand in the sediment, as described in Chapter 4, Section 4.3.

In the same manner, Figure 5.2 presents the longitudinal pattern of the SOD and TOC concentration along the Athabasca River in winter 2007. The mean SOD in winter 2007 varied from 0.02 g/m^2•d at DMSW to 0.48 g/m^2•d at DSCR. Similar to the fall 2006 pattern, the SOD in winter 2007 are observed higher at the downstream part of the river. The variability of replication of cores was relatively higher at some sites compared to the fall. The TOC concentration increased along the flow of the Athabasca River water, indicating that the nutrient discharges from pulp mills and municipal wastes are contributing to an increase in the TOC concentration. This was obvious from the more than six-fold increase in TOC concentration from USHP to DSMW, where three pulp mills and two municipal wastewater treatment plants contribute to the organic load in the river water. In the winter months, the tributaries received less flow and organic loads from non-point sources, as the catchment area was covered with snow and the upstream sub-tributaries were frozen. Therefore the contribution of organic load from the non-point was negligible.

The SOD and the TOC concentration did not show significant correlation in winter 2007 (Fig. 5.2). The reason could be that the TOC is in less bio-available form (labile) for microbial activity in the river water. But once this TOC is

deposited onto the sediment surface, the bacterial community could consume the TOC for its metabolism inside the sediment.

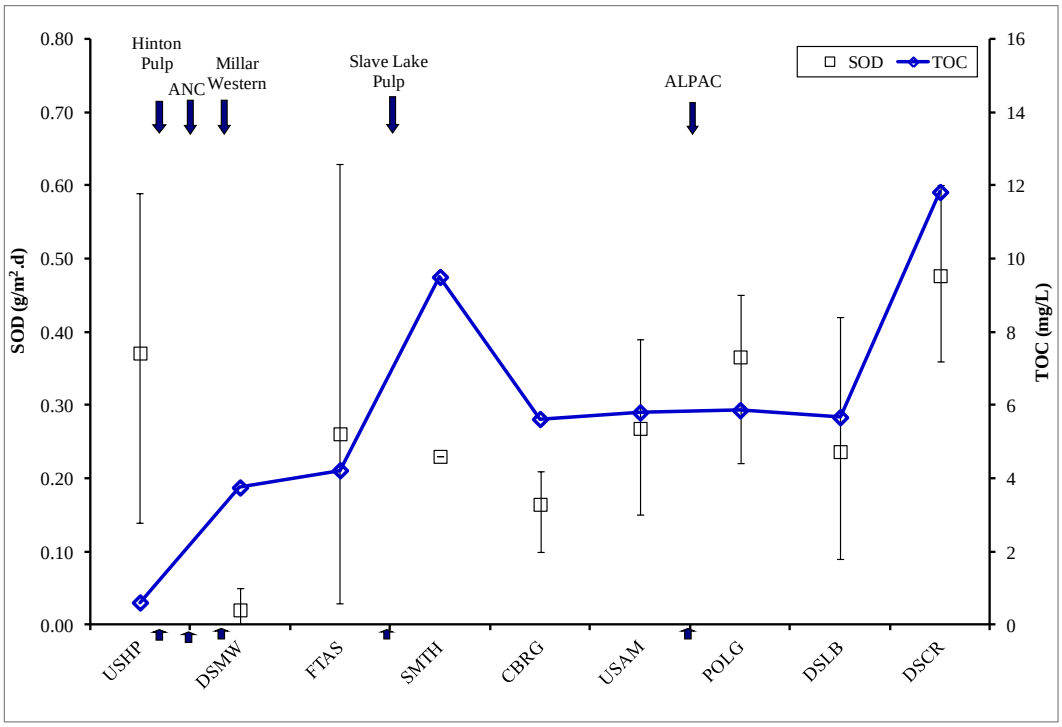

Figure 5.2 Longitudinal pattern of the SOD (at 4±1°C) & TOC concentration along Athabasca River in the winter 2007. The arrows represent approximate discharge points to the River

5.3 Influence of Water Characteristics on SOD Along the Athabasca River

As observed earlier, the variation of the SOD along the Athabasca River was different in the fall and winter. Therefore it would be prudent to determine the relationship between water chemistry and the SOD for an individual season. For clarity of content, the water chemistry and the SOD for fall 2006 and winter 2007

are presented in the following sections. Another reason for choosing the fall 2006 and winter 2007 data set as representative is that more sampling locations were covered (15 sites in fall 2006 and 10 sites in winter 2007). For statistical analysis, all the data sets obtained in the fall or winter of different years, were used.

5.3.1 Water Chemistry and SOD Relationship in Fall

The physical and chemical water quality parameters along the Athabasca River in this study varied among the sites (Table 5.1) as presented in Figure 5.3. The ambient DO ranged from 9.0 mg/L to 11.8 mg/L, the temperature ranged from 3.1^{o}C to 11.8^{o}C during the field sampling period, pH was stable at 8.1 to 8.2, alkalinity ranged from 93 mg/L to 149 mg/L as $CaCO_3$, and conductivity ranged from 118 μS/cm to 247 μS/cm. In general, total and dissolved constituent concentrations increased moving downstream in the Athabasca River. For example, the lowest and highest concentration of TOC, BOD_5, TDP, Chlorophyll-a, and conductivity were at USHP and at DSCR, respectively.

The TOC concentrations revealed the clear impact of tributaries and point source loading along the river. The TOC at EMBG, downstream of the Hinton Pulp mill, was about three times higher than the TOC upstream of the mill. Similarly, the TOC was about one-and-a-half times higher downstream of DSMW, below the discharge points of the ANC and Millar Western pulp mills, than it was at UANC, upstream of the pulp mills. Similarly, the TOC concentration downstream of the

ALPAC pulp mill, at POLG, was one-and-a-quarter times higher than at USAM. Tributaries were also significant sources of constituent load, with clear increases in concentrations of TOC, TDP, and Chlorophyll-a downstream of the confluences with the Athabasca River. The increase in the TOC concentration at CBRG as compared to SMTH was likely due to the load from the Town of Athabasca wastewater treatment plant, as it is the only large contributor between SMTH and CBRG. The increased TOC concentration at DSCR was the result of loading from the Calling River. TIN and TSS concentrations were variable but correlated with each other. The TDP and Chlorophyll-a concentrations follow the trend of TOC. BOD_5 values do not exhibit an appreciable variation along the river, indicating a relative steady state in oxygen consumption within the water column itself. Table 5.2 shows the total nutrient load in the Athabasca River on the sampling day at a particular site. The loads were estimated from the river flow and river water chemistry on the sampling date. Generally, on the sampling day, loads are higher downstream of the nutrient source.

For statistical analysis we used 26 data sets of all water quality parameters except BOD_5, which had 15 data sets of fall sampling in 2006, 2007, and 2008. Pair-wise correlation among data sets of all fall sampling revealed strong associations among independent variables (conductivity, alkalinity, TOC, BOD_5, TSS, TIN, TDP, Chlorophyll-a, and Fe) and the response variable (SOD) (Table 5.3). The SOD was positively correlated with TOC, TDP, Chlorophyll-a, and Fe. TOC was negatively correlated with conductivity and alkalinity, indicating that higher

Table 5.1 Water Chemistry of Athabasca River Samples (Sept 19 - Oct 16, 2006)

Parameter	USHP	EMBG	UANC	USML	DSMW	BLRG	FTAS	DSTR	CHLM	SMTH	CBRG	USAM	POLG	DSLB	DSCR
Ambient DO, mg/L	10.4	11.1	10.0	9.3	9.7	10.2	9.8	10.1	9.9	9.0	10.3	10.2	10.2	11.6	11.8
Ambient Temp., ^{o}C	5.6	5.7	7.5	7.6	9.5	9.1	8.3	6.6	11.8	11.7	11.4	3.7	11.6	3.1	3.3
Conductivity, µS/cm	210.7	222.7	199.5	270.5	243.7	221.3	206.9	126.2	247.2	238.5	236.0	240.6	239.8	197.9	118.4
pH	8.1	8.2	8.1	8.1	8.2	8.2	8.1	8.1	8.2	8.2	8.2	8.1	8.2	8.1	8.0
Alkalinity, mg/L as $CaCO_3$	107.5	109.7	107.3	106.4	147.9	123.9	118.4	117.6	137.5	127.6	131.7	130.3	133.2	126.8	93.3
TOC, mg/L	0.8	2.1	2.2	2.2	3.3	3.6	4.9	5.6	5.6	5.5	6.3	5.1	6.1	5.0	14.7
BOD_5, mg/L	2.0	2.0	2.0	2.0	2.0	2.0	2.4	2.0	2.0	2.0	2.0	2.0	4.5	2.0	2.1
TSS, mg/L	19.0	2.0	3.5	1.0	2.5	1.5	<0.05	5.0	5.0	7.0	7.0	4.0	1.0	<0.05	21.0
NH_4^+, µg/L	2.0	2.0	5.4	4.2	2.0	2.0	6.2	4.2	2.0	2.0	2.0	2.0	2.0	3.7	4.0
NO_x, µg/L	79.0	40.0	2.5	3.0	12.5	3.8	5.9	5.5	3.8	3.9	4.1	3.2	5.1	5.6	27.7
TIN, µgN/L	81.0	42.0	7.9	7.2	14.5	5.8	12.2	9.7	5.0	5.9	6.1	5.2	7.1	9.4	31.7
TDP, µg/L	1.0	1.4	1.4	2.0	1.8	2.1	2.8	2.1	3.4	4.0	4.7	3.3	3.5	4.1	28.0
Chlorophyll-a, µg/L	0.4	4.7	1.1	1.4	0.7	1.9	2.6	2.2	2.1	2.4	3.3	2.7	3.0	2.9	13.3
Fe, mg/L	0.1	0.1	0.0	0.0	0.0	0.1	<0.02	0.1	0.3	0.3	0.3	0.3	0.0	0.2	0.3
SOD, $g/m^2.d$	0.13	0.38	0.29	0.29	0.25	0.09	0.19	0.21	0.25	0.23	0.30	0.50	0.12	0.25	0.71
SOD_{20}, $g/m^2.d$	0.24	0.71	0.54	0.54	0.47	0.17	0.36	0.39	0.47	0.43	0.56	0.94	0.22	0.47	1.33

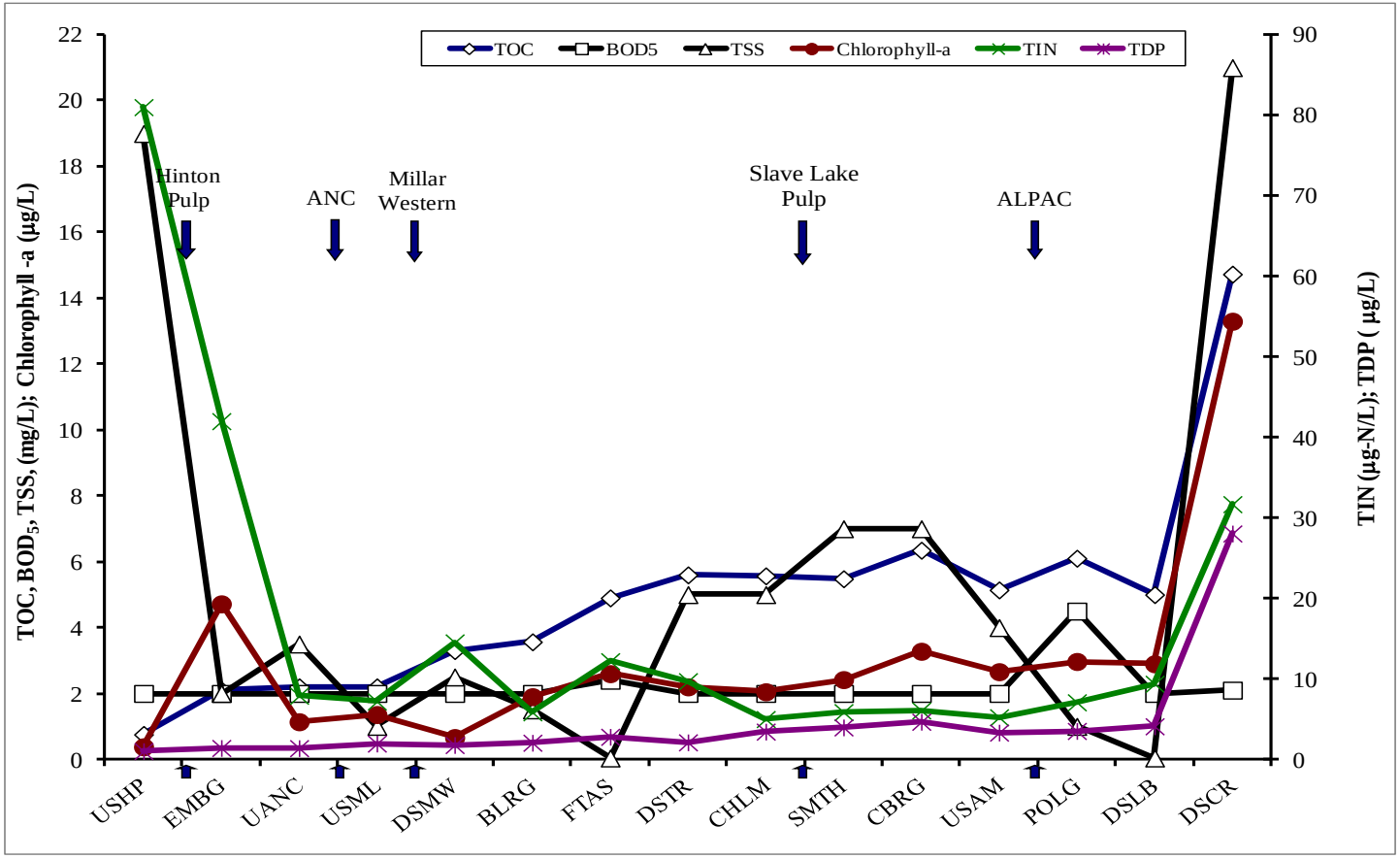

Figure 5.3 Spatial variability of water characteristics along the Athabasca River in fall 2006. The arrows represent the approximate location of effluent discharges from pulp mills.

concentrations were likely associated with surface runoff being lower in ions compared to groundwater. The significant negative correlation of Chlorophyll-a with conductivity and alkalinity indicated that algal biomass is sensitive to inorganic loads. The synergistic impact of TDP and Chlorophyll-a, which is correlated with TOC, showed a positive correlation with the SOD. TSS was correlated with TDP, but BOD_5 was not correlated with any other variables.

The factor analysis identified three principal components that explained 82 % of the variability in the SOD (Table 5.4). The principal component 1 was driven by TOC, TSS, TDP, Chlorophyll-a, and (negative) conductivity and alkalinity. The principal component 2 was driven by TIN and the principal component 3 was driven by Fe.

The ANOVA for the three factors analysis was significant ($F = 5.89$ adjusted $R^2 = 0.512$; $P<0.012$). The SOD was only significantly related to the principal component 1 ($\beta = 0.393$; $P < 0.01$) in the regression analysis (Table 5.5). The result of the pair-wise correlation and linear regression confirmed the dependency of the SOD on TOC, TDP, and Chlorophyll-a. The SOD is stimulated by adding organic carbon with synergistic effects of N and P only in the presence of additional organic carbon (Yu, 2006). Interestingly, BOD_5 was not correlated with the TOC or the SOD. This could be because the SOD is created by the microbially mediated degradation of organic matter (labile or refractory) deposited on the river bed over a period of time, whereas BOD_5 is only sensitive to easily

Table 5.2 Instantaneous Load in the Athabasca River (Sept 19 – Oct 16, 2006)

Parameter	USHP	EMBG	UANC	USML	DSMW	BLRG	FTAS	DSTR	CHLM	SMTH	CBRG	USAM	POLG	DSLB	DSCR
River Flow (m^3/s)	97.00	98.23	176.44	179.01	281.49	281.63	294.60	294.82	381.23	402.09	452.41	206.02	453.19	209.50	210.37
Alkalinity, t/d as $CaCO_3$	901.02	930.69	1635.40	1644.84	3597.06	3015.10	3013.43	2995.26	4530.04	4431.83	5149.03	2319.53	5217.09	2295.13	1695.41
TOC, t/d	6.34	17.82	33.54	34.03	79.36	86.80	121.95	142.64	183.47	190.45	248.09	91.55	239.05	90.50	267.73
BOD_5, t/d	16.76	16.97	30.49	30.93	48.64	48.67	61.09	50.94	65.88	69.48	78.18	35.60	176.20	36.20	38.17
TSS, t/d	159.24	16.97	53.35	15.47	60.80	36.50	0.64	127.36	164.69	243.18	273.61	71.20	39.16	0.45	381.69
TIN, kg/d	678.84	356.46	120.43	111.36	353.14	142.10	310.02	247.08	164.69	203.58	236.87	92.92	277.22	169.78	575.98
TDP, kg/d	8.54	11.94	21.19	30.21	43.19	50.05	71.14	53.75	113.31	137.71	182.31	59.06	137.83	73.49	509.79
Chlorophyll-a, kg/d	3.18	40.06	17.38	21.03	16.05	46.23	66.18	56.04	67.52	84.07	128.21	47.35	116.29	53.03	241.73
Fe, t/d	0.92	1.19	0.30	0.46	0.97	2.68	0.25	1.53	9.55	8.69	12.12	5.34	0.78	3.26	4.73

Table 5.3 Pearson's correlation between the SOD and water chemistry for all fall sampling

	SOD	TOC	BOD_5	TSS	TIN	TDP	Chlo-a	Cond	Alkal
SOD	1.000								
TOC	0.567**	1.000							
BOD_5	-0.275	0.141	1.000						
TSS	0.153	0.290	-0.196	1.000					
TIN	0.008	0.253	-0.130	0.214	1.000				
TDP	0.608**	0.896**	-0.006	0.532**	0.301	1.000			
Chlo-a	0.718**	0.624**	0.032	0.341	0.155	0.707**	1.000		
Cond	-0.504*	-0.208	0.131	-0.089	0.365	-0.120	-0.533*	1.000	
Alkal	-0.487*	-0.164	0.199	-0.297	0.235	-0.201	-0.445*	0.804**	1.000
Fe	0.484*	0.340	-0.338	0.170	0.237	0.229	0.496**	-0.463*	-0.244

** Correlation is significant at 0.01 level (2-tailed)
* Correlation is significant at 0.05 level (2-tailed)

Table 5.4 Orthogonal Rotated factor loadings of variables in principal component axes 1-3

	Component		
	1	2	3
TOC	0.827	0.539	-0.100
BOD_5	-0.127	0.319	-0.747
TSS	0.780	-0.369	0.216
TIN	0.313	-0.817	0.066
TDP	0.944	0.230	-0.076
Chlorophyll-a	0.921	0.231	-0.120
Conductivity	-0.731	0.156	0.264
Alkalinity	-0.592	0.577	0.229
Fe	0.414	0.399	0.749
% Variation explained	46.69	20.21	14.70

Extraction Method: Principal Component Analysis
Rotation Method: Varimax with Kaiser Normalization
Rotation Converged in 5 Iterations

biodegradable (labile) organic matter in the water column. Although BOD_5 contributes to the SOD, the relationship between these two parameters may be uncertain. As found in Table 5.1, the BOD_5 concentration is in a narrow range of

2 mg/L and does not vary significantly at sites along the river, whereas, the SOD varies significantly at all sites along the river. Therefore BOD_5 is not correlated with SOD. A negative correlation between the SOD and conductivity as well as alkalinity suggested that the SOD is primarily determined by carbonaceous degradation.

Table 5.5 Regression analysis - on principal components and SOD

Model	Unstandardized Coefficients		Standardized Coefficient Beta	t	Significance
	β	Std. Error			
(Constant)	0.393	0.04		9.842	0
Score for Factor 1	0.153	0.041	0.69	3.693	0.004
Score for Factor 2	0.031	0.041	0.141	0.755	0.466
Score for Factor 3	0.077	0.041	0.347	1.859	0.09

Model F = 5.89
Regression Degree of Freedom = 3
Error Degree of Freedom = 22
Adjusted R^2 = 0.512
Number of Cases 26

But at the same time, there was no strong relationship between the SOD and TIN (nitrogen loading). The ammonium oxidation in the river water column may be slow at low temperature (Tchobanoglous et al., 2003). It is also to be noted that the TIN composition (NH_4^+ and $NO_2^- + NO_3^-$) could be responsible for not having correlation with SOD because nitrate acts as electron acceptor during microbial degradation. When nitrate in river water column diffuses into sediment due to chemical gradient across the SWI, nitrate does not consume oxygen, thus showing no effect on SOD.

5.3.2 Water Chemistry and SOD Relationship in the Winter of 2007

The physical and chemical water quality parameters varied along the river (Table 5.6) as presented in Figure 5.4. The ambient DO ranged from 7.9 mg/L to 11.4 mg/L. There is a clear indication that the DO declined gradually from the upstream site, USHP, to the downstream site, DSCR. The sampling dates were random to avoid any bias. The temperature was at the freezing mark most of the time, the pH was stable at 7.5 to 7.9, alkalinity ranged from 104.5 mg/L as $CaCO_3$ to 210 mg/L as $CaCO_3$, and conductivity ranged from 198 μS/cm to 470 μS/cm. The alkalinity and conductivity were higher in winter 2007 compared to fall 2006. As in fall 2006, total and dissolved constituent concentrations increased moving downstream in the Athabasca River. For example, the lowest and highest concentrations of TOC and TDP were at USHP and at DSCR, respectively. However the TSS concentration was very low and below the detection limit at the majority of sites. The chlorophyll-a concentration was always below 1 μg/L, which indicated that growth of algal biomass was negligible in the winter as the river was frozen and covered with snow.

The increase in TOC concentration revealed the impact of discharges from point and non-point sources, a similar trend as in fall 2006. TOC at USML, downstream of two pulp mills, was four times higher than at USHP, upstream of the discharge point. Similarly, at DSMW, downstream of Millar Western Pulp Mill, the TOC was one-and-one-half times higher than at USML, upstream of the pulp mill. The

Table 5.6 Water Chemistry of Athabasca River Samples in the winter (Feb 10 – March 13, 2007)

Parameter	USHP	USML	DSMW	FTAS	SMTH	CBRG	USAM	POLG	DSLB	DSCR
Ambient DO, mg/L	11.3	10.3	10.1	10.7	9.1	9.2	9.1	9.5	8.3	7.9
Ambient Temperature, ^{0}C	0.1	0.1	0.1	0.0	-0.2	0.1	0.1	0.1	0.1	-0.1
Conductivity, µS/cm	206.0	243.8	253.4	227.4	472.2	240.8	242.3	237.6	197.6	82.4
pH	7.8	7.9	7.8	7.8	7.7	7.7	7.6	7.7	7.7	7.5
Alkalinity, mg/L as $CaCO_3$	104.5	156.4	210.0	167.8	190.7	169.4	176.6	176.5	171.5	119.4
TOC, mg/L	0.6	2.5	3.8	4.2	9.0	5.6	5.8	5.9	5.7	11.8
BOD_5, mg/L	2.7	1.3	1.6	1.8	3.4	1.5	3.1	3.1	2.6	2.0
TSS, mg/L	2.0	<0.05	<0.05	2.5	<0.05	4.0	<0.05	<0.05	3.0	19.0
TIN, µgN/L	110.7	157.1	233.7	167.3	234.9	262.3	254.2	249.3	245.5	247.3
TDP, µg/L	1.6	7.5	6.2	9.1	12.5	10.8	11.3	12.3	8.7	48.3
Chlorophyll-a, µg/L	0.1	1.0	0.8	0.2	0.3	0.2	0.3	0.2	0.1	0.8
Fe, mg/L	<0.02	<0.02	<0.02	<0.02	0.1	0.2	0.2	0.2	0.2	<0.02
SO_4, mg/L	85.5	70.8	48.1	47.8	69.7	55.0	56.4	55.4	55.2	14.5
SOD, g/m^2.d	0.37	NA	0.02	0.26	0.23	0.16	0.27	0.37	0.24	0.48
SOD_{20}, g/m^{2}d	0.69	NA	0.04	0.49	0.43	0.30	0.51	0.69	0.45	0.90

< denotes below detection limit

NA Not available

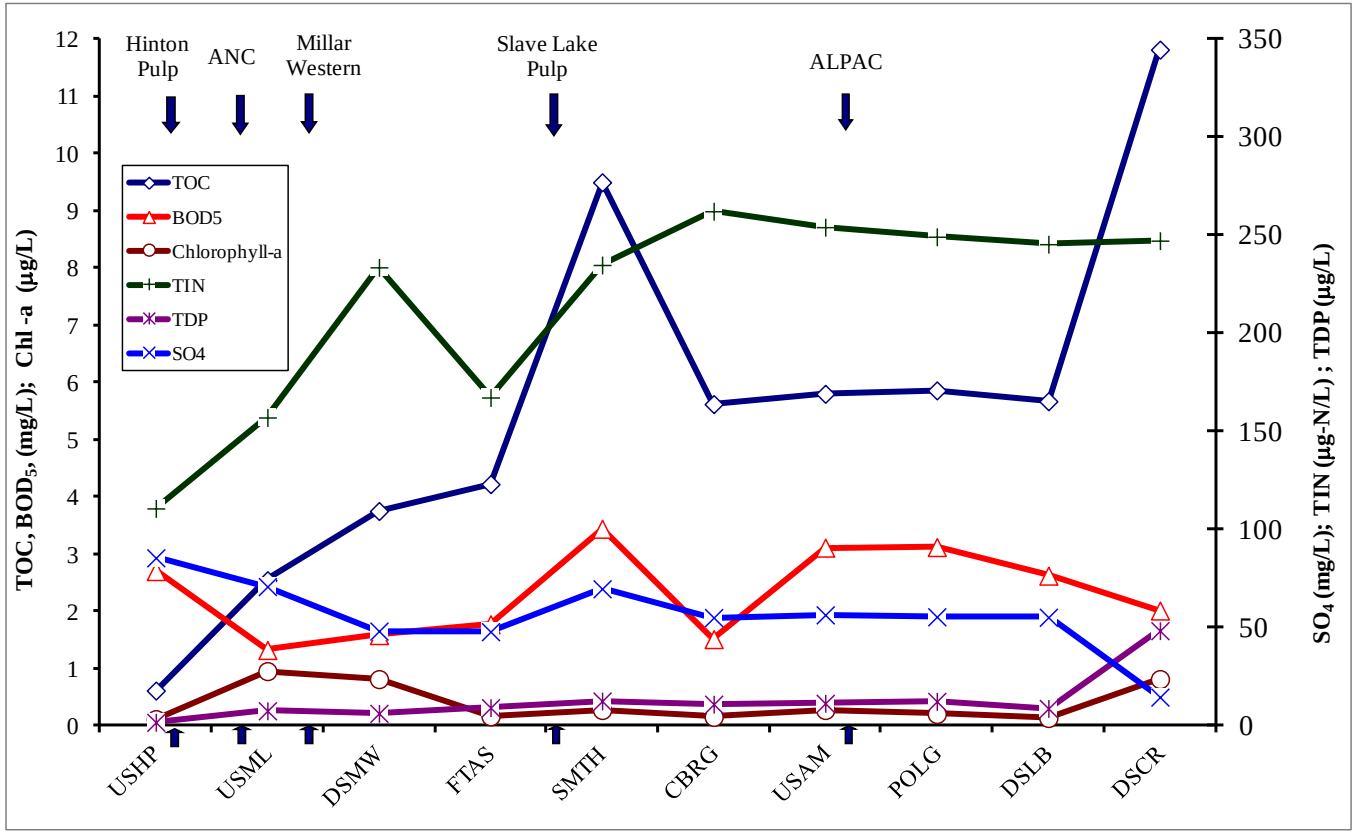

Figure 5.4 Spatial variability of water characteristics along the Athabasca River in winter 2007. The arrows represent the approximate location of effluent discharges from Pulp Mills

TOC was two times higher at SMTH than at FTAS, a contribution of the Slave Lake Pulp Mill. At FTAS, the TOC was higher than at DSMW. The only contributing source is the Freeman River upstream of FTAS. The BOD_5 concentration varied among sites along the Athabasca River in the range of 1.3 mg/L to 2.1 mg/L. The TIN concentration was ten times higher in winter 2007 compared to fall 2006 because the NO_x^- concentration was higher in the winter. Below SMTH, the NO_x^- concentration is stable. The reason for the increased NO_x^- concentration in winter could be the contribution from pulp mill discharge and groundwater seepage. Table 5.7 shows the total nutrient load in the Athabasca River on sampling day at a particular site. The nutrient load in the river confirms the above findings.

Table 5.7 Instantaneous Load in the Athabasca River (Feb 10 – March 13, 2007)

Parameter	USHP	USML	DSMW	FTAS	SMTH	CBRG	USAM	POLG	DSLB	DSCR
River flow (m^3/s)	45.40	46.74	56.12	59.83	68.60	73.91	73.11	74.10	NA	NA
Alkalinity, t/d as $CaCO_3$	410	631	1018	867	1130	1082	1116	1130	-	-
TOC, t/d	2.4	10.3	18.2	21.8	53.3	35.9	36.6	37.5	-	-
BOD_5, t/d	10.59	5.33	7.66	9.15	20.39	9.64	19.64	19.97	-	-
TSS, t/d	7.8	0.2	0.2	12.9	0.3	25.5	0.3	0.3	-	-
TIN, kg/d	434	634	1133	865	1392	1675	1606	1596	-	-
TDP, kg/d	6.3	30.2	29.9	46.9	73.8	69.3	71.3	78.5	-	-
Chlorophyll-a, kg/d	0.4	3.8	3.9	0.8	1.6	1.0	1.7	1.3	-	-
SO_4, t/d	335	286	233	247	413	351	356	355	-	-
Fe, t/d	0.1	0.1	0.1	0.1	0.3	1.0	0.9	1.0	-	-

NA - the river discharge was not available

In order to establish a relationship between the SOD and water chemistry in all winter seasons, a pair-wise correlation was used. Pair-wise correlation among 12 data sets of all winter sampling revealed associations among independent

variables (conductivity, alkalinity, TOC, BOD_5, TSS, TIN, TDP, Chlorophyll-a and Fe) and the response variable, i.e. the SOD (Table 5.8). The SOD was positively correlated only with TSS. Unlike the strong correlation of the SOD with TOC in all fall, there was no strong correlation of the SOD with TOC, TDP, and Chlorophyll-a in winter. TOC was negatively correlated with alkalinity. BOD_5 was not correlated with any other variables. TSS consists of nutrients and debris in addition to suspended inorganic particles in river water (Wetzel, 2007). Therefore the TSS is positively correlated with TDP in both fall and winter. TDP is also positively correlated with TOC in both seasons. In the Athabasca River TSS also consists of suspended carbonaceous organic compound from the point and non-point sources, the above relationship implies that the TSS is also derived by oxygen demanding organic compounds represented by TOC. Although there was no statistical correlation between SOD and TOC in winter, but TOC appeared to be controlling factor of SOD in winter.

Table 5.8 Pearson's correlation between the SOD and water chemistry for all winter sampling

	SOD	TOC	BOD_5	TSS	TIN	TDP	Chlo-a	Cond	Alkal	Fe
SOD	1.000									
TOC	0.275	1.000								
BOD_5	0.358	0.123	1.000							
TSS	0.596*	0.486	-0.344	1.000						
TIN	-0.001	0.384	0.023	0.253	1.000					
TDP	0.515	0.847**	-0.134	0.827**	0.305	1.000				
Chlorophyll-a	-0.071	0.384	-0.378	0.535	0.325	0.586*	1.000			
Conductivity	-0.348	-0.152	0.474	-0.571	-0.086	-0.525	-0.305	1.000		
Alkalinity as $CaCO_3$	-0.653*	-0.052	0.009	-0.406	0.714*	-0.277	0.179	0.349	1.000	
Fe	-0.039	0.123	0.296	-0.183	0.623*	-0.065	-0.325	-0.068	0.433	1.000

* Correlation is significant at the 0.05 level (2-tailed).

** Correlation is significant at the 0.01 level (2-tailed).

In the fall TDP could be a limiting factor for microbial activities inside sediment, as suggested by Yu (2006). The fall TDP concentration in the Athabasca River is about one-third of the winter TDP concentration averaged at all sites, as shown in Table 5.1 and Table 5.6. It is likely that the assimilation of TDP by algal biomass for their growth led to the decrease in concentration of TDP in the fall. In winter the biomass growth was low, shown by smaller concentration of Chlorophyll-a. Because of low assimilation of TDP by algal biomass, higher concentration of TDP was observed in winter than in fall in the Athabasca River water. However, there was downward flux of TDP in winter as shown by nutrient flux analysis, Table 4.2. This result indicates that there could be TDP limitation in the fall and not necessarily in the winter, since TDP could get diffused inside sediment from the TDP available in the river water column.

5.4 Use of SOD for Water Quality Modeling in the Athabasca River

The use of the SOD values in calibrating DO models is not consistent and depends on the modeler's judgement. Tian (2005) calibrated the WASP 6 model for the Athabasca River using the SOD of 0.01 $g/m^2 \cdot d$ to 0.59 $g/m^2 \cdot d$ for different segments of the Athabasca River. Miao (2006) calibrated the CE-QUAL W2 model using an average SOD for the Athabasca River (0.15 $g/m^2 \cdot d$) as input to the model for DO prediction. Alternatively, the CE-QUAL W2 model could be

calibrated by incorporating interpolated SOD values between river segments using water and sediment quality data.

More importantly, river water TOC, TDP and Chlorophyll-a concentrations significantly influence the SOD and could be used to predict the SOD for model use. The positive correlation of TOC with TDP and Chlorophyll-a in the fall was not observed in the winter because of the low quantity of algal mass, although there was a positive correlation between TDP and Chlorophyll-a TOC was positively correlated with TDP in the winter season. These results indicated that in both seasons, TOC was the driving force that synergistically impacted the SOD. This led us to assume that TOC could be taken as representative of TDP and Chlorophyll-a in other analysis. Based on the results from this study and combining the factors that affect the SOD, i.e. sediment porosity and river water TOC, a generalized approach can also be developed. The correlation between the SOD and porosity (Figure 4.8, Chapter 4) for the fall is: SOD (g/m^2•d) = 0.0081 x Porosity (%) – 0.3262. While the correlation between the SOD and TOC for the fall season is: SOD (g/m^2•d) = 0.0302 x TOC (mg/L) + 0.0845. Based on these relationships, SOD classification is suggested, as in Table 5.9.

The SOD has been correlated with water column BOD_5 in tidal creeks, coastal sediment, and river sediment (MacPherson 2003). The use of BOD_5 as an important factor in predicting the SOD depends on the availability of the labile

carbon source in the water column. In addition, the temperature should be appropriate for the heterotrophic bacteria to work on. But in northern rivers, the BOD_5 parameter is not suitable because of low bacterial activity during the winter.

Table 5.9 Suggested SOD classification against available nutrient concentration and sediment quality in the Athabasca River

SOD ($g/m^2 \cdot d$) Range (4^oC)	SOD ($g/m^2 \cdot d$) Value to be Used in a River Reach	TOC (mg/L)	Porosity (%)
Low (<0.15)	0.1	<3	<60
Medium (0.16 - 0.3)	0.2	3 - 7	61-75
High (>0.31)	0.4	>7	>75

This study in the Athabasca River sediment confirms that BOD_5 is not a major factor affecting the SOD. Therefore, the selection of TOC in river water is appropriate. Moreover, researchers have correlated SOD positively with land use patterns (Utley 2008), organic content of sediment (Heckathorn and Gibbs 2010), and negatively correlated with sand content in the sediment (Steeby et al., 2004). As the organic matter content and sediment content are related to sediment porosity, selection of porosity as a predictor of the SOD in the Athabasca River was appropriate. The model developed (Equation 5.1) fits well (Table 5.10) with the fall water column TOC and sediment porosity (R^2 = 0.497; F = 11.375; P < 0.001). The predictive model:

$$SOD\ (g/m^2 \cdot d) = -0.281 + 0.19 * TOC\ (mg/L) + 0.006 * Porosity\ (\%) \quad (5.1)$$

Table 5.10 Regression analysis on TOC, porosity, and SOD

Model	Unstandardized Coefficients		Standardized Coefficients Beta	t	Significance	95.0% Confidence Interval for B	
	B	Std. Error				Lower Bound	Upper Bound
(Constant)	-0.281	0.137		-2.042	0.053	-0.565	0.004
TOC	0.019	0.008	0.366	2.246	0.035	0.001	0.036
Porosity	0.006	0.002	0.468	2.867	0.009	0.002	0.010

5.5 Summary and Conclusion

The SOD in the Athabasca River varied from 0 $g/m^2 \cdot d$ to 0.71 $g/m^2 \cdot d$ (at 4 ± 1^oC) in the fall samplings in 2006, 2007, and 2008. But the SOD varied from 0.02 $g/m^2 \cdot d$ to 0.48 $g/m^2 \cdot d$ (at 4 ± 1^oC) in the winter samplings in 2007 and 2008. Fifteen locations were sampled along the Athabasca River in fall 2006 and ten locations in the same area in winter 2007. Sampling was not possible in as many locations during other periods. In general, the SOD was higher downstream of nutrient sources that were discharged into the Athabasca River. However, at some locations the SOD did not follow this trend.

Upon analyzing sediment characteristics in the same locations, it was found that SOD is statistically correlated with porosity. The porosity was correlated with the

finer portion of the sediment as well as with the organic carbon content in the sediment. Most of the SOD is reported worldwide to be influenced by the water chemistry, so the Athabasca River's water chemistry was regressed with SOD. The results indicated that in general, SOD is correlated with TOC, TDP, and Chlorophyll-a during the fall, but not during the winter. In winter TSS was correlated with TDP, and TDP was correlated with TOC. As explained earlier TSS was derived by carbonaceous organic matters represented by TOC. Although winter SOD was not correlated with water chemistry, the TOC did appear to exert some control on SOD in the Athabasca River.

One of the most challenging issues with modeling DO is the variability of SOD from year to year and reach to reach. The SOD is difficult to measure, making inclusion on a model even more difficult. A simple approach for establishing SOD for use in model applications, based on easy-to-measure water quality parameters, was presented.

Based on the results on the relationship between water chemistry and the SOD the following conclusions are made:

(1) The SOD values vary in time and space along the Athabasca River, with values ranging from 0 $g/m^2 \cdot d$ to 0.71 $g/m^2 \cdot d$ (at $4 \pm ^oC$) in the fall and from 0.02 $g/m^2 \cdot d$ to 0.48 $g/m^2 \cdot d$ (at 4 ± 1^oC) in the winter.

(2) SOD values generally increase at downstream sites along the Athabasca River, however certain reaches show significant declines at downstream sites.

(3) The SOD is positively correlated to the river water quality parameters, TOC, TDP, Chlorophyll-a in the fall. Although SOD was not correlated to the river water quality parameters in winter, the TOC was driving force for the SOD variation in the fall and winter.

(4) The SOD is also correlated to the sediment porosity in both seasons.

(5) A SOD classification was presented, as an important input to the DO modeling in the Athabasca River in the winter. The SOD could be estimated from the easily measurable water quality parameter, the TOC and sediment porosity.

Chapter 6

EVALUATION OF MICROSENSORS AT NEAR-ZERO TEMPERATURE

6.1 Introduction

Microsensors are electrochemical sensors that allow for measurements with a spatial resolution of <0.1 mm (Kuhl and Revsbech, 2001). Microsensors are robust with very high spatial resolution, making them a reliable tool to elucidate the concentration profiles of chemical species with no or minimized physical disturbance (Revsbech et al., 1980). Because they are small, microsensors are useful tools to investigate processes occurring at a very fine scale, as is the case with sediment (de Beer, 1999), where diffusion and reaction processes create steep physiochemical gradients within micrometre distances. The use of microsensors minimizes the disturbance of these gradients and other microenviromental conditions such as boundary layers, diffusion, and flow patterns on the microscale (Amann and Kuhl, 1998). Moreover, the microsensor's fine spatial resolution allows the functional separation of different layers where biochemical processes occur in close vicinity (e.g. nitrification and denitrification). Therefore, using microsensors one can determine the activity of the microorganism that mediates the chemical transformation.

The electrochemical microsensors can be divided into (1) simple Ag/Ag^+ half cells, (2) ion-exchange-based electrodes, (3) simple cathodes or anodes with continuous, varying, or no polarization, and (4) Clark-type gas sensors where the chemical species must pass an ion-impermeable membrane before oxidation or reduction or, alternatively, induction of pH changes in the internal electrolyte (Kuhl and Revsbech, 2001). Clark-type oxygen and H_2S microsensors are amperometric sensors that measure partial pressure of the gas in an experimental solution. The ion-exchange-based microsensors are potentiometric sensors that measure the potential difference between working and reference electrodes.

The fabrication and evaluation procedures for oxygen microsensors are abundant (Lu and Yu, 2002; Revsbech, 1989; Revsbech, 1986). The combined oxygen microsensor has been the most widely used microsensor in the environmental field. In the same fashion, abundant literature is available about the fabrication and evaluation of ion-selective microsensors (Amman, 1986; Carlini and Ransom, 1991; Miller and Wells, 2006). The combined oxygen microsensor has now been well established. But the ISmEs bear the brunt of interferences, due mainly to the presence of other ions and temperature variation. The important part of an ISmE is the ion-selective ionophore at its tip. Different ionophores for different ions are commercially available (Fluka, 1996).

Accurate measurements and reporting of ISmE data are longstanding problems caused by the effect of varying temperature (Barron et al., 2008). An increase in any solutions' temperature will decrease the viscosity and increase the mobility of its ions in solution. An increase in temperature may also lead to an increase in the number of ions in solution due to the dissociation of molecules. In addition, changes in temperature will also influence the sensor's measurement performance. Therefore the relationship between temperature and ISmE's performance (e.g. slope response) is complex (Carlini and Ransom, 1991). In view of the complexity of the relationship between temperature and ISmE slope response, it is best to avoid temperature fluctuations in sample solution during experiments. Vaughan-Jones and Kaila (1986) reported that the temperature gradient along the length of the ion-selective column or cocktail altered the ISmE response.

If the experiment requires varying the temperature, careful calibrations of the ISmEs over the experimental temperature range are recommended to determine empirical correction factors; given the known differences in electrode characteristics between ion-selective macro- and microelectrodes (Ammann, 1986), calculated adjustments based on theoretical models of ion-selective macroelectrode behavior cannot be relied upon to yield accurate temperature correction factors (Carlini and Ransom, 1991).

As regards to the complex relationship between temperature change and the ISmE slope response, there is no literature that could give a temperature correction factor other than the theoretical Nernst slope for ideal electrode. Moreover, literature is available that mostly describes the fabrication and evaluation of microsensors at room temperature. In-situ studies reported use of the oxygen microsensors at lower temperatures, but there are no reports of using the ISmEs at lower temperatures. Shabala et al. (2006) evaluated the pH ISmE at 4^{o}C, 25^{o}C, and 40^{o}C, and found that the slope responses varied with tested temperatures. The study concluded that for practical purposes, no temperature correction was needed in the temperature range between 4^{o}C and 22^{o}C for the research. This study led us to ponder the evaluation and applicability of pH, NH_4^+, and NO_3^- ISmEs at near zero temperatures.

Since the SOD study in the Athabasca River required use of microsensors at near zero temperatures, it was imperative to carry out an investigation on the evaluation and applicability of microsensors at near zero temperatures. In this chapter we describe the impact of temperature change on the performance of oxygen microsensor and ISmEs. The performance of pH, NH_4^+, and NO_3^- ISmEs was based on the slope of the calibration curve.

6.2 Microsensor Fabrication

6.2.1 Combined Oxygen Microsensor

An oxygen microsensor is an amperometric type of sensor. The procedure to fabricate and calibrate a combined oxygen microsensor for this research was adapted from Lu and Yu (2002). The calibration and application of the oxygen microsensor was extended to near zero temperature and in the river sediment, respectively. In brief, the combined oxygen microsensor consisted of a cathode of platinum wire plated with gold at its tip, a reference electrode of Ag/AgCl, and a guard cathode of Ag wire, assembled inside a glass casing tapered at one end. The tapered end was the tip of the microsensor of size 20 to 50 μm which consisted of a silicon membrane. The glass casing was filled with electrolytes and sealed with glue. The working theory behind the oxygen microsensor is that when oxygen diffuses inside the membrane, it reduces on the very tip surface of platinum wire, thus creating an electrical signal in the electrolyte circuitry medium against the reference electrode. The current originating from the reduction of the oxygen at the tip surface is proportional to oxygen partial pressure in the surrounding medium (Revsbech and Jorgensen, 1986).The guard cathode along side of the cathode consumes oxygen that might exist behind the working cathode's tip (Revsbech, 1989).

Each microsensor was checked against response time, stirring effect, and residual current during calibration. The response time was below two seconds, fast enough

for oxygen measurement in sediment and at a lower temperature. The stirring effect, which is the fraction of current change when the microsensor is subject to stirring and stagnant conditions, was always less than 2%. The residual current was below 15 pA when the signal was measurable in pA, and below 0.2 nA when the signal was measured in nA. Each oxygen microsensor was calibrated before and after its experimental use. Normally, the same calibration curve was obtained, which indicated that the microsensor tip was stable and usable.

6.2.2 Ion Selective Liquid Membrane Microsensors (ISmEs)

An ISmE contains an ion-selective membrane in the tip of the glass micropipette and is responsive both to the membrane potential and the activity (not concentration) of the ion sensed by the selective membrane (Miller and Wells, 2006). Three ion selective microsensors: pH, NH_4^+, and NO_3^- were fabricated and calibrated in this research. The similarity of their microsensor structures, fabrication procedures, and calibration methods makes it logical to describe the fabrication and evaluation process of these ISmEs in one group (Yu, 2000). There are numerous fabrication procedures available (Miller and Wells, 2006; Li, 2001; Yu, 2000; Fluka, 1996; de Beer and Sweerts, 1989; de Beer and Van Huevel, 1988). In this research, we followed the fabrication procedures of the three ISmEs given by Yu (2000). The only addition was the coating of the microsensor tip with protein, described by de Beer et al. (1997) to overcome the interference problem.

A brief summary of the fabrication and calibration procedure is described here. The fabrication procedure can be divided into six stages: (1) pulling the glass micropipettes, (2) silanizing the tip of micropipettes, (3) backfilling with an internal reference solution, (4) front filling with an ion selective cocktail, (5) coating with protein, and (6) conditioning the microsensors. Stages (1), (2) and (5) were the same for all three ISmEs but stages (3), (4) and (6) were different for each type of ISmE. Each ISmE was calibrated before being used to measure concentration profiles in river sediment.

A 15 cm (1.2 mm O.D.) borosilicate micropipette (World Precision Instruments # BF120-69-15) was pulled with a PUL-100 Vertical Pipette Puller (World Precision Instruments). The pulling program was designed in such a way that the tip of pulled micropipette was 6 to 12 μm. Micropipettes with smaller tip sizes (6 to10 μm) were used for NH_4^+ and pH ISmEs, but those with larger tip sizes (9 to12 μm)were used for NO_3^- ISmE. The hair-like pipette tips were broken to the required size using a pair of fine tweezers (Roboz Surgical Instrument Co. Catalog No. RS 4905) under a microscope.

The micropipette tips obtained in this fashion were silanized immediately, using a dip-and-bake method (Fluka, 1996). The silanization makes the tip surface hydrophobic by causing the glass surface to react with dry N,N-Dimethyltrimethylsilylamine so that the liquid membrane can be held inside the

micropipette tips. The micropipettes with silanized tips were baked in an oven at 200^{o}C for 10 hours. After being cooled in a desiccator, the micropipettes were ready for front and backfilling. The backfilling was performed with the help of injection needles and plastic syringes. The internal reference solutions for backfilling the micropipette for pH, ammonium, and nitrate ISmEs were: pH 7 buffer solution (Fisher Catalog # SB108-500), 0.01M NH_4Cl, and 0.1M KNO_3 + 0.1M KCl, respectively. The backfilling solutions were degassed under the vacuum and filtered through a 0.2 μm Milipor membrane.

Immediately after the backfilling procedure, the micropipettes were front-filled with neutral carrier liquid membrane cocktails. This procedure was done as soon as possible to avoid air bubbles forming between the internal reference solution and the membranes. The front-filling was done by dipping the micropipette tips into a reservoir of liquid membrane cocktail, so that the cocktail was drawn into the micropipette's shank by capillary forces. The typical dipping times in our research for pH, ammonium, and nitrate were 15 seconds, 30 seconds, and 180 seconds. The length of the liquid membrane could be controlled by varying the dipping time. Also, the membrane length could be decreased by changing the pressure being applied by the syringe to the back end of the micropipette. The cocktails used for pH, ammonium, and nitrate were Hydrogen Ionophore I - Cocktail B (Fluka # 95293), Ammonium Ionophore I - Cocktail A (Fluka # 09879), and Nitrate Ionophore Cocktail A (Fluka # 72549), respectively.

The back and front filled micropipettes were then dried for half an hour before protein coating. For coating, the micropipette tips were briefly dipped into a priming solution of 10% (w/w) cellulose acetate in acetone. This was done as briefly as possible to avoid having the membrane dissolved in the acetone. Immediately after priming with cellose acetate, the tips were dipped into a mixture of 1 mL of protein solution containing 10 % (w/v) bovine serum albumin (BSA) in 50 mM sodium phosphate (pH 7.0) and 10 μL of 25% glutaraldehyde (De Beer et al., 1997). Li (2001) used 10 μL of 50% glutaraldehyde, but we found that 50% glutaraldehyde produced a viscous protein coating which dried quickly, thus bending the tips and affecting the performance. After drying, a cross-linked protein layer coating was formed, which was water insoluble and firmly fixed. Protein- coated micropipette tips were stored in conditioning solutions of pH buffer, 0.02M NH_4Cl, and 0.1M KNO_3 for pH, ammonium and nitrate ISmEs, respectively. The pH and ammonium ISmEs were conditioned for at least one hour, but nitrate ISmEs were conditioned for a shorter time, at least 30 minutes. Conditioned ISmEs tend to have more stable, faster, and more reproducible responses (Koryta and Stulik, 1983) than non-conditioned ones.

6.3 Microsensor Calibration

6.3.1 Oxygen Sensor Calibration

The two-point calibration (Stief et al., 2003; Lorenzen et al., 1998; McConn and Robinson, 1963) of each oxygen microsensor was performed in zero oxygen and air saturation conditions (Lu and Yu, 2002) at different temperatures, including room temperature and near zero temperature. The reason for calibrating the microsensor at near zero temperature was to examine its applicability in experimental sediment at that temperature. The temperatures used for calibration were 3^{o}C, 10^{o}C, 15^{o}C, and 23^{o}C. All the electrodes, i.e., cathode, reference electrode and guard cathode, were connected to a picoammeter (Unisense, Denmank Model No. PA2000) that gave readouts of current. The current signal was converted to an oxygen concentration using a calibration curve of current vs. dissolved oxygen concentration. Figure 6.1 presents a typical calibration curve with error bars of an oxygen microsensor at room temperature.

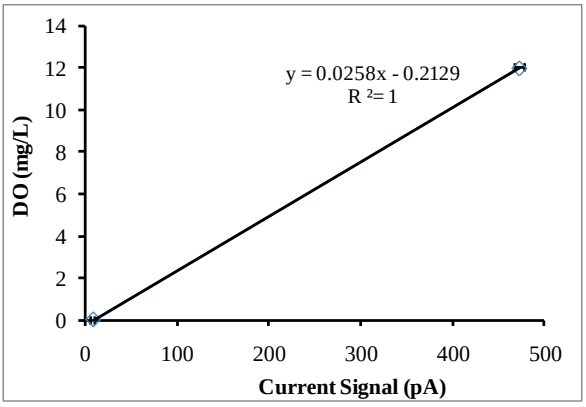

Figure 6.1 Calibration of a combined oxygen microsensor at room temperature

6.3.2 Ion Selective Microsensor Calibration

Individual ISmEs, even if they are of the same design and the same batch, may differ qualitatively in their ion activity vs. their EMF relationship. Therefore, each ISmE must be individually tested and calibrated before being used (Amman, 1986). The aim of this research was to calibrate ISmEs at different temperatures and evaluate their applicability at near zero temperature. ISmEs are best calibrated in calibrating solutions that resemble the experimental solution(s) as closely as possible (Ammann, 1986). At the minimum, calibrating solutions should have an ionic strength and pH equal to or near that of experimental solution(s) (Miller and Wells, 2006) and, when in use, their temperature should be within $\pm 0.5^{o}C$ of that of the experimental solution (Amman, 1986).

Before calibration, an Ag/AgCl wire was inserted into the conditioned ISmE from the back end. This was the working electrode. Another Ag/AgCl mili-electrode (Microelectrode Inc. # MI-409) was used as the reference electrode. These two electrodes were connected to Kiethly's Electrometer (Model # 6517A) for potential measurement in mV. A series of standard solutions at different concentrations for a specific microsensor were used to calibrate that microsensor. For pH ISmE, the standard solutions were pH buffer solutions at pH 6, 7, 8, 9, 10. For ammonium ISmE, the standard solutions were NH_4Cl solutions at concentrations of 10^{-7}, 10^{-6}, 10^{-5}, 10^{-4}, 10^{-3}, and 10^{-2} M. For nitrate ISmE, the

standard solutions were KNO_3 solutions at concentrations of 10^{-7}, 10^{-6}, 10^{-5}, 10^{-4}, 10^{-3}, and 10^{-2} M. The calibrations were performed inside a Faraday Cage to avoid possible electromagnetic interferences.

For calibration of ISmEs at different temperatures, the standard solutions were stored in temperature controlled refrigerators at 3^oC, 8^oC, 14^oC, and room temperature at 23^oC. Thermometers were used to monitor liquid temperatures in standard solutions. The bottles that contain standard solutions for calibration were jacketed with gel-packs as a means of insulation, so that the solution temperature could be maintained for the calibration periods. Each bottle with a particular standard solution was taken out of the refrigerator for calibration and stored back inside the refrigerator after calibration. The duration required for standard solution change between two standards was minimized to 3 seconds (Shabala et al., 2006). If the duration between the two standards solution change was longer, the ISmE tip would be exposed to room temperature that could alter the ISmE performance. Therefore, great care was taken during calibration to minimize the temperature change in the tip and the standard solution.

Figure 6.2 presents the calibration curve of three pH microsensors, calibrated at room temperature in a pH range of 6 to 10. The slope of the individual pH ISmE ranged from 58.2 to 55.8 mV/decade change. The slope is very close to the Nernst slope, 58.16 mV/decade change of an ideal pH electrode. The negative sign of the

slope indicates that as pH increases, the hydrogen ion activity decreases. In the same manner, Figure 6.3 shows the average calibration curve of three NH_4^+ microsensors. The slope of the individual NH_4^+ ISmE ranged from 55.6 to 54.7 mV/decade change. The NH_4^+ ISmEs fabricated in our laboratory had detection limits of 10^{-6} M concentration of NH_4^+. The potential reading became larger on increasing the NH_4^+ concentration in standard solution, resulting in a positive slope. The potential readout for standard solution with NH_4^+ concentration of 10^{-7} M was not included in the calibration curve. The average calibration curve of three NO_3^- microsensors is presented in Figure 6.4. The slope of the individual NO_3^- ISmE ranged from 55.8 to 50.7 mV/decade change. The slope was the opposite of the NH_4^+ microsensor, but the detection limit is the same, i.e., 10^{-6} M concentration of NO_3^-.

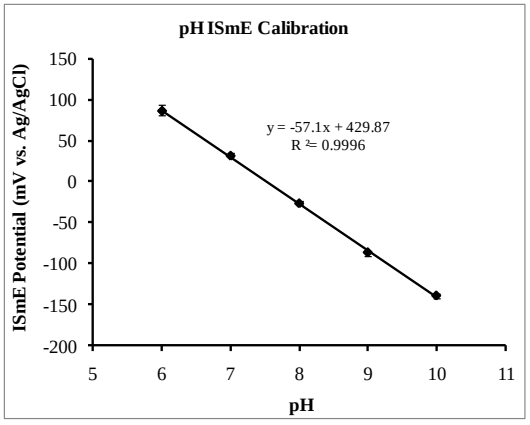

Figure 6.2 Calibration of pH ISmE at room temperature

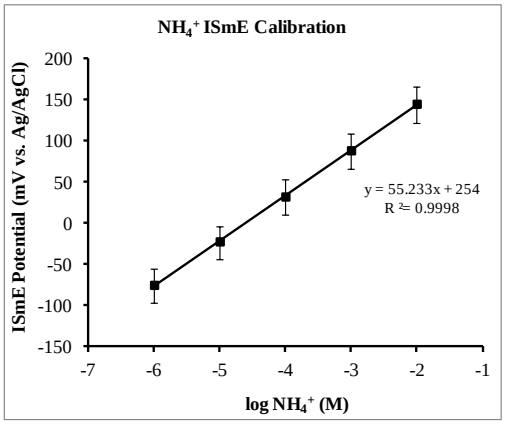

Figure 6.3 Calibration of NH_4^+ ISmE at room temperature

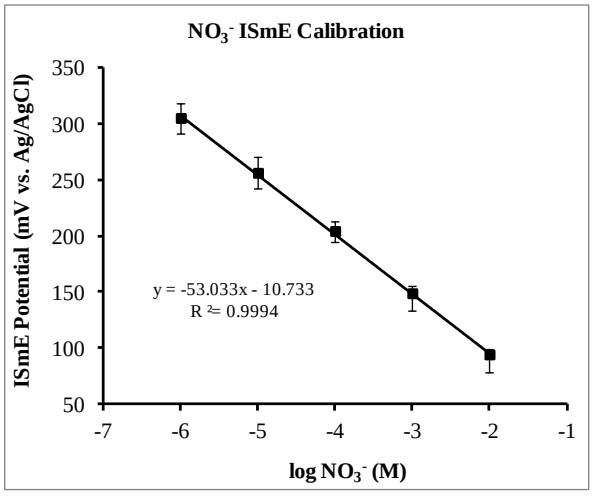

Figure 6.4 Calibration of NO_3^- ISmE at room temperature

6.4 Temperature Effect On Microsensor Evaluation

6.4.1 Temperature Effect on Combined Oxygen Microsensor Evaluation

Figure 6.5 shows the calibration curves of two oxygen microsensors calibrated at 23^{o}C (room temperature), 15^{o}C, 10^{o}C and 3^{o}C in de-ionized water. From the figure it was inferred that the current signal became smaller as the temperature decreased for air saturated conditions, thereby rendering a higher slope of the calibration curve at a lower temperature. The result demonstrated that for same current reading the dissolved oxygen concentration is higher in water at a lower temperature. The trend of oxygen concentration measured by the microsensor is, in principle, similar to the theoretical concentration of dissolved oxygen in water based on its solubility (barometric pressure = 760 mm Hg and salinity = 0). Figure

6.6 compares the effect of temperature on an O_2 concentration obtained from an O_2 mcrosensor calibration and based on theoretical solubility at different temperatures. To determine the O_2 concentration at a particular

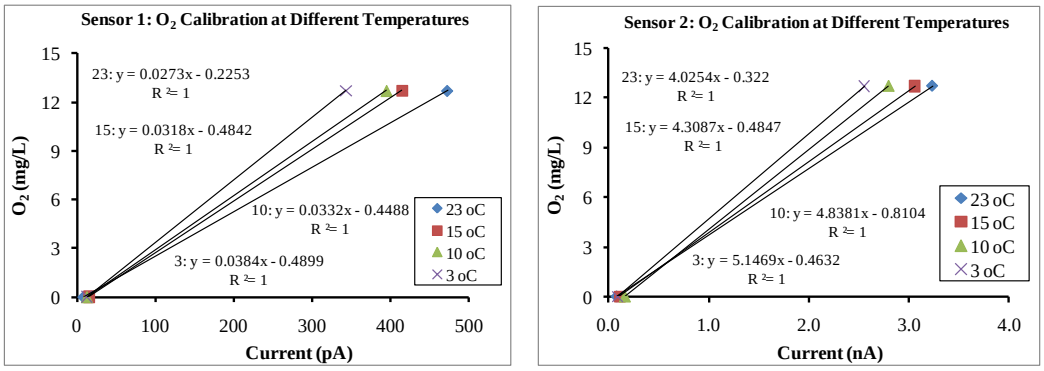

Figure 6.5 Combined O_2 microsensor calibration at different temperatures. The current values are average of three cycles of calibration in air saturated and zero oxygen conditions

temperature, a standard saturation concentration of O_2 was fixed at 3^oC, which matches with the highest solubility concentration of O_2 in water. The measured O_2 concentrations were interpolated among temperatures of interest based on the calibration curve given in Figure 6.5. The result (Figure 6.6) demonstrated that the O_2 concentration decreased with the temperature increase. A slight deviation in O_2 concentration was observed from the theoretical value as the temperature decreased. At 3^oC, the O_2 concentration was 6% less than the theoretical solubility value, whereas the difference was less than 1% at 15^oC. Therefore it could be concluded that temperature does not affect the O_2 microsensor performance.

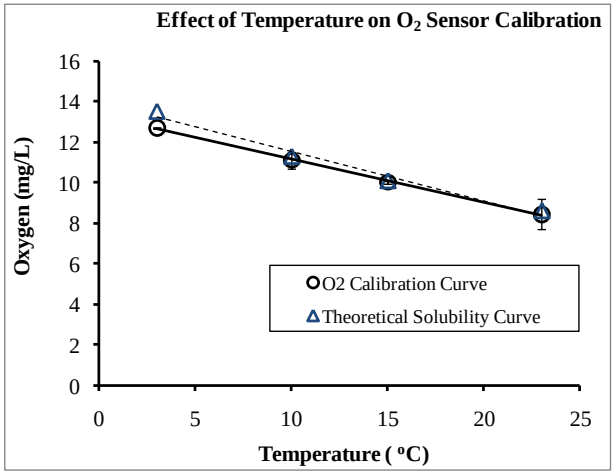

Figure 6.6 Comparison of O_2 concentration in water at different temperatures between microsensor measurement and theoretical solubility

6.4.2 Temperature Effect on pH ISmE Evaluation

This study was conducted to investigate the effect of temperature change on pH microsensor performance based on its slope. Three individual ISmEs were calibrated at different temperatures (23^{o}C, 14^{o}C , 8^{o}C, and 3^{o}C) in a pH range of 6 to 10 and performances of ISmEs at temperatures of interest were compared. Figure 6.7 shows the change of average slope of calibration curve of three pH microsensor at different temperatures. The slopes of ISmEs increased with the temperature increase. The slopes of tested ISmEs at room temperature were similar to the Nernst's slope of ideal microsensors. At lower temperatures, the tested ISmEs' slopes were slightly flat as compared to the Nernst's slope. The slope change could be interpreted as follows: the fabricated ISmEs gave a slightly lower concentration than ideal electrodes for a particular temperature. Shabala et al. (2006) using same commercial cocktail reported a slope change (from room

temperature to 4^{o}C) in their pH ISmEs to be below 8%. This research found that such a slope change was below 6% (from 23^{o}C to 3^{o}C).

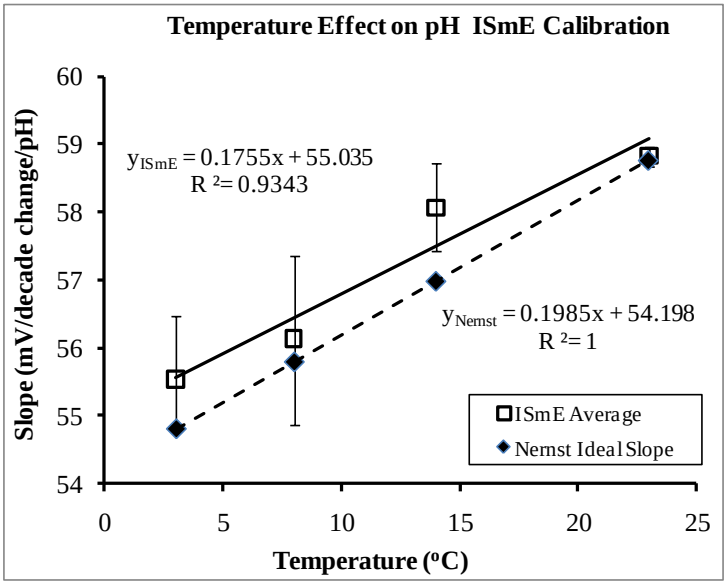

Figure 6.7 Average calibration curve's slope change of pH ISmEs at different temperatures

As expected, the slope of tested ISmEs increased with a temperature increase. The slope change deviation of tested ISmES from the Nernst slope change for an ideal electrode could be attributed to many factors that are temperature dependent. Since we used a commercial cocktail, the membrane resistance, due possibly change to cocktail's characteristics at different temperature, could be a major factor. In addition, the effect of temperature on a buffer solution could also be a factor. However, we did not use a buffer solution; therefore, the quantification of this influence on de-ionized water was negligible. Although the performance characteristics of the pH microsensor were close to that of ideal electrode (slope

above 54 mv/decade change) at a lower temperature, we recommend calibrating the microsensors at a temperature equal to the experiment.

6.4.3 Temperature Effect on NH_4^+ ISmE Evaluation

To study the temperature effect on the NH_4^+ ISmE performance, four individual NH_4^+ ISmEs were calibrated in a standard solution at varying temperatures of 23^oC, 14^oC , 8^oC, and 3^oC. The calibration procedure was same as mentioned earlier for pH ISmEs. The average of slopes of four individual ISmEs at specified temperature were compared with the slope of an ideal electrode (Figure 6.8). The slopes of ISmEs are more flat than slope of ideal electrode at all the temperatures of interest. The trend of slope change against temperature of fabricated ISmEs was found to be different from the change of slopes of ideal electrodes at lower temperature.

The trend of slope change against temperature for ISmEs was non-linear, whereas that for the ideal electrode was linear. The change of slope from 23^oC up to 14^oC of fabricated ISmEs was linear and steeper than the slope change for ideal slopes. But the trend of slope change of ISmEs from 14^oC to 3^oC was almost constant. Had temperature affected the NH_4^+ ion dissociation and ionic concentration, we would have observed a linear trend of slope change at a lower temperature.

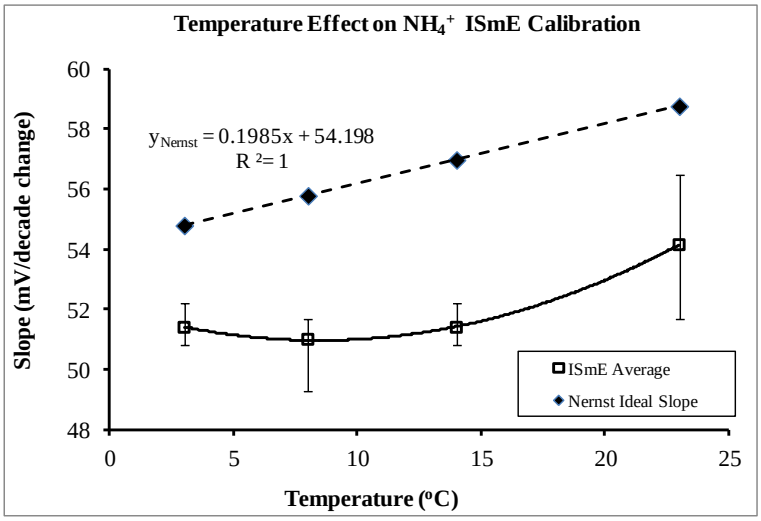

Figure 6.8 Average slope change of NH_4^+ ISmEs at different temperatures

From Figure 6.8, it is clear that the shift in thermodynamic equilibrium of NH_4^+ ion is ruled out. This suggests that temperature affects NH_4^+ ISmE's performance at certain temperatures below room temperature, below which the temperature change does not affect the ISmE performance based on slope. The effect could be attributed to the cocktail property, which is also temperature dependent. The result confirmed the practical usability of NH_4^+ ISmEs at a lower temperature, as the slopes are above 50 mV/decade change (Shabala, et al., 2006). The deviation of slopes from the mean slope of ISmEs at a particular temperature does not show any kind of trend, since the deviation is highest at 23^{o}C followed by 8^{o}C.

6.4.4 Temperature Effect on NO_3^- ISmE Evaluation

Three NO_3^- ISmEs were individually calibrated in a standard solution of KNO_3 at a concentration range of 10^{-6} M to 10^{-2} M of NO_3^- with varying temperatures of 23°C, 14°C, 8°C, and 3°C. The calibration procedure was the same as mentioned earlier for all ISmEs. The average slopes of calibration curves of three individual NO_3^- ISmEs at specified temperatures were compared with the slope of the ideal electrode. Figure 6.9 shows the comparison of calibration slopes. The slopes of ISmEs were smaller than the slope of ideal electrodes at all temperatures. In addition, the slope change against temperature was steeper than that of the ideal electrode. The slope change was slightly non-linear.

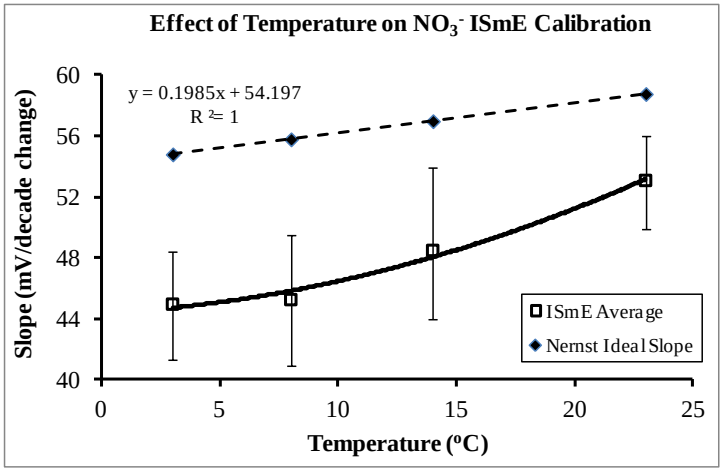

Figure 6.9 Average slope change of NO_3^- ISmEs at different temperatures

The reason for the smaller slope of individual NO_3^- ISmE compared to the slope of an ideal electrode could be attributed to selectivity of ionophore or cocktail. During calibration it was noted that the cocktail for the NO_3^- microelectrode was

slightly more viscous than the other ISmEs' cocktails. Also, the response time was slower than other ISmEs.

6.5 Summary and Conclusion

Any laboratory with apparatus and technical know-how can fabricate and calibrate microsensors. Moreover, chemicals used to fabricate and evaluate are tested at 25^{o}C, thus making them best suitable for room temperature. The was a lack of literature that evaluated microsensors' performances at various temperatures. Therefore, in order to understand the practical usability of microsensors at temperatures other than room temperature, combined oxygen microsensors, pH, NH_4^+, and NO_3^- ISmEs were fabricated and evaluated at temperatures 23^{o}C, 14^{o}C , 8^{o}C, and 3^{o}C based on the calibration slopes.

The oxygen concentrations measured at different temperature with two oxygen microsensors were compared with oxygen concentrations based on solubility of oxygen in water (at barometric pressure of 760 mm Hg and salinity of 0 ppm). The result demonstrated that the oxygen microsensors gave similar results with the concentrations due to solubility. Thus it was found that the effect of temperature on the oxygen microsensor performance was not prominent.

In the same manner, three to four pH, NH_4^+, and NO_3^- ISmEs with protein coating were calibrated in respective standard solutions at specified temperatures. The calibration curve's slopes of the ISmEs were compared with the Nernst's calibration curve's slope of an ideal electrode to determine the effect of temperature on sensor evaluation. The calibration curve's slope of pH ISmE did not differ with the calibration curve's slope of an ideal pH electrode at varying temperatures. The calibration curve's slopes of NH_4^+ and NO_3^- ISmEs were smaller than the calibration curve's slope of the ideal NH_4^+ and NO_3^- electrode at varying temperatures. The change in calibration curve's slopes against temperature were not necessarily linear in both cases. The calibration curve's slope change was negligible in NH_4^+ ISmEs below 14^{o}C. The reason could be that the cocktail property did not change below 14^{o}C, thus giving rise to a negligible slope change against temperature. The NO_3^- ISmEs followed the performance of the ideal electrode to 8^{o}C; below this the temperature the change in calibration curve's slope against temperature was non-linear.

The results of this research confirmed that oxygen microsensors and pH, NH_4^+, and NO_3^- ISmEs can be evaluated at different temperatures and used at a tested temperature range (3 to 23^{o}C). However, the microsensors must be calibrated at the experimental solution's temperature before being used for measurements.

In conclusion, the O_2 and ISmEs selective of pH, NH_4^+, and NO_3^- microsensors can be used in the temperature as low as 3^oC. Temperature correction may not be applicable for these microsensors, but microsensors need to be calibrated at the same temperature of the experiment before their use.

Chapter 7

MICROBIALLY MEDIATED AMMONIUM OXIDATION IN RIVER SEDIMENT UNDER ICE COVER MEASURED WITH MICROSENSORS

7.1 Introduction

This chapter presents the use of microsensors to profile the chemical concentration along the vertical depth of sediment cores. A combined O_2 microsensor and three ISmEs selective to NH_4^+, NO_3^-, and pH were used. The concentration profiles were used to develop activity profiles using Fick's laws of diffusion. Rates of oxygen consumption and ammonium oxidation were evaluated for various conditions such as nutrient loading, flowing and stagnant water and sediment exposure to light or dark.

Microbial degradation of organic matter in fresh water sediment releases primarily dissolved organic carbon (DOC), CO_2, dissolved organic nitrogen (DON), and NH_4^+ (Hansen et al., 1998). There exists a competition between heterotrophs and autotrophs, in the environment, including sediment, for substrates such as NH_4^+ and O_2 (Stief et al., 2003), but heterotrophs outcompete the autotrophs. However, in oxygen-limiting condition, autotrophs get benefit for NH_4^+ oxidation, (Satoh et al., 2004). The addition of ammonia in the river system due to anthropogenic

activities causes eutrophication, therefore its removal is necessary. Removing ammonia from the river system is carried out by nitrification and denitrification in sediment (Jensen et al., 1994).

The addition of ammonia to the river sediment could happen in two pathways: transport of NH_4^+ from the river water column to the aerobic zone of the sediment, and diffusion of NH_4^+ from the deeper anaerobic zone to the shallower aerobic zone of the sediment. The continuous supply of NH_4^+ onto the river bed creates a concentration gradient at the SWI; consequently, NH_4^+ is diffused to the sediment's aerobic zone. When organic matter degrades in the anaerobic zone, NH_4^+ is produced. The accumulation of NH_4^+ in the anaerobic zone develops a concentration gradient which causes a diffusion of NH_4^+ to the aerobic zone. These two pathways create an elevated level of ammonia useful for heterotrophic as well as autotrophic bacteria.

The ammonia oxidation occurs in the aerobic zone where oxygen is abundant, whereas denitrification normally occurs in the sediment's anoxic layer. Ammonia oxidation undergoes numerous steps before it is oxidized to nitrite and finally nitrate. Thus, nitrate production is normally understood as nitrification (Tchobanoglous et al., 2003). Complete ammonia oxidation and nitrification have been obtained in engineered wastewater treatment systems (Henze et al., 2002). The two most important factors for regulating nitrification are the availability of

oxygen and the supply of NH_4^+ by mineralization (Jensen et al., 1994; Nielsen et al., 1990). Temperature has a great impact on nitrification rates (Henze et al., 2002). Therefore it is imperative to determine ammonium oxidation at a lower temperature that could be related to the river sediment system of Canada's northern rivers.

It is well known that microorganisms living in diffusion-limited environments are exposed to steep chemical gradients (Revsbech, 1989) generated by the microorganisms themselves as a consequence of their tendency to locate themselves (by movement and/or proliferation) in layers in which optimal growth conditions prevail (Dalsgaard and Bak, 1992). The stratification of the organisms will be reorganized when external perturbations are imposed upon the community (e.g., changes in O_2 conditions), which will again be readily reflected in the other chemical gradients. In such environments, microsensor techniques are ideal tools for studying the principles of microbial regulation (Revsbech and Jorgensen, 1986).

The oxidation of ammonia coupled with nitrification and denitrification in fresh water sediment has been studied in the past decade (Revsbech et al., 2006; Altman et al., 2003; Stief et al., 2003, Meyer et al., 2001; Lorenzen et al., 1998). The general method used for determining the nitrogen cycle in sediment is to remove macro benthic fauna by sieving sediment and re-establishing the environment

inside the sediment (Altman et al., 2003; Jensen et al., 1994). Sometimes this re-established sediment is called model sediment (Jensen et al., 1994). Nitrogen transformation has also been found coupled with benthic macro and micro fauna (Henrikson and Kemp, 1988). Lorenzen et al. (1998) reported ammonia oxidation coupled with nitrification and denitrification in undisturbed diatom-inhabited fresh water sediment. It was also found that the nitrification rate increased when the sediment surface was exposed to light (Meyer et al., 2001; Lorenzen 1998). When light was absent, adding ammonia to overlying water of the sediment core did not influence nitrification rates (Lorenzen et al., 1998).

There is a considerable amount of literatures about nitrogen transformation studies in sediment, either at room temperature or above 10^{o}C. However, we could not find any work done at near zero temperature. Given the background of the Athabasca River in the ice-covered stage in winter, it is imperative to determine a nitrogen transformation process in the river sediment which could enable us to determine its impact on dissolved oxygen balance in the river. It is also assumed that the carbon and nutrient load that the Athabasca River receives continuously might be responsible for the DO deficit. The nitrogen transformation process inside sediment may also be influenced by the presence or absence of the light or diurnal changes. In Athabasca River the river water is under ice in the winter creating dark condition, but in the spring the river is exposed to light because of ice-break. This change of exposure condition from dark to light may also affect

the oxygen budget in the river. In order to investigate these scenarios experiment was conducted on sediment samples obtained from the Athabasca River.

The objectives of this research were: to understand the ammonium oxidation process in Athabasca River sediment at near zero temperature and its impact on oxygen consumption in order to establish a relationship between ammonium oxidation and SOD; to determine the impact of spiked load of NH_4^+ and TOC on ammonium oxidation; and to determine the impact of illumination on the ammonium oxidation process. In order to achieve research aims, a suite of microsensors including Clark's type O_2 microsensor, ISmEs selective of NH_4^+, NO_3^-, and pH were employed to obtain O_2, NH_4^+, NO_3^-, and pH profiles in sediment. The sediment cores were subjected to the spiked concentration of NH_4^+ and TOC. The sediment cores were also subjected to dark and light cycles to evaluate the impact of light in ammonium oxidation and nitrate production in the sediment. The concentration profiles of the chemicals were used to estimate ammonium oxidation rates and nitrate production rates.

7.2 Microsensor Measurement of Chemical Concentrations

7.2.1 Oxygen Penetration Depth and Oxygen Flux In Sediment

The oxygen penetration depth inside sediment indicates the aerobic zone inside sediment where microbes oxidize ammonium to nitrite and nitrate by the process of nitrification. Below this layer is the anoxic or anaerobic zone, where the microbial metabolic process occurs in absence of oxygen. In anaerobic conditions, reduced chemicals such as ammonium are diffused back to the aerobic zone. Figures 7.1, 7.2, and 7.3 show the oxygen profiles obtained by microsensor measurement. The broken lines in all figures represent the SWI. The depths are measured vertically downwards from the SWI. The concentration of oxygen at 100% air saturation at 3^{o}C is 13.45 mg/L (pressure = 760 mm Hg, salinity = 0 ppm). The oxygen profiles in all figures in the dark and illuminated conditions did not show much difference, but the profiles in flow conditions show a higher oxygen concentration in overlying water as well as inside sediment.

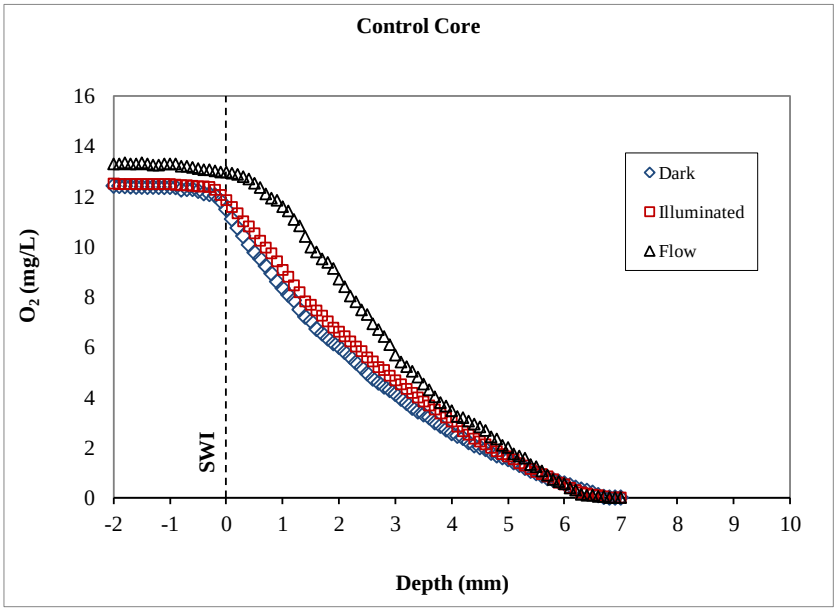

Figure 7.1 Oxygen profiles in control core at various conditions

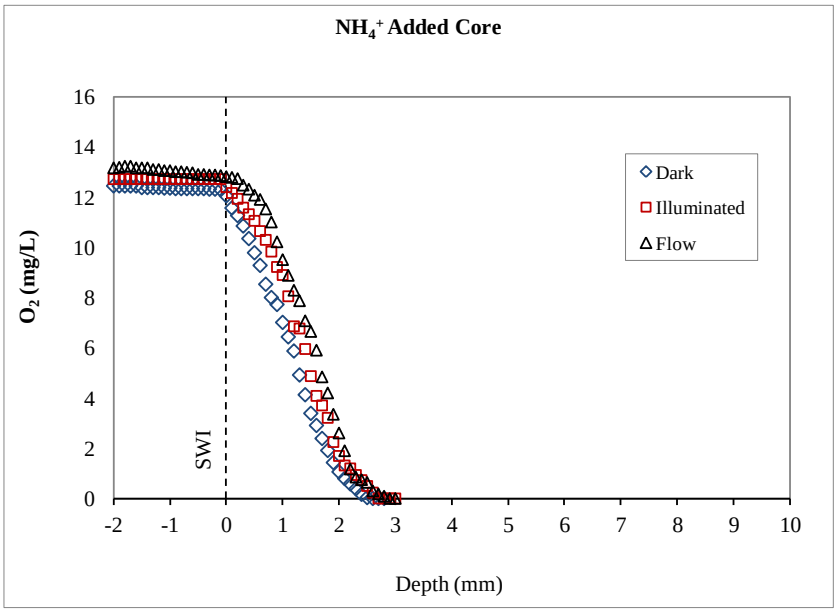

Figure 7.2 Oxygen profiles in NH_4^+ spiked core at various conditions

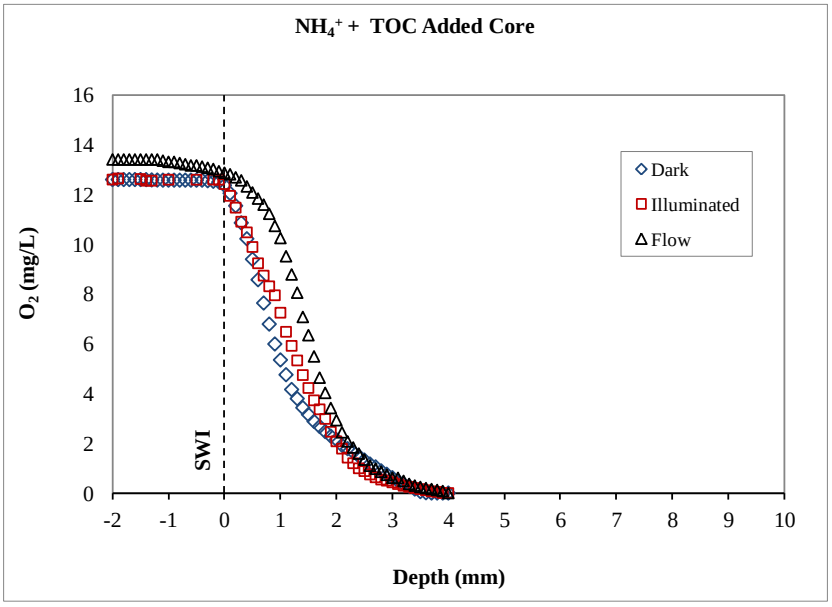

Figure 7.3 Oxygen profiles in NH_4^+ + TOC spiked core at various conditions

The depth of oxygen penetration changes once the nutrient is added (Figure 7.2

and Figure 7.3). As shown in Table 7.1, the oxygen penetration depth or thickness of aerobic zone in the control core in the dark was 6.8 mm. The aerobic zone reduced to 2.6 mm when ammonium was spiked in the overlying water. This reduction of the thickness of aerobic zone was also observed in other conditions too. But the aerobic zone of 3.7 mm was thicker in the core spiked with NH_4^+ + TOC than the core spiked with NH_4^+ alone. The reason could be that the TOC spiked in particulate form might have provided carbon to benthic microorganisms, particularly algal biomass, for their metabolism. The algae, being capable of photosynthesis, might have influenced the oxygen balance, thus giving a slightly thicker aerobic zone compared to the core spiked with only NH_4^+.

The oxygen penetration depth defines the thickness of aerobic zone. The aerobic zone is most important for redox reactions in the sediment-porewater systems. Ammonium is also oxidized in this aerobic zone. The more oxidation of organic matter and ammonium occurs, thinner the aerobic zone becomes. In this case the decrease in aerobic zone is due to the increased oxygen demand for more organic matter and ammonium oxidation. Moreover, the reduction of the aerobic zone means increase in anoxic/anaerobic zone leading to the transport of reduced chemicals to aerobic zone in elevated quantity.

The results of this research lead to conclude that the oxygen penetration depth reduces once the overlying water is loaded with nutrients irrespective of tested

conditions. This indicates that addition of nutrient in the water increases demand of the oxygen inside sediment which leads to decrease in oxygen penetration depth. In the Athabasca River, the nutrient load, either from point source discharges or efflux of nutrient from sediment to water column, can reduce the aerobic zone by exerting higher oxygen demand. Ultimate effect of this elevated oxygen demand is on the decrease in the river DO.

Table 7.1 Oxygen penetration depth in the sediment measured from the SWI

Condition	O_2 Penetration Depth in Sediment		
	Control Core	NH_4^+ Added Core	NH_4^+ + TOC Added Core
Stagnant	6.8 mm	2.6 mm	3.7 mm
Illuminated	6.8 mm	2.7 mm	3.9 mm
Flow	6.8 mm	2.9 mm	3.8 mm

Owing to sediment heterogeneity, a direct comparison of chemical profiles within a core and in between cores may give false information. Therefore the comparison of microbial activities is intended to show trends rather than to determine accurate values. Researchers have used the depth-specific activities to compare local consumption or production rates at different loading scenarios, e.g. the nutrient loading (Revsbech et al., 2006; Altman, 2003; Lorenzen, 1998), and the dark and the illuminated condition (Meyer et al., 2001).

The impact of oxygen penetration depth on the flux of oxygen can better be understood using oxygen consumption activities of microbes. The microbial

activities of oxygen consumption or production are calculated from the O_2 concentration profiles obtained by microsensor measurement. The activities are the local conversion rates in a layer. These activities are again used to determine flux of the oxygen. This flux can only be calculated for a specific depth. This flux is the local flux for an active layer of that specific depth in the sediment. In this way, to get the local flux, the net oxygen activity (sum of consumption activities or production activities) is multiplied by the depth to which the activity is integrated, as explained in Chapter 3, Section 3.10.3. For oxygen consumption activities, the depth of integration was selected based on oxygen penetration depth and the point at which oxygen consumption and production overlap. In most cases the depth was 2.4 mm. This depth was suitable to oxygen penetration depth for NH_4^+ spiked core, and other cores where oxygen consumption activities changed to production activities.

Table 7.2 presents the depth-specified oxygen flux in control, NH_4^+ spiked, and NH_4^+ + TOC spiked cores in stagnant and flow conditions in the sediment. The comparison of local flux was done between flowing and stagnation condition because flow of water over the sediment affects the oxygen consumption rate by increasing the oxygen transfer across the SWI (Revsbech et al., 1980). In addition to the flow, the illumination also affects the oxygen consumption/production rate (Revsbech et al., 1981). Because there was no significant impact of the illumination on O_2 concentration profiles as observed in the Figure 7.1, Figure

7.2, and Figure 7.3 we did not include the local fluxes at illuminated condition for comparison. Therefore a comparison of local oxygen flux between the stagnant and flowing water was used to determine impact of the water flow on oxygen flux inside sediment.

Table 7.2 Local oxygen flux in different scenarios in the dark

Depth-integrated Flux	Control Core		NH_4^+ Spiked Core		NH_4^+ + TOC Spiked Core	
	Stagnant	Flow	Stagnant	Flow	Stagnant	Flow
O_2 Flux of (g/m^2•d)	2.13	2.78	5.92	6.26	4.06	5.29
Ratio of O_2 flux (Flow to Stagnant)	1.31		1.06		1.3	

In Table 7.2 it is observed that the oxygen flux in the flow condition was higher than in the stagnant condition in all nutrient load conditions. About 30% more oxygen flux was observed at the flow condition in the control core as well as in the NH_4^+ + TOC spiked core. When TOC is added, bioturbation due to benthic fauna can increase the oxygen flux. However, the flow condition had a smaller effect (6% more) on oxygen flux than the stagnant condition in NH_4^+ spiked core. The reason for this smaller effect of the flow on the flux could be that diffusive transport was dominant over advective transport. The local oxygen fluxes in nutrient spiked cores are two to three times higher than those in the control core. The results lead to conclude that higher flux of oxygen means higher demand of oxygen or SOD in the sediment, when there is load of nutrient in water. This result showed that due to flow the high SOD rate can be obtained in the river

system than lake systems when loading and benthic properties are same. The result of increased O_2 flux due to flow also confirms the importance of water mixing in SOD determination apparatus used in river sediments, as discussed in 3.3.2.

The oxygen penetration depth, as shown in Table 7.1, decreased once the nutrient was spiked in the overlying water of the core. As a result, the oxygen flux increased in the nutrient-spiked core compared to the control core, as shown in Table 7.2. Because the oxygen flux in the NH_4^+ + TOC spiked core was smaller than in the NH_4^+ spiked core, which was not consistent with the oxygen penetration depth, the addition of particulate organic carbon along with NH_4^+ did not enhance oxygen consumption. This can be interpreted that the incubation duration was not sufficient for particulate organic carbon biodegradation. The duration of incubation was based on the duration of ice-cover on the river when sediment sampling was performed. This observation indicates that freshly deposited particulate organic carbon in the riverbed may not affect the benthic oxygen consumption under ice-cover until particulate organic carbon is converted to solubilised form.

In Table 7.2, the depth-integrated O_2 fluxes in the control core are greater than the SOD (which is also an oxygen flux) in the same location (USAM) of the Athabasca River derived by core incubation in Chapter 4 and Chapter 5. It should

be noted that the experimental sediment cores, collected from USAM, were incubated for 70 days, changing overlying water twice every week. Moreover, the river nutrient concentration was elevated by adding NH_4Cl to satisfy the microsensor measurement. The results lead to the conclusion of having higher oxygen fluxes in the control core than the oxygen fluxes of the river sediment determined by whole core method. Based on the results of this study, addition of nutrient increased oxygen flux.

7.2.2 Estimation of Ammonium Oxidation Activities Under Ice Cover

The NH_4^+ oxidation activities represent the microbial processes that convert ammonium to nitrite or nitrate by consuming oxygen. By measuring ammonium oxidation activities, the volume conversion rates of ammonium oxidation can be estimated. This study, designed to estimate microbial activities for ammonium oxidation, was conducted in the dark, so that the conditions were similar to those beneath the ice cover.

It is imperative to obtain comparative conversion rates of oxygen consumption, ammonium oxidation, and ultimate nitrification. Ammonium oxidation is also deammonification such that all of the ammonium is not nitrified, but a portion of it is assimilated during the benthic faunal and microbial metabolic activities. Therefore ammonium oxidation does not mean nitrification. For clarity the

nitrification is presented as nitrate production in this study. Moreover, denitrification is not considered, because of instrumental limitations during microsensor measurements. Normally denitrification occurs below the nitrification layer, well below the layer where oxygen becomes zero.

The microbial activities are estimated from the chemical profiles of the microenvironments inside sediment. Figure 7.4 shows the microenvironment inside sediment of the control core in the dark. The broken line shows the SWI. In Figure 7.4, the O_2 was observed to the depth of 6.8 mm. Accordingly, other chemicals were profiled to this depth. The NH_4^+-N concentration decreased from 280 mg-N/L at the SWI to 120 mg-N/L at 1.2 mm depth inside sediment. Below this depth, the NH_4^+-N concentration started to increase. The decrease in the NH_4-N concentration indicated autotrophic microbial activity. This de-ammonification process is related to the amount of oxygen consumption inside sediment, thus leading to ammonium oxidation. The occurrence of nitrification can be observed in Figure 7.4. The NO_3^--N concentration increased from 66 mg-N/L at the SWI to 98 mg-N/L at 0.9 mm depth inside the sediment. The occurrence of the nitrification process is also supported by the decrease in pH (Figure 7.4) at and below the SWI, since alkalinity is consumed during nitrification process (Tchobanoglous et al., 2003).

In Figure 7.4 the concentration of O_2, NO_3^-, and pH in the bulk water (above the SWI) were constant, however, the NH_4^+ concentration increased slightly near SWI in the bulk water. There could be two possible reasons for this increase in NH_4^+ concentration. One of the possible reasons could be the performance of microsensor at very low concentration. The NH_4^+ ISmE was calibrated before and after measurement and the same calibration curve was obtained without any distortion in the signal. The calibration results rule out the possibility of microsensor's malfunction at low concentration of NH_4^+. The other is the nitrogen fixation and mineralization of ammonium near the SWI. Nitrogen fixation by microfauna at the SWI could contribute to the increase in NH_4^+ concentration. Revsbech et al. (2006) have reported that nitrogen fixation is carried out by cyanobacterial species on or near the sediment surface in the dark or the illuminated condition, where NH_4^+ is produced. Other benthic fauna mineralize organic nitrogen to NH_4^+ at the sediment surface (Jensen et al., 1994). Stief and de Beer (2006) found NH_4^+ production in the vicinity of a burrow made by macrofauna. The sediment samples used in the research did not exclude existing habitants including benthal fauna, microalgae, and other plant and animal species. The existence of these benthic flora and fauna and their activities on nitrogen fixation and ammonium mineralization might have contributed to the increase in the NH_4^+ concentration near the SWI.

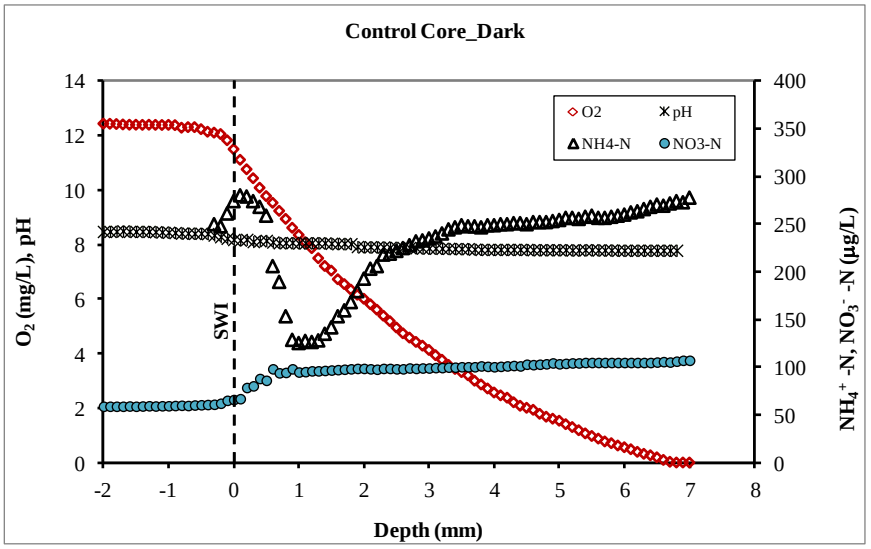

Figure 7.4 Profiles of O_2, NH_4^+, NO_3^-, and pH in control core in the dark

The fast increase in NO_3^--N concentration in Figure 7.4 to the depth of 1.0 mm from SWI, where NH_4^+-N concentration was at minimum, changed to gradual increase below this depth. Also down to the 1.0 mm depth from the SWI, there was ammonium oxidation and nitrate production. Below this depth the NH_4^+-N concentration started increasing. The increase in NH_4^+-N concentration slowed ammonium oxidation due to less availability of oxygen. Although the nitrate production in this region also slowed down, but the nitrate concentration continued to increase gradually in deeper section of the sediment. The gradual increase in the concentrations of NH_4^+-N and NO_3^--N in the deeper section can be explained by the diffusion and accumulation phenomenon.

The increase in NH_4^+-N concentration was observed in the river sediment, as described earlier in Chapter 4, Section 4.5. This increase could be due to

continuous diffusion of NH_4^+-N from water column to the sediment. At the same time, organic matters in the anaerobic zone of the sediment undergo microbial degradation releasing reduced compounds including NH_4^+. The continuous degradation of organic matter in anaerobic zone gives off elevated concentration of NH_4^+. The continuous accumulation of NH_4^+ in the deeper sections of sediment was the reason for elevated concentration in the deeper sections of the river sediment, as found in Section 4.5. This accumulated NH_4^+ diffuses to upper layers due to concentration gradient. The diffusion of NH_4^+-N reaches beyond the SWI to the river water for the same reason of concentration gradient. This hypothesis is confirmed by the efflux of NH_4^+-N observed in the river sediment, as described in the Section 4.5.

For the gradual increase in NO_3^--N in deeper section, as shown in Figure 7.4, same diffusion and accumulation hypothesis can be applied. There is continuous diffusion of NO_3^- from the river water to the sediment. In addition to this, ultimate result of the ammonium oxidation is nitrate production, through nitrification. The nitrification process leads to increased NO_3^- concentration in the sediment. Because of instrument limitation we were not able to profile NO_3^- concentration in deeper sections of the sediment. In order to determine the NO_3^- concentration in the deeper sections of the sediment, we sliced the sediment in 2 cm depth sections of all cores (control, NH_4^+ added, and NH_4^+ + TOC added) after microsensor measurement was completed. The NO_3^--N concentration of the pore water of the

sliced section were analyzed. Figure 7.5 shows that the NO_3^- concentration, indeed increased in top section (within 2 cm depth) of the sediment from the SWI. The nitrate was completely denitrified in the next second (2 to 4 cm depth) or third (4 to 6 cm depth) sections of the sediment from the SWI. Because complete denitrification occurred in anaerobic zone in deeper section, the diffusion of the NO_3^-, due to concentration gradient, was in downward direction in the sediment. Therefore it can be concluded that the gradual increase in NO_3^--N concentration in the deeper section of Figure 7.4 is due to the accumulation and diffusion phenomenon.

Pelegri and Blackburn (1996) reported that the nitrification was altered by the presence and actions of benthic macrofauna in the lake sediment. In this research undisturbed sediment samples, which included benthic micro-macrofauna, microalgae and other animals and plants, were used. Quantification of the effect of macrofauna was beyond the scope of the research, but it could also be one of the reasons for the trend of nitrification in Figure 7.4.

The oxygen consumption inside the sediment for ammonium oxidation and ultimately nitrification due to the microbial metabolism could better be presented by determining microbial activities. As described earlier, the microbial activities (also called local conversion rates or simply conversion rates) are obtained by the method of discrete differentiation of chemical fluxes, as explained in Section

3.10.3. In this research, the microbial activities were obtained by taking 5 data points (i.e. consecutive readings at equally spaced depths) of concentration, such that activities were calculated for a layer of 0.4 mm depth. In other words, the local conversions were performed within this layer. The reason for taking higher number of data points was to get smoother activity profiles.

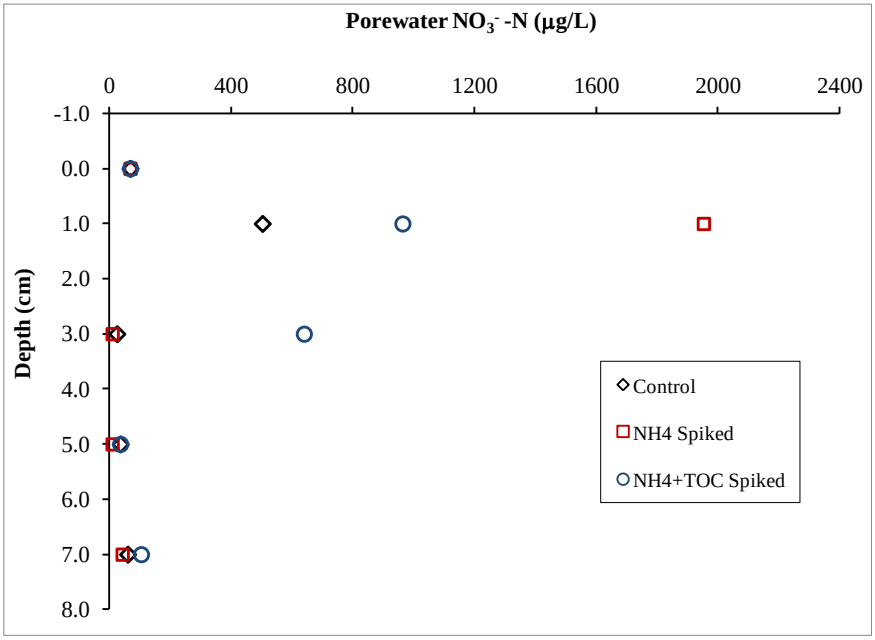

Figure 7.5 Porewater NO_3^--N concentration in the sediment sections of all cores in different loading condition

Figure 7.6, Figure 7.7, and Figure 7.8 show the profiles of activities of oxygen consumption, NH_4^+ oxidation and NO_3^- production, respectively. For simplicity, the negative and positive values of the activities (in x-axis) are the consumption activities and the production activities, respectively. It was observed that the

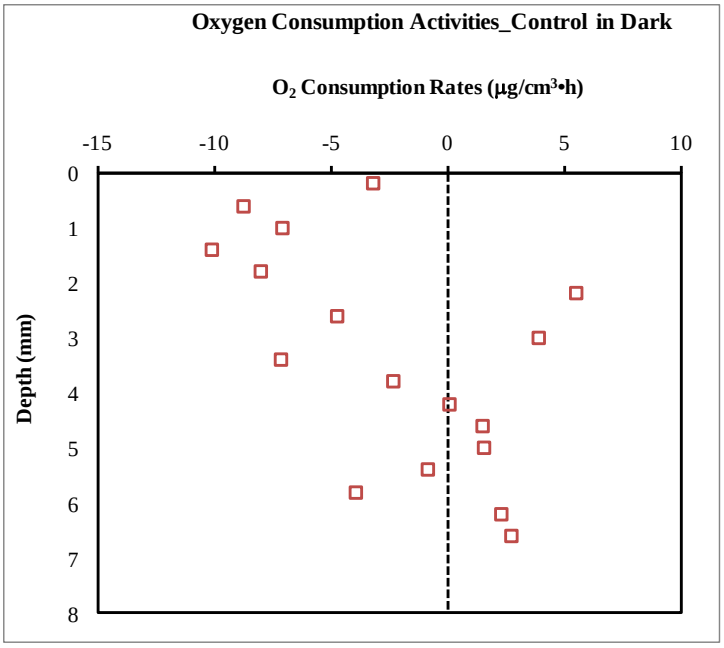

Figure 7.6 Oxygen Activities of Microbes in Control Core in Dark

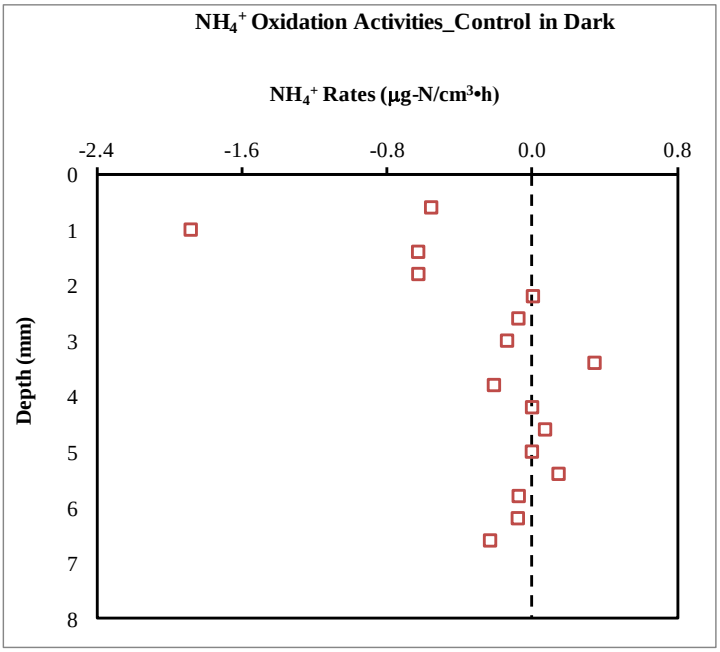

Figure 7.7 NH_4^+ Oxidation Activities of Microbes in Control Core in Dark

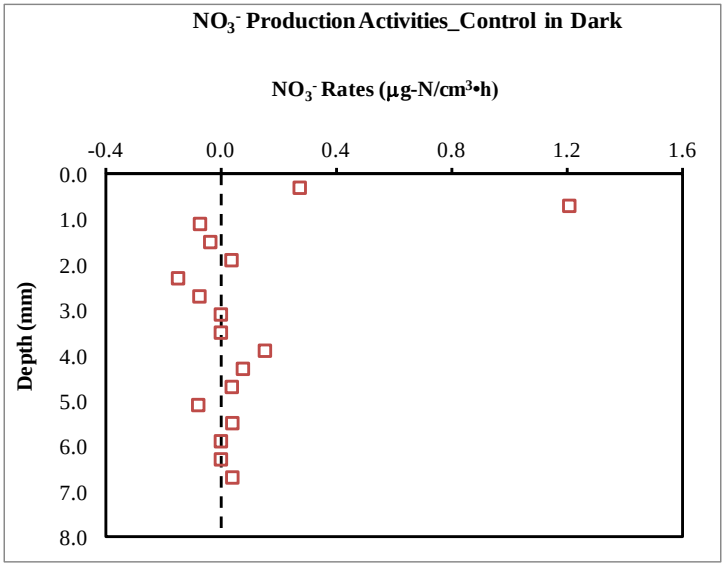

Figure 7.8 NO_3^- Activities of Microbes in Control Core in Dark

activity profiles are smooth for a certain depth from SWI, but smeared below this depth. Similar phenomena of smeared activities below a certain depth have also been observed by Satoh et al. (2004) in a biofilm. We used undisturbed sediment in our experiment and the benthic inhabitants of the sediment were not eliminated. The actions of benthic inhabitants could have had the effect on the alteration of the activities.

In Figure 7.6, the oxygen consumption activity or rate of oxygen removal was observed up to 4.2 mm of depth inside the sediment from the SWI, except at some odd data points. The peak activity of 10.01 µg/cm^3•h, occurred at 1.4 mm depth of the sediment. The NH_4^+ oxidation activity was also observed at depth of 4.2 mm from the SWI, as oxygen consumption activity. The peak deammonification

activity of 1.88 μg/cm^3•h occurred at the depth of 1.0 mm from the SWI. At the same time, smooth nitrate production activity was observed at the top 1.0 mm depth of sediment from the SWI, with the peak nitrification activity of 1.21 μg/cm^3•h at 0.6 mm depth from the SWI. Below this depth, the NO_3^- activity profiles were smeared. In Figure 7.8, very small activity of NO_3^- consumption was observed in the depth below 1.0 mm from SWI. There could possibly be assimilation or denitrification occurring. However, this activity of NO_3^- consumption changes to the activity of NO_3^- production below 3.4 mm from the SWI. The alteration of consumption and production of NO_3^- could either be caused by benthic fauna due to assimilation of NO_3^- in their metabolic activities, as described earlier, or there is denitrification occurring. Since the peak activities of ammonium oxidation and nitrate production occurred at a depth shallower than the 1.0 mm depth of the sediment, it can be concluded that nitrification occurred inside the sediment. At this depth high amount of oxygen consumption activity occurred. The oxygen consumption activity and NH_4^+ oxidation activity below 1.0 mm depth of the sediment indicate that there was partial oxidation of NH_4^+ but no production of nitrate. Nitrite production might have happened, but we were unable to quantify nitrite production. At low O_2 concentration and high NH_4^+ concentration, the nitrite build up could inhibit nitrification (Park et al., 2010), a sign of no nitrate production. Considering the very existence of benthic fauna, the assimilation of NH_4^+ and NO_3^- in their metabolic activity could also alter the local activities.

From the results it can be concluded that peak activities of O_2 consumption, NH_4^+ oxidation and NO_3^- production occurred at shallower depth (1.0 mm from the SWI). Nitrification occurred during the process of NH_4^+ oxidation, but not all NH_4^+ was converted to NO_3^-. There was possibility of producing nitrite during NH_4^+ oxidation. It was assumed that some of the NH_4^+ was used by benthic fauna in their metabolic activities, adding to NH_4^+ oxidation.

7.2.3 Impact of Nutrient Load on Ammonium Oxidation Activities Under Ice Cover

To study the impact of the nutrient load on ammonium oxidation, the overlying water in the core was spiked with 3 mg/L of NH_4Cl. In order to maintain the NH_4^+ concentration, overlying water was replaced twice a week. The microsensor measurement was performed 24 hours after the nutrient spiking. Figure 7.9 presents the microsensor measured profiles of O_2, NH_4^+, NO_3^-, and pH in the sediment core spiked with NH_4^+. It was observed that oxygen was not available below the depth of 2.6 mm from the SWI, which is much shallower than the oxygen availability depth of the control core (6.8 mm). Therefore it can be interpreted that once ammonium was spiked in the overlying water, the rate of oxygen consumption inside the sediment increased because the ammonium oxidizing bacteria were more active with the availability of the substrate.

The O_2 concentration in the overlying water (above the SWI) was constant. The NH_4^+-N concentration and pH were decreasing, while, NO_3^--N concentration was increasing in the overlying water. The NH_4^+-N concentration decrease in overlying water was due mainly to two reasons: diffusion of NH_4^+ inside sediment and assimilation or oxidation by microbial metabolic activities. The NH_4^+ oxidation is also supported by the increase in NO_3^--N concentration and decrease in pH, indicating nitrification process.

The NH_4^+-N concentration inside sediment decreased from 1.79 mg/L at the SWI to 1.0 mg/L at a depth of 1.6 mm from the SWI. Below this depth of sediment, the NH_4^+-N concentration increased. The reason for this increase in the NH_4^+-N concentration is that there was continuous NH_4^+-N production and accumulation at deeper sections where the anoxic/anaerobic environment existed. The NH_4^+-N could be diffused to the upper layers due to a concentration gradient, thereby increasing the NH_4^+-N concentration in the aerobic zone. In Figure 7.9, the NO_3^--N concentration was observed increasing below the SWI. This increase is due to nitrate production in the aerobic zone. The continuous increase in the NO_3^--N concentration in the deeper section could also be attributed to the accumulation due to the diffusion of the NO_3^--N concentration from the deeper section.

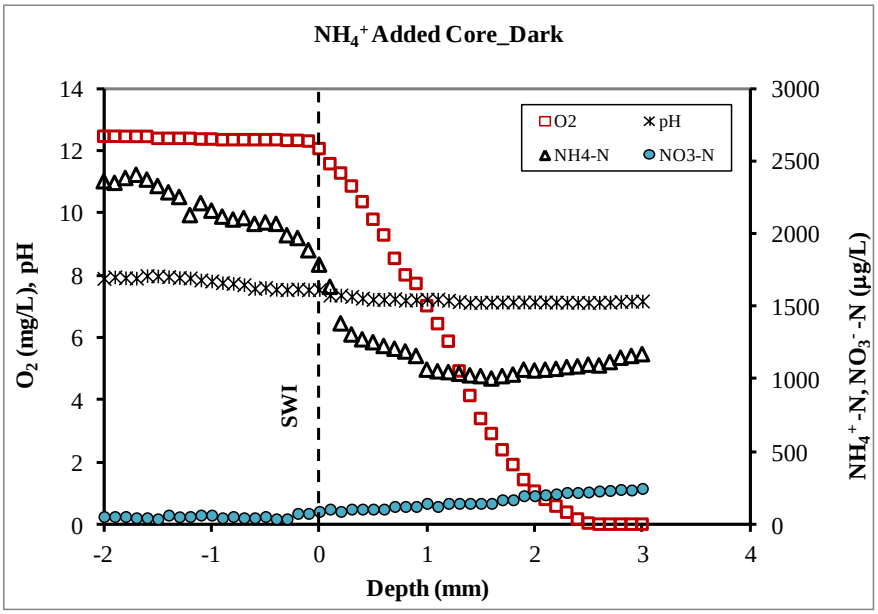

Figure 7.9 Profiles of O_2, NH_4^+, NO_3^-, and pH in NH_4^+ Spiked Core in the Dark

The concentration profiles lead to conclude that when NH_4^+ is added to overlying water, the oxidation of NH_4^+ occurs by consuming oxygen. Increased consumption of oxygen by the added ammonium for its oxidation causes the aerobic zone to be shallower inside sediment. In the Athabasca River, the increase in NH_4^+ load could take place by the waste discharges from pulp mills and municipal waste treatment plants, and ammonium flux from deeper anaerobic zone to aerobic zone in the sediment. As explained earlier, in Section 7.2.2, an efflux of NH_4^+-N from sediment to the overlying water adds to the NH_4^+ load to the Athabasca River. The increased load exerts more oxygen demand in the sediment thus reducing the DO level in the Athabasca River.

The process of NH_4^+ oxidation and nitrification inside the sediment in the nutrient spiked core is further explained by the activity profiles as presented in Figure 7.10, Figure 7.11, and Figure 7.12. The microbial activities of oxygen consumption, ammonium oxidation, and nitrification or nitrate production were observed up to a depth of 2.4 mm from the SWI inside the sediment. The peak activities of O_2, NH_4^+, and NO_3^- of values 39.63 $\mu g/cm^3 \bullet h$, 17.71 $\mu g/cm^3 \bullet h$, and 1.41 $\mu g/cm^3 \bullet h$ occurred at the depths of 1.4 mm, 0.2 mm, and 1.4 mm from the SWI, respectively. In Figure 7.11, the NH_4^+ oxidation activities were smeared below 1.6 mm from the SWI. There was the activity of NO_3^- production up to 0.6 mm from the SWI, below this depth there was NO_3^- consumption activity. At this depth there was no NH_4^+ oxidation activity, as observed in Figure 7.11. This means that either assimilation or denitrification occurred at this region or the nitrification was inhibited. Revsbech et al. (2006) reported that assimilation or denitrification was observed in aerobic zone of the sediment. This observation also explains the reason for 0.25 mg/L NO_3^--N production against 1.0 mg/L NH_4^+-N oxidation. Moreover, not all NH_4^+-N was converted to NO_3^--N.

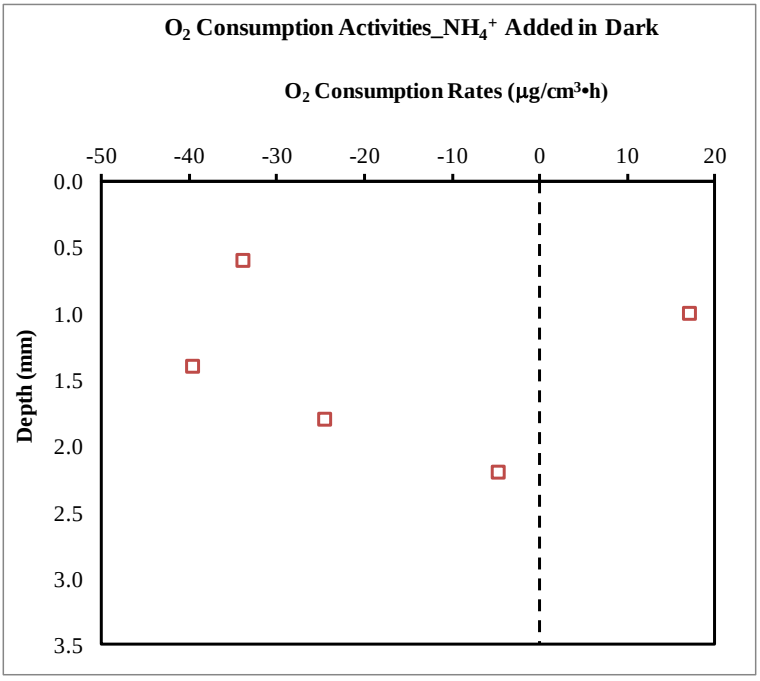

Figure 7.10 Oxygen Activities of Microbes in NH_4^+ Spiked Core in Dark

All peak activities in the NH_4^+ spiked core were higher than those in the control core, particularly ammonium oxidation. However, these activities are local conversion rates of chemicals; and the comparison of peak activities does not give net activities throughout the active layer inside the sediment. Therefore comparison of peak activities cannot be performed. For comparison of these activities in different loading scenario we have to calculate net activities for an active layer of the specific depth. The benefit of doing this is that fluxes of chemicals are calculated from these depth-specific net activities.

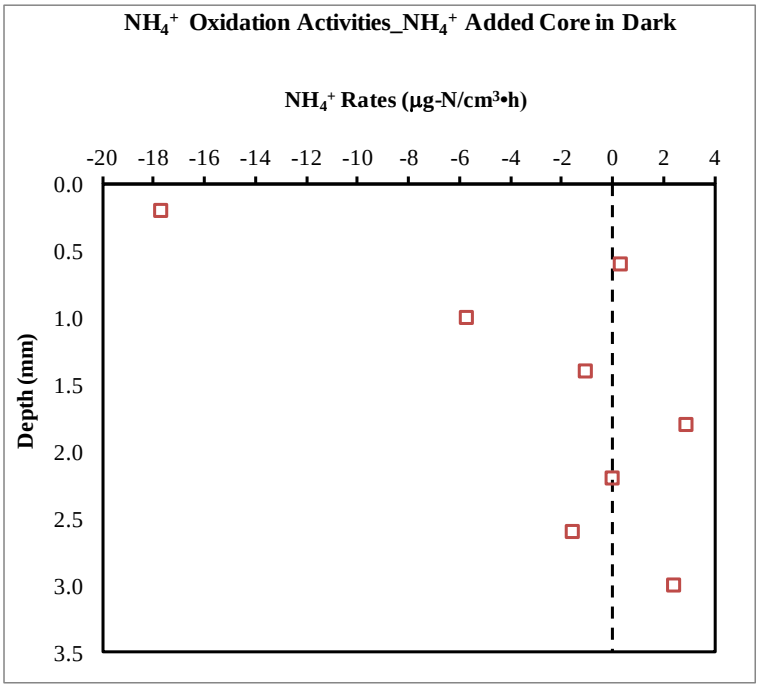

Figure 7.11 NH_4^+ Oxidation Activities of Microbes in NH_4^+ Spiked Core in Dark

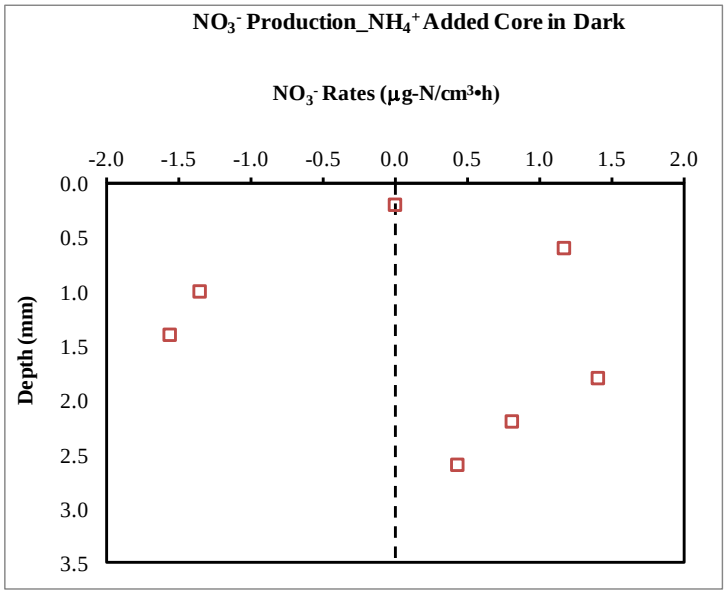

Figure 7.12 NO_3^- Production Activities of Microbes in NH_4^+ Spiked Core in Dark

The depth of the active layer for calculating net activities was 2.4 mm based on oxygen consumption/production activities, as explained in the Section 3.10.3, Chapter 3. Table 7.3 gives the net activities or conversion rates in control and NH_4^+ added cores. The net activity results showed that depth-integrated conversion rates of O_2, NH_4^+, and NO_3^- were three times, seven times, and two times higher, respectively, in nutrient added cores than control core. In the Athabasca River if 3 mg/L NH_4^+ is added to the river water in winter, the increased NH_4^+ load increases oxygen consumption rate three times of the normal rate, requiring higher flux of O_2 across the SWI to be diffused from water to the sediment. The amount of the O_2 flux required is such that this creates DO decline in the river water. In this analysis it is assumed that DO in the river is sufficient to meet the increased O_2 flux from bulk water to the sediment. On increasing NH_4^+ load to the river further, decrease in the DO would take place, thus degrading river water quality. Therefore in order to maintain the DO concentration in the river either the NH_4^+ load should be reduced or supply of oxygen to the river water should be increased.

Table 7.3 Depth-Integrated Net Activities or Conversion Rates in the Dark

Net Activities or Conversion Rates	Control Core	NH_4^+ Added Core
O_2 Consumption ($\mu g/cm^3 \bullet hr$)	-37.01	-102.80
NH_4^+ Consumption ($\mu g\text{-}N/cm^3 \bullet hr$)	-3.69	-24.52
NO_3^- Production ($\mu g\text{-}N/cm^3 \bullet hr$)	1.52	3.39

The results of microbial activities lead us to conclude that higher oxygen consumption rate was observed for higher ammonium oxidation rate, when nutrient load was added to the overlying water. This shrunk the DO penetration depth causing thinner aerobic zone. At the same time nitrate production rate also increased due to nitrification, however, not all ammonium oxidized was converted to nitrate due to partial nitrification.

7.2.4 Impact of Organic Carbon Load on Ammonium Oxidation Activities Under Ice Cover

The experiment was performed to observe the impact of organic carbon addition in the ammonium oxidation process. Organic carbon in particulate form was spiked in the core that contained 3 mg/L spiked ammonium. Starch was added as particulate organic carbon and measured as TOC. The spiked concentration was 4 mg/L of TOC. Figure 7.13 presents the microsensor measured profiles of O_2, NH_4^+, and NO_3^-, and pH in the sediment core spiked with NH_4^+ + TOC. Oxygen was available up to 3.7 mm depth of sediment in NH_4^+ + TOC spiked core. This aerobic depth was deeper than the depth in the NH_4^+ spiked core.

The concentration profiles, as shown in Figure 7.13, are similar to the concentration profiles of NH_4^+-N added core, except NH_4^+ profiles. The oxygen

was available to a depth 3.7 mm from the SWI, deeper than the depth in NH_4^+ added core. The NH_4^+-N concentration decreased from 1.27 mg/L at the SWI to 0.53 mg/L at 1.7 mm depth and gradually reached 0.43 mg/L at 3.1 mm depth. As observed in other loading conditions, below this depth of the sediment, the NH_4^+-N concentration started increasing. The process of deammonification was greater within the first 2.0 mm depth of the sediment in all loading conditions. Nitrate concentration gradually increased from 92.47 mg/L at the SWI to a higher concentration in deeper layers. The pH decline at the SWI also showed the nitrification process occurring. The phenomenon of ammonium removal could have occurred in two ways: by the assimilation of ammonium in microbial and benthic metabolism, and by nitrification.

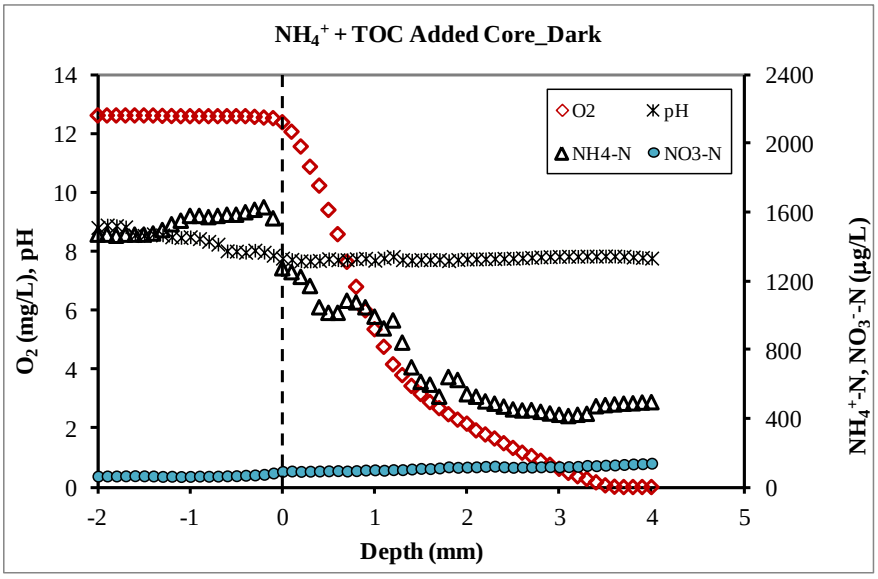

Figure 7.13 Profiles of O_2, NH_4^+, NO_3^-, and pH in NH_4^+ + TOC Spiked Core in the Dark

The concentration profiles showed that adding particulate organic carbon did not enhance oxygen consumption activities compared to the NH_4^+ addition. The reason could be that particulate organic carbon was not solubilised within the incubation period of 70 days. Yu (2006) reported that the addition of labile carbon source to the overlying water enhanced the oxygen consumption by reducing oxygen penetration depth. Although the TOC spiking concentration was selected based on the annual TOC peak value in the Athabasca River, spiked TOC in particulate form might not have influenced the oxygen consumption activities within the incubation period. Another reason could be that the heterogeneity of the sediment might have influenced the oxygen penetration depth. The ammonium oxidation and nitrate production could be better explained by activity profiles as shown in Figure 7.14, Figure 7.15, and Figure 7.16.

In Figure 7.14, the oxygen consumption activity was observed down to the depth of 3.4 mm in NH_4^+ + TOC spiked sediment core with the peak activity of 34.43 $\mu g/cm^3$•hr at 1.0 mm depth. Similarly, as shown in Figure 7.15 and Figure 7.16, the ammonium oxidation and nitrate production activities were observed down to 3.8 mm of depth with the peak activities of 11.09 $\mu g/cm^3$•hr and 0.80 $\mu g/cm^3$•hr occurring at a depth of 1.4 mm and 0.2 mm, respectively. Ammonium production activity near the SWI was observed since the NH_4^+ concentration increased at the SWI. A lower production of nitrate could be attributed to the assimilation of ammonium by microbes.

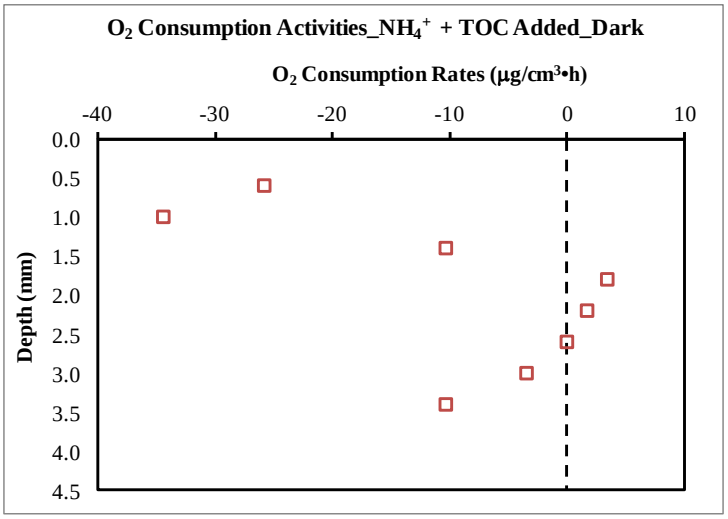

Figure 7.14 Oxygen Activities of Microbes in NH_4^+ + TOC Spiked Core in Dark

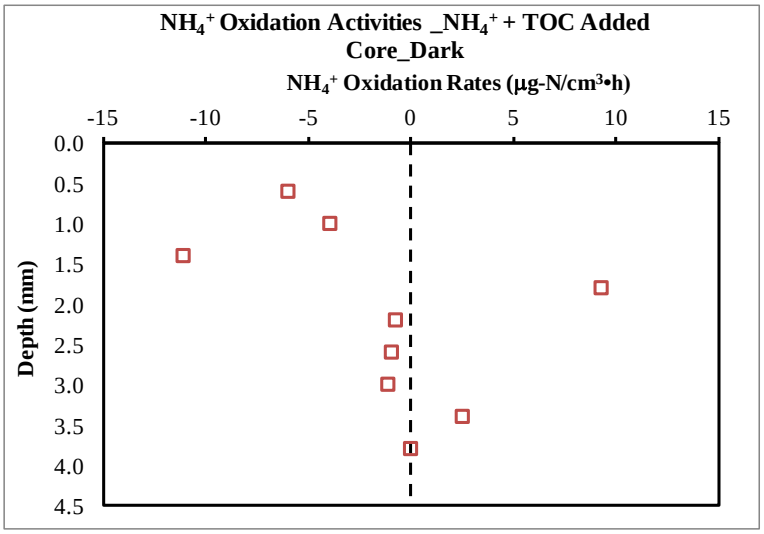

Figure 7.15 NH_4^+ Oxidation Activities of Microbes in NH_4^+ + TOC Spiked Core in Dark

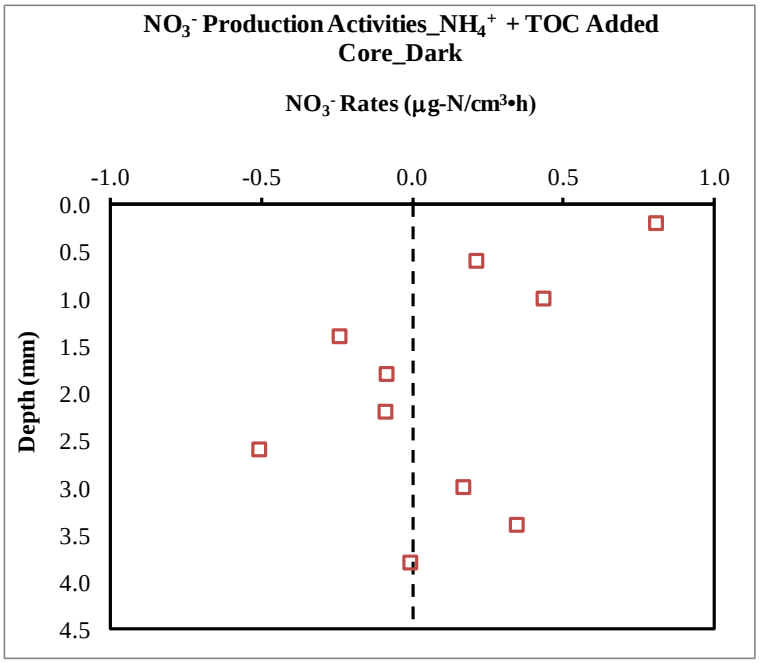

Figure 7.16 NO_3^- Production Activities of Microbes in NH_4^+ + TOC Spiked Core in Dark

The depth-integrated net activities of O_2 consumption, NH_4^+ oxidation, and NO_3^- production for specified depth of 2.4 mm from the SWI are 70.58 µg/cm^3•hr, 21.76 µg/cm^3•hr, and 1.45 µg/cm^3•hr, respectively. These conversion rates in NH_4^+ + TOC core were smaller than the conversion rates of the sediment spiked with NH_4^+ only. The selection of the integration depth might have played some role here. Since oxygen penetration in the NH_4^+ + TOC spiked core was 1.0 mm deeper than in the NH_4^+ spiked core, some activities were still occurring below the depth of integration, which could bring the activities in these cores at the same level. However, adding organic carbon was supposed to enhance the microbial metabolism, thus affecting oxygen consumption as well as nitrate production,

which did not happen. This indicates that the net conversion rates near the SWI remained the same even if particulate organic carbon was added. In addition, the TOC added was in particulate form and solubilization to labile organic carbon could not happen within the incubation period to enhance oxygen consumption activities.

7.2.5 Effect of Light in Oxygen Consumption and Ammonium Oxidation

Light affects oxygen availability in the water column as well as inside the sediment (Wetzel, 2003; Revsbech and Jorgensen, 1986). The Athabasca River is under ice cover in winter and the ice cover breaks in spring. The breaking of ice allows light penetration inside the shallow river water. Therefore the riverbed receives a light source to stimulate photosynthesis mediated by algal biomass. The light intensity might not be at the level of open water. However, this condition could be created during microsensor measurement since researchers have simulated illuminated conditions in laboratory experiments (Lorenzen et al., 1998; Meyer et al., 2001). In this study, sediment cores incubated in the dark were subject to one or two cycles of 12-h/12-h dark-light cycles by a source emitting a light intensity of 100 lux. All microsensor measurements were performed in illuminated conditions.

Figure 7.17, Figure 7.18, and Figure 7.19 present the microsensor measured profiles at the illuminated condition of O_2, NH_4^+, NO_3^-, and pH in three sediment cores: the control, spiked with NH_4^+, and spiked with NH_4^+ + TOC, respectively. The availability of oxygen inside the sediment was up to a depth of 6.8 mm, 2.7 mm, and 3.9 mm in the control core, NH_4^+ spiked core and NH_4^+ + TOC spiked core, respectively. The depths in the illuminated core were slightly higher than the depths in dark core, except for the control core, where depths were same in dark and illuminated condition. This indicates that illumination stimulates the activity of benthic fauna at the upper layer of the sediment. The profile of the NH_4^+ concentration in the overlying water of the control core was similar to the control core in the dark. As explained earlier in Section 7.2.2, the nitrogen fixation and ammonium mineralization by certain species of bacteria in the sediment might have caused the increase in the NH_4^+ concentration. The concentration profiles in other loading conditions are similar to those in the dark condition.

The NH_4^+-N concentration of 0.32 mg/L at the SWI in the control core decreased to 0.2 mg/L at the depth of 0.9 mm, and then the concentration gradually increased in the control core. In the NH_4^+ spiked core, the NH_4^+-N concentration of 1.94 mg/L at the SWI drastically decreased to 1.14 mg/L at 0.7 mm and further decreased gradually to 2.4 mm. Then, the NH_4^+-N concentration started increasing. While the NH_4^+-N concentration of 2.16 mg/L at the SWI in

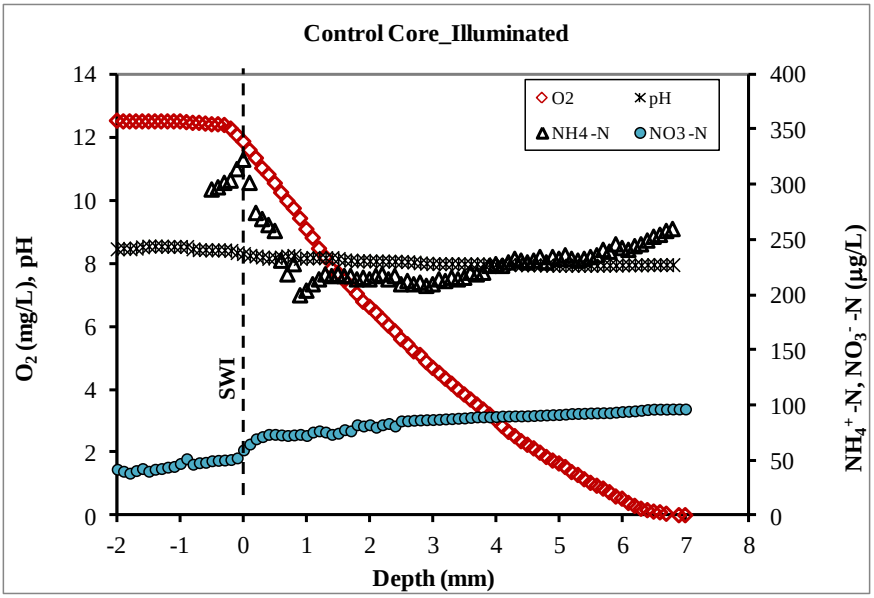

Figure 7.17 Profiles of O_2, NH_4^+, NO_3^-, and pH in Control Core Illuminated

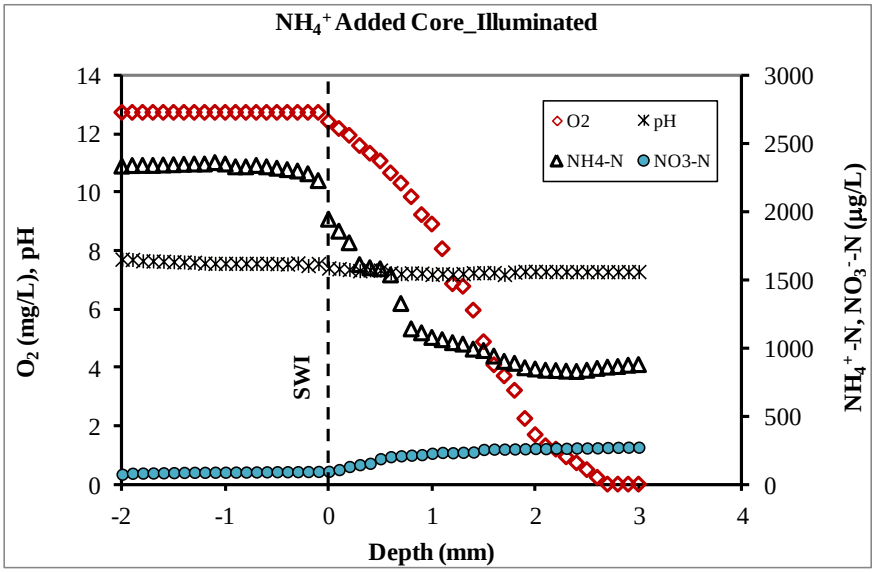

Figure 7.18 Profiles of O_2, NH_4^+, NO_3^-, and pH in NH_4^+ Spiked Core Illuminated

NH_4^+ + TOC spiked core decreased to 0.47 mg/L at 2.1 mm depth and continued decreasing gradually to a concentration of 0.39 mg/L. Similar to what occurred in

the condition of darkness, the NH_4^+-N concentration decreased within 2 mm depth from the SWI. The NO_3^--N concentration increased gradually to deeper sections due to nitrification.

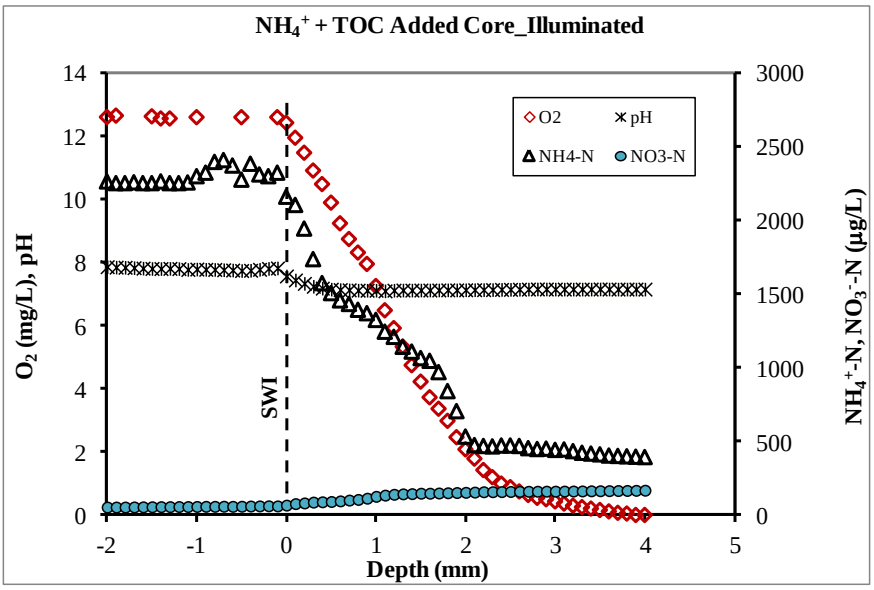

Figure 7.19 Profiles of O_2, NH_4^+, NO_3^-, and pH in NH_4^+ + TOC Spiked Core Illuminated

The process of ammonium oxidation in sediment cores in illuminated conditions could be better explained by microbial activities. The microbial activity profiles in the control core in illuminated conditions are presented in Figure 7.20, Figure 7.21, and Figure 7.22. The NH_4^+ oxidation activities were observed at the top 1.0 mm. Below this depth the activities were smeared. The trends of microbial activities were similar to those in dark conditions. Figure 7.23, Figure 7.24, and Figure 7.25 present activities in NH_4^+ spiked sediment cores in illuminated conditions. In Figure 7.23 the oxygen activity indicated oxygen production is

possible with photosynthetic activity of microalgae near the SWI. NO_3^- production was observed in deeper sections.

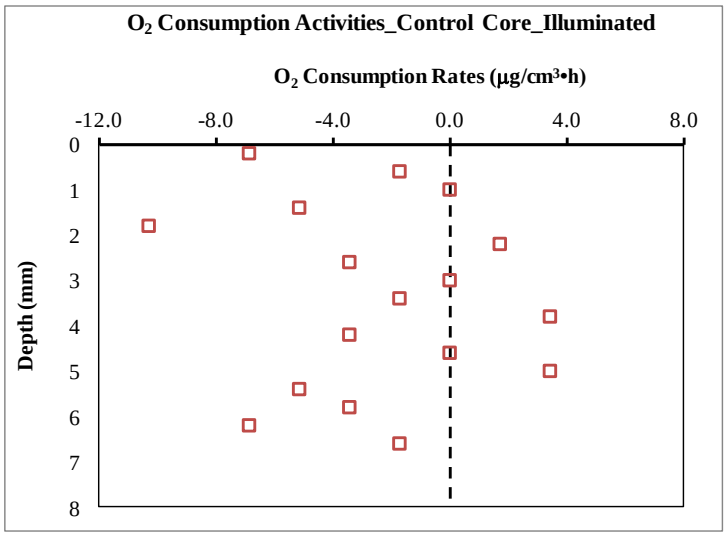

Figure 7.20 O_2 Consumption Activities of Microbes in Control Core Illuminated

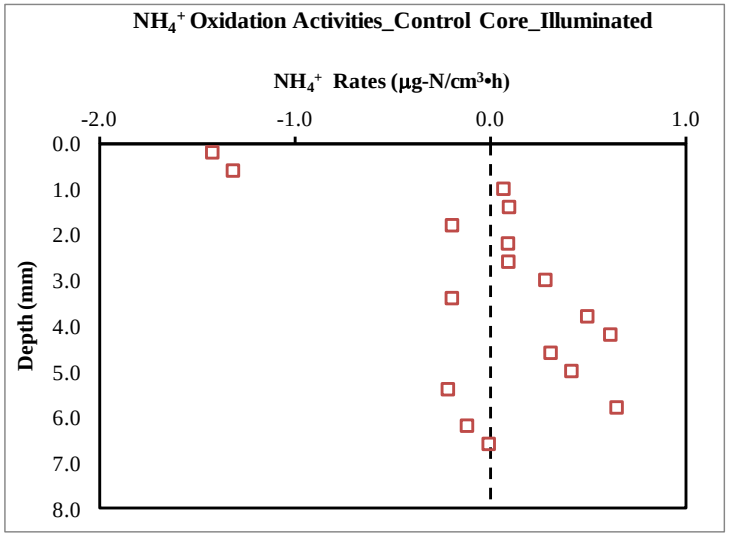

Figure 7.21 NH_4^+ Oxidation Activities of Microbes in Control Core Illuminated

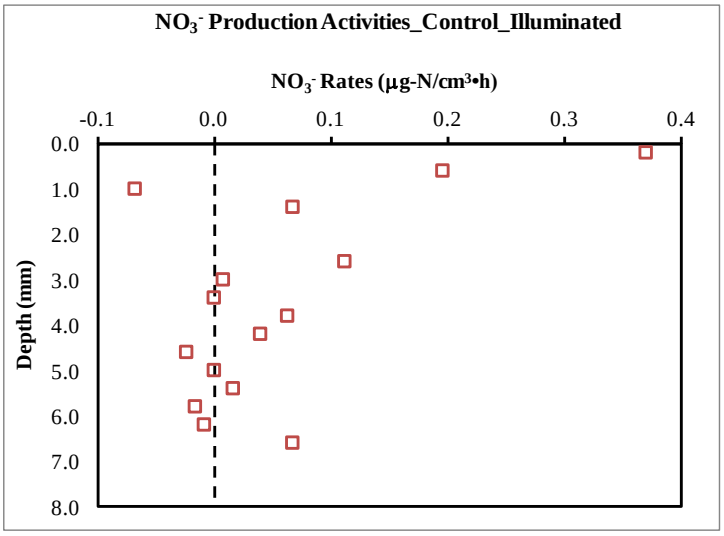

Figure 7.22 NO_3^- Production Activities of Microbes in Control Core Illuminated

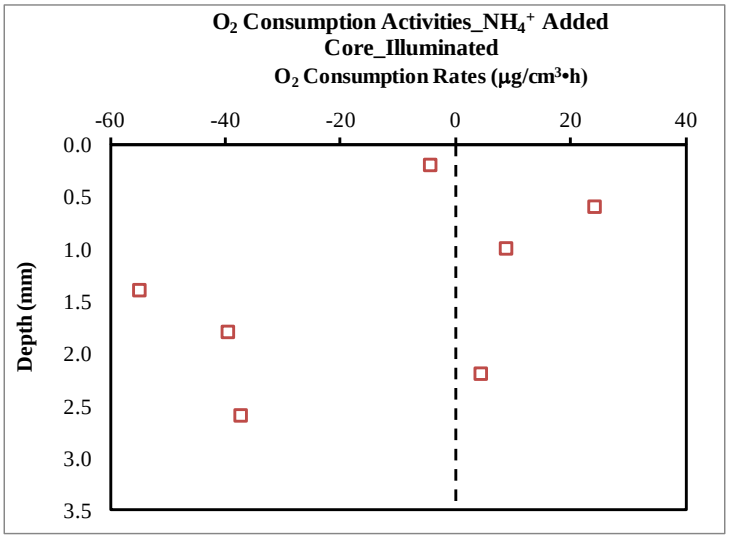

Figure 7.23 O_2 Consumption Activities of Microbes in NH_4^+ Spiked Core Illuminated

A good oxygen consumption activity and ammonium oxidation activity was observed in NH_4^+ + TOC spiked core illuminated, as shown in Figure 7.26 and Figure 7.27. At the same time in Figure 7.28, the trend of nitrate production

activity also coincides with O_2 consumption activities and NH_4^+ oxidation activities. A pH change was observed in the NH_4^+ + TOC spiked core when illuminated.

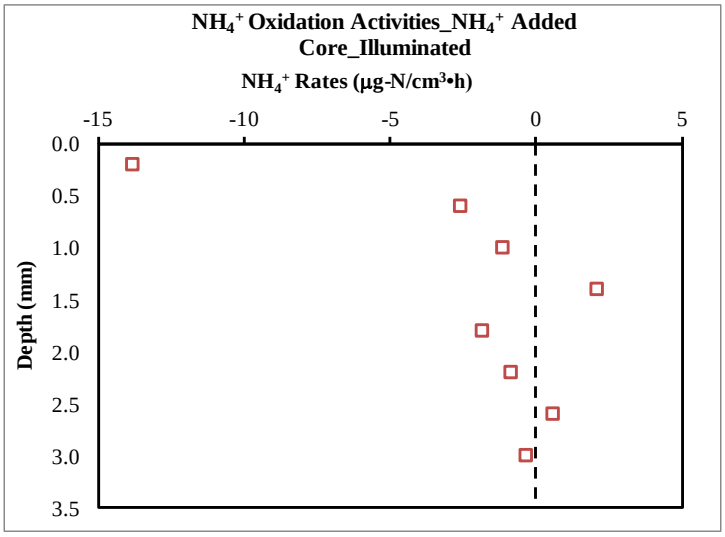

Figure 7.24 NH_4^+ Oxidation Activities of Microbes in NH_4^+ Spiked Core Illuminated

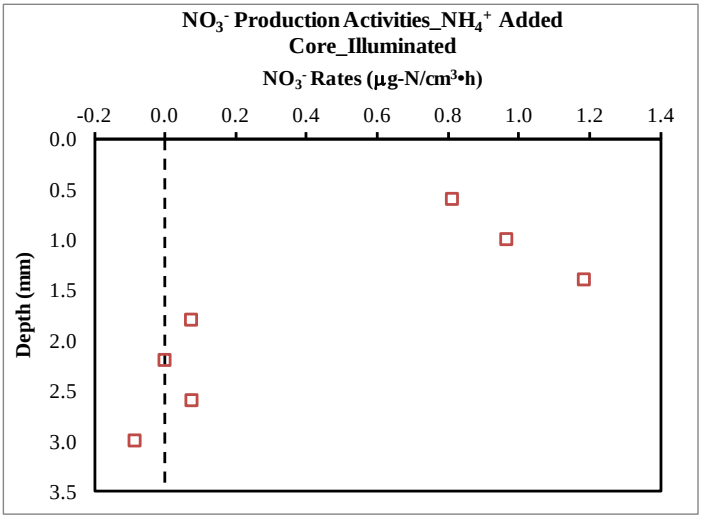

Figure 7.25 NO_3^- Production Activities of Microbes in NH_4^+ Spiked Core Illuminated

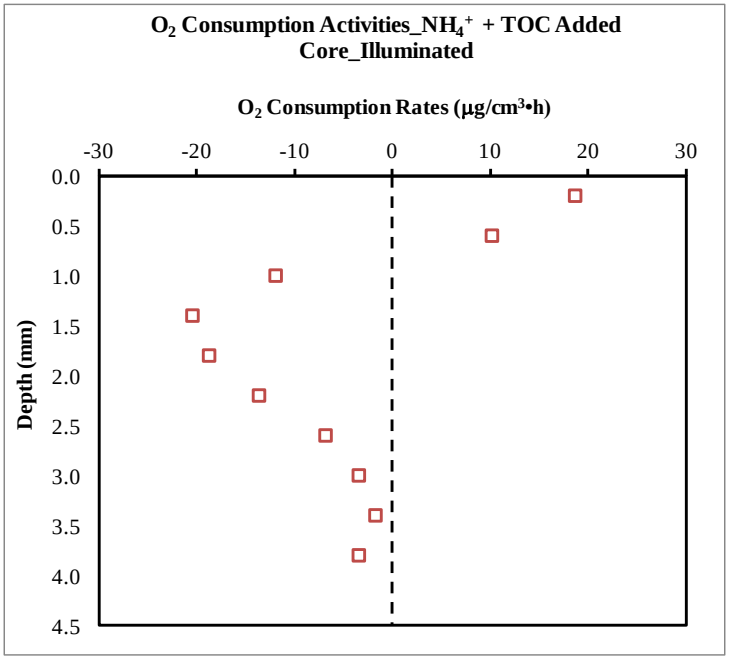

Figure 7.26 O_2 Consumption Activities of Microbes in NH_4^+ + TOC Spiked Core Illuminated

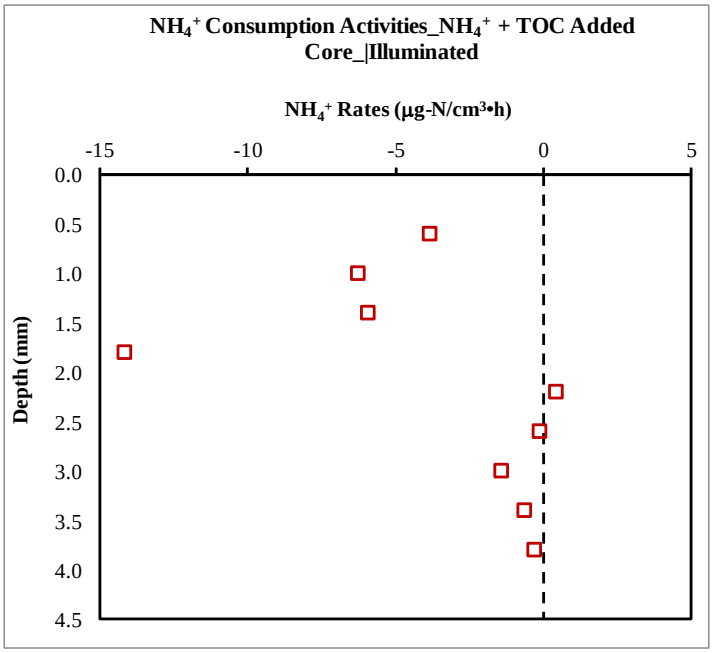

Figure 7.27 NH_4^+ Oxidation Activities of Microbes in NH_4^+ + TOC Spiked Core Illuminated

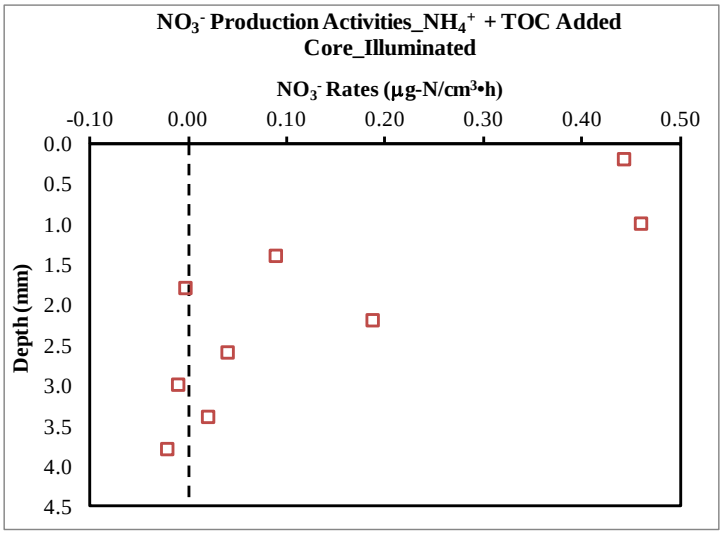

Figure 7.28 NO_3^- Production Activities of Microbes in NH_4^+ + TOC Spiked Core Illuminated

The microbial activities in different scenario can be compared by depth-specific net activities, or volume conversion rates, for an active layer. Table 7.4 gives a comparative volume conversion rates in the sediment cores having different nutrient loading. The negative and positive sign indicate the consumption and the production, respectively. Table 7.5 gives the flux of chemicals calculated based on

Table 7.4 Net microbial activities in different cores in dark and light conditions

Activities	Net Activities or Volume Conversion Rates (µg-N/cm^3•hr)*					
	Control Core		NH_4^+ Added Core		NH_4^+ + TOC Added Core	
	Dark	Illumi-nated	Dark	Illumi-nated	Dark	Illumi-nated
O_2 Activity	-37.01	-24.01	-102.80	-98.85	-70.58	-64.60
NH_4^+ Activity	-3.69	-2.93	-24.52	-19.72	-21.76	-21.42
NO_3^- Activity	1.52	0.74	3.39	3.03	1.45	1.18

*The unit for O_2 conversion rate is in µg-O_2/cm^3•hr

the net activities and depth of integration.

Generally, the net microbial activities are higher in nutrient added cores than those activities in control core. This shows that conversion rates increase when nutrient is added to the system. The net oxygen consumption activities were smaller in the illuminated core than the dark core in all nutrient conditions, including control core. The main reason for the smaller oxygen consumption activity in illuminated core than in the dark core is photosynthetic activity of bacteria in the sediment. In Figure 7.20 the activity of oxygen consumption changed to the activity of oxygen production below the selected depth for integration when control core was illuminated. Moreover, there were activities of oxygen production at 0.5 to 1.0 mm depth in both nutrient spiked cores when

Table 7.5 Depth-Integrated Flux of chemicals in different cores in dark and light conditions

Depth-Integrated Flux[#]*	Control Core		NH_4^+ Added Core		NH_4^+ + TOC Added Core	
	Dark	Illuminated	Dark	Illuminated	Dark	Illuminated
O_2	-2.13	-1.85	-5.92	-5.69	-4.07	-3.72
NH_4^+	-212.43	-196.87	-1412.47	-1168.00	-1253.1	-1233.70
NO_3^-	72.93	50.03	195.09	174.67	83.74	67.94
Depth of Integration	2.4	2.4	2.4	2.4	2.4	2.4

[#] The unit of O_2 flux is $g/m^2 \cdot d$; unit of the flux of NH_4^+ and NO_3^- is $mg/m^2 \cdot d$; unit of depth is mm

***** The units of flux were used for consistency with SOD and nutrient flux in Chapter 4

illuminated. A similar trend of activities of oxygen production was observed in NH_4^+ loaded condition, as shown in Figure 7.23 and Figure 7.26. The photosynthetic activity of bacteria was responsible for the activity of oxygen production inside the sediment. The photosynthetic activity of bacteria also caused reduction in the activity of oxygen consumption. This led to smaller net activities of oxygen consumption in the illuminated condition than in the dark in the control cores. Revsbech et al. (1981) observed increase in oxygen concentration inside sediment due to photosynthetic activity when the sediment was exposed to the light.

The activity of oxygen consumption is the result of ammonium oxidation activity, since the autotrophic bacteria require oxygen to oxidize ammonium. In Table 7.4, higher net oxygen consumption activities were observed when net ammonium activities increased, in most of the scenarios. Net ammonium oxidation activities were about six times higher in nutrient spiked cores than in the control core. During ammonium oxidation, nitrate was produced by nitrification process. Therefore nitrification or nitrate production activities are dependent on ammonium oxidation.

Considering nitrate production as nitrification we can determine the amount of nitrification from the total amount of ammonium oxidised by comparing the local fluxes. As observed in Table 7.5, the ammonium oxidation resulted in 25% to

34% of nitrification in the control core, about 15% in the NH_4^+ spiked core, and about 6% in the NH_4^+ + TOC spiked core. This means that only 15% of the ammonium oxidized was converted to nitrate in the NH_4^+ spiked core. Similarly, the amounts of nitrification were 15% and 36% more in the NH_4^+ +TOC spiked core compared to the amounts of nitrification in the control core in the dark and illuminated conditions, respectively. This shows that nitrification was more in the illuminated core than in the dark core. Lorenzen et al. (1998) have found that nitrification could be up to 50% of ammonium oxidation. Given the experimental temperature, the amounts of nitrification are within the range. The nitrate production activity profiles in nutrient spiked cores (Figure 7.11, Figure 7.15, Figure 7.24, and Figure 7.27) have been observed to have shifted in the deeper sections when illuminated. Such shifts have been observed when benthic fauna are active (Lorenzen et al., 1998). The shift in nitrification activities led to decreased nitrification rates in nutrient added cores. The nitrification rates would increase if total activity profiles were taken into account. This indicates that nitrification increases when ammonium is added, but the addition of organic matter reduces the nitrification rates. The organic carbon enhances denitrification in layers with low or no oxygen (Tchobanoglous et al., 2003). Therefore, the possibility of denitrification occurring in TOC added core cannot be ruled out.

The extent of oxygen penetration into the sediment has been shown to affect nitrate production and consumption (Nielsen et al., 1990). If oxygen is limiting

nitrification, increased oxygen penetration will stimulate nitrification. The effect on nitrate consumption can either be positive or negative. If nitrate consumption is closely coupled to nitrification, it will be stimulated by the increased nitrate production (Lorenzen, et al., 1998; Jensen et al., 1994). If not, consumption may decrease as the increased oxygen penetration pushes the anoxic nitrate reduction zone further into the sediment and increases the diffusion path of nitrate from the water phase to the consumption zone (Lorenzen et al., 1998; Nielsen et al., 1990). In our case the addition of the nutrient has caused the nitrification zone to extend, although the oxygen penetration depth did not change, therefore nitrate consumption or denitrification was pushed further deeper sections of the sediment.

The results of the impact of illumination on the ammonium oxidation revealed that oxygen consumption rates, ammonium oxidation rates and nitrate production rates were higher in the nutrient added cores compared to control core when illuminated. However, the oxygen consumption rate and ammonium oxidation rate were smaller in illuminated cores than their counterpart in the dark. The illumination increased the nitrification rate in nutrient spiked cores compared to control core. The nitrification increases when ammonium is added, but the addition of organic matter reduces the nitrification rates.

7.3 Summary and Conclusion

The chemical profiles of O_2, NH_4^+, NO_3^-, and pH at near zero temperature were obtained using Clark type O_2 microsensors, ISmEs selective of NH_4^+, NO_3^-, and pH in undisturbed sediment samples collected from the Athabasca River bed, for the first time in our knowledge. The undisturbed sediment samples were incubated at near zero temperature in the dark with the addition of NH_4^+ alone, and NH_4^+ + TOC for 70 days mimicking Athabasca River under ice cover in winter. O_2 was profiled in stagnant as well as flow conditions (flow velocity 0.83 cm/s) in a flow-through cell, while NH_4^+, NO_3^-, and pH could only be profiled in stagnant conditions. Thus, the impact of flow on solute diffusion and nitrogen transformation could not be determined. To study the impact of nutrient loading on the oxygen consumption rate in the sediment, the overlying water of each core was spiked with either 3 mg/L of NH_4^+ or 3 mg/L of NH_4^+ and 4 mg/L of TOC. The volumetric conversion rates were obtained from concentration profiles of each sediment core by integrating the activities of O_2 consumption, NH_4^+ oxidation, and NO_3 production to a depth.

The oxygen concentration profiling revealed that the O_2 penetration depth decreased significantly when the incubation core's overlying water was spiked with NH_4^+ or NH_4^+ + TOC. It was observed that adding particulate organic carbon (starch) represented by TOC did not affect the oxygen penetration depth. This

indicates that either solubilisation of particulate organic matter could not happen during the period, or that adding TOC enhanced the growth of other benthic fauna that suppressed oxygen consumption but increased NH_4 assimilation. The fluid flow over the sediment, mimicking river flow over the bed, increased the oxygen consumption rate, estimated from depth-integrated oxygen consumption activities in stagnant and flow conditions. The water flow result supports the proper mixing requirement to any SOD determination apparatus.

Based on depth-specific microbial activities the oxygen consumption rates of 37.07 $\mu g/cm^3 \bullet hr$ (dark) and 24.01 $\mu g/cm^3 \bullet hr$ (illuminated) in control core increased to 102.8 $\mu g/cm^3 \bullet hr$ (dark) and 98.85 $\mu g/cm^3 \bullet hr$ (illuminated), respectively, in 3 mg/L NH_4^+ added core. Similarly, the oxygen consumption rates increased to 70.58 $\mu g/cm^3 \bullet hr$ (dark) and 64.6 $\mu g/cm^3 \bullet hr$ (illuminated) in 3 mg/L NH_4^+ and 4 mg/L TOC added core. Therefore oxygen consumption increases when NH_4^+ load is added to the water. Addition of particulate organic carbon could not enhance oxygen consumption rate further due to lack of solubilisation at near zero temperature. Based on the above results, if 3 mg/L of extra NH_4^+ alone or together with 4 mg/L of TOC is added in the Athabasca River in winter the oxygen flux or SOD would rise about three times of the normal nutrient load. This increase in SOD would certainly reduce the DO concentration in the River.

The depth-integrated rate of ammonium removal, termed as the NH_4^+ oxidation rate of 3.69 $\mu g/cm^3 \bullet hr$ (dark) and 2.93 $\mu g/cm^3 \bullet hr$ (illuminated) in control core increased to 24.52 $\mu g/cm^3 \bullet hr$ (dark) and 20.29 $\mu g/cm^3 \bullet hr$ (illuminated), respectively in NH_4^+ added core, which is about six fold in the nutrient-spiked core as compared to in the control core. This demonstrated that addition of NH_4^+ increased ammonium oxidation rate. The NH_4^+ oxidation rates were almost same in the NH_4^+ spiked and NH_4^+ + TOC spiked core when illuminated. The results confirmed the increase in oxygen demand or SOD by the increased ammonium oxidation rate in the river sediment, in the event of increased nutrient load in the Athabasca River. All the NH_4^+ oxidized was not converted to nitrate. A part of the NH_4^+ was incorporated to benthic assimilation. The presence of micro and macro fauna in the sediment impacted the nitrification rate. There was a range of 6% to 34% of nitrification out of all NH_4^+ oxidation in different cores in dark and illuminated conditions. The addition of NH_4^+ increased nitrification, but the addition of organic carbon reduced nitrification. Also, it was observed that there is a shift in nitrate production in the deeper section in the nutrient and organic carbon spiked core at the illuminated stage due to shift in benthic fauna. When considering biologically mediated nitrogen transformation, pH plays role in clarifying nitrification and denitrification. The pH decreases during nitrification and increases during denitrification. In this study, the pH profiles supported nitrification because pH decreased at the SWI and along the depth. A higher pH drop at the SWI was observed in cores with nutrient and organic carbon addition.

Based on the analysis of the concentration profiles of O_2, pH, NH_4^+, and NO_3^- in the sediment for consumption and production activities of microbes in different loading scenarios, the following conclusions are made:

(1) The oxygen penetration depth decreased from 6.8 mm in control core to 2.6 mm when the core was added with NH_4^+ and 2.7 mm when the core was added with NH_4^+ and particulate TOC.

(2) The decrease in the penetration depth was due to high oxygen consumption in the sediment due to aerobic ammonium oxidation.

(3) The flow of water over the sediment increased the oxygen flux in the sediment, indicating increased SOD. This result also confirms the requirement of mixing in SOD determination apparatus.

(4) Ammonium oxidation increased in the sediment with the addition of nutrient, resulting in higher oxygen consumption. The depth-specific oxygen consumption rate increased to three times of the normal rate once 3 mg/L of NH_4^+ was added in the core under the experimental conditions, because of increased ammonium oxidation. The result indicates that in the event of increased load of nutrient in the Athabasca River, the SOD may increase considerably leading to decline of DO in the river water. This may lead to lower DO level in the river. Therefore to maintain the DO level in the river either the NH_4^+ load should be reduced or supply of O_2 to the river water should be increased.

(5) Although the particulate TOC addition did not increase oxygen consumption rate further than the rate of NH_4^+ addition, the addition of nutrient increased the oxygen consumption rate. The reason could be that particulate TOC was not solubilised within the duration of the experiment. This indicates that freshly added particulate organic carbon in the Athabasca River in winter may not increase oxygen consumption rate before particulate organic carbon is converted to labile organic carbon.

(6) The NH_4^+ concentration profiles revealed that there is accumulation and diffusion of NH_4^+ occurring in the sediment. The NH_4^+ diffuses upwards to aerobic zone from deeper anaerobic zone, confirming the NH_4^+ efflux from sediment to water as described in Chapter 5 using whole core incubation method.

(7) The increased depth-specific flux of NH_4^+ consumption as a result of the efflux contributed to the increased oxygen consumption rate.

(8) The nitrate production was observed in all loading scenarios but not all ammonium oxidized was converted to nitrate. Some of the ammonium oxidized was incorporated to benthic assimilation.

(9) Although the illumination did not enhance oxygen consumption rate and ammonium oxidation rate, the nitrate production was increased in the illuminated condition when the water was spiked with NH_4^+.

Chapter 8

CONCLUSIONS AND RECOMMENDATATIONS

This dissertation explores on the SOD in the Athabasca River in the winter when the river is covered with ice. At the scenario of reduced light penetration for photosynthetic activity and no reaeration, the oxygen demand from the sediment is the main sink for oxygen balance in the river. The factors that affect SOD in Athabasca River include chemical and physical properties of river water and sediment. One of the aims of the research was to relate these chemical and physical properties of water and sediment with the SOD. Also, these chemical and physical properties play role in microbial activities in the river water and inside sediment. Although the river water temperature is near zero in the winter, microbially mediated activities occur inside the sediment due to availability of food and suitable environment. Thus, it was imperative to understand whether microbially mediated chemical conversions are part of the SOD variation. To clearly understand microbially mediated chemical conversions, the research aimed at determining flux of chemicals including oxygen and nutrients (food for microbes) above and inside the sediment, using the whole core as well as the innovative and robust microsensor methods.

8.1 CONCLUSIONS

This research aimed to determine the factors affecting the SOD in the winter in the Athabasca River. The foremost part of the research was to develop SOD measurement technique, test and use the technique in the Athabasca River. A new laboratory based SOD measurement technique was developed for winter SOD determination applicable to river sediment under ice cover. The following conclusions are made based on the results of this research.

Based on the development and deployment of the new SOD measuring technique:

(1) A laboratory based SOD measurement apparatus was developed that addressed the issues of hydrodynamics inside sediment chamber; shape, size and enclosure of the chamber; continuous DO monitoring; and flexibility in operation. The apparatus is suitable for SOD determination in the Athabasca River, especially in winter, although it can be used for SOD determination in other aquatic systems.

(2) The apparatus was successfully used in determining nutrient flux across the SWI because of the added function of intermittent water sampling.

Based on the SOD of the Athabasca River sediment in alternate fall and winter seasons from fall 2006 through fall 2008, and the study of relationships of the SOD with water chemistry, sediment properties and nutrient flux:

(3) The SOD along the Athabasca River sediment at $4 \pm 1^{o}C$ varied in time and space ranging from 0 $g/m^2 \cdot d$ to 0.71 $g/m^2 \cdot d$ in the fall and 0.02 $g/m^2 \cdot d$ to 0.48 $g/m^2 \cdot d$ in the winter. In general, the SOD at the downstream sites was higher than the upstream sites of the Athabasca River.

(4) The SOD was positively correlated with TOC, TDP, and Chlorophyll-a in the fall. Although SOD was not correlated with TOC, TDP, and Chlorophyll-a in the winter, but TOC was the driving force in the SOD variation in both seasons. A generalized classification of SOD, based on the relationship of SOD and water chemistry in the fall, was made such that the SOD could be estimated from the easily measurable water quality parameter, the TOC. The classification of SOD is assumed to be important input to the DO modeling of the Athabasca River in winter.

(5) The sediment porosity was positively correlated to the SOD in both the fall and the winter, indicating porosity to be one of the factors affecting the SOD in the Athabasca River. The sediment porewater system provides food and shelter for microbial activities. These microbial activities exert demand for oxygen thus relating to the SOD.

(6) SOD was positively correlated with the efflux of NH_4^+ from sediment to the water column measured with the new apparatus at near zero temperature. The NH_4^+ efflux was the result of upward diffusion of NH_4^+ from anaerobic zone, the deeper section of the river sediment, where

NH_4^+ is accumulated due to anaerobic degradation of organic matter. In the Athabasca River the increased NH_4^+ flux would increase the SOD in winter.

In order to determine on NH_4^+ oxidation due to the microbial activities and the impact of the oxidation on the oxygen flux or the SOD, this research used a suite of microsensors. Impact of the nutrient addition on ammonium oxidation was also included in this research. The research evaluated and used ISmEs selective of NH_4^+, NO_3^-, and pH, and an O_2 microsensor at near zero temperature. Based on microsensor measured concentration profiles in the sediment subjected to different loading conditions, the following conclusions are made:

(7) The oxygen penetration depth decreased from 6.8 mm in control core to 2.6 mm when the core was added with NH_4^+ and 2.7 mm when the core was added with NH_4^+ and particulate TOC. The oxygen flux required within a depth-specified layer of the sediment for the aerobic oxidation of NH_4^+ was responsible for the decrease in the oxygen penetration depth.

(8) When the nutrient load is increased in the water column, the NH_4^+ oxidation increases resulting in increased oxygen consumption. The nutrient discharges the Athabasca River receives from the point and the non-point sources can increase the nutrient load in the river. Also, an

efflux of NH_4^+ from nutrient rich sediment to the water column may contribute to the increased oxygen consumption.

(9) If 3 mg/L of extra NH_4^+ alone or together with 4 mg/L of particulate TOC is added in the Athabasca River in winter the oxygen flux or SOD would rise about three times of the normal nutrient load. This increase in SOD would reduce the DO concentration in the River. Therefore to maintain the DO level in the river either the NH_4^+ load should be reduced or supply of O_2 to the river water should be increased.

(10) Although the particulate TOC addition did not increase oxygen consumption rate further than the rate of NH_4^+ addition, the addition of nutrient increased the oxygen consumption rate. The reason could be that particulate TOC was not solubilised within the duration of the experiment. This indicates that freshly added particulate organic carbon in the Athabasca River in winter may not increase oxygen consumption rate before particulate organic carbon is converted to labile organic carbon.

(11) Not all NH_4^+ oxidized produced nitrate by nitrification, a part of the total NH_4^+ oxidation could be accounted for benthic assimilation.

(12) Although illumination did not enhance oxygen consumption and NH_4^+ oxidation, but illumination increased nitrate production.

8.2 RECOMMENDATIONS FOR FUTURE STUDIES

(1) Improvement of SOD measurement technique is a continuous process. Because flow influences SOD, mixing mechanism is an integral and important part of the SOD measurement apparatus. In this research we used average flow velocity of the Athabasca River to design the mixing capacity of the apparatus. To improve the applicability of the apparatus in different locations with different flow velocities, it is recommended to evaluate the mixing in the apparatus with various rotational speeds of the motor so that close to *in situ* condition could be achieved and correct SOD value could be obtained for those locations.

(2) This research investigated impact of nitrogen dynamics on SOD in the Athabasca River sediment. Because of the instrumental limitation, carbon recycling inside sediment could not be investigated. Carbon burial and recycling is important factor for early diagenesis and the SOD, new techniques, such as carbon isotopes etc., could be used to investigate carbon burial and recycling inside river sediment.

(3) The microsensor profiling showed chemical environment for ammonium oxidation and nitrification inside sediment at near zero temperature. In order to supplement the microbial activities determined from microsensor profiling it is recommended to study the population dynamics of

microbial species responsible for ammonium oxidation and nitrate production.

(4) Nutrient flux across the SWI is found to be an important factor for the SOD in the Athabasca River, based on this study on sediment at representative but limited sites of the Athabasca River. The nutrient flux can be used to estimate nutrient budget across the SWI. In order to determine waste load allocation along the river by the regulatory authority, using these nutrient budgets, study of nutrient flux at more locations along the river is recommended.

REFERENCES

Adams, D. A. (1994). "Sediment Pore Water Sampling". In: *Handbook of Techniques for Aquatic Sediments Sampling* (Alena Murdoch and Scott D. MacKnight Ed.), 2nd Edition, Lewis Publishers, Boca Raton.

Arega, F. and Lee, J. H. W. (2000). "Diffusional Mass Transfer at Sediment–Water Interface of Cylindrical Sediment Oxygen Demand Chamber". *Journal of Environmental Engineering*, 131(5):755-766.

Altmann, D. (2003). "Nitrification in Freshwater Sediments as Studied with Microsensors and Fluorescence In Situ Hybridization". Ph. D. Dissertation, University of Bremen, Germany.

Altmann, D., Stief, P., Amann, R., de Beer, D., Schramm, A. (2003). "In situ distribution and activity of nitrifying bacteria in freshwater sediment". *Environmental Microbiology*, 5(9):798–803.

Amann, R. and Kuhl, M. (1998). "In Situ Methods for Assessment of Microorganisms and Their Activities". *Current Opinion in Microbiology*, 1:352-358.

Amann, R. and Kuhl, M. (1998). "In situ Methods for Assessment of Microorganisms and Their Activities, *Current Opinion in Microbiology*, 1:353-358.

Ammann D. (1986). "Ion-Selective Microelectrodes". Springer Verlag, New York, USA.

ASTM, (1994) “Annual Book of Standards (Section 4) Construction: Soil and Rock (I), Vol. 8”. American Society for Testing and Materials (ASTM), Philadelphia, PA.

Baity, H. G. (1938). “Some factors affecting the aerobic decomposition of sewage sludge deposits”. *Sewage Works Journal*, 10:539-68.

Barron, J. J., Ashton, C., Geary, L. (2008). “The Effects of Temperature on pH Measurement”. *TSP-01, Issue 1*, Reagecon Diagnostics Ltd, Ireland.

Belanger, T. V. (1981). “Benthic Oxygen Demand in Lake Apopka, Florida”. *Water Research*, 15:267-274.

Bennett, J. P., and Rathburn, R. E. (1972). “Reaeration in Open-Channel Flow”. USGS Professional paper 737:75.

Berner, R. A. (1980). “ Early Diagenesis A Theoretical Approach”. Princeton University Press, N J.

Boudreau, B. P. (1997). “Diagenetic Models and Their Implementation”. Springer Verlag, Heidelberg, Germany.

Boudreau, B. P. and Jorgensen B. B. (2001). “The Benthic Boundary Layer: Transport Processes and Biogeochemistry”. Oxford University Press, New York.

Bouldin D. R. (1968). “Models for Describing the Diffusion of Oxygen and Other Mobile Constitutents Acrosss the Mud-Water Interface”. *Journal of Ecology*, 56(77):77-87.

Bowie, G. L., Mills, W. B., Porcella, D. B., Campbell, C. L., Pagenkopf, J. R., Rupp, G. L., Johnson, K. M., Chan, P. W. H., Gherini, S. A., Chamberlin, C. E., (1985). "Rates, Constants and Kinetic Formulations in Surface Water Quality Modeling". 2nd Edition, EPA Office of Research and Development, Athens, GA.

Bowman, G. T. and Delfino, J. J. (1980). "Sediment Oxygen Demand Techniques: Review and Comparison of Laboratory and In Situ Systems". *Water Research*, 14:491-499.

Broecker, W. S. and Peng, T.-H. (1974). "Gas Exchange Rates Between Air and Sea". *Tellus*, 26:21–35.

Cai, W.-J., Sayles, F. L., (1996). "Oxygen penetration depths and fluxes in marine sediments". *Marine Chemistry*, 52:123-131.

Caldwell, J. M. and Doyle, M. C., (1995). "Sediment Oxygen Demand in the Lower Willamette River, Oregon, 1994". U. S. Geological Survey, Water-Resources Investigations Report 95–4196, Portland, Oregon.

Carlini, W. G. and Ransom, B. R. (1991). "Fabrication and Implementation of Ion-Selective Microelectrodes". *Neurophysiological Techniques Neuromethods*, 14:227-320.

Casey, R.J. (1990). "Sediment Oxygen Demand During the Winter in the Athabasca River and Wapiti-Smoky River System". Alberta Environment, Edmonton, AB.

Casey, R. J.; Noton, L.R. (1989). "Method Development and Measurement of Sediment Oxygen Demand During the Winter on the Athabasca River". Alberta Environment, Environmental Assessment Division, Environmental quality Monitoring Branch, Edmonton, AB.

Chambers, P. A., Brown, S., Culp, J. M., Lowell, R. B., and Pietroniro, A. (2000). "Dissolved Oxygen Decline in Ice-Covered Rivers of Northern Alberta and its Effects on Aquatic Biota". *Journal of Aquatic Ecosystem Stress and Recovery* ,8:27–38.

Chambers, P. A., Culp, J. M., Glozier, N. E., Cash, K. J., Wrona, F. J., Noton, L. (2006). "Northern Rivers Ecosystem Initiative: Nutrients and Dissolved Oxygen – Issues and Impacts". *Environmental Monitoring and Assessment*, 113:117–141.

Chambers, P. A., G. J. Scrimgeour & A. Pietroniro, (1997). "Winter oxygen conditions in ice-covered rivers: the impact of pulp mill and municipal effluents". *Canadian Journal of Fisheries and Aquatic Sciences*, 54:2796–2806.

Chen, G. H., Leong, I. M., Liu, J., Huang, J. C., Lo, I. M. C., Yen, B. C. (2000). "Oxygen Deficit Determinations for a Major River in Eastern Hong Kong, China". *Chemosphere*, 41:7-13.

Cowan, J. L. W. and Boynton, W. R., (1996). "Sediment-Water Oxygen and Nutrient Exchanges along the Longitudinal Axis of Chesapeake Bay:

Seasonal Patterns, Controlling Factors and Ecological Significance". *Estuaries*, 19(3):562-580.

Cox, B. A. (2003). "A Review of Dissolved Oxygen Modeling Techniques for Lowland Rivers". *The Science of the Total Environment*, 314-316:303-334.

Crank, J. (1983). "The Mathematics of Diffusion". Oxford University Press, London.

Dalsgaard, T., and Bak, F. (1992). "Effect of Acetylene on Nitrous Oxide Reduction and Sulfide Oxidation in Batch and Gradient Cultures of *Thiobacillus Denitrificans*". *Applied and Environmental Microbiology*, 58:1601-1608.

de Beer, D. (1999). "Use of Micro-Electrodes to Measure In Situ Microbial Activities in Biofilms, Sediments, and Microbial Mats". In: *Molecular Microbial Ecology Manual* (A. D. L. Akkermans,et al. Ed.), Kluwer Academic Press.

de Beer, D. and Heuvel, J. C. V. D., (1988). "Response of Ammonium-Selective Microelectrodes Based on the Neutral Carrier Nonactin". *Talanta*, 35(9):728-730.

de Beer, D. and Sweerts, J.-P. R. A. (1989). "Measruement of Nitrate Gradients with an Ion-Selective Microelectrode", *Analytica chimica Acta*, 219:351-356.

de Beer, D., Schramm, A., Santegoeds, C. M, Kuhl, M. (1997). "A nitrite Microsensor for Profiling Environmental Biofilms". *Applied and Environmental Microbiology*, 63(3):973-977.

Denis, L., and Grenz, G., (2003). "Spatial Variability in Oxygen and Nutrient Fluxes at the Sediment–Water Interface on a Continental Shelf in the Gulf of Lions (NW Mediterranean)". *Oceanologica Acta*, 26:373-389.

Denis, L., Grenz, C., Alliot, E., and Rodier, M. (2001). "Temporal Variability in Dissolved Inorganic Nitrogen Fluxes at the Sediment-Water Interface and Related Annual Budget on A Continental Shelf (NW Mediterranean)". *Oceanologica Acta*, 24(1):85-97.

Di Toro, D. M. (1986). "A diagenetic Oxygen Equivalents Model of Sediment Oxygen Demand". In: *Sediment Oxygen Demand: Processes, Modeling and Measurement* (K. J. Hatcher Ed.), INR, University of Georgia, Georgia, pp. 171-208.

Di Toro, D. M. (2001). "Sediment Flux Modeling". John Wiley & Sons, New York.

Di Toro, D. M., Paquin, P. R., Subburamu, K., and Gruber, D. A. (1990). "Sediment Oxygen Demand Model: Methane and Ammonia Oxidation". *Journal of Environmental Engineering, ASCE*, 116(5):945-986.

Doyle, M. C. and Lynch, D. D. (2005). "Sediment Oxygen Demand in Lake Ewauna and the Klamath River, Oregon June 2003". U. S. Geological Survey, Scientific Investigation Report 2005-5228.

Eaton, A. D., Clesceri, L. S., Rice, E. W., Greenberg, A. E. (2005). "Standard Methods for the Examination of Water and Wastewater", 21st Edition, American Public Health Association (APHA), American Water Works Association (AWWA) and Water Environment Federation (WEF).

Ellis, C. R. and Stefan, H. G. (1989). "Oxygen Demand in Ice Covered Lakes as It Pertains to Winter Aeration". *Water Resources Bulletin*, 25(6):1169-1176.

Fair, G. M., Moore, E. W., and Thomas Jr., H. A. (1941). "The Natural Purification of River Muds and Pollutional Sediment". *Journal of Sewage Works*, 13(2):270-307.

Fenchel, T. M. and Balckburn, T. H. (1979). "Bacteria and Mineral Cycling". Academic Press.

Fluka (1996). "Selectophore: Ionophores, Membranes, Mini-ISE". Fluka Chemical Corp., Switzerland.

Gelda, R. K., Auer, M. T., and Effler, S. W. (1995). "Determination of Sediment Oxygen Demand by Direct Measurement and by Inference from Reduced Species Accumulation". *Marine and Freshwater Research*, 46:81-88.

Grenz, C., Denis, L., Boucher, G., Chauvaud, L., Clavier, J., Fichez, R., Pringault, O. (2003). "Spatial variability in Sediment Oxygen Consumption under Winter Conditions in a Lagoonal System in New Caledonia (South Pacific)". *Journal of Experimental Marine Biology and Ecology*, 285–286:33– 47.

Haag, I., Gerhard Schmid, G., and Westrich, B. (2006). “Dissolved Oxygen and Nutrient Fluxes across the Sediment–Water Interface of the Neckar River,Germany: In-Situ Measurements and Simulations”. *Water, Air, and Soil Pollution: Focus*, 6:49–58.

Hall, D. C. and Berkas, W. R. (1988). “Comparison of Instream and Laboratory Methods of Measuring Sediment Oxygen Demand”. *Water Resources Bulletin*, 24(3):571-575.

Han, P. and Bartels, D. M. (1996). “Temperature Dependence of Oxygen Diffusion in H_2O and D_2O”. *The Journal of Physical Chemistry*, 100(51):5597-5602.

Hansen, K. and Kristensen, E. (1998). “The impact of the Polychaete Nereis Diversicolor and Enrichment with Macroalgal (*Chaetomorpha Linum*) Detritus on Benthic Metabolism and Nutrient Dynamics in Organic-Poor and Organic-Rich Sediments”. *Journal of Experimental Marine Biology and Ecology*, 231:201-223.

Hargrave, B. T. (1969). “Similarity of Oxygen Uptake by Benthic Communities”. *Limnology and Oceanography*, 14(5):801-805.

Hargrave, B. T. (1973). “Coupling Carbon Flow through Some Pelagic and Benthic Communities”. *Journal of Fisheries Research Board, Canada*, 30:1317-1326.

Hargreaves, J. A. (1998). “Nitrogen Biogeochemistry of Aquaculture Ponds”. *Aquaculture*, 166:181-212.

Hatcher, K. J. (1986). “Introduction to Sediment Oxygen Demand Modeling”. In: *Sediment Oxygen Demand: Processes, Modeling and Measurement* (K. J. Hatcher Ed.), INR, University of Georgia, Georgia, pp. 113-120.

HBT AGRA Ltd., (1993). “Sediment Oxygen Demand Investigations on the Athabasca River During the Winter of 1993”. Prepared for Alberta Forest Products Association, Calgary, Alberta.

Heckathorn, H. A. and Gibs, J. (2010). “Sediment Oxygen Demand in the Saddle River and Salem River Watersheds, New Jersey, July–August 2008”. U.S. Department of the Interior and U.S. Geological Survey, Scientific Investigations Report 2010–5093.

Henriksen, K., and Kemp, M. W. (1988). “Nitrification in estuarine and coastal marine sediments”. In: *Nitrogen Cycling in Coastal Marine Environments, SCOPE 33* (T. H. Blackburn, and J. Sørensen Ed.),. Wiley Interscience, Chichester, United Kingdom.

Henze, M., Harremoës, P., and Jansen, J. C., and Arvin, E. (2002). “Wastewater Treatment Biological and Chemical Processes”. Springer Verlag, Berlin, Germany.

House, W. A. (2003). “Factors Influencing the Extent and Development of the Oxic Zone in Sediments”. *Biogeochemistry*, 63:317-333.

Huettel, M., Webster, I. T. (2001) “Porewater Flow in Permeable Sediments”, In: *The Benthic Boundary Layer: Transport Processes and Biogeochemistry* (B.

P. Boudreau and B. B. Jorgensen Ed.), Oxford University Press, New York, USA, pp: 144-179.

Jahnke, R. A. (2001) Constraining Organic Matter Cycling with Benthic Fluxes. In: *The Benthic Boundary Layer: Transport Processes and Biogeochemistry* (B. P. Boudreau and B. B. Jorgensen Ed.), Oxford University Press, New York, USA.

Jensen, K. Revesbech, N. P., Nielsen, L. P. (1993) "Microscale Distribution of Nitrification Activity in Sediment Determined with a Shielded Microsensor for Nitrate". *Applied and Environmental Microbiology*, 59(10):3287-3296.

Jensen, K., Sloth, N. P., Risgaard, P. N, Rysgaard, S., Revsbech, N. P. (1994) "Estimation of Nitrification and Denitrification from Microprofiles of Oxygen and Nitrate in Model Sediment Systems". *Applied and Environmental Microbiology*, 60:2094–2100.

Jorgensen, B. B. (2001). "Diagenesis and Sediment-Water Exchange". In: *The Benthic Boundary Layer: Transport Processes and Biogeochemistry* (B. P. Boudreau and B. B. Jorgensen Ed.), Oxford University Press, New York, USA..

Klapwijk, A. Snodgrass, W. J. (1986). "Biofilm Model for Nitrification, Denitrification, and Sediment Oxygen Demand in Hamilton Harbor" In: *Sediment Oxygen Demand: Processes, Modeling and Measurement* (K. J. Hatcher Ed.), INR, University of Georgia, Georgia, pp. 75-97.

Koryta J. and Stulik, K. (1983). “Ion-selective Electrodes”. Cambridge University Press, Cambridge, UK.

Kuhl, M. and Revsbech, N. P. (2001). “Biogeochemical Microsensors for Boundary Layer Studies” In: *The Benthic Boundary Layer: Transport Processes and Biogeochemistry* (B. P. Boudreau and B. B. Jorgensen Ed.), Oxford University Press, New York, USA, pp. 181-210.

Li, J. (2001). “Azo Dye Biodegradation and Inhibition Effects on Aerobic Nitrification and Anoxic Denitrification Processes”. Ph D Dissertation. University of Cincinnati.

Li, Y. H. and Gregory, S. (1974). “Diffusion of Ions in Sea Water and in Deep-Sea Sediments”. *Geochimica Cosmochimica Acta*, 38:703–714.

Ling, T.-Y., Ng, C.-S., Lee, N., Buda, D., (2009). “Oxygen Demand of the Sediment from the Semariang Batu River, Malaysia”. *World Applied Sciences Journal*, 7(4):440-447.

Liu, W. C., (2009). “Measurement of Sediment Oxygen Demand for Modelling Dissolved Oxygen Distribution in Tidal Keelung River”. *Water and Environment Journal*, 23(2):100-109.

Lorenzen, J., Larsen, L. H., Kjær, T., Revsbech, N. P. (1998). “Biosensor Determination of the Microscale Distribution of Nitrate, Nitrate Assimilation, Nitrification, and Denitrification in a Diatom-Inhabited Freshwater Sediment”. *Applied and Environmental Microbiology*, 64(9):3264–3269.

Lu, R. and Yu, T. (2002). "Fabrication and Evaluation of an Oxygen Microelectrode Applicable to Environmental Engineering and Science". *Journal of Environmental Engineering and Science*, 1:225-235.

Mackenthum, A. A. and Stefan, S. G. (1998). "Effect of Flow Velocity in the Sediment Oxygen Demand: Experiments". *Journal of Environmental Engineering*, 124(3):222-230.

Matisoff, G. and Neeson, T. M. (2005). "Oxygen Concentration and Demand in Lake Erie Sediments". *Journal of the Great Lakes Research*, 31(Supplement 2):284–295.

Matlock, M. D., Kasprzak, K. R., Osborn, G. S. (2003). "Sediment Oxygen Demand in the Arroyo Colorado River". *Journal of the American Water Resources Association (JAWRA)*, 39(2):267-275

McConn, R. and Robinson, J. S. (1963). "Notes on the Oxygen Electrode". *British Journal of Anaesthesia*, 35:679-683.

McDonnel, A. J. and Hall, S. D. (1969). "Effects of environmental Factors on Benthal Oxygen Uptake". *Journal of Water Pollution Control Federation Research*, 41(Supplement):353-363.

Meyer, R. L., Kjær, T., Revsbech, N. P. (2001). "Use of NO_x^- Microsensors to Estimate the Activity of Sediment Nitrification and No_x^- Consumption Along an Estuarine Salinity, Nitrate, and Light Gradient". *Aquatic Microbial Ecology*, 26:181–193.

Miller, A. J. and Wells, D. M. (2006). "Electrochemical Methods and Measuring Transmembrane Ion Gradient". In: *Plant Electrophysiology - Theory and Methods* (A. Volkov Ed.), Springer-Verlag, Berlin, Heidelberg.

Murphy, P. J. and Hicks, D. B. (1986). "In-Situ Method for Measuring Sediment Oxygen Demand". In: *Sediment Oxygen Demand: Processes, Modeling and Measurement* (K. J. Hatcher Ed.), INR, University of Georgia, Georgia, pp. 307-322.

Nakamura, Y. and Stefan, H. G. (1994). "Effect of Flow Velocity on Sediment Oxygen Demand: Theory". *Journal of Environmental Engineering*, 120(5):996-1016.

Neumann, D., Kramer, M., Raschke, I., Grafe, B. (2001). "Detrimental Effects of Nitrite on the Development of Benthic *Chironomus* Larvae in Relation to Their Settlement in Muddy Settlements". *Archive of Hydrobiology*, 153:103-128.

Nielsen, L. P., Christensen, P. B., Revsbech, N. P., Sorensen, J. (1990). "Denitrification and Photosynthesis in Stream Sediment Studied with Microsensor and Whole-Core Techniques". *Limnology and Oceanography*, 35:1135–1144

Noton L.R. (1996). "Investigations of Streambed Oxygen Demand, Athabasca River, October 1994 to March 1995". Northern River Basins Study Project; Report No. 94. Edmonton, Alberta, Canada.

NREI (2004). "*Northern Rivers Ecosystem Initiative 1998-2003: Final Report"*. Alberta Environment, Edmonton, Alberta, Canada.

Osborn, G. S., Charbonnet, D. A., Smith, P. K., Matlock, M. D. (2008). "A Chamberless Method for Determining SOD". *Transactions of ASABE*, 51(3):1123-1131.

Park, S., Bae, W., Rittman, B. E. (2010). "Operational Boundaries for Nitrite Accumulation in Nitrification Based on Minimum/Maximum Substrate Concentration That Include Effect of Oxygen Limitation, pH and Free Ammonia and Free Nitrous Acid Inhibition". *Environmental Science and Technology*, 44(1):335-342.

Park, S. S. and Jaffe, P. R. (1996). "Development of a Sediment Redox Potential Model for the Assessment of Postdepositional Metal Mobility". *Journal of Ecological Modeling*, 91:169-181.

Parkhill, K. L. and Gulliver J. S. (1997). "Discussion on: Comparision of Two Sediment Oxygen Demand Techniques by Traus et al., in J. Env. Eng. 121(9), 1995". *Journal of Environmental Engineering*, 123(1):97-98.

Pelegri, S. P. and Blackburn, T. H. (1996). "Nitrogen Cycling in Lake Sediments Bioturbated by *Chironomous plumosus* Larvae, Under Different Degree of Oxygenation". *Hydrobiologia*, 325:231-238.

Percival, J. B. and Lindsay, P. J. (1996). "Measurement of Physical Properties of Sediment". In: *Manual of Physico-Chemical Analysis of Aquatic Sediments* (Alena Mudroch et al. Ed.), CRC Press, Lewis Publishers, Boca Raton.

Rabouille, C., Denis, L., Dedieua, K., Storac G., Lansard, B., and Grenz, C. (2003). "Oxygen Demand in Coastal Marine Sediments: Comparing In-Situ

Microelectrodes and Laboratory Core Incubations". *Journal of Experimental Marine Biology and Ecology*, 285–286:49-69.

Revsbech, N. P. (1989). "An Oxygen Microsensor with a Guard Cathode". *Limnology and Oceanography*, 34(2):474–478.

Revsbech, N. P. and Jorgensen, D. B. (1986). "Microelectrodes: Their Use in Microbial Ecology". *Advances in Microbial Ecology*, 9:293-352.

Revsbech, N. P., Jorgensen, B. B., Blackburn, T. H. (1980). "Oxygen in the Seabottom Measured with a Microelectrode". *Science*, 207:1355-1356.

Revsbech, N. P., Jørgensen, B. B., Brix, O. (1981). "Primary Production of Microalgae in Sediments Measured by Oxygen Microprofile, $H^{14}CO_3^-$ Fixation, and Oxygen Exchange Methods". *Limnology Oceanography*, 26:717–730.

Revsbech, N. P. (2005). "Analysis of Microbial Communities with Electrochemical Microsensors and Microscale Biosensors". *Methods in Enzymology*, 397:147-166.

Revsbech, N. P., Risgaard-Petersen, N., Schramm, A., Nielsen, L. P. (2006). "Nitrogen transformations in stratified aquatic microbial ecosystems". *Antonie van Leeuwenhoek* 90:361–375.

Revsbech, N. P., Sorensen, J., and Blackburn, T. H. (1980). "Distribution of Oxygen in marine Sediments Measured with Microelectrodes" *Limnology and Oceanography*, 25(3):403-411.

Rounds, S. A., Doyle, M. C. (1997). “Sediment Oxygen Demand in the Tulatin River Basin, Oregon”. U.S. Geological Survey, USA.

Satoh, H., Ono, H., Rulin, B., Kamo, J., Okabe, S., Fukushi, K.-I. (2004). “Macroscale and Microscale Analyses of Nitrification and Denitrification in Biofilms Attached on Membrane Aerated Biofilm Reactors”. *Water Research,* 38:1633–1641.

Seiki, T., Izawa, H., Date, E., Sunahara, H., (1994). “Sediment Oxygen Demand in Hiroshima Bay”. *Water Research*, 28(2):385-393.

Shabala, L., Ross, T., McMeekin, T., Shabala, S. (2006). “Non-invasive Microelectrode Ion Fux Measurements to Study Adaptive Responses of Microorganisms to the Environment”. *FEMS Microbiology Review*, 30:472–486.

Steeby, J. A., Hargreaves, J. A., Tucker, C. S. (2004). “Factors Affecting Sediment Oxygen Demand in Commercial Channel Catfish Ponds”. *Journal of the World Aquaculture Society*, 35(3):322 – 334.

Stefan, H. G. (1992). “Sedimentary Oxygen Demand and its Effect on Winterkill in Lakes”. *Proceedings, US Army Corps of Engineers Workshop on Sediment Oxygen Demand*, 21-22 August 1990, pp. 137-142.

Stief, P. and de Beer, D. (2006). “Probing the Microenvironment of Freshwater Sediment Macrofauna: Implications of Deposit-Feeding and Bioirrigation for Nitrogen Cycling”. *Limnology and Oceanography*, 51(6):2538-2548.

Stief, P., de Beer, D., Nuemann, D. (2002). "Small Scale Distribution of Interstitial Nitrite in Freshwater Sediment Microcosms: The Role of nitrate and Oxygen Availability, and Sediment Permeability". *Microbial Ecology*, 43:367-378.

Stief, P., Schramm, A., Altaman, D., De Beer, D. (2003). "Temporal Variation of Nitrification Rates in Experimental Freshwater Sediments Enriched with Ammonia or Nitrite". *FEMS Microbiology Ecology*, 46:63-71.

Tchobanoglous, G., Burton, F. L., Stensel, H. D. (2003). "Wastewater Engineering Treatment and Reuse". Metcalf and Eddy Inc., McGraw Hill.

Thomann, R. V. and Mueller J. A. (1987). "Principles of Surface Water Quality Modeling and Control". Harper Collins Publisher, New York, pp. 261-384.

Thornton, D. C. O., Dong, L. F., Underwood, G. J. C., Nedwell, D. B. (2007). "Sediment–Water Inorganic Nutrient Exchange and Nitrogen Budgets in the Colne Estuary, UK". *Marine Ecology Progress Series*, 337:63-77.

Tian, Y. (2005) "A Dissolve Oxygen Model and Sediment Oxygen Demand Study in the Athabasca River" Master's Thesis, University of Alberta, Edmonton, Alberta.

Traux, D. D., Shindala, A., and Sartain, H. (1995). "Comparision of Two Sediment Oxygen Demand Techniques". *Journal of Environmental Engineering*, 21(9):619-624.

Utley, B. C., Vellidis, G., Lowrance, R., Smith, M. C., (2008). "Factors Affecting Sediment Oxygen Demand Dynamics in Blackwater Streams of Georgia's

Coastal Plain". *Journal of the American Water Resources Association*, 44(3):742 -753.

Veenstra, J. N. and Nolen, S. L. (1991) "In-Situ Sediment Oxygen Demand in Five Southwestern U.S. Lakes". *Water Research*, 25(3):351-35.

Walker, R. R. and Snodgrass, W. J. (1986). "Model for Sediment Oxygen Demand in Lakes". *Journal of Environmental Engineering*, 112(1):25-43.

Wetzel, R. C. (2007). "Limnology: Lakes and River Ecosystem", Third Edition, Academic Press, New York, USA.

Whittemore, R. C. (1986). "Problems with In-Situ and Laboratory SOD Measurements and their Implementation in Water Quality Modeling Studies". In: *Sediment Oxygen Demand: Processes, Modeling and Measurement* (K. J. Hatcher Ed.), INR, University of Georgia, Georgia, pp. 331-341.

Wood, T. M. (2001). "Sediment Oxygen Demand in Upper Klamath and Agency Lakes, Oregon, 1999". U.S. Geological Survey Water-Resources Investigations Report 01–4080.

Yu, M. (2006). "Sediment Oxygen Demand Investigation and CE-QUAL-W2 Model Calibration in the Athabasca River". Master's Thesis, University of Alberta, Edmonton, Alberta.

Yu, T. (2000). "Stratification of Microbial Processes and Redox Potential Changes in Biofilms". Ph D Dissertation. University of Cincinnati.

APPENDICES

Appendix A

Details of SOD Determination Sediment Core

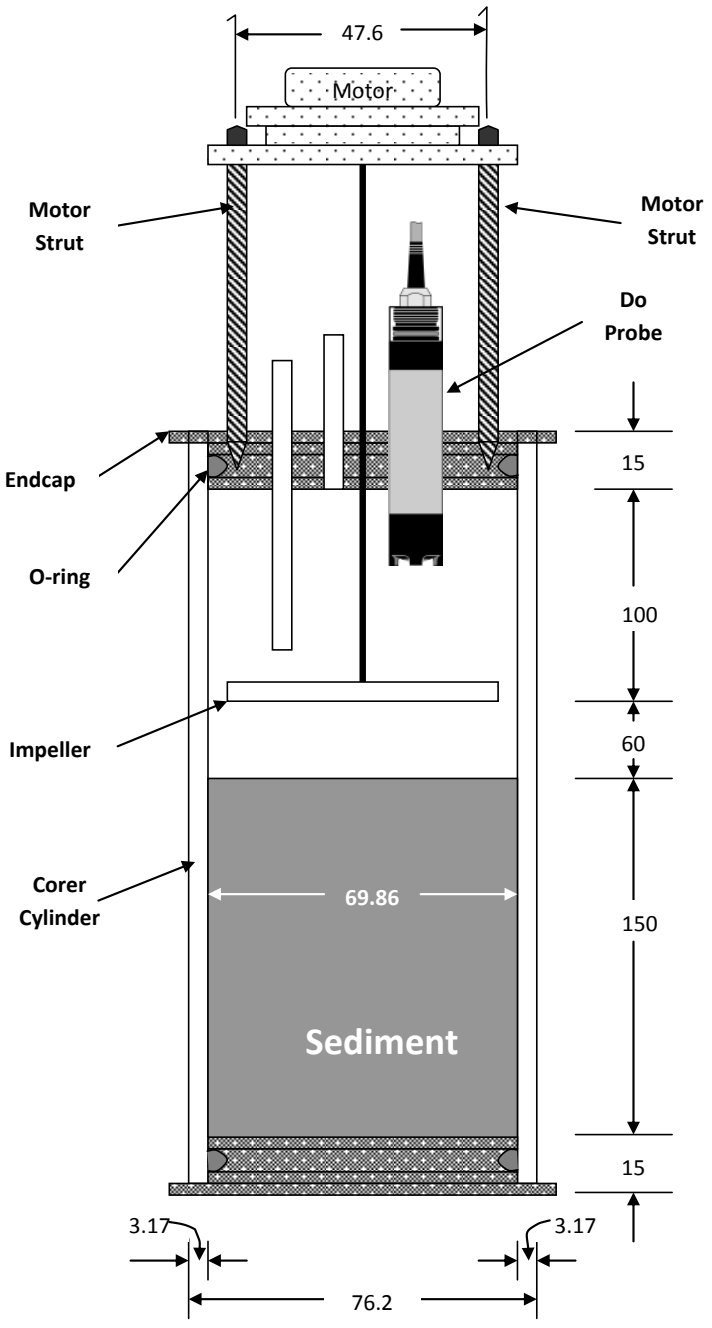

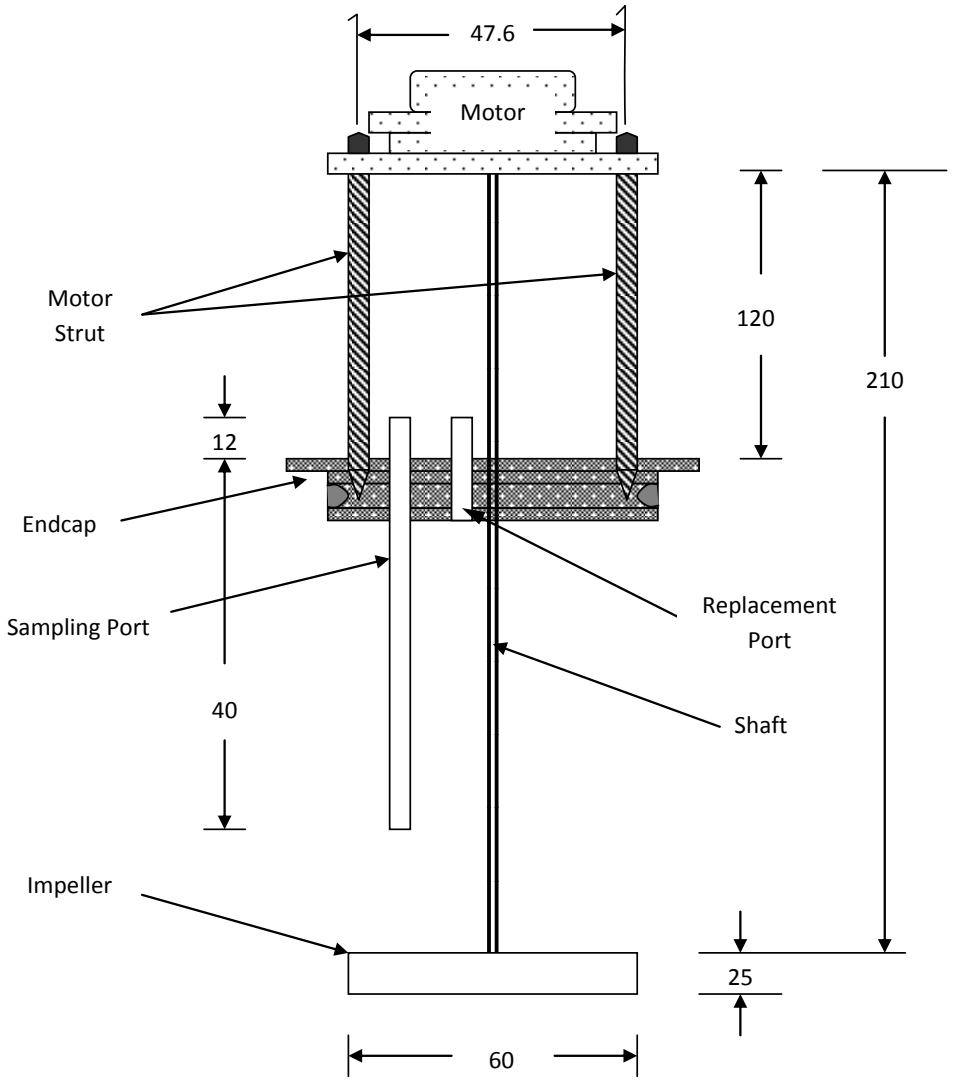

Dimensions all in mm

APPENDIX B
Data for Chapter 4

Data for Figure 4.1 Longitudinal pattern of SOD along Athabasca River in fall

Location	SOD (g/m^2•d) Standardized at 4±1°C										
	Fall 2006			Fall 2007*				Fall 2008*			
	Core 1	Core 2	Average	Core 1	Core 2	Core 3	Average	Core 1	Core 2	Core 3	Average
USHP	0.03	0.21	0.13	-	-	-	-	-	-	-	-
EMBG	0.36	0.40	0.38	-	-	-	-	-	-	-	-
UANC	0.35	0.23	0.29	-	-	-	-	-	-	-	-
USML	0.28	0.30	0.29	0.21	0.09	0.18	0.16	0.14	0.04	-	0.09
DSMW	0.23	0.27	0.25	0.07	0.10	0.46	0.21	-	-	-	-
BLRG	0.12	0.06	0.09	-	-	-	-	-	-	-	-
FTAS	0.18	0.20	0.19	-	-	-	-	0.27	0.15	0.09	0.17
DSTR	0.23	0.19	0.21	-	-	-	-	-	-	-	-
CHLM	0.19	0.31	0.25	-	-	-	-	-	-	-	-
SMTH	0.30	0.16	0.23	0.00	0.00	0.00	0.00	0.04	-	-	0.04
CBRG	0.28	0.32	0.30	-	-	-	-	-	-	-	-
USAM	0.54	0.46	0.50	0.25	0.25	0.25	0.25	0.21	0.27	-	0.24
POLG	0.06	0.17	0.12	0.17	0.11	-	0.14	-	-	-	-
DSLB	0.38	0.11	0.25	-	-	-	-	-	-	-	-
DSCR	0.78	0.64	0.71	0.06	0.47	0.92	0.48	0.36	0.27	0.31	0.32

* The SOD rate measured at 3±1°C are standardized at 4±1°C for compatibility using Equation 3.3

Data for Figure 4.2 Longitudinal pattern of SOD along the Athabasca River in the winter

Location	SOD (g/m^2•d) Standardized at 4±1 °C								
	Winter 2007					Winter 2008*			
	Core 1	Core 2	Core 3	Core 4	Average	Core 1	Core 2	Core 3	Average
USHP	0.14	0.38	0.59	-	0.37	-	-	-	-
USML	-	-	-	-	-	-	-	-	-
DSMW	0.05	0.00	0.01	-	0.02	-	0.28	0.35	0.32
FTAS	0.63	0.03	0.12	-	0.26	-	-	-	-
SMTH	-	-	0.23	-	0.23	-	-	-	-
CBRG	0.21	0.10	0.18	-	0.16	-	-	-	-
USAM	0.39	-	0.15	-	0.27	0.21	0.22	0.19	0.21
POLG	0.45	0.22	0.42	-	0.37	-	-	-	-
DSLB	0.42	0.09	0.20	-	0.24	-	-	-	-
DSCR	0.36	0.60	0.49	0.46	0.48	0.29	0.22	0.24	0.25

* The SOD rate measured at 3±1°C are standardized at 4±1°C for compatibility using Equation 3.3

Measured Data for SOD in the Fall and Winter seasons at $3 \pm 1^{o}C$

Location	SOD ($g/m^2 \cdot d$) Measured at $3 \pm 1^{o}C$											
	Fall 2007				Fall 2008				Winter 2008			
	Core 1	Core 2	Core 3	Average	Core 1	Core 2	Core 3	Average	Core 1	Core 2	Core 3	Average
USHP	-	-	-	-	-	-	-	-	-	-	-	-
EMBG	-	-	-	-	-	-	-	-	-	-	-	-
UANC	-	-	-	-	-	-	-	-	-	-	-	-
USML	0.20	0.08	0.17	0.15	0.13	0.04	-	0.09	-	0.27	0.34	0.31
DSMW	0.07	0.09	0.44	0.20	-	-	-	-	-	-	-	-
BLRG	-	-	-	-	-	-	-	-	-	-	-	-
FTAS					0.26	0.14	0.08	0.16				
DSTR	-	-	-	-	-	-	-	-	-	-	-	-
CHLM	-	-	-	-	-	-	-	-	-	-	-	-
SMTH	0.00	0.00	0.00	0.00	0.04	-	-	0.04				
CBRG	-	-	-	-	-	-	-	-	-	-	-	-
USAM	0.24	0.24	0.24	0.24	0.20	0.26	-	0.23	0.20	0.21	0.18	0.20
POLG	0.16	0.11	-	0.13	-	-	-	-	-	-	-	-
DSLB	-	-	-	-	-	-	-	-	-	-	-	-
DSCR	0.06	0.45	0.88	0.46	0.35	0.26	0.30	0.30	0.28	0.21	0.23	0.24

Data for Figure 4.3 Sediment porosity in the fall at different sites along the Athabasca River

Location	Porosity (%) Fall 2006			Porosity (%) Fall 2007			Porosity (%) Fall 2008		
	Sample 1	Sample 2	Average	Sample 1	Sample 2	Average	Sample 1	Sample 2	Average
USHP	56.9	65.3	62.1	-	-	-	-	-	-
EMBG	74.1	71.1	72.6	-	-	-	-	-	-
UANC	71.4	66.2	68.8	-	-	-	-	-	-
USML	84.8	72.0	78.4	60.5	63.5	62.0	83.3	75.7	79.5
DSMW	60.6	66.2	63.4	72.9	62.3	67.6	-	-	-
BLRG	64.1	40.1	52.1	-	-	-	-	-	-
FTAS	69.6	79.2	74.4	-	-	-	73.5	62.7	68.1
DSTR	66.6	64.3	65.5	-	-	-	-	-	-
CHLM	59.0	75.4	67.2	-	-	-	-	-	-
SMTH	51.0	69.3	60.1	38.7	46.3	42.5	53.9	68.7	61.3
CBRG	72.4	70.2	71.3	-	-	-	-	-	-
USAM	74.5	88.7	81.6	81.4	77.2	79.3	77.3	81.1	79.2
POLG	49.5	55.9	52.7	89.0	84.2	86.6	-	-	-
DSLB	56.2	68.4	62.3	-	-	-	-	-	-
DSCR	92.1	76.3	84.2	82.9	98.1	90.5	78.4	88.0	83.2

Data for Figure 4.4 Sediment porosity in the winter at different sites along the Athabasca River

Location	Porosity (%)						
	Winter 2007			Winter 2008			
	Sample 1	Sample 2	Average	Sample 1	Sample 2	Sample 3	Average
USHP	60.1	78.5	69.3	-	-	-	-
USML	-	-	-	84.3	80.7	83.7	82.9
DSMW	43.5	47.5	55.5	-	-	-	-
FTAS	81.0	71.2	75.6	-	-	-	-
SMTH	-	-	61.8	-	-	-	-
CBRG	65.4	61.6	63.5	-	-	-	-
USAM	79.3	73.7	76.5	70.7	64.5	74.5	69.9
POLG	60.9	76.5	68.7	-	-	-	-
DSLB	68.7	62.3	65.5	-	-	-	-
DSCR	80.8	97.6	89.2	65.8	75.4	-	70.6

Data for Table 4.1 Sediment Composition and Porosity at Various Sites

White Court

Depth	Silt + Clay (%)					Clay (%)					Sand (%)					Porosity (%)					
(cm)	1	2	Mean	Min	Max	1	2	Mean	Min	Max	1	2	Mean	Min	Max	1	2	3	Mean	Min	Max
1	39.7	36.2	37.95	1.71	1.71	9.2	9.8	9.51	0.32	0.32	60.3	63.8	62.05	1.71	1.71	84.31	80.70	83.65	82.89	2.19	1.42
3	54.4	36.6	45.47	8.90	8.90	11.5	9.3	10.38	1.08	1.08	45.6	63.4	54.53	8.90	8.90	81.53	86.32	73.72	80.52	6.80	5.80
5	43.3	50.7	47.01	3.67	3.67	11.5	10.2	10.82	0.64	0.64	56.7	49.3	52.99	3.67	3.67	83.41	78.91	84.14	82.15	3.24	1.98
7	48.8	43.4	46.08	2.69	2.69	12.7	10.4	11.56	1.15	1.15	51.2	56.6	53.92	2.69	2.69	77.15	77.98	81.62	78.92	1.77	2.71
9	45.9	40.7	43.31	2.63	2.63	12.5	10.0	11.27	1.24	1.24	54.1	59.3	56.69	2.63	2.63	76.30	79.57	90.91	82.26	5.96	8.65

ALPAC

Depth	Silt + Clay (%)					Clay (%)					Sand (%)					Porosity (%)					
(cm)	1	2	Mean	Min	Max	1	2	Mean	Min	Max	1	2	Mean	Min	Max	1	2	3	Mean	Min	Max
1	30.82	32.66	31.74	0.92	0.92	10.01	14.66	12.33	2.33	2.33	69.18	67.34	68.26	0.92	0.92	66.13	59.95	69.87	65.32	5.37	4.56
3	36.77	28.12	32.44	4.33	4.33	15.86	11.60	13.73	2.13	2.13	63.23	71.88	67.56	4.33	4.33	72.77	64.73	67.57	68.36	3.63	4.41
5	37.54	26.83	32.18	5.36	5.36	17.36	8.71	13.03	4.33	4.33	62.46	73.17	67.82	5.36	5.36	68.57	71.19	62.98	67.58	4.60	3.61
7	44.01	30.17	37.09	6.92	6.92	17.96	10.05	14.01	3.95	3.95	55.99	69.83	62.91	6.92	6.92	70.96	66.03	66.90	67.96	1.94	2.99
9	38.58	33.90	36.24	2.34	2.34	14.30	11.45	12.88	1.42	1.42	61.42	66.10	63.76	2.34	2.34	70.38	65.90	64.93	67.07	2.14	3.31

Calling River

Depth	Silt + Clay (%)					Clay (%)					Sand (%)					Porosity (%)				
(cm)	1	2	Mean	Min	Max	1	2	Mean	Min	Max	1	2	Mean	Min	Max	1	2	Mean	Min	Max
1	35.02	33.27	34.14	0.87	0.87	9.69	8.61	9.15	0.54	0.54	64.98	66.73	65.86	0.87	0.87	65.76	75.44	70.60	4.84	4.84
3	26.13	20.00	23.07	3.06	3.06	7.28	6.94	7.11	0.17	0.17	73.87	80.00	76.93	3.06	3.06	71.35	67.58	69.46	1.88	1.88
5	20.96	16.33	18.65	2.31	2.31	5.89	5.61	5.75	0.14	0.14	79.04	83.67	81.35	2.31	2.31	64.33	68.23	66.28	1.95	1.95
7	22.60	18.70	20.65	1.95	1.95	8.12	5.78	6.95	1.17	1.17	77.40	81.30	79.35	1.95	1.95	63.06	63.51	63.29	0.22	0.22
9	28.18	22.49	25.33	2.84	2.84	9.87	6.34	8.10	1.77	1.77	71.82	77.51	74.67	2.84	2.84	62.33	69.31	65.82	3.49	3.49

Data for Table 4.1 Sediment Nutrient Content at Various Sites

White Court

Depth	Total Nitrogen (%, wt/dry wt)					Total Carbon (%, wt/dry wt)					Total Organic Carbon (%, wt/dry wt)					Total Organic Matter (%, wt/dry wt)					
(cm)	1	2	Mean	Min	Max	1	2	Mean	Min	Max	1	2	Mean	Min	Max	1	2	3	Mean	Min	Max
1	0.15	0.19	0.17	0.02	0.02	6.54	7.52	7.03	0.49	0.49	3.68	4.38	4.03	0.35	0.35	13.06	10.95	11.51	11.84	0.89	1.22
3	0.16	0.18	0.17	0.01	0.01	6.64	8.21	7.42	0.79	0.79	3.55	5.23	4.39	0.84	0.84	11.81	13.18	6.32	10.44	4.12	2.74
5	0.27	0.15	0.21	0.06	0.06	9.61	6.50	8.05	1.56	1.56	6.42	3.56	4.99	1.43	1.43	13.56	9.15	10.80	11.17	2.02	2.39
7	0.15	0.13	0.14	0.01	0.01	6.79	5.75	6.27	0.52	0.52	3.83	2.74	3.28	0.54	0.54	7.52	8.21	11.69	9.14	1.62	2.55
9	0.21	0.13	0.17	0.04	0.04	7.56	5.86	6.71	0.85	0.85	4.57	2.97	3.77	0.80	0.80	7.44	9.21	10.79	9.14	1.71	1.64

ALPAC

Depth	Total Nitrogen (%, wt/dry wt)					Total Carbon (%, wt/dry wt)					Total Organic Carbon (%, wt/dry wt)					Total Organic Matter (%, wt/dry wt)					
(cm)	1	2	Mean	Min	Max	1	2	Mean	Min	Max	1	2	Mean	Min	Max	1	2	3	Mean	Min	Max
1	0.04	0.05	0.04	0.00	0.00	1.60	1.51	1.55	0.05	0.05	0.71	0.73	0.72	0.01	0.01	2.72	1.41	2.75	2.29	0.88	0.45
3	0.07	0.04	0.06	0.02	0.02	2.12	1.48	1.80	0.32	0.32	1.10	0.67	0.88	0.21	0.21	2.03	1.84	2.23	2.03	0.19	0.20
5	0.05	0.03	0.04	0.01	0.01	1.68	1.41	1.55	0.14	0.14	0.69	0.48	0.58	0.11	0.11	2.26	1.20	1.97	1.81	0.61	0.45
7	0.06	0.04	0.05	0.01	0.01	1.78	1.58	1.68	0.10	0.10	0.79	0.66	0.72	0.07	0.07	3.15	1.81	2.04	2.33	0.52	0.82
9	0.05	0.03	0.04	0.01	0.01	1.60	1.43	1.52	0.09	0.09	0.73	0.50	0.61	0.12	0.12	2.76	2.18	2.16	2.37	0.21	0.39

Calling River

Depth	Total Nitrogen (%, wt/dry wt)					Total Carbon (%, wt/dry wt)					Total Organic Carbon (%, wt/dry wt)					Total Organic Matter (%, wt/dry wt)				
(cm)	1	2	Mean	Min	Max	1	2	Mean	Min	Max	1	2	Mean	Min	Max	1	2	Mean	Min	Max
1	0.07	0.06	0.06	0.01	0.01	1.61	1.56	1.58	0.03	0.03	0.97	0.88	0.92	0.04	0.04	3.02	2.75	2.88	0.14	0.14
3	0.03	0.03	0.03	0.00	0.00	1.37	1.27	1.32	0.05	0.05	0.46	0.40	0.43	0.03	0.03	2.22	2.60	2.41	0.19	0.19
5	0.02	0.03	0.02	0.00	0.00	1.21	1.09	1.15	0.06	0.06	0.34	0.42	0.38	0.04	0.04	1.74	1.58	1.66	0.08	0.08
7	0.03	0.03	0.03	0.00	0.00	1.34	0.85	1.09	0.24	0.24	0.51	0.35	0.43	0.08	0.08	1.77	1.81	1.79	0.02	0.02
9	0.04	0.02	0.03	0.01	0.01	1.28	0.97	1.12	0.16	0.16	0.62	0.29	0.46	0.16	0.16	2.68	2.05	2.37	0.31	0.31

Data for Table 4.1 Sediment Pore Water Nutrients

White Court

Depth (cm)	NH_4^+ (mg-N/L)					NO_x^- (µg-N/L)				
	1	2	Mean	Min	Max	1	2	Mean	Min	Max
1	4.5	5.2	4.9	0.4	0.4	16.0	14.0	15.00	1.00	1.00
3	10.7	9.8	10.3	0.4	0.4	13.0	14.6	13.80	0.80	0.80
5	14.7	15.7	15.2	0.5	0.5	13.0	15.0	14.00	1.00	1.00
7	17.9	20.0	19.0	1.1	1.1	36.0	43.5	39.75	3.75	3.75
9	62.2	44.4	53.3	8.9	8.9	9.0	18.4	13.70	4.70	4.70

ALPAC

Depth (cm)	NH_4^+ (µg-N/L)					NO_x^- (µg-N/L)				
	1	2	Mean	Min	Max	1	2	Mean	Min	Max
1	125	132.0	128.5	3.50	3.50	16.0	17.2	16.6	0.6	0.6
3	252	263.0	257.5	5.50	5.50	41.0	57.3	49.2	8.2	8.2
5	285	276.6	280.8	4.2	4.20	15.0	18.0	16.5	1.5	1.5
7	335	327.4	331.2	3.8	3.80	12.0	17.2	14.6	2.6	2.6
9	473	498.3	485.7	12.7	12.7	17.0	15.8	16.4	0.6	0.6

Calling River

Depth (cm)	NH_4^+ (µg-N/L)					NO_x^- (µg-N/L)				
	1	2	Mean	Min	Max	1	2	Mean	Min	Max
1	1050	929	990	60.50	60.50	12	14	13.00	1.0	1.0
3	1990	1930	1960	30.00	30.00	17	28	22.50	5.5	5.5
5	1880	2000	1940	60.00	60.00	246	220	233.0	13.0	13.0
7		2870	2870	0	0.00		67	67.0	0.0	0.0

Data for Figure 4.11 DO Concentration of Overlying Water of Sediment Core at Whitecourt, USML

Time	DO of Overlying Water (mg/L)					Corrected DO (mg/L)			
(hours)	Sample 1	Sample 2	Sample 3	Control	Average	Sample 1	Sample 2	Sample 3	Average
0.00	10.65	10.41	10.44	10.55	10.43				
0.50	10.45	10.23	10.28	10.46	10.25	10.36	10.14	10.18	10.16
1.50	10.23	9.93	10.06	10.47	9.99	10.15	9.85	9.98	9.91
2.50	10.06	9.66	9.87	10.47	9.77	9.97	9.58	9.79	9.68
3.50	9.93	9.47	9.71	10.47	9.59	9.85	9.39	9.64	9.51
4.50	9.81	9.30	9.57	10.44	9.44	9.70	9.19	9.46	9.32
5.50	9.72	9.17	9.45	10.44	9.31	9.62	9.06	9.35	9.20
6.50	9.65	9.04	9.33	10.44	9.19	9.54	8.93	9.22	9.07
7.50	9.60	8.94	9.23	10.44	9.08	9.49	8.82	9.12	8.97
8.50	9.56	8.84	9.13	10.43	8.99	9.44	8.72	9.00	8.86
9.50	9.54	8.76	9.02	10.42	8.89	9.41	8.62	8.89	8.75
10.50	9.51	8.68	8.92	10.42	8.80	9.37	8.55	8.79	8.67
11.50	9.47	8.61	8.81	10.42	8.71	9.33	8.48	8.68	8.58
12.50	9.44	8.54	8.72	10.42	8.63	9.31	8.41	8.58	8.50
13.50	9.41	8.45	8.59	10.40	8.52	9.26	8.30	8.44	8.37
14.50	9.39	8.35	8.48	10.41	8.42	9.24	8.21	8.34	8.27
15.50	9.35	8.29	8.35	10.38	8.32	9.18	8.11	8.18	8.14
16.50	9.32	8.22	8.24	10.36	8.23	9.12	8.02	8.04	8.03
17.50	9.29	8.15	8.13	10.36	8.14	9.11	7.96	7.95	7.95
18.50	9.24	8.09	8.03	10.38	8.06	9.07	7.92	7.86	7.89
19.50	9.19	8.03	7.95	10.37	7.99	9.01	7.85	7.77	7.81
20.50	9.17	7.98	7.87	10.35	7.92	8.97	7.78	7.67	7.72
21.50	9.16	7.92	7.79	10.32	7.85	8.93	7.69	7.56	7.63
22.50	9.15	7.86	7.71	10.33	7.78	8.92	7.63	7.49	7.56
23.50	9.13	7.81	7.63	10.33	7.72	8.91	7.60	7.41	7.50
24.50	9.12	7.76	7.55	10.34	7.65	8.91	7.54	7.33	7.44
25.50	9.10	7.70	7.47	10.34	7.59	8.89	7.49	7.25	7.37
26.50	9.08	7.66	7.39	10.33	7.52	8.86	7.44	7.17	7.30
27.50	9.05	7.62	7.31	10.34	7.46	8.85	7.41	7.10	7.25
28.50	9.02	7.58	7.23	10.35	7.40	8.82	7.37	7.02	7.20
29.50	9.00	7.54	7.15	10.35	7.34	8.80	7.34	6.95	7.14
30.50	8.98	7.50	7.07	10.35	7.28	8.78	7.30	6.88	7.09
31.50	8.96	7.46	7.02	10.35	7.24	8.77	7.26	6.82	7.04
32.50	8.95	7.42	6.96	10.37	7.19	8.77	7.23	6.78	7.00
33.50	8.94	7.38	6.90	10.39	7.14	8.78	7.21	6.74	6.97
34.50	8.93	7.34	6.83	10.34	7.08	8.72	7.13	6.62	6.87
35.50	8.91	7.30	6.78	10.31	7.04	8.67	7.05	6.54	6.79
36.50	8.90	7.26	6.73	10.35	6.99	8.70	7.06	6.53	6.79
37.50	8.89	7.22	6.67	10.36	6.94	8.69	7.02	6.47	6.75
38.50	8.87	7.18	6.62	10.35	6.90	8.67	6.98	6.41	6.70
39.50	8.85	7.16	6.58	10.34	6.87	8.64	6.95	6.37	6.66
40.50	8.84	7.14	6.54	10.32	6.84	8.61	6.91	6.32	6.61
41.50	8.82	7.11	6.52	10.34	6.82	8.61	6.90	6.31	6.60
42.50	8.80	7.09	6.51	10.33	6.80	8.58	6.87	6.29	6.58
43.50	8.78	7.06	6.48	10.33	6.77	8.56	6.84	6.26	6.55
44.50	8.75	7.04	6.46	10.30	6.75	8.50	6.79	6.21	6.50
45.50	8.73	7.02	6.44	10.28	6.73	8.45	6.75	6.16	6.46
46.50	8.71	7.01	6.41	10.32	6.71	8.48	6.77	6.17	6.47
47.50	8.71	6.99	6.38	10.31	6.68	8.47	6.75	6.14	6.45
48.00	8.7	6.98	6.37	10.31		8.46	6.74	6.13	6.44

Data for Figure 4.12 Nutrient Concentrations of Overlying Water for Flux Calculations at Whitecourt, USML

Time (hours)	NH_4^+ (µg-N/L)							
	Overlying Water 1	Overlying Water 2	Overlying Water 3	OL Water Mean	Min	Max	Control	Corrected Mean
0	101.40	78.16	255.51	145.02	66.86	110.49	28.75	145.02
12	141.61	105.76	310.14	185.84	80.08	124.31	27.72	186.87
24	157.10	117.41	356.05	210.19	92.78	145.86	24.74	214.20
36	186.39	118.42	444.54	249.78	131.36	194.75	22.90	255.64
48	192.78	150.77	346.68	230.08	79.31	116.61	21.18	237.64

Time (hours)	NO_x^- (µg-N/L)							
	Overlying Water 1	Overlying Water 2	Overlying Water 3	OL Water Mean	Min	Max	Control	Corrected Mean
0	27.80	27.75	24.00	25.90	1.90	3.80	25.93	25.90
12	26.85	25.00	24.80	25.82	1.02	2.05	23.03	28.73
24	29.61	24.87	25.69	27.65	1.96	3.92	23.96	29.63
36	29.64	25.77	25.69	27.66	1.98	3.95	23.93	29.67
48	29.59	22.99	27.03	28.31	1.28	2.56	22.97	31.28

Time (hours)	PO_4^{3-} (µg/L)							
	Overlying Water 1	Overlying Water 2	Overlying Water 3	OL Water Mean	Min	Max	Control	Corrected Mean
0	2.75	3.39	3.55	3.23	0.48	0.32	3.05	3.23
12	3.79	4.62	3.16	3.86	0.70	0.76	3.29	3.62
24	3.82	3.31	2.97	3.37	0.40	0.46	3.54	2.88
36	3.05	4.99	3.40	3.81	0.77	1.17	3.32	3.55
48	2.86	3.68	3.15	3.23	0.37	0.45	3.60	2.68

Time (hours)	SO_4^{2-} (mg/L)							
	Overlying Water 1	Overlying Water 2	Overlying Water 3	OL Water Mean	Min	Max	Control	Corrected Mean
0	59.01	58.47	58.27	58.58	0.31	0.43	59.17	58.58
12	58.92	58.40	58.52	58.62	0.21	0.31	58.39	59.39
24	49.50	58.59	58.75	55.61	6.11	2.98	58.23	56.55
36	58.95	58.17	58.69	58.60	0.44	0.34	58.68	59.09
48	58.37	58.28	58.51	58.39	0.11	0.12	58.05	59.50

Data for Figure 4.13 DO Concentration of Overlying Water of Sediment Core at ALPAC Site (USAM)

Time	DO in Overlying Water (mg/L)						Corrected DO (mg/L)			
(hours)	Sample1	Sample 2	Sample 3	Control	Average	Time (hr)	Sample1	Sample 2	Sample 3	Average
0.00	10.27	9.91	9.84	9.34	10.01	0.00				
0.50	10.25	9.88	9.82	9.35	9.98	0.50	10.26	9.89	9.83	9.99
1.50	10.19	9.81	9.75	9.34	9.92	1.50	10.19	9.81	9.75	9.92
2.50	10.14	9.76	9.70	9.34	9.87	2.50	10.14	9.76	9.70	9.87
3.50	10.10	9.69	9.65	9.34	9.81	3.50	10.10	9.69	9.65	9.81
4.50	10.04	9.63	9.59	9.32	9.75	4.50	10.02	9.61	9.57	9.73
5.50	10.00	9.57	9.54	9.32	9.70	5.50	9.98	9.55	9.52	9.68
6.50	9.96	9.50	9.48	9.32	9.65	6.50	9.94	9.48	9.46	9.63
7.50	9.90	9.46	9.43	9.31	9.60	7.50	9.87	9.43	9.40	9.57
8.50	9.86	9.40	9.38	9.32	9.55	8.50	9.84	9.38	9.36	9.53
9.50	9.82	9.33	9.33	9.30	9.49	9.50	9.78	9.29	9.29	9.45
10.50	9.77	9.29	9.28	9.30	9.45	10.50	9.73	9.25	9.24	9.41
11.50	9.73	9.24	9.24	9.29	9.40	11.50	9.68	9.19	9.19	9.35
12.50	9.69	9.19	9.19	9.30	9.36	12.50	9.65	9.15	9.15	9.32
13.50	9.65	9.14	9.15	9.30	9.31	13.50	9.61	9.10	9.11	9.27
14.50	9.61	9.09	9.10	9.28	9.27	14.50	9.55	9.03	9.04	9.21
15.50	9.58	9.06	9.07	9.27	9.24	15.50	9.51	8.99	9.00	9.17
16.50	9.54	9.01	9.03	9.26	9.19	16.50	9.46	8.93	8.95	9.11
17.50	9.50	8.96	8.98	9.26	9.15	17.50	9.42	8.88	8.90	9.07
18.50	9.47	8.92	8.95	9.26	9.11	18.50	9.39	8.84	8.87	9.03
19.50	9.43	8.89	8.91	9.25	9.08	19.50	9.34	8.80	8.82	8.99
20.50	9.39	8.84	8.87	9.25	9.03	20.50	9.30	8.75	8.78	8.94
21.50	9.36	8.80	8.83	9.25	9.00	21.50	9.27	8.71	8.74	8.91
22.50	9.33	8.76	8.80	9.24	8.96	22.50	9.23	8.66	8.70	8.86
23.50	9.30	8.71	8.76	9.24	8.92	23.50	9.20	8.61	8.66	8.82
24.50	9.25	8.69	8.72	9.23	8.89	24.50	9.14	8.58	8.61	8.78
25.50	9.22	8.64	8.68	9.21	8.85	25.50	9.09	8.51	8.55	8.72
26.50	9.19	8.60	8.65	9.21	8.81	26.50	9.06	8.47	8.52	8.68
27.50	9.16	8.57	8.62	9.21	8.78	27.50	9.03	8.44	8.49	8.65
28.50	9.12	8.52	8.57	9.22	8.74	28.50	9.00	8.40	8.45	8.62
29.50	9.09	8.48	8.54	9.21	8.70	29.50	8.96	8.35	8.41	8.57
30.50	9.06	8.46	8.51	9.20	8.68	30.50	8.92	8.32	8.37	8.54
31.50	9.03	8.42	8.48	9.18	8.64	31.50	8.87	8.26	8.32	8.48
32.50	9.00	8.39	8.45	9.19	8.61	32.50	8.85	8.24	8.30	8.46
33.50	8.96	8.36	8.41	9.20	8.58	33.50	8.82	8.22	8.27	8.44
34.50	8.94	8.31	8.38	9.19	8.54	34.50	8.79	8.16	8.23	8.39
35.50	8.91	8.30	8.36	9.20	8.52	35.50	8.77	8.16	8.22	8.38
36.50	8.88	8.26	8.32	9.19	8.49	36.50	8.73	8.11	8.17	8.34
37.50	8.85	8.22	8.29	9.19	8.45	37.50	8.70	8.07	8.14	8.30
38.50	8.82	8.20	8.26	9.19	8.43	38.50	8.67	8.05	8.11	8.28
39.50	8.77	8.17	8.24	9.19	8.39	39.50	8.62	8.02	8.09	8.24
40.50	8.72	8.14	8.20	9.18	8.35	40.50	8.56	7.98	8.04	8.19
41.50	8.66	8.09	8.16	9.16	8.30	41.50	8.48	7.91	7.98	8.12
42.50	8.62	8.06	8.13	9.17	8.27	42.50	8.45	7.89	7.96	8.10
43.50	8.55	8.04	8.10	9.17	8.23	43.50	8.38	7.87	7.93	8.06
44.50	8.48	8.01	8.08	9.15	8.19	44.50	8.29	7.82	7.89	8.00
45.50	8.42	7.98	8.05	9.13	8.15	45.50	8.21	7.77	7.84	7.94
46.50	8.34	7.95	8.01	9.13	8.10	46.50	8.13	7.74	7.80	7.89
47.50	8.27	7.91	7.98	9.11	8.05	47.50	8.04	7.68	7.75	7.82
48.00	8.26	7.91	7.98	9.13	8.05	48.00	8.05	7.70	7.77	7.84

Data for Figure 4.14 Nutrient Concentrations in Overlying Water for Flux Calculations at ALPAC Site (USAM)

Time (hours)	NH_4^+ (µg-N/L)							
	Overlying Water 1	Overlying Water 2	Overlying Water 3	OL Water Mean	Min	Max	Control	Corrected Mean
0	28.00	59.11	30.85	39.32	8.47	19.79	29.93	39.32
12	34.39	60.94	27.00	40.78	6.38	20.16	29.88	40.83
24	27.13	75.06	28.11	43.43	15.33	31.63	29.00	44.36
36	24.19	73.13	34.60	43.97	9.37	29.16	28.93	44.97
48	26.33	74.37	37.85	46.18	8.33	28.18	26.61	49.50

Time (hours)	NO_x^- (µg-N/L)							
	Overlying Water 1	Overlying Water 2	Overlying Water 3	OL Water Mean	Min	Max	Control	Corrected Mean
0	3.06	3.06	3.05	3.05	0.00	-0.01	4.96	3.05
12	6.62	4.83	4.85	5.43	0.60	1.19	4.88	5.52
24	4.13	5.06	14.91	8.03	3.90	6.88	5.04	7.96
36	4.94	6.82	14.45	8.74	3.80	5.71	3.04	10.66
48	4.42	8.18	13.85	8.82	4.39	5.03	4.25	9.53

Time (hours)	PO_4^{3-} (µg/L)							
	Overlying Water 1	Overlying Water 2	Overlying Water 3	OL Water Mean	Min	Max	Control	Corrected Mean
0	4.62	5.90	5.37	5.30	0.68	0.61	5.00	5.30
12	4.01	5.04	6.70	5.25	1.24	1.45	4.75	5.49
24	5.07	4.68	6.16	5.30	0.23	0.86	6.37	3.93
36	3.93	5.12	5.52	4.86	0.93	0.67	6.62	3.23
48	4.74	4.94	4.95	4.88	0.13	0.07	6.96	2.91

Time (hours)	SO_4^{2-} (mg/L)							
	Overlying Water 1	Overlying Water 2	Overlying Water 3	OL Water Mean	Min	Max	Control	Corrected Mean
0	37.73	37.87	38.25	37.95	0.22	0.30	38.11	37.95
12	37.89	38.02	37.81	37.91	0.01	0.11	38.51	37.51
24	38.03	38.13	38.25	38.14	0.11	0.11	38.77	37.48
36	38.17	38.20	38.73	38.37	0.20	0.36	38.19	38.29
48	37.98	38.52	38.15	38.22	0.24	0.30	38.37	37.96

Data for Figure 4.15 DO Concentration of Overlying Water of Sediment Core at Calling River (DSCR)

Time	DO in Overlying Water (mg/L)					DO Corrected (mg/L)			
(hours)	Sample 1	Sample 2	Sample 3	Average	Control	Sample 1	Sample 2	Sample 3	Average
0.00	10.57	10.56	10.46	10.53	10.52				
0.50	10.50	10.50	10.40	10.47	10.47	10.45	10.45	10.35	10.42
1.50	10.42	10.43	10.30	10.38	10.39	10.30	10.30	10.17	10.25
2.50	10.31	10.35	10.20	10.29	10.32	10.11	10.15	10.00	10.09
3.50	10.23	10.27	10.13	10.21	10.28	9.98	10.03	9.88	9.97
4.50	10.16	10.22	10.06	10.15	10.25	9.89	9.96	9.79	9.88
5.50	10.09	10.17	10.00	10.09	10.22	9.79	9.87	9.70	9.79
6.50	10.04	10.13	9.94	10.03	10.18	9.70	9.79	9.60	9.69
7.50	9.97	10.08	9.88	9.98	10.17	9.63	9.73	9.54	9.63
8.50	9.92	10.05	9.82	9.93	10.15	9.55	9.68	9.45	9.56
9.50	9.86	10.00	9.77	9.88	10.13	9.47	9.61	9.37	9.48
10.50	9.81	9.97	9.72	9.83	10.11	9.40	9.56	9.31	9.43
11.50	9.76	9.93	9.66	9.78	10.10	9.34	9.51	9.25	9.37
12.50	9.70	9.90	9.62	9.74	10.09	9.27	9.47	9.19	9.31
13.50	9.65	9.86	9.57	9.69	10.07	9.20	9.41	9.12	9.24
14.50	9.59	9.82	9.52	9.64	10.07	9.14	9.37	9.06	9.19
15.50	9.54	9.79	9.47	9.60	10.06	9.08	9.33	9.01	9.14
16.50	9.49	9.75	9.42	9.56	10.05	9.02	9.28	8.95	9.08
17.50	9.45	9.72	9.37	9.51	10.03	8.96	9.23	8.88	9.02
18.50	9.40	9.69	9.33	9.47	10.03	8.91	9.20	8.84	8.98
19.50	9.35	9.65	9.29	9.43	10.01	8.85	9.15	8.78	8.93
20.50	9.31	9.62	9.24	9.39	10.00	8.79	9.10	8.72	8.87
21.50	9.25	9.58	9.19	9.34	10.00	8.74	9.07	8.68	8.83
22.50	9.22	9.56	9.15	9.31	10.00	8.70	9.04	8.64	8.79
23.50	9.17	9.51	9.10	9.26	10.00	8.65	8.99	8.58	8.74
24.50	9.11	9.47	9.05	9.21	9.99	8.58	8.94	8.52	8.68
25.50	9.07	9.44	9.00	9.17	9.99	8.54	8.91	8.47	8.64
26.50	9.03	9.41	8.97	9.13	9.98	8.49	8.87	8.43	8.60
27.50	8.98	9.37	8.92	9.09	9.98	8.44	8.84	8.39	8.56
28.50	8.93	9.34	8.88	9.05	9.99	8.40	8.80	8.34	8.51
29.50	8.89	9.31	8.84	9.01	9.98	8.35	8.77	8.30	8.47
30.50	8.85	9.27	8.80	8.97	9.98	8.31	8.73	8.26	8.43
31.50	8.80	9.24	8.75	8.93	9.98	8.26	8.70	8.21	8.39
32.50	8.76	9.20	8.72	8.89	9.98	8.22	8.67	8.18	8.36
33.50	8.71	9.17	8.68	8.86	9.98	8.17	8.63	8.14	8.31
34.50	8.67	9.14	8.64	8.82	9.97	8.12	8.59	8.09	8.27
35.50	8.63	9.10	8.60	8.78	9.97	8.08	8.56	8.05	8.23
36.50	8.59	9.07	8.56	8.74	9.98	8.05	8.53	8.01	8.20
37.50	8.54	9.04	8.52	8.70	9.97	8.00	8.49	7.97	8.15
38.50	8.51	9.01	8.48	8.67	9.97	7.96	8.46	7.93	8.12
39.50	8.47	8.98	8.44	8.63	9.97	7.92	8.43	7.90	8.08
40.50	8.42	8.95	8.40	8.59	9.97	7.88	8.40	7.86	8.04
41.50	8.38	8.91	8.37	8.55	9.97	7.83	8.36	7.82	8.00
42.50	8.34	8.88	8.33	8.52	9.98	7.80	8.34	7.78	7.97
43.50	8.31	8.85	8.29	8.49	9.97	7.76	8.30	7.74	7.94
44.50	8.28	8.82	8.26	8.45	9.97	7.73	8.27	7.71	7.90
45.50	8.24	8.79	8.22	8.41	9.97	7.69	8.24	7.67	7.87
46.50	8.20	8.75	8.18	8.38	9.98	7.66	8.21	7.64	7.84
47.50	8.15	8.72	8.14	8.34	9.98	7.62	8.18	7.60	7.80
48.00	8.13	8.70	8.11	8.31	9.99	7.60	8.17	7.58	7.78

Data for Figure 4.16 Nutrient Concentrations in Overlying Water for Flux Calculations at Callling River (DSCR)

Time (hours)	NH_4^+ (µg-N/L)							
	Overlying Water 1	Overlying Water 2	Overlying Water 3	OL Water Mean	Min	Max	Control	Corrected Mean
0	20.00	20.00	21.00	20.33	0.33	0.67	28.00	20.33
12	21.77	32.22	25.58	26.52	4.75	5.70	29.65	24.88
24	26.43	24.71	20.07	23.74	3.67	2.69	25.80	25.94
36	24.65	27.50	23.72	25.29	1.57	2.21	29.62	23.67
48	20.29	23.11	25.95	23.12	2.83	2.83	26.93	24.19

Time (hours)	NO_x^- (µg-N/L)							
	Overlying Water 1	Overlying Water 2	Overlying Water 3	OL Water Mean	Min	Max	Control	Corrected Mean
0	3.00	4.00	3.00	3.33	0.33	0.67	2.00	3.33
12	0.96	0.96	2.00	1.31	0.35	0.69	2.97	0.34
24	4.61	3.78	5.64	4.67	0.90	0.96	7.71	-1.04
36	0.96	0.96	1.06	0.99	0.03	0.06	2.00	0.99
48	4.76	3.82	5.75	4.78	0.95	0.97	7.76	-0.98

Time (hours)	PO_4^{3-} (µg/L)							
	Overlying Water 1	Overlying Water 2	Overlying Water 3	OL Water Mean	Min	Max	Control	Corrected Mean
0	17.80	23.80	21.40	21.00	3.20	2.80	28.40	21.00
12	20.71	22.04	18.06	20.27	2.21	1.77	25.56	23.11
24	19.81	23.78	15.98	19.86	3.88	3.92	25.98	22.27
36	20.01	20.76	16.70	19.16	2.46	1.61	27.25	20.31
48	21.35	25.22	16.99	21.18	4.20	4.03	29.87	19.72

Time (hours)	SO_4^{2-} (mg/L)							
	Overlying Water 1	Overlying Water 2	Overlying Water 3	OL Water Mean	Min	Max	Control	Corrected Mean
0	11.86	8.93	11.73	10.84	1.91	0.89	8.69	10.84
12	13.80	11.00	13.86	12.89	1.89	0.97	9.62	11.96
24	12.86	14.03	13.64	13.51	0.65	0.13	10.90	11.30
36	10.75	9.16	12.43	10.78	1.62	1.65	8.58	10.88
48	9.25	8.48	11.42	9.72	1.23	1.70	7.54	10.87

Flux Calculation Results for Table 4.2

Relationship Used:

$$Flux = \frac{\Delta C}{\Delta t} \times \frac{Volume}{Area_{Chamber}}$$

White Court

Sample	OL Water Volume (cm^3)	Core Surface Area (cm^2)	Height (cm)	O_2			NH_4^+-N		NO_x^--N		PO_4^{3-}		SO_4^{2-}	
				Slope (ΔC/Δt)	SOD (g/m^2•d)	Mean SOD (g/m^2•d)	Slope (ΔC/Δt)	Mean Flux (mg/m^2•d)	Slope (ΔC/Δt)	Mean Flux (mg/m^2•d)	Slope (ΔC/Δt)	Mean Flux (mg/m^2•d)	Slope (ΔC/Δt)	Mean Flux (mg/m^2•d)
1	700	38.31	18.27	0.0607	0.27	0.32	2.1168	10.09	0.0978	0.46	-0.0097	-0.05	0.0128	61.04
2	660		17.23	0.0831	0.34									
3	780		20.36	-	-	-								

ALPAC

Sample	OL Water Volume (cm^3)	Core Surface Area (cm^2)	Height (cm)	O_2			NH_4^+-N		NO_x^--N		PO_4^{3-}		SO_4^{2-}	
				Slope (ΔC/Δt)	SOD (g/m^2•d)	Mean SOD (g/m^2•d)	Slope (ΔC/Δt)	Mean Flux (mg/m^2•d)	Slope (ΔC/Δt)	Mean Flux (mg/m^2•d)	Slope (ΔC/Δt)	Mean Flux (mg/m^2•d)	Slope (ΔC/Δt)	Mean Flux (mg/m^2•d)
1	752	38.31	19.63	0.0426	0.20	0.20	0.2042	0.91	0.151	0.67	-0.0586	-0.026	0.0086	38.43
2	760		19.84	0.0447	0.21									
3	700		18.27	0.0421	0.18									

Calling River

Sample	OL Water Volume (cm^3)	Core Surface Area (cm^2)	Height (cm)	O_2			NH_4^+-N		NO_x^--N		PO_4^{3-}		SO_4^{2-}	
				Slope (ΔC/Δt)	SOD (g/m^2•d)	Mean SOD (g/m^2•d)	Slope (ΔC/Δt)	Mean Flux (mg/m^2•d)	Slope (ΔC/Δt)	Mean Flux (mg/m^2•d)	Slope (ΔC/Δt)	Mean Flux (mg/m^2•d)	Slope (ΔC/Δt)	Mean Flux (mg/m^2•d)
1	810	38.31	21.10	0.0543	0.28	0.24	0.0542	0.23	-0.0633	-0.28	-0.0447	-0.19	-0.0084	-35.93
2	798		20.80	0.0423	0.21									
3	710		18.5	0.0522	0.23									

Data for the relationship Between Nutrient Flux and Sediment Nutrient Content

Location	NH_4^+ Flux ($mg\text{-}N/m^2 \cdot d$)	% (wt/dry wt)			
		TN	TOC	OM	Porosity
Whitecourt	10.095	0.17	4.03	11.84	82.89
ALPAC	0.913	0.04	0.72	2.29	65.32
Calling River	0.000	0.06	0.92	2.88	70.60

Location	NO_x^- Flux ($mg/m^2 \cdot d$)	% (wt/dry wt)			
		TN	TOC	OM	Porosity
Whitecourt	0.464	0.17	4.03	11.84	82.89
ALPAC	0.675	0.04	0.72	2.29	65.32
Calling River	0.000	0.06	0.92	2.88	70.60

Data for the Relationship Between Nutrient Flux and Sediment Classification and Porosity

Location	NH_4^+ Flux ($mg\text{-}N/m^2 \cdot d$)	% (wt/dry wt)		
		Clay	Sand	Porosity
Whitecourt	9.301	9.51	62.05	82.89
ALPAC	0.630	12.33	68.26	65.32
Calling River	0.000	9.15	65.86	70.60

Location	NO_x^- Flux ($mg/m^2 \cdot d$)	% (wt/dry wt)		
		Clay	Sand	Porosity
Whitecourt	0.265	9.51	62.05	82.89
ALPAC	0.552	12.33	68.26	65.32
Calling River	0.000	9.15	65.86	70.60

Data for Figure 4.17 and Figure 4.18 Relationship Between SOD and Nutrient Flux

Location	SOD ($g/m^2 \cdot d$)	Flux ($mg\text{-}N /m^2 \cdot d$)	
		NH_4^+	NO_x^-
Whitecourt	0.32	10.09	0.46
ALPAC	0.20	0.91	0.67
Calling River	0.24	0.000	0.000

APPENDIX C
Data for Chapter 5

Calculations for Instantaneous Load in the Athabasca River Tributaries in the Fall of 2006 Supplementing Table 5.2

Tributary	Flow (m^3/s)	Concentration							Load						
		TOC (mg/L)	BOD_5 (mg/L)	TSS (mg/L)	TIN (µg/L)	TDP (µg/L)	Chl-α (µg/L)	Fe (mg/L)	TOC (t/d)	BOD_5 (t/d)	TSS (t/d)	TIN (kg/d)	TDP (kg/d)	Chl-α (kg/d)	Fe (kg/d)
McLeod River	38.8	3.13	2.00	1.00	11.46	1.62	0.75	0.01	10.49	6.70	3.35	38.42	5.42	2.51	33.52
Freeman River	5.32	9.43	2.00	2.50	4.61	5.50	1.95	0.52	4.33	0.92	1.15	2.12	2.53	0.90	239.02
Pembina River	31.4	5.77	2.00	1.00	3.09	3.89	2.24	0.24	15.65	5.43	2.71	8.38	10.56	6.08	651.11
Lesser Slave River	20.8	14.38	2.00	1.00	23.53	17.51	15.77	0.42	25.84	3.59	1.80	42.29	31.47	28.34	754.79
La Biche River	2.69	15.41	2.00	26.00	165.60	58.56	14.17	0.23	3.58	0.46	6.04	38.49	13.61	3.29	53.46
Calling River	0.86	13.65	2.00	3.00	35.20	51.76	23.64	0.40	1.01	0.15	0.22	2.62	3.85	1.76	29.72

APPENDIX D

Data for Chapter 6

Data for Figure 6.1 - Oxygen Calibration Curve at Room Temperature

DO (mg/L)	Current Signal (pA)						
	1	2	3	4	Average	Min	Max
12	479	473	473	468	473.25	5.25	5.75
0	9	10	6	8	8.25	2.25	1.75

Data for Figure 6.2 pH Microsensor Calibration at Room Temperature

pH	Potential (mV) for pH ISmE # 1			Potential (mV) for pH ISmE # 2			Potential (mV) for pH ISmE # 3			Potentail (mV) of all ISmEs		
	1st Reading	2nd Reading	Average	1st Reading	2nd Reading	Average	1st Reading	2nd Reading	Average	Average	Min	Max
6	92	91	92	89	88	89	80	78	79	87	8	5
7	33	31	32	33	37	35	28	27	28	32	4	0
8	-27	-23	-25	-26	-26	-26	-31	-27	-29	-27	2	2
9	-84	-82	-83	-86	-88	-89	-87	-88	-88	-87	1	4
10	-139	-135	-137	-139	-140	-140	-141	-142	-142	-140	2	3
Regression Equation	$y_1 = -57.3x + 434.2$			$y_2 = -58.2x + 439.4$			$y_3 = -55.8x + 416$			$y_{AVE} = -57.1x + 429.87$		
Slope	-57.30			-58.20			-55.80			-57.10		

Data for Figure 6.3 NH_4^+ Microsensor Calibration at Room Temperature

log NH_4^+ (M)	Potential (mV) for NH_4^+ ISmE # 1			Potential (mV) for NH_4^+ ISmE # 2			Potential (mV) for NH_4^+ ISmE # 3			Potentail (mV) of all NH_4^+ ISmEs		
	1st Reading	2nd Reading	Average	1st Reading	2nd Reading	Average	1st Reading	2nd Reading	Average	Average	Min	Max
-6	-58	-52	-55	-75	-79	-77	-95	-97	-96	-76	20	21
-5	-3	0	-2	-23	-26	-25	-40	-44	-42	-23	19	21
-4	52	56	54	30	29	30	10	11	11	32	21	22
-3	109	110	110	87	86	87	66	67	67	88	21	22
-2	166	167	167	144	144	144	123	123	123	145	22	22
Regression Equation	$y_1 = 55.6x + 277.2$			$y_2 = 55.4x + 253.4$			$y_3 = 54.7x + 231.4$			$y_{AVE} = 55.233x + 254$		
Slope	55.60			55.40			54.70			55.23		

Data for Figure 6.4 NO_3^- Microsensor Calibration at Room Temperature

log NO_3^- (M)	Potential (mV) for NO_3^- ISmE # 1			Potential (mV) for NO_3^- ISmE # 2			Potential (mV) for NO_3^- ISmE # 3			Potential (mV) for all NO_3^- ISmEs		
	1st Reading	2nd Reading	Average	1st Reading	2nd Reading	Average	1st Reading	2nd Reading	Average	Average	Min	Max
-6	302	308	305	290	292	291	317	321	319	305	14	14
-5	254	258	256	240	244	242	268	271	270	256	14	14
-4	202	203	203	193	196	195	213	214	214	204	9	10
-3	139	140	140	142	139	141	164	163	164	148	7	16
-2	83	84	84	88	87	88	109	109	109	94	6	15
Regression Equation	$y_1 = -55.8x - 25.6$			$y_2 = -50.7x - 11.4$			$y_3 = -52.6x + 4.8$			$y_{AVE} = -53.033x - 10.733$		
Slope	-55.80			-50.70			-52.60			-53.03		

Data for Figure 6.5 O_2 Calibration at Different Temperature for Sensor #1

Calibration Condition	23°C		15°C		10°C		3°C	
	Current (nA)	O_2 (mg/L)	Current (nA)	O_2 (mg/L)	Current (nA)	O_2 (mg/L)	Current (nA)	O_2 (mg/L)
Air Saturated	473.25	12.7	415.25	12.7	395.50	12.7	343.25	12.7
N_2 Flushed	8.25	0	15.25	0	13.50	0	12.75	0
Slope	0.0273		0.0318		0.0332		0.0384	

Data for Figure 6.5 O_2 Calibration at Different Temperature for Sensor #2

Calibration Condition	23°C		15°C		10°C		3°C	
	Current (nA)	O_2 (mg/L)	Current (nA)	O_2 (mg/L)	Current (nA)	O_2 (mg/L)	Current (nA)	O_2 (mg/L)
Air Saturated	3.24	12.7	3.06	12.7	2.79	12.7	2.56	12.7
N_2 Flushed	0.08	0	0.11	0	0.17	0	0.09	0
Slope	4.0254		4.3087		4.8381		5.1469	

Data for Figure 6.6 Comparison of O_2 concentration in water at different temperatures between microsensor measurement and theoretical solubility

Temp (^oC)	O_2 (mg/L)					
	Sensor 1	Sensor 2	Average	Min	Max	Based on O_2 Solubility in Water
3	12.70	12.70	12.70	0.00	0.00	13.52
10	10.69	11.51	11.10	0.41	0.41	11.30
15	9.93	10.11	10.02	0.09	0.09	10.10
23	7.71	9.17	8.44	0.73	0.73	8.62

Data for Figure 6.7 Temperature Effect on pH ISmE Calibration

Temp ^oC	Fabricated pH ISmE Slope (mV/decade change)						Nernst Ideal Slope (mV/decade change)
	ISmE # 1	ISmE # 2	ISmE # 3	ISmE Average	Min	Max	
23	58.8	59.0	58.7	58.8	0.1	0.2	58.8
14	58.7	58.1	57.4	58.1	0.7	0.6	57.0
8	56.1	54.9	57.4	56.1	1.2	1.3	55.8
3	55.8	54.6	56.2	55.5	0.9	0.7	54.8
Linear Regression Equation:				y = 0.1755x + 55.035			y = 0.1985x + 54.198

Data for Figure 6.8 Temperature Effect on NH_4^+ ISmE Calibration

Temp (^oC)	Fabricated NH_4^+ ISmE Slope (mV/decade change)							Nernst Slope for Ideal Electrode (mV/decade change)
	ISmE # 1	ISmE # 2	ISmE # 3	ISME # 4	ISmE Average	Min	Max	
23	56.6	51.8	54.9	53.3	54.2	2.4	2.5	58.8
14	52.0	50.6	51.6	51.4	51.4	0.8	0.6	57.0
8	49.4	52.7	50.3	51.6	51.0	0.7	1.7	55.8
3	52.0	50.6	51.6	51.4	51.4	0.8	0.6	54.8
Linear Regression Equation:								y = 0.1985x + 54.198

Data for Figure 6.9 Temperature Effect on NO_3^- ISmE Calibration

Temp (^oC)	Fabricated NO_3^- ISmE Slope (mV/decade change)						Nernst Slope for Ideal Electrode (mV/decade change)
	ISmE # 1	ISmE # 2	ISmE # 3	ISmE Average	Min	Max	
23	56.3	50.1	52.8	53.1	3.0	3.2	58.8
14	53.0	43.0	49.4	48.5	5.5	4.5	57.0
8	49.6	41.0	45.1	45.2	4.2	4.4	55.8
3	48.6	41.5	44.7	44.9	3.4	3.7	54.8
Linear Regression Equation:							y = 0.1985x + 54.198

APPENDIX E

Chapter 7

Data for Figure 7.1 O_2 Profiles in Control Core in the Dark, Illuminated and Flow Condition

Depth	O_2 (mg/L)			Depth	O_2 (mg/L)			Depth	O_2 (mg/L)		
mm	Dark	Illuminated	Flow	mm	Dark	Illuminated	Flow	mm	Dark	Illuminated	Flow
-2.0	12.43	12.52	13.30	1.1	8.08	8.80	11.43	4.1	2.46	2.83	3.23
-1.9	12.43	12.49	13.30	1.2	7.86	8.46	11.09	4.2	2.38	2.64	3.19
-1.8	12.42	12.49	13.35	1.3	7.49	8.19	10.83	4.3	2.21	2.51	3.05
-1.7	12.40	12.49	13.30	1.4	7.21	7.82	10.41	4.4	2.08	2.35	2.93
-1.6	12.39	12.49	13.30	1.5	7.04	7.68	9.98	4.5	2.01	2.23	2.82
-1.5	12.39	12.49	13.35	1.6	6.72	7.46	9.79	4.6	1.93	2.12	2.68
-1.4	12.39	12.49	13.30	1.7	6.54	7.25	9.51	4.7	1.79	1.98	2.42
-1.3	12.39	12.49	13.25	1.8	6.34	7.02	9.37	4.8	1.68	1.85	2.34
-1.2	12.39	12.49	13.25	1.9	6.15	6.77	9.13	4.9	1.61	1.73	2.08
-1.1	12.38	12.49	13.30	2.0	6.01	6.61	8.71	5.0	1.53	1.64	2.00
-1.0	12.39	12.49	13.30	2.1	5.81	6.43	8.41	5.1	1.41	1.53	1.74
-0.9	12.37	12.47	13.30	2.2	5.61	6.22	8.04	5.2	1.30	1.37	1.66
-0.8	12.28	12.45	13.21	2.3	5.38	6.02	7.80	5.3	1.18	1.28	1.57
-0.7	12.30	12.45	13.21	2.4	5.18	5.84	7.48	5.4	1.07	1.14	1.32
-0.6	12.30	12.43	13.16	2.5	4.95	5.59	7.30	5.5	0.97	1.03	1.23
-0.5	12.23	12.40	13.12	2.6	4.74	5.43	6.93	5.6	0.88	0.93	1.06
-0.4	12.13	12.40	13.07	2.7	4.58	5.20	6.70	5.7	0.77	0.84	0.89
-0.3	12.10	12.38	13.07	2.8	4.42	5.08	6.42	5.8	0.71	0.73	0.72
-0.2	12.05	12.27	13.02	2.9	4.29	4.86	6.10	5.9	0.62	0.59	0.64
-0.1	11.82	12.06	12.98	3.0	4.13	4.67	5.68	6.0	0.56	0.52	0.55
0.0	11.49	11.86	12.98	3.1	3.94	4.51	5.40	6.1	0.49	0.39	0.38
0.1	11.10	11.58	12.93	3.2	3.77	4.33	5.22	6.2	0.39	0.30	0.30
0.2	10.76	11.33	12.88	3.3	3.58	4.17	5.03	6.3	0.32	0.21	0.13
0.3	10.43	11.01	12.79	3.4	3.43	3.99	4.80	6.4	0.27	0.16	0.09
0.4	10.08	10.81	12.70	3.5	3.32	3.83	4.53	6.5	0.19	0.11	0.09
0.5	9.77	10.53	12.53	3.6	3.20	3.67	4.29	6.6	0.10	0.09	0.05
0.6	9.53	10.24	12.36	3.7	3.00	3.51	4.02	6.7	0.03	0.05	0.05
0.7	9.23	9.96	12.11	3.8	2.86	3.35	3.79	6.8	0.00	0.00	0.00
0.8	8.94	9.74	11.94	3.9	2.72	3.19	3.65	6.9	0.00	0.00	0.00
0.9	8.61	9.42	11.85	4.0	2.57	3.03	3.46	7.0	0.00	0.00	0.00
1.0	8.35	9.07	11.60	4.1	2.46	2.83	3.23				

Data for Figure 7.2 O_2 Profiles in NH_4^+ Spiked Core in the Dark, Illuminated and Flow Condition

Depth	O_2 (mg/L)			Depth	O_2 (mg/L)		
mm	Dark	Illuminated	Flow	mm	Dark	Illuminated	Flow
-2.0	12.46	12.73	13.18	1.1	6.44	8.06	8.89
-1.9	12.46	12.73	13.20	1.2	5.88	6.86	8.30
-1.8	12.46	12.73	13.25	1.3	4.92	6.77	7.88
-1.7	12.46	12.73	13.25	1.4	4.13	5.96	7.08
-1.6	12.46	12.73	13.18	1.5	3.39	4.88	6.66
-1.5	12.39	12.73	13.18	1.6	2.91	4.09	5.91
-1.4	12.39	12.73	13.18	1.7	2.39	3.71	4.85
-1.3	12.39	12.73	13.11	1.8	1.91	3.21	4.21
-1.2	12.39	12.73	13.11	1.9	1.43	2.25	3.35
-1.1	12.37	12.73	13.07	2.0	1.06	1.69	2.61
-1.0	12.37	12.73	13.07	2.1	0.80	1.31	1.90
-0.9	12.35	12.73	13.03	2.2	0.58	1.20	1.17
-0.8	12.35	12.73	13.03	2.3	0.38	0.93	0.85
-0.7	12.35	12.73	13.00	2.4	0.17	0.73	0.75
-0.6	12.35	12.73	12.98	2.5	0.04	0.50	0.64
-0.5	12.35	12.73	12.92	2.6	0.00	0.23	0.30
-0.4	12.35	12.73	12.92	2.7	0.00	0.00	0.18
-0.3	12.33	12.73	12.90	2.8	0.00	0.00	0.09
-0.2	12.33	12.73	12.90	2.9		0.00	0.00
-0.1	12.31	12.73	12.87	3.0		0.00	0.00
0.0	12.06	12.41	12.83				
0.1	11.58	12.18	12.80				
0.2	11.28	11.94	12.75				
0.3	10.86	11.59	12.49				
0.4	10.36	11.33	12.33				
0.5	9.79	11.07	12.09				
0.6	9.29	10.66	11.92				
0.7	8.54	10.31	11.54				
0.8	8.01	9.84	11.02				
0.9	7.73	9.23	10.23				
1.0	7.02	8.91	9.52				

Data for Figure 7.3 O_2 Profiles in NH_4^+ + TOC Spiked Core in the Dark, Illuminated and Flow Condition

Depth	O_2 (mg/L)			Depth	O_2 (mg/L)		
mm	Dark	Illuminated	Flow	mm	Dark	Illuminated	Flow
-2.0	12.61	12.61	13.42	1.1	4.76	6.49	9.53
-1.9	12.61	12.65	13.42	1.2	4.16	5.92	8.79
-1.8	12.61		13.42	1.3	3.80	5.33	8.06
-1.7	12.61		13.42	1.4	3.43	4.75	7.08
-1.6	12.61		13.42	1.5	3.16	4.23	6.35
-1.5	12.61	12.63	13.42	1.6	2.88	3.73	5.50
-1.4	12.61	12.56	13.42	1.7	2.68	3.37	4.64
-1.3	12.60	12.56	13.42	1.8	2.47	2.98	4.03
-1.2	12.59		13.42	1.9	2.29	2.46	3.42
-1.1	12.59		13.37	2.0	2.15	2.08	2.93
-1.0	12.59	12.61	13.32	2.1	1.92	1.79	2.44
-0.9	12.59		13.32	2.2	1.78	1.42	2.08
-0.8	12.59		13.28	2.3	1.65	1.20	1.83
-0.7	12.59		13.23	2.4	1.49	0.99	1.59
-0.6	12.59		13.18	2.5	1.33	0.88	1.34
-0.5	12.59	12.61	13.18	2.6	1.17	0.75	1.10
-0.4	12.59		13.13	2.7	1.05	0.63	0.98
-0.3	12.56		13.08	2.8	0.89	0.54	0.86
-0.2	12.54	12.61	13.04	2.9	0.76	0.50	0.73
-0.1	12.52	12.61	12.95	3.0	0.62	0.43	0.61
0.0	12.38	12.43	12.88	3.1	0.48	0.36	0.61
0.1	12.06	11.95	12.82	3.2	0.37	0.29	0.49
0.2	11.56	11.48	12.70	3.3	0.27	0.25	0.37
0.3	10.87	10.91	12.58	3.4	0.16	0.20	0.30
0.4	10.23	10.49	12.33	3.5	0.06	0.16	0.24
0.5	9.40	9.90	12.09	3.6	0.01	0.11	0.20
0.6	8.58	9.24	11.85	3.7	0.00	0.07	0.16
0.7	7.64	8.75	11.60	3.8	0.00	0.05	0.12
0.8	6.80	8.32	11.24	3.9	0.00	0.00	0.08
0.9	6.00	7.95	10.75	4.0	0.00	0.00	0.00
1.0	5.35	7.25	10.26				

Data for Figure 7.4 Profiles of O_2, NH_4^+, NO_3^-, and pH in Control Core in the Dark

Depth (mm)	O_2 (mg/L)	NH_4^+-N (µg/L)	NO_3^--N (µg/L)	pH	Depth (mm)	O_2 (mg/L)	NH_4^+-N (µg/L)	NO_3^--N (µg/L)	pH	Depth (mm)	O_2 (mg/L)	NH_4^+-N (µg/L)	NO_3^--N (µg/L)	pH
-2.0	12.43		59.08	8.48	1.1	8.08	127.43	95.36	8.06	4.1	2.46	249.74	100.91	7.82
-1.9	12.43		59.09	8.48	1.2	7.86	126.31	96.20	8.07	4.2	2.38	249.74	101.35	7.82
-1.8	12.42		59.09	8.48	1.3	7.49	127.99	96.20	8.06	4.3	2.21	250.84	101.80	7.82
-1.7	12.40		59.09	8.50	1.4	7.21	134.92	96.62	8.06	4.4	2.08	250.84	101.35	7.82
-1.6	12.39		59.34	8.48	1.5	7.04	141.61	97.04	8.04	4.5	2.01	249.74	103.13	7.82
-1.5	12.39		59.09	8.48	1.6	6.72	153.28	97.46	8.03	4.6	1.93	251.95	102.69	7.81
-1.4	12.39		59.34	8.48	1.7	6.54	159.47	97.89	8.04	4.7	1.79	251.95	103.13	7.81
-1.3	12.39		59.60	8.48	1.8	6.34	168.11	98.31	8.03	4.8	1.68	251.95	103.58	7.81
-1.2	12.39		59.34	8.47	1.9	6.15	179.57	98.74	7.93	4.9	1.61	253.06	104.49	7.81
-1.1	12.38		59.60	8.46	2.0	6.01	192.66	98.74	7.91	5.0	1.53	254.17	103.58	7.81
-1.0	12.39		59.60	8.45	2.1	5.81	203.10	98.31	7.92	5.1	1.41	256.42	104.03	7.81
-0.9	12.37		59.86	8.44	2.2	5.61	205.80	97.89	7.91	5.2	1.30	256.42	104.49	7.80
-0.8	12.28		60.12	8.42	2.3	5.38	217.91	98.74	7.91	5.3	1.18	255.29	104.49	7.80
-0.7	12.30		59.86	8.42	2.4	5.18	218.87	98.74	7.90	5.4	1.07	257.55	104.94	7.81
-0.6	12.30		60.38	8.41	2.5	4.95	221.78	98.31	7.89	5.5	0.97	258.68	104.94	7.81
-0.5	12.23		60.65	8.41	2.6	4.74	224.72	98.31	7.89	5.6	0.88	256.42	104.94	7.80
-0.4	12.13		60.91	8.40	2.7	4.58	227.71	99.17	7.89	5.7	0.77	256.42	104.94	7.80
-0.3	12.10	249.74	61.18	8.35	2.8	4.42	231.75	98.74	7.88	5.8	0.71	257.55	104.94	7.80
-0.2	12.05	247.55	62.25	8.29	2.9	4.29	232.77	99.17	7.87	5.9	0.62	258.68	104.94	7.79
-0.1	11.82	260.97	65.31	8.23	3.0	4.13	234.83	99.17	7.87	6.0	0.56	259.82	104.94	7.79
0.0	11.49	273.90	66.16	8.19	3.1	3.94	236.90	99.60	7.86	6.1	0.49	262.12	104.94	7.79
0.1	11.10	279.99	67.03	8.16	3.2	3.77	240.05	99.60	7.86	6.2	0.39	263.27	104.94	7.79
0.2	10.76	278.76	78.74	8.19	3.3	3.58	244.31	100.04	7.86	6.3	0.32	265.60	104.94	7.79
0.3	10.43	273.90	80.48	8.11	3.4	3.43	246.47	100.04	7.85	6.4	0.27	267.95	104.94	7.79
0.4	10.08	267.95	88.18	8.14	3.5	3.32	248.64	100.48	7.85	6.5	0.19	270.31	105.40	7.79
0.5	9.77	258.68	86.28	8.15	3.6	3.20	247.55	100.48	7.85	6.6	0.10	269.13	105.86	7.79
0.6	9.53	205.80	98.31	8.09	3.7	3.00	247.55	100.48	7.83	6.7	0.03	271.51	105.40	7.79
0.7	9.23	189.30	94.13	8.07	3.8	2.86	246.47	101.35	7.82	6.8	0.00	273.90	106.32	7.79
0.8	8.94	153.28	94.54	8.07	3.9	2.72	248.64	100.91	7.82	6.9	0.00	272.70	107.25	
0.9	8.61	128.55	98.31	8.07	4.0	2.57	248.64	100.48	7.82	7.0	0.00	277.54	107.25	
1.0	8.35	125.20	94.95	8.05										

Data for Figure 7.5 Porewater NO_3^--N Concentration in the Sediment Sections of all Cores in Different Loading Conditions

Depth (mm)	Concentration of NO_3^- µg-N/L		
	Control Core	NH_4^+ Spiked Core	NH_4^+ + TOC Spiked Core
0.0	67.74	67.74	67.74
0.5	-	-	-
1.0	502.68	1953.39	963.46
1.5	-	-	-
3.0	24.25	8.82	639.37
5.0	35.28	8.82	35.28
7.0	59.53	41.89	103.62

Data for Figure 7.6, Figure 7.7, 7.8 Microbial Activities in Control Core in the Dark

Depth (mm)	Activity (µg/cm^3•h) in Control Core		
	O_2	NH_4^+-N	NO_3^--N
0.2	-3.18	-	0.27
0.6	-8.72	-0.56	1.21
1.0	-7.04	-1.88	-0.07
1.4	-10.09	-0.63	-0.04
1.8	-7.98	-0.63	0.04
2.2	5.55	0.00	-0.15
2.6	-4.74	-0.08	-0.07
3.0	3.92	-0.14	0.00
3.4	-7.10	0.34	0.00
3.8	-2.30	-0.21	0.15
4.2	0.06	0.00	0.08
4.6	1.49	0.07	0.04
5.0	1.56	0.00	-0.08
5.4	-0.81	0.15	0.04
5.8	-3.92	-0.07	0.00
6.2	2.30	-0.08	0.00
6.6	2.74	-0.23	0.04

Data for Figure 7.9 Profiles of O_2, NH_4^+, NO_3^-, and pH in NH_4^+ Spiked Core in the Dark

Depth (mm)	O_2 (mg/L)	NH_4^+ -N (µg/L)	NO_3^- -N (µg/L)	pH	Depth (mm)	O_2 (mg/L)	NH_4^+ -N (µg/L)	NO_3^- -N (µg/L)	pH
-2.0	12.46	2360.70	54.13	7.90	1.1	6.44	1052.23	123.69	7.23
-1.9	12.46	2349.66	54.12	7.95	1.2	5.88	1046.61	144.92	7.20
-1.8	12.46	2382.91	54.12	7.92	1.3	4.92	1035.45	144.92	7.16
-1.7	12.46	2405.28	45.55	7.91	1.4	4.13	1024.39	144.92	7.13
-1.6	12.46	2371.79	45.55	7.99	1.5	3.39	1018.90	144.92	7.13
-1.5	12.39	2327.71	38.26	7.98	1.6	2.91	1002.57	144.92	7.14
-1.4	12.39	2284.30	64.14	7.96	1.7	2.39	1018.90	169.41	7.14
-1.3	12.39	2252.18	52.29	7.93	1.8	1.91	1029.90	169.41	7.14
-1.2	12.39	2127.36	54.12	7.92	1.9	1.43	1063.54	197.57	7.14
-1.1	12.37	2209.93	64.14	7.85	2.0	1.06	1057.87	197.57	7.15
-1.0	12.37	2158.02	64.14	7.82	2.1	0.80	1063.54	203.69	7.14
-0.9	12.35	2117.22	45.55	7.76	2.2	0.58	1069.24	209.98	7.14
-0.8	12.35	2097.05	54.12	7.74	2.3	0.38	1080.71	219.73	7.14
-0.7	12.35	2107.11	45.55	7.70	2.4	0.17	1086.49	219.73	7.13
-0.6	12.35	2067.10	45.55	7.58	2.5	0.04	1098.12	223.07	7.13
-0.5	12.35	2077.05	54.12	7.61	2.6	0.00	1092.29	229.89	7.13
-0.4	12.35	2067.10	38.26	7.55	2.7	0.00	1115.76	233.37	7.14
-0.3	12.33	1988.94	38.26	7.54	2.8	0.00	1145.71	240.48	7.16
-0.2	12.33	1969.79	75.85	7.56	2.9	0.00	1157.87	236.90	7.17
-0.1	12.31	1885.46	75.85	7.54	3.0	0.00	1170.15	247.77	7.18
0.0	12.06	1786.47	89.48	7.54					
0.1	11.58	1633.80	105.32	7.37					
0.2	11.28	1382.15	89.48	7.37					
0.3	10.86	1305.89	105.32	7.32					
0.4	10.36	1272.42	105.32	7.27					
0.5	9.79	1252.68	105.32	7.23					
0.6	9.29	1226.78	105.32	7.23					
0.7	8.54	1207.65	123.69	7.25					
0.8	8.01	1188.77	123.69	7.20					
0.9	7.73	1157.87	123.69	7.22					
1.0	7.02	1063.54	144.92	7.23					

Data for Figure 7.10, Figure 7.11 and Figure 7.12 Activities in NH_4^+ Spiked Core in the Dark

Depth (mm)	Activity ($\mu g/cm^3 \cdot h$) in NH_4^+ Spiked Core		
	O_2	NH_4^+-N	NO_3^--N
0.2	-	-17.71	0.00
0.6	-33.88	0.31	1.17
1.0	17.09	-5.73	-1.35
1.4	-39.63	-1.07	-1.56
1.8	-24.55	2.88	1.41
2.2	-4.74	-0.02	0.81
2.6	-	-1.58	0.43

Data for Figure 7.13 Profiles of O_2, NH_4^+, NO_3^-, and pH in NH_4^+ + TOC Spiked Core in the Dark

Depth (mm)	O_2 (mg/L)	NH_4^+-N (µg/L)	NO_3^--N (µg/L)	pH	Depth (mm)	O_2 (mg/L)	NH_4^+-N (µg/L)	NO_3^--N (µg/L)	pH
-2.0	12.61	1468.55	65.02	8.82	1.1	4.76	922.84	99.17	7.78
-1.9	12.61	1468.55	65.84	8.90	1.2	4.16	969.32	102.66	7.83
-1.8	12.61	1462.00	65.84	8.88	1.3	3.80	840.21	102.66	7.72
-1.7	12.61	1468.55	66.67	8.84	1.4	3.43	696.48	106.25	7.71
-1.6	12.61	1468.55	67.50	8.56	1.5	3.16	611.85	109.93	7.73
-1.5	12.61	1468.55	66.67	8.55	1.6	2.88	595.67	108.69	7.72
-1.4	12.61	1475.12	65.84	8.60	1.7	2.68	525.64	112.45	7.73
-1.3	12.60	1495.02	63.40	8.56	1.8	2.47	639.81	118.93	7.69
-1.2	12.59	1528.79	64.21	8.50	1.9	2.29	622.89	116.30	7.73
-1.1	12.59	1549.42	62.61	8.48	2.0	2.15	539.92	117.61	7.75
-1.0	12.59	1577.35	63.40	8.50	2.1	1.92	525.64	118.93	7.75
-0.9	12.59	1577.35	65.02	8.44	2.2	1.78	498.20	121.60	7.75
-0.8	12.59	1570.32	64.21	8.34	2.3	1.65	485.03	122.95	7.76
-0.7	12.59	1577.35	65.02	8.25	2.4	1.49	468.00	118.93	7.77
-0.6	12.59	1584.41	66.67	8.02	2.5	1.33	451.57	116.30	7.77
-0.5	12.59	1584.41	67.50	8.01	2.6	1.17	445.56	117.61	7.78
-0.4	12.59	1598.63	70.07	7.98	2.7	1.05	447.56	117.61	7.80
-0.3	12.56	1612.98	71.82	8.05	2.8	0.89	437.67	118.93	7.82
-0.2	12.54	1627.45	75.43	7.98	2.9	0.76	428.00	120.26	7.83
-0.1	12.52	1563.32	83.10	7.87	3.0	0.62	420.42	118.93	7.83
0.0	12.38	1272.94	92.47	7.78	3.1	0.48	412.98	120.26	7.84
0.1	12.06	1250.40	94.66	7.73	3.2	0.37	420.42	121.60	7.84
0.2	11.56	1222.78	92.47	7.69	3.3	0.27	426.10	127.08	7.85
0.3	10.87	1169.36	93.56	7.68	3.4	0.16	470.10	125.69	7.84
0.4	10.23	1045.80	94.66	7.70	3.5	0.06	476.44	128.48	7.85
0.5	9.40	1013.60	95.77	7.76	3.6	0.01	480.72	129.89	7.85
0.6	8.58	1013.60	96.89	7.72	3.7	0.00	485.03	132.75	7.84
0.7	7.64	1083.85	94.66	7.72	3.8	0.00	487.20	135.66	7.81
0.8	6.80	1074.21	96.89	7.75	3.9	0.00	491.57	137.13	7.80
0.9	6.00	1045.80	100.32	7.77	4.0	0.00	493.77	140.11	7.78
1.0	5.35	991.22	101.48	7.71					

Data for Figure 7.14, Figure 7.15 and Figure 7.16 Activities in NH_4^+ + TOC Spiked Core in Dark

Depth (mm)	Activity ($mg/cm^3 \cdot h$) in NH_4^+ + TOC Spiked Core		
	O_2	NH_4^+-N	NO_3^--N
0.2	-	-	0.81
0.6	-25.82	-5.98	0.21
1.0	-34.43	-3.94	0.43
1.4	-10.33	-11.09	-0.24
1.8	3.44	9.29	-0.09
2.2	1.72	-0.74	-0.09
2.6	0.00	-0.94	-0.51
3.0	-3.44	-1.11	0.17
3.4	-10.33	2.52	0.35
3.8	-	-0.01	-0.01

Data for Figure 7.17 Profiles of O_2, NH_4^+, NO_3^-, and pH in Control Core Illuminated

Depth (mm)	O_2 (mg/L)	NH_4^+-N (μg/L)	NO_3^--N (μg/L)	pH	Depth (mm)	O_2 (mg/L)	NH_4^+-N (μg/L)	NO_3^--N (μg/L)	pH	Depth (mm)	O_2 (mg/L)	NH_4^+-N (μg/L)	NO_3^--N (μg/L)	pH
-2.0	12.52		41.87	8.46	1.1	8.80	209.36	75.59	8.19	4.1	2.83	226.04	90.08	7.97
-1.9	12.49		40.05	8.48	1.2	8.46	213.80	76.66	8.17	4.2	2.64	229.19	90.08	7.96
-1.8	12.49		38.30	8.46	1.3	8.19	218.32	75.59	8.18	4.3	2.51	232.39	90.21	7.96
-1.7	12.49		40.65	8.48	1.4	7.82	216.80	73.50	8.18	4.4	2.35	230.79	90.21	7.95
-1.6	12.49		42.49	8.52	1.5	7.68	218.32	74.54	8.15	4.5	2.23	229.19	90.33	7.95
-1.5	12.49		40.05	8.55	1.6	7.46	216.80	77.74	8.11	4.6	2.12	230.79	90.58	7.95
-1.4	12.49		41.87	8.55	1.7	7.25	216.80	76.66	8.10	4.7	1.98	234.00	90.83	7.95
-1.3	12.49		42.49	8.55	1.8	7.02	213.80	82.21	8.07	4.8	1.85	229.19	91.08	7.94
-1.2	12.49		43.77	8.53	1.9	6.77	215.29	81.07	8.09	4.9	1.73	234.00	91.33	7.94
-1.1	12.49		44.41	8.54	2.0	6.61	213.80	82.21	8.08	5.0	1.64	232.39	91.46	7.94
-1.0	12.49		47.10	8.53	2.1	6.43	216.80	79.95	8.07	5.1	1.53	235.63	91.84	7.93
-0.9	12.47		51.41	8.53	2.2	6.22	218.32	82.21	8.07	5.2	1.37	232.39	92.34	7.94
-0.8	12.45		46.42	8.46	2.3	6.02	213.80	83.36	8.07	5.3	1.28	230.79	92.47	7.94
-0.7	12.45		47.79	8.43	2.4	5.84	216.80	81.07	8.07	5.4	1.14	232.39	92.60	7.94
-0.6	12.43		48.15	8.44	2.5	5.59	209.36	85.70	8.06	5.5	1.03	234.00	92.85	7.93
-0.5	12.40	295.26	49.57	8.42	2.6	5.43	212.31	85.82	8.05	5.6	0.93	235.63	92.98	7.94
-0.4	12.40	297.26	49.93	8.43	2.7	5.20	209.36	86.30	8.04	5.7	0.84	240.56	93.11	7.94
-0.3	12.38	301.30	50.23	8.42	2.8	5.08	210.83	86.54	8.01	5.8	0.73	238.91	93.11	7.94
-0.2	12.27	303.34	50.67	8.41	2.9	4.86	207.91	86.78	8.00	5.9	0.59	245.59	93.62	7.94
-0.1	12.06	313.72	52.16	8.34	3.0	4.67	209.36	86.90	7.99	6.0	0.52	242.23	94.14	7.95
0.0	11.86	322.26	59.39	8.31	3.1	4.51	213.80	87.14	7.99	6.1	0.39	240.56	94.40	7.95
0.1	11.58	301.30	64.71	8.25	3.2	4.33	212.31	87.50	7.99	6.2	0.30	243.90	94.79	7.95
0.2	11.33	274.02	69.47	8.23	3.3	4.17	215.29	87.75	7.99	6.3	0.21	245.59	95.31	7.95
0.3	11.01	268.48	71.46	8.20	3.4	3.99	213.80	88.11	7.99	6.4	0.16	248.99	95.97	7.96
0.4	10.81	263.03	73.50	8.16	3.5	3.83	215.29	88.36	7.99	6.5	0.11	252.43	96.36	7.96
0.5	10.53	257.68	73.50	8.19	3.6	3.67	219.84	88.85	7.98	6.6	0.09	254.17	96.36	7.96
0.6	10.24	230.79	72.98	8.20	3.7	3.51	218.32	89.34	7.98	6.7	0.05	257.68	96.36	7.95
0.7	9.96	218.32	72.47	8.23	3.8	3.35	219.84	89.34	7.98	6.8	0.00	259.45	96.49	7.96
0.8	9.74	227.61	72.98	8.25	3.9	3.19	226.04	89.34	7.98	6.9	0.00	263.03	96.49	7.96
0.9	9.42	199.34	73.50	8.15	4.0	3.03	227.61	89.58	7.97	7.0	0.00	270.31	96.49	7.96
1.0	9.07	203.58	72.47	8.17										

Data for Figure 7.18 Profiles of O_2, NH_4^+, NO_3^-, and pH in NH_4^+ Spiked Core Illuminated

Depth (mm)	O_2 (mg/L)	NH_4^+-N (µg/L)	NO_3^--N (µg/L)	pH	Depth (mm)	O_2 (mg/L)	NH_4^+-N (µg/L)	NO_3^--N (µg/L)	pH
-2.0	12.73	2333.39	74.73	7.71	1.1	8.06	1059.87	234.48	7.21
-1.9	12.73	2337.52	81.71	7.70	1.2	6.86	1038.11	232.40	7.20
-1.8	12.73	2338.55	82.81	7.66	1.3	6.77	1027.37	235.53	7.22
-1.7	12.73	2338.55	83.56	7.65	1.4	5.96	990.51	237.65	7.24
-1.6	12.73	2341.65	85.06	7.64	1.5	4.88	980.18	256.40	7.25
-1.5	12.73	2343.72	86.21	7.63	1.6	4.09	939.76	258.70	7.25
-1.4	12.73	2346.83	87.76	7.62	1.7	3.71	900.75	258.70	7.19
-1.3	12.73	2348.90	88.55	7.60	1.8	3.21	886.47	259.86	7.27
-1.2	12.73	2348.90	88.55	7.58	1.9	2.25	853.89	261.02	7.29
-1.1	12.73	2359.28	89.35	7.57	2.0	1.69	844.77	263.36	7.29
-1.0	12.73	2348.90	89.35	7.57	2.1	1.31	835.73	262.19	7.29
-0.9	12.73	2328.24	90.15	7.57	2.2	1.20	833.48	265.73	7.29
-0.8	12.73	2328.24	90.55	7.57	2.3	0.93	829.01	264.54	7.29
-0.7	12.73	2338.55	91.36	7.57	2.4	0.73	826.77	266.91	7.28
-0.6	12.73	2328.24	92.18	7.57	2.5	0.50	835.73	266.91	7.28
-0.5	12.73	2317.97	93.01	7.56	2.6	0.23	849.32	268.11	7.28
-0.4	12.73	2307.72	93.01	7.55	2.7	0.00	858.48	270.52	7.28
-0.3	12.73	2297.52	93.43	7.58	2.8	0.00	863.10	271.73	7.28
-0.2	12.73	2277.21	94.27	7.50	2.9	0.00	872.38	272.94	7.29
-0.1	12.73	2227.04	95.11	7.56	3.0	0.00	877.06	272.94	7.29
0.0	12.41	1943.69	95.96	7.41					
0.1	12.18	1855.79	108.75	7.38					
0.2	11.94	1771.04	131.19	7.36					
0.3	11.59	1610.75	144.74	7.32					
0.4	11.33	1587.74	154.77	7.35					
0.5	11.07	1580.13	188.39	7.34					
0.6	10.66	1535.07	203.25	7.25					
0.7	10.31	1325.04	209.71	7.21					
0.8	9.84	1139.01	214.44	7.24					
0.9	9.23	1110.20	218.31	7.23					
1.0	8.91	1076.43	228.28	7.19					

Data for Figure 7.19 Profiles of O_2, NH_4^+, NO_3^-, and pH in NH_4^+ + TOC Spiked Core Illuminated

Depth (mm)	O_2 (mg/L)	NH_4^+-N (µg/L)	NO_3^--N (µg/L)	pH	Depth (mm)	O_2 (mg/L)	NH_4^+-N (µg/L)	NO_3^--N (µg/L)	pH
-2.0	12.61	2265.16	55.32	7.88	1.1	6.49	1244.68	136.30	7.11
-1.9	12.65	2253.43	55.32	7.86	1.2	5.92	1209.66	141.95	7.13
-1.8		2253.43	55.32	7.86	1.3	5.33	1142.15	144.84	7.14
-1.7		2259.29	55.99	7.84	1.4	4.75	1109.63	146.30	7.13
-1.6		2253.43	56.66	7.83	1.5	4.23	1065.45	149.26	7.14
-1.5	12.63	2253.43	57.35	7.82	1.6	3.73	1046.98	149.26	7.14
-1.4	12.56	2265.16	58.04	7.82	1.7	3.37	970.13	150.76	7.14
-1.3	12.56	2253.43	58.04	7.82	1.8	2.98	841.03	152.27	7.14
-1.2		2253.43	58.74	7.81	1.9	2.46	705.24	153.79	7.14
-1.1		2258.12	58.74	7.79	2.0	2.08	532.53	155.32	7.14
-1.0	12.61	2300.66	59.44	7.80	2.1	1.79	474.69	156.87	7.15
-0.9		2324.58	60.16	7.79	2.2	1.42	468.62	159.20	7.15
-0.8		2397.57	60.16	7.79	2.3	1.20	465.62	159.52	7.15
-0.7		2409.92	60.88	7.78	2.4	0.99	471.65	160.15	7.16
-0.6		2373.03	60.16	7.77	2.5	0.88	471.65	161.09	7.16
-0.5	12.61	2276.94	60.88	7.75	2.6	0.75	468.62	161.73	7.16
-0.4		2385.28	62.34	7.76	2.7	0.63	453.75	162.36	7.17
-0.3		2312.59	63.08	7.79	2.8	0.54	447.92	162.68	7.17
-0.2		2300.66	63.83	7.82	2.9	0.50	450.83	163.16	7.17
-0.1	12.61	2324.58	63.08	7.83	3.0	0.43	442.16	163.32	7.17
0.0	12.43	2161.38	68.48	7.58	3.1	0.36	445.03	163.64	7.17
0.1	11.95	2105.46	78.62	7.45	3.2	0.29	433.64	164.12	7.17
0.2	11.48	1944.88	83.20	7.35	3.3	0.25	422.51	164.60	7.17
0.3	10.91	1737.40	88.98	7.25	3.4	0.20	417.03	165.57	7.17
0.4	10.49	1574.72	90.98	7.20	3.5	0.16	411.63	166.05	7.17
0.5	9.90	1506.67	93.01	7.16	3.6	0.11	403.63	166.70	7.17
0.6	9.24	1457.29	97.19	7.15	3.7	0.07	401.00	167.35	7.17
0.7	8.75	1433.12	102.62	7.14	3.8	0.05	398.38	168.00	7.17
0.8	8.32	1393.60	107.14	7.13	3.9	0.00	395.78	168.82	7.17
0.9	7.95	1370.34	115.43	7.13	4.0	0.00	393.19	169.64	7.17
1.0	7.25	1324.81	128.15	7.13					

Data for Figure 7.20, Figure 7.21, Figure 7.22 Microbial Activities in Control Core Illuminated

Depth (mm)	Activity (μg/cm^3•h) in Illuminated Control Core		
	O_2	NH_4^+-N	NO_3^--N
0.2	-6.86	-1.42	0.37
0.6	-1.72	-1.31	0.20
1.0	0.00	0.07	-0.07
1.4	-5.15	0.10	0.07
1.8	-10.29	-0.19	-0.15
2.2	1.72	0.09	-0.29
2.6	-3.43	0.09	0.11
3.0	0.00	0.28	0.01
3.4	-1.72	-0.19	0.00
3.8	3.43	0.50	0.06
4.2	-3.43	0.62	0.04
4.6	0.00	0.31	-0.02
5.0	3.43	0.42	0.00
5.4	-5.15	-0.22	0.02
5.8	-3.43	0.65	-0.02
6.2	-6.86	-0.12	-0.01
6.6	-1.72	-0.01	0.07

Data for Figure 7.23, Figure 7.24 and Figure 7.25 Activities in NH_4^+ Spiked Core Illuminated

Depth (mm)	Activity (μg/cm^3•h) in NH_4^+ Spiked Core_Illuminated		
	O_2	NH_4^+-N	NO_3^--N
0.2	-4.39	-13.82	-0.49
0.6	24.16	-2.60	0.81
1.0	8.79	-1.15	0.96
1.4	-54.91	2.08	1.18
1.8	-39.54	-1.85	0.07
2.2	4.39	-0.87	0.00
2.6	-37.32	0.57	0.07

Data for Figure 7.26, Figure 7.27 and Figure 7.28 Activities in NH_4^+ + TOC Spiked Core Illuminated

Depth (mm)	Activity ($\mu g/cm^3 \cdot h$) in NH_4^++TOC Spiked Core_Illuminated		
	O_2	NH_4^+-N	NO_3^--N
0.2	-	-	0.44
0.6	-	-3.86	-
1.0	-11.90	-6.29	0.46
1.4	-20.40	-5.95	0.09
1.8	-18.70	-14.18	0.00
2.2	-13.60	0.41	0.19
2.6	-6.80	-0.14	0.04
3.0	-3.40	-1.44	-0.01
3.4	-1.70	-0.66	0.02
3.8	-3.40	-0.32	-0.02